Improved Resilience of Rigid Pavement Systems

FINAL REPORT

FDOT Contract Number: BEB14

October 2023

Submitted By:
Hyung S. Lee, Ph.D., P.E.
Shreenath Rao, Ph.D., P.E.

100 Trade Centre Dr., Suite 200
Champaign, Illinois 61820

DISCLAIMER

The opinions, findings, and conclusions expressed in this publication are those of the authors and not necessarily those of the State of Florida Department of Transportation.

SI* (MODERN METRIC) CONVERSION FACTORS

APPROXIMATE CONVERSIONS TO SI UNITS

Symbol	When You Know	Multiply By	To Find	Symbol
		LENGTH		
in	inches	25.4	millimeters	mm
ft	feet	0.305	meters	m
yd	yards	0.914	meters	m
mi	miles	1.61	kilometers	km
		AREA		
in^2	square inches	645.2	square millimeters	mm^2
ft^2	square feet	0.093	square meters	m^2
yd^2	square yard	0.836	square meters	m^2
ac	acres	0.405	hectares	ha
mi^2	square miles	2.59	square kilometers	km^2
		VOLUME		
fl oz	fluid ounces	29.57	milliliters	mL
gal	gallons	3.785	liters	L
ft^3	cubic feet	0.028	cubic meters	m^3
yd^3	cubic yards	0.765	cubic meters	m^3
	NOTE: volumes greater than 1000 L shall be shown in m^3			
		MASS		
oz	ounces	28.35	grams	g
lb	pounds	0.454	kilograms	kg
T	short tons (2000 lb)	0.907	megagrams (or "metric ton")	Mg (or "t")
		TEMPERATURE (exact degrees)		
°F	Fahrenheit	5 (F-32)/9 or (F-32)/1.8	Celsius	°C
		ILLUMINATION		
fc	foot-candles	10.76	lux	lx
fl	foot-Lamberts	3.426	$candela/m^2$	cd/m^2
		FORCE and PRESSURE or STRESS		
lbf	poundforce	4.45	newtons	N
lbf/in^2	poundforce per square inch	6.89	kilopascals	kPa

APPROXIMATE CONVERSIONS FROM SI UNITS

Symbol	When You Know	Multiply By	To Find	Symbol
		LENGTH		
mm	millimeters	0.039	inches	in
m	meters	3.28	feet	ft
m	meters	1.09	yards	yd
km	kilometers	0.621	miles	mi
		AREA		
mm^2	square millimeters	0.0016	square inches	in^2
m^2	square meters	10.764	square feet	ft^2
m^2	square meters	1.195	square yards	yd^2
ha	hectares	2.47	acres	ac
km^2	square kilometers	0.386	square miles	mi^2
		VOLUME		
mL	milliliters	0.034	fluid ounces	fl oz
L	liters	0.264	gallons	gal
m^3	cubic meters	35.314	cubic feet	ft^3
m^3	cubic meters	1.307	cubic yards	yd^3
		MASS		
g	grams	0.035	ounces	oz
kg	kilograms	2.202	pounds	lb
Mg (or "t")	megagrams (or "metric ton")	1.103	short tons (2000 lb)	T
		TEMPERATURE (exact degrees)		
°C	Celsius	1.8C+32	Fahrenheit	°F
		ILLUMINATION		
lx	lux	0.0929	foot-candles	fc
cd/m^2	$candela/m^2$	0.2919	foot-Lamberts	fl
		FORCE and PRESSURE or STRESS		
N	newtons	0.225	poundforce	lbf
kPa	kilopascals	0.145	poundforce per square inch	lbf/in^2

*SI is the symbol for the International System of Units. Appropriate rounding should be made to comply with Section 4 of ASTM E380.
(Revised March 2003)

Technical Report Documentation Page

1. Report No.	2. Government Accession No.	3. Recipient's Catalog No.

4. Title and Subtitle	5. Report Date
Improved Resilience of Rigid Pavement Systems	October, 13, 2020
	6. Performing Organization Code
7. Author(s)	8. Performing Organization Report No.
Hyung S. Lee and Shreenath Rao.	Contract No. BEB14
9. Performing Organization Name and Address	10. Work Unit No. (TRAIS)
Applied Research Associates, Inc. 100 Trade Centre Dr., Suite 200 Champaign, IL 61820	11. Contract or Grant No. BEB14
12. Sponsoring Agency Name and Address	13. Type of Report and Period Covered
Florida Department of Transportation State Materials Office 5007 N.E. 39th Avenue Gainesville, FL 32609	Draft Final Report April 2021 to September 2023
	14. Sponsoring Agency Code

15. Supplementary Notes

16. Abstract

The primary objective of this study was to evaluate the impact that inundation may have on concrete pavements and to identify cost-effective and implementable solutions to improve the resilience of new and existing rigid pavement systems subjected to the combined effects of flooding and sea level rise. To meet these objectives, a mechanistic-empirical methodology for assessing the resiliency of Florida's rigid pavements was developed. The new rigid pavement resiliency tool was implemented in a macro-enabled Excel spreadsheet environment. In addition, a preliminary vulnerability study indicated that FDOT's existing rigid pavement sections are not free from the threats of flooding and sea level rise. Several examples have been provided in the report to demonstrate the use of the newly developed resiliency tool for the purpose of rigid pavement resiliency under various moisture conditions. However, it is emphasized that the tool was implemented based on numerous existing models that were found in literature, without any further calibration or validation. As such, it is strongly recommended that FDOT examine the results from the resiliency tool against any available field data.

17. Key Word	18. Distribution Statement
Rigid Pavement, Resilience, Resiliency, Flooding, Sea Level Rise (SLR), Inundation, Concrete, Climate Change	No restrictions

19. Security Classif. (of this report)	20. Security Classif. (of this page)	21. No. of Pages	22. Price
Unclassified	Unclassified	159	

Form DOT F 1700.7 (8-72) Reproduction of completed page authorized

EXECUTIVE SUMMARY

The primary objective of this study was to evaluate the impact that inundation may have on concrete pavements and to identify cost-effective and implementable solutions to improve the resilience of new and existing rigid pavement systems subjected to the combined effects of flooding and sea level rise. To meet these objectives, a Mechanistic-Empirical methodology for assessing the resiliency of Florida's rigid pavements was developed. Based on the thorough review of available literature, three main components were identified and implemented into the mechanistic-empirical "Rigid Pavement Resiliency Tool" developed as part of this project.

FDOT's new Rigid Pavement Resiliency Tool was implemented in a macro-enabled Excel spreadsheet environment. The primary purpose of the tool is to allow the user to analyze the structural response and performance of rigid pavement systems under various moisture-related scenarios.

In addition to the resiliency tool development, a preliminary effort was carried out to assess the vulnerability of FDOT's existing rigid pavement sections under flooding and sea level rise (SLR). Based on the results of the preliminary analysis, it was found that FDOT's existing rigid pavements may be vulnerable to flooding and SLR.

Several examples have been provided in the report to demonstrate the use of the newly developed resiliency tool. Since FDOT's rigid pavement design tables were not developed to incorporate the effect of SLR, a series of sensitivity analyses were conducted to develop preliminary design strategies using FDOT's Rigid Pavement Resiliency Tool. The results from the sensitivity analyses were used to develop preliminary damage ratios that can be used to adjust the PCC or the base thickness for different levels of ground water table depth. A couple of example problems were provided in which a rigid pavement design could be modified based on the damage ratios provided in this report.

However, it is emphasized that the tool was implemented based on numerous, existing models that were found in literature. These models include those for the moisture flow, hydraulic conductivity, resilient modulus of the soil, structural response, transfer functions, etc. These models were implemented based on the available information documented in literature, without any further calibration or validation. As such, it is emphasized that the examples on the damage ratios developed herein should only be used as a general guide on how the tool may be used in the future with additional research to support the validity of the resiliency tool. Furthermore, it is strongly recommended that FDOT examine the results from the resiliency tool against any available field data.

TABLE OF CONTENTS

LIST OF FIGURES

LIST OF TABLES

1. INTRODUCTION

In recent years, several studies have recognized the impact of climate change on highway pavements (Kopp et al. 2014; FHWA 2014). Climate change can cause higher temperature, flooding, and sea level rise, as well as devastating hurricanes. Over the past few decades, flooding and hurricanes have significantly impacted transportation infrastructure, including pavements, foundations, and bridges, resulting in closure of roadways, delay in traffic, and economic loss in the U.S. and worldwide. The National Oceanic and Atmospheric Administration (NOAA) reported a $306.2 billion loss in the U.S. for the year 2017 due to intensive hurricanes (NOAA, 2020a). In addition, the increase in sea level induced by both climate-related and non-climate-related changes has the potential to degrade highway pavements through inundation of foundation layers (i.e., unbound materials).

State highway agencies (SHA) are already spending millions of dollars per year constructing and maintaining safe, smooth, and durable pavements. Highway pavement deterioration due to severe weather events, including flooding and rising sea level are very costly, and may require a significant increase in SHAs' budgets to recover the infrastructure damaged due to severe weather, as illustrated in the following examples.

- Within the last decade, states in the Midwest, including Missouri, Illinois, and Arkansas, were impacted by flooding and experienced a period of heavy rainfall up to 15 inches, which caused severe damage to infrastructure. These severe weather conditions incurred an estimated cost of $1.8 billion (Smith et al., 2020).

- Flooding of Missouri River in 2011 impacted several cities in Missouri and Iowa and caused traffic closures on several interstate highways. The average modulus of inundated pavement foundation was about 1.3 to 3.6 times lower than the non-inundated pavements (Vennapusa et al., 2013, 2016). The damage caused by Missouri River flooding on primary and secondary highways was about $63.5 million (Vennapusa et al., 2013).

- Gaspard et al. (2007) evaluated the inundated pavements in Louisiana due to Hurricane Katrina and found a strength reduction in the foundation layers of both concrete and asphalt pavements. The study showed that the strength and resilient modulus of inundated asphalt pavement foundations were more significantly impacted than those of rigid pavements. The estimated rehabilitation cost for 200 miles of inundated roadways was $50 million.

Excessive moisture in pavement foundation layers can significantly reduce the load-bearing capacity, stiffness, and the longevity of pavement foundation (Rada and Witczak, 1981; Cary and Zapata, 2011; and Ceylan et. al., 2013). SHAs recognized the complexity of evaluating inundated pavement behavior during a flood and after flood water receded from the pavement surface. Therefore, the time to reopen an inundated pavement after flooding has frequently been determined based on past experience along with visual inspection of pavement (Vennapusa et al., 2013; Elshaer, 2017). In addition, SHAs are faced with the challenge of precisely evaluating the structural capacity of the inundated pavement and selecting remedial measures to extend the

pavement service life. Such challenges, combined with the lack of assessment or evaluation of the inundated pavement foundation (i.e., base/subbase and subgrade) and continuing climate change, may increase the rate of foundation degradation and cause extensive rehabilitation.

1.1. BACKGROUND

Inundated highways due to storms, hurricanes, and sea level rise have caused dramatic losses in Florida's economy. Historically, Florida has experienced a number of hurricanes and storms due to its geographical location and ongoing climate change. Hurricane Opal was one of the most devastating natural disasters that impacted Florida (Leadon et al., 1998). This hurricane hit the Panhandle Coast of Florida in 1995. Many structures and roads located in different counties were significantly damaged and inundated. About a mile-long stretch of U.S. Highway 98 was damaged near Eglin Air Force Base and other highways were inundated.

The most unprecedented number of hurricanes in Florida was observed in 2004, which caused significant damage to transportation infrastructure as well as to other properties. These hurricanes were Charley, Frances, Ivan, and Jeanne. The estimated damage due to these hurricanes was $41 billion (FDOT, 2005). Pavement sections were damaged resulting in closure of roadways. In 2005, Hurricane Dennis caused severe damage to a section of State Route 30 (US-98) in Florida from strong storms. This storm damaged a 14.6-mile stretch of highway in Franklin County, Florida.

In 2012, Storm Debby caused significant flooding and heavy rainfall for 36 to 48 hours across north Florida. As an example, Figure 1 shows a photo of a pavement completely submerged under water due to this storm (NOAA, 2020b). The estimated rainfall was over 10 inches with a peak of 28.78 inches in 24 hours. Significant flooding struck many highways including a section of US 90, leading to closure of this section for a period of two weeks. The estimated cost of flood damage across Florida was over $40 million and the total storm damage was estimated at $250 million.

Figure 1. Flooding at Suncoast Parkway in Hernando County, FL (courtesy: *Tampa Bay Times*/Will Vragovic).

More recently, hurricane Michael struck the south of Panama City in Florida, which caused catastrophic damage and large inundated areas from Tyndall Air Force base down through Mexico Beach (Cleary et al., 2018). The pavements were damaged due to raised water levels and high levels of storm surge, and a number of highways had to remain closed.

In addition to the devastating storms and hurricanes, sea level continues to rise in Florida with a large uncertainty in projections (Berry et al., 2012). Based on different predictions, the researchers expected that sea level will continue to rise up to six to twelve inches by 2030. The major cause of sea level rise in Florida is contributed by the impact of global warming (Bloetscher et al., 2014). Infrastructure closer to the shoreline in Florida are more prone to the impact of sea level rise and has higher potential for storm surge damage, surface water flooding, and damaged coastal infrastructure (Knott et al., 2017).

1.2. STUDY OBJECTIVES

Moisture within the foundation of Florida's pavements may lead to detrimental impacts. The consequence may range from total washout of the pavement (under very severe storms and hurricanes) to short-term and long-term inundation that may lead to serviceability loss of the pavement structure. The short-term effect may result from opening the roadway to traffic as soon as the flooded water is receded from the pavement surface while the long-term effect may be caused by excessive moisture within the base, subbase, subgrade, and embankment that requires a long period of time to drain out.

The primary objective of this study is to evaluate the impact that inundation may have on concrete pavements and to identify cost-effective and implementable solutions to improve the resilience of new and existing rigid pavement systems subjected to the combined effects of flooding and sea level rise. It should be noted that the scope of this study is limited to structural effect of short-term and long-term inundation on Florida's rigid pavements, i.e., total washout of the pavement structure is beyond the scope of this study.

2. LITERATURE REVIEW

In this chapter, a summary of the literature gathered and reviewed for resiliency of rigid pavement systems is provided. The review included an overview of pavement resiliency, existing agency practice, recent developments, and components of mechanistic-empirical models for the resiliency tool that is to be developed in this project.

2.1. DEFINITION OF RESILIENCY

A generic definition of resilience or resiliency provided by United Nations (UN) is given as the following (UN, 2016).

"The ability of a system, community or society exposed to hazards to resist, absorb, accommodate, adapt to, transform and recover from the effects of a hazard in a timely and efficient manner, including through the preservation and restoration of its essential basic structures and functions through risk management."

The above definition is applicable to a broad range of systems, communities, and societies exposed to a wide range of hazards (e.g., a nation's resilience to COVID-19). For pavements and roadway infrastructure systems, a more focused or narrower definition of resilience is provided by the Federal Highway Administration as the following (FHWA, 2014).

"The ability to anticipate, prepare for, and adapt to changing conditions and withstand, respond to, and recover rapidly from disruptions."

The above definition implies that resiliency is not represented by a single action nor a single outcome (e.g., a post-disaster activity or action for recovering). Instead, the above definition emphasizes that resiliency includes the activities and focuses on the ability of an infrastructure system to serve its purpose before, during, and after the event. Therefore, resiliency is a "cradle-to-grave" engineering philosophy that is represented by a combination of actions for designing, constructing, and operating a transportation infrastructure system that is fault-tolerant, safe, secure, smart, efficient, survivable, and sustainable (Barami, 2013).

2.2. PERFORMANCE CRITERIA AND COMPONENTS INFRASTRUCTURE RESILIENCY

Barami (2013) indicated that there are three performance criteria for infrastructure resiliency. These criteria are listed as the following.

- **Efficiency**: The infrastructure is capable of meeting its specific functions (technical efficacy) at the lowest cost (cost-effectiveness).
- **Sustainability**: The infrastructure uses the natural, human, and manufactured resources in a sustainable manner not only to meet the current needs but also to protect resources for the future.

- **Survivability**: The infrastructure is capable of withstanding damage with minimal adverse impact for the safety, security, and survival of the people as well as the infrastructure assets and the ecosystem.

Bowers and Gu (2021) noted that the above performance criteria align with the triple bottom line of infrastructure sustainability which includes economy, environment, and social. As such, although the existing practices pertaining to resiliency and sustainability are similar and overlap to a certain degree, resiliency and sustainability are two distinct concepts with sustainability being a key criterion for resiliency, as pointed out by Barami (2013) and Bowers and Gu (2021).

2.3. RESILIENCY FRAMEWORK

According to FHWA, there are five major steps in the pavement resiliency framework, as shown Figure 2 (Dylla and Hyman, 2018). These five major steps are:

1. Set Objectives and Define Scope
2. Compile Data
3. Assess Vulnerability
4. Analyze Adaptation Options
5. Incorporate Results into Decision Making

Additional details on the above steps are provided in the following.

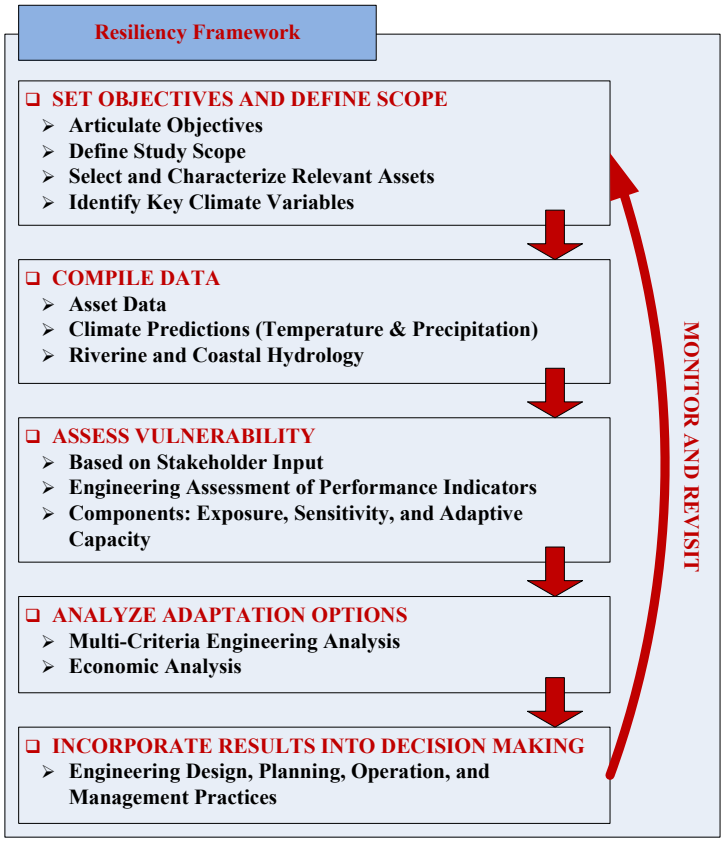

Figure 2. Resiliency framework (after Dylla and Hyman, 2018)

2.3.1. Set Objectives and Define Scope

In this step, the assets to be analyzed for resiliency need to be defined. The value of these identified assets and the climate variables (or climate impacts) affecting their condition and value should also be identified. The three major climate impacts for pavements are summarized as the following (Muench and Van Dam, 2015).

1. Temperature Impacts
    a. General (slow) increase in temperature
    b. Higher extreme temperatures
    c. Fewer freezing days
2. Precipitation Impacts
    a. Changes in average annual precipitation
    b. Wetter winters and drier summers
    c. Increased precipitation intensity
    d. More frequent and severe hurricanes
3. Sea Level Impacts
    a. Sea-level rise

It is also beneficial to define the metrics for quantifying the vulnerability of the identified assets under climate change and extreme weather events as well as the metrics for resiliency performance criteria discussed previously. Although not exhaustive, some examples of these metrics are provided below.

1. Metrics for technical efficacy may include structural capacity, remaining life, or other measures of pavement strength or service life. Metrics for cost-effectiveness may include life-cycle cost or other cost measures for building and maintaining the infrastructure system.

2. Metrics for sustainability may include emitted greenhouse gas (GHG) or other measures quantifying the extent or amount of inputs and resources used and their social, economic, and environmental impacts.

3. Metrics for survivability may include the speed at which a pavement structure recovers after a weather-related hazard. Other metrics may include the performance deviation due to an extreme weather event or comparisons of pre-disaster and post-disaster performances of a pavement system.

Flannery et. al. (2018) noted that although the above metrics may also be used to provide an overall measure or quantification of resilience, the majority of SHAs currently have not defined their resiliency metrics. Furthermore, they noted that there is no standard or universally adopted metric within the highway community. Establishment of a universal measure of resiliency still remains theoretical and discipline-specific, and may or may not be more meaningful than the practical, pavement-related indices or qualitative metrics (Pavement Interactive, 2021; Tamvakis and Xenidis, 2013). As such, the SHAs may need to define their resiliency metrics depending on the agency's preference and focus areas and/or adopt other measures that are already being used (e.g., life-cycle cost, pavement performance indices, etc.).

2.3.2. Compile Data

After the pavement assets and the climate variables have been identified, it is necessary to gather the relevant data for assessing vulnerability.

The pavement data should include information regarding the pavement structure itself (e.g., thickness) as well as the monitored performance data of the pavement and their trends. As noted by Muench and Van Dam (2015) and Dylla and Hyman (2018), climate impacts such as temperature increase or sea-level rise (with a possible exception of hurricanes) are projected to occur relatively slowly when considering the typical design lives of pavements. As such, Muench and Van Dam (2015) pointed out that the trend in key pavement performance parameters should be monitored, and the changes in these trends (e.g., in the rate and/or type of distress development) may be attributed to climatic changes over time. The key performance parameters or indicators identified for rigid pavements are shown in the following.

1. Blow-ups for Jointed Plain Concrete Pavements (JPCP)
2. Slab cracking
3. Punch-outs for Continuously Reinforced Concrete Pavements (CRCP)
4. Joint Spalling
5. Freeze-thaw durability
6. Faulting, pumping, and corner breaks
7. Slab warping

The climate data should include not only the information pertaining to current weather and climate, but also the predicted, long-term changes in climate that is narrowed down to the project level. If the climate change is anticipated to be minimal during the life-cycle of the pavement (i.e., climate is predicted to change very slowly compared to the pavement life, or if the pavement rehabilitation cycles are planned to occur relatively quickly), it may not be necessary to account for the climate change in the analysis of that particular pavement (i.e., the SHA may use the historical climate data for the analysis or watch out for any changes in the key performance indicators discussed above). On the other hand, if the climate change is predicted to impact the pavement during its service life (i.e., predicted to occur relatively quickly), then it may be necessary to compare the current and predicted climate conditions to develop the appropriate adaptation options for the changing climate (Dylla and Hyman, 2018).

2.3.3. Assess Vulnerability

In this context, vulnerability is defined as the assessment of exposure, sensitivity, and adaptive capacity (Pavement Interactive, 2021). These components are briefly summarized below.

1. **Exposure**: The pavements that are exposed to climate change or extreme weather events need to be identified.
2. **Sensitivity**: This involves assessing the impact of climate change or extreme weather events on pavements.
3. **Adaptive Capacity**: This involves the assessment of the pavement's ability to withstand and/or recover from the effect of climate change or extreme weather events.

2.3.4. Analyze Adaptation Options

According to FHWA, adaptation is defined as the following.

"Adjustment in natural or human systems in anticipation of or response to a changing environment in a way that effectively uses beneficial opportunities or reduces negative effects"

Note that the above definition aligns with the resiliency performance criteria of efficiency (response to a changing environment), sustainability (effectively use beneficial opportunities), and survivability (reduce negative effects). As such, for a given pavement that is determined to be vulnerable to climate change or extreme weather events, a wide variety of adaptation options (including the most expensive options all the way down to the option of no cost, no action) need to be considered and the one that maximizes the benefit in terms of the performance criteria should be selected (Pavement Interactive, 2021).

Although a thorough research documenting all available adaptation options for rigid pavements was not found, the following options were identified from multiple sources (Mack, 2020; Dylla and Hyman, 2018; Pavement Interactive, 2021).

1. Elevating the road above flooding elevation: This is likely the most expensive option.
2. Hardening of the pavement system: Using stiffer and/or better-quality materials.
3. Reduce joint spacing: For reducing blow-ups caused by increasing temperature.
4. Stabilized base and subbase layers: For areas where the ground water table may rise or higher precipitation is expected.
5. Road abandonment: If detours are available. i.e., this option is not always possible. This option does not increase the adaptive capacity of the pavement.

The functionality of a resilient pavement (i.e., those that were treated to increase the adaptive capacity) can be explained based on its short-term effects during flood and/or hurricane events as well as long-term performance as shown in Figure 3. As shown in the figure, mitigation efforts (i.e., increasing the adaptive capacity) can be utilized prior to a flooding or hurricane event to reduce the risk of performance loss by alleviating the impact of flood at the initial stage (Hemmati et. al., 2020). This strategy can result in a significantly faster rate of recovery for the inundated pavement, but requires a substantial investment and planning to mitigate the impact of future flooding events. On the other hand, a pavement that has not received any mitigation efforts before the event may cost more to repair and take longer to recover. As such, in order to determine the most adequate level of mitigation (in terms of cost and pavement performance), it is crucial that the SHAs are equipped with a means for assessing the rate of pavement recovery which depends on the existing conditions of the pavement as well as its design criteria, percentage of cracks, and level of maintenance (Lounis and McAllister, 2016).

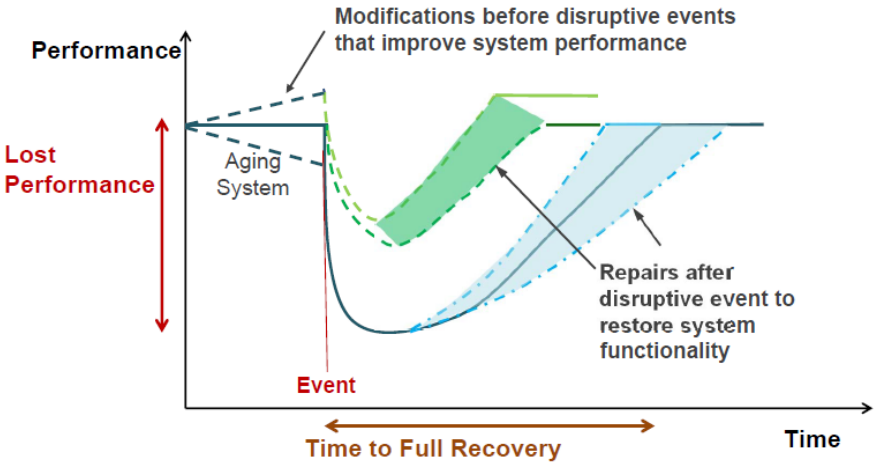

Figure 3. Effects of performance and recovery time on pavement resilience (Dean, 2020)

2.3.5. Incorporate Results into Decision Making

The final step is to implement the adaptation options in the pavement design, planning, operation, and management practices as determined applicable. The condition as well as the performance of these pavements should continue to be monitored, and the effectiveness of the adaption option should be evaluated.

2.3.6. Remarks on Pavement Resiliency

As seen from the above, resiliency is a broad philosophy that is focused not only on the post-disaster activities but also on pre-disaster and during disaster activities that many different branches of an SHA (e.g., planning, design, construction, and maintenance) need to work together. Nevertheless, the concept of resiliency is still fairly new to the transportation sector and is continuing to evolve. As such, a detailed, easy-to-use guidance on implementing resiliency and quantitative assessment of resiliency (i.e., resiliency metrics) for the transportation community is yet to be developed (Flannery et. al., 2018).

It is also to be noted that the general scope of resiliency is not limited to disruptions related to natural hazards such as extreme weather events and climate change. In other words, other societal stressors such as conflict, human rights, welfare, and wellbeing are also important aspects of transportation infrastructure resiliency. However, these are beyond the scope of this study which is focused on the structural resiliency of inundated rigid pavements in Florida.

2.4. REVIEW OF FDOT'S EXISTING PRACTICE

2.4.1. FDOT's Resiliency Initiatives

Along with the FHWA's initiatives and nationwide focus on resiliency discussed above, FDOT has incorporated resiliency into all phases of transportation planning within the last decade (Carver and Spirio, 2019). FDOT's resiliency initiatives are briefly reviewed in the following.

2.4.1.1. FDOT's Definition of Resiliency

Similar to FHWA's definition of resiliency reviewed previously, several SHAs including FDOT have developed their definitions of resiliency. FDOT's definition of resiliency is given as the following (FDOT, 2020a).

"The ability of the transportation system to adapt to changing conditions and prepare for, withstand, and recover from disruption."

Similarly, Table 1 summarizes the definitions of resiliency from other State DOTs obtained from a recent survey conducted under a National Cooperative Highway Research Program (NCHRP) study (Flannery et. al., 2018). It is noted that while FHWA and FDOT definitions of resiliency focus on all periods (i.e., before, during, and after the event as indicated by the terms such as "adapt" and "prepare"), many other State DOT resiliency definitions fall short and focus on the post-event period, as pointed out by Flannery et. al. (2018).

Table 1. State DOT Definitions of Resiliency (Flannery et al. 2018).

State Agency	Definition of Resilience
Minnesota DOT	Reducing vulnerability and ensuring redundancy and reliability to meet essential travel needs.
Oregon DOT	Uses a definition from the Oregon DOT (ODOT) seismic report: "To achieve rapid recovery, require government continuity, resilient physical infrastructure, and business continuity."
Arizona DOT	ADOT developed the Resilience Program to support its mission to provide a safe, efficient, cost-effective transportation system that can be compromised from the effects of heat extremes, dust storms, wildfires, flooding, landslides, rockfall incidents, and slope failures, and cope with the ever-growing cost of these threats.
Delaware DOT	Uses the concept in the Delaware Executive Order 41, which outlines resiliency practices to help mitigate climate impacts and reduce emissions.
Colorado DOT	Uses a definition provided by the Governor's Resiliency Framework: "The ability of communities to rebound, positively adapt to or thrive amidst changing conditions or challenges – including disasters and climate change – and maintain quality of life, healthy growth, durable systems, and conservation of resources for present and future generations."
New York State DOT	Uses the recommended guidance provided by the NYS 2100 Commission, which outlines how the state plans to identify areas where further resilience practices are needed.
New Hampshire DOT	Uses the NAS definition by default, which states "resilience is the ability to plan, absorb, recover and adapt."
Illinois DOT	Plan and invest in the state's transportation system to ensure that infrastructure is prepared for extreme weather events.

2.4.1.2. Florida Transportation Plan (FTP)

The Florida Transportation Plan (FTP) was first published in 2015 and was recently updated in 2020 (FDOT, 2020a). The recent FTP was published in 4 distinct elements: Vision, Policy, Performance, and Implementation. The Vision Element established seven long-range goals for FDOT one of which is to achieve "Agile, Resilient, and Quality Infrastructure" in Florida by 2045.

The Policy Element defines a total of fifteen objectives in support of the seven long-range goals, four of which are tailored to infrastructure. These objectives are:

1. Maintain Florida's transportation assets in a state of good repair for all modes.
2. Increase the resiliency of infrastructure.
3. Meet customer expectations for infrastructure quality and service.
4. Improve transportation system connectivity.

Furthermore, the Policy Element stipulates a total of twelve progress indicators for measuring progress toward the above objectives. Among them, the following four indicators are related to infrastructure (or pavements, to be more specific) resiliency.

1. Pavement condition.
2. Vulnerability to flooding or storm surge.
3. Hours or days of transportation facility closure due to smoke, fire, flooding, wind, or extreme temperature.
4. Frequency of repairs due to damage from extreme weather or other events.

The Performance Element reports how Florida's assets are performing in terms of a few key measures that could be assessed currently. For example, the Performance Element indicated that Florida's pavement and bridge conditions have met or exceeded the targets established for 2019 (measured using the 2017 data as baseline). However, the Element also notes that various climatic threats (such as hurricanes, storm surge, and sea level rise) may have a significant impact on performance (or condition) of Florida's pavements and bridges. While the progress metrics were not provided for all of the above-mentioned indicators, FDOT has assessed the risk or vulnerability of Florida's Strategic Intermodal Systems (SIS) in a separate study. This study is described subsequently.

The Implementation Element, which was developed as a web-based application defines the short-term and midterm actions to be carried out by FDOT and other local transportation authorities. While the details are still being developed and updated on a continuous basis, the four major action items pertaining to infrastructure are listed as the following:

1. Continue to enhance asset management practices at the state and local levels.
2. Develop policies and standards for next-generation transportation corridors.
3. Strengthen research, development, and deployment of new technologies and practices.
4. Retrofit, adapt, or provide more diversity in the location of critical infrastructure to reduce vulnerability to extreme weather and other environmental conditions.

2.4.1.3. Risk Assessment of SIS Facilities

As a first step towards achieving the goal of "Agile, Resilient, and Quality Infrastructure", FDOT conducted a study to assess the vulnerability and risk of various Strategic Intermodal Systems (SIS) within the state (FDOT, 2018).

The vulnerability was assessed using three components mentioned previously (see Section 2.3.3): Exposure, Sensitivity, and Adaptive Capacity. Exposure of SIS facilities to climate hazard was determined based on GIS analysis of various datasets (see Figure 4 as an example). Sensitivity was assessed by the condition of the asset (e.g., pavement condition) and Adaptive Capacity was assessed by Daily Vehicle Miles Travelled (DVMT).

The overall vulnerability or risk was assessed for SIS highways, bridges, and military access facilities under different climate-related issues including storm surge (Categories 1, 3, and 5), projected flooding (100-year), and sea level rise (1 ft. and 2 ft.). The centerline miles and DVMT of SIS highways that were determined to be vulnerable to these natural hazards are summarized in Table 2.

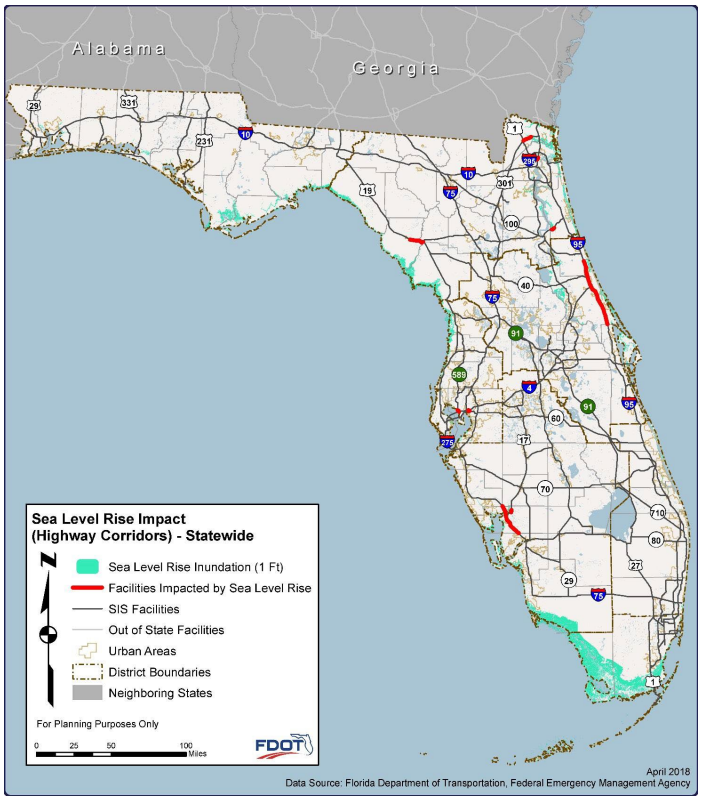

Figure 4. SIS highway facilities impacted by 1-foot sea level rise projections (FDOT, 2018).

Table 2. SIS highway corridor impacted by different hazards (FDOT, 2018).

Hazard Type	Hazard Category / Level	Centerline Miles at Risk (% of Statewide)*	Potentially Impacted DVMT, ×1000 (% of Statewide)*
Storm Surge	Category 1	160 (3%)	10,659 (5%)
	Category 2	621 (13%)	28,833 (13%)
	Category 3	983 (21%)	48,751 (23%)
Exposure to Flooding	Low (≤ 3 ft.)	215 (4.5%)	14,092 (6.6%)
	Medium (3 ft. to 10 ft.)	268 (5.6%)	10,999 (5.1%)
	High (> 10 ft.)	62 (1.3%)	2,196 (1.0%)
Sea Level Rise (SLR)	1 ft. SLR	39 (0.8%)	1,939 (0.9%)
	2 ft. SLR	248 (5.2%)	24,018 (11.0%)

Note*: The centerline miles and DVMT are not cumulative (e.g., centerline miles under high flooding risk do not include those of medium risk).

2.4.1.4. The 2020 update of Freight Mobility and Trade Plan (FMTP)

In alignment of FDOT's effort on resiliency, the Freight Mobility and Trade Plan (FMTP) was updated in 2020 to reflect the long-range goals set forth by FTP (FDOT, 2020c). While the focus of FMTP is on resilient freight mobility & infrastructure and its scope is relatively broad (roads, bridges, seaports, airports, etc.), it also provides a framework for scenario-based planning for resilience.

More specifically, the FMTP outlined possible consequences for the following scenario – Florida experiences over 4.0°F of temperature increase, 1.0 ft. sea level rise, increased frequencies of stronger hurricanes and extreme rainfall (greater than 4 in.) events by the year 2045. It was indicated that this scenario may result in significant FDOT investments in pervious pavements, ultra-high strength concrete, roadway elevation projects, bio swales, pumping/lift stations, and other washout prevention strategies.

2.4.1.5. Sea-Level Scenario Sketch Planning Tool

In collaboration with University of Florida (UF) GeoPlan Center, FDOT developed the Sea-Level Scenario (SLS) Sketch Planning Tool (https://sls.geoplan.ufl.edu/view-maps/). The purpose of this online tool was to assist in the identification of transportation infrastructure exposed to current and future risks of flooding. The tool allows for visualization of floodplains (100-yr and 500-yr) and various scenarios for future sea level rise (e.g., 1.0 ft. and 2.0 ft) based on the data made available by the U.S. Army Corps of Engineers (USACE) and the National Oceanic and Atmospheric Administration (NOAA). The tool also implemented the Digital Elevation Model (DEM) of the entire State of Florida as well as a number of GIS layers for transportation assets including FDOT's Road Characteristic Inventory (RCI) data.

It is also noted that the SLS Sketch Planning Tool was a major source of data for the risk assessment of SIS facilities discussed previously: the DEM and the sea level projections from USACE data were used for assessing the exposure of SIS facilities to flooding.

2.4.1.6. Closing Remarks on FDOT's Resiliency Efforts

As mentioned previously, FDOT has incorporated resiliency into all phases of transportation planning. Based on FDOT's resiliency efforts reviewed above, the authors are of the opinion that FDOT's efforts are in alignment with FHWA's 5 steps for resiliency framework (shown in Section 2.3). More specifically, FDOT has defined goals and objectives for their resiliency initiative (Step 1), compiled or identified source of necessary data (Step 2), and assessed vulnerability for at least the most critical transportation assets namely the SIS facilities (Step 3).

While Implementation Element of FDOT's FTP outlined the action items for resilient infrastructure within the State, detailed adaptation options that need to be implemented during design, construction, maintenance, and operation of different transportation assets are still being developed.

It is also to be noted that the objective of this study is closely related to FDOT's continued efforts on implementing resiliency, but with a scope that is limited to structural resiliency of rigid pavements under inundated conditions.

2.5. FDOT'S RIGID PAVEMENT DESIGN PRACTICE

As noted earlier, FDOT has incorporated resiliency into all phases of transportation planning and completed the vulnerability assessment of the State's most critical infrastructure (i.e., SIS facilities). While the Implementation Element of the FTP outlines the generic action items for infrastructure resiliency, detailed strategies pertaining to design, construction, maintenance, and operation for resilient infrastructure are yet to be developed (FDOT, 2020a). A detailed review of FDOT's existing practice on all of the aforementioned activities is beyond the scope of this study. However, since the scope of this study is limited to structural resiliency of Florida's rigid pavements, a brief review of FDOT's rigid pavement design practice and its limitations are discussed in the following.

According to FDOT's current Rigid Pavement Design Manual, there are two rigid pavement design options in which the primary difference is in the foundation layers (FDOT, 2021). These options are the asphalt base option and the special select soil subbase option, as visualized in Figure 5. The asphalt base option is the recommended option because (1) it allows for the use of standard (and readily available) materials and (2) the asphalt base contributes to the structural capacity of the rigid pavement and the design thickness of the Portland Cement Concrete (PCC) layer is generally thinner than the special select soil subbase option. Nonetheless, the minimum thickness of PCC is specified to be 8.0 in., regardless of the design option.

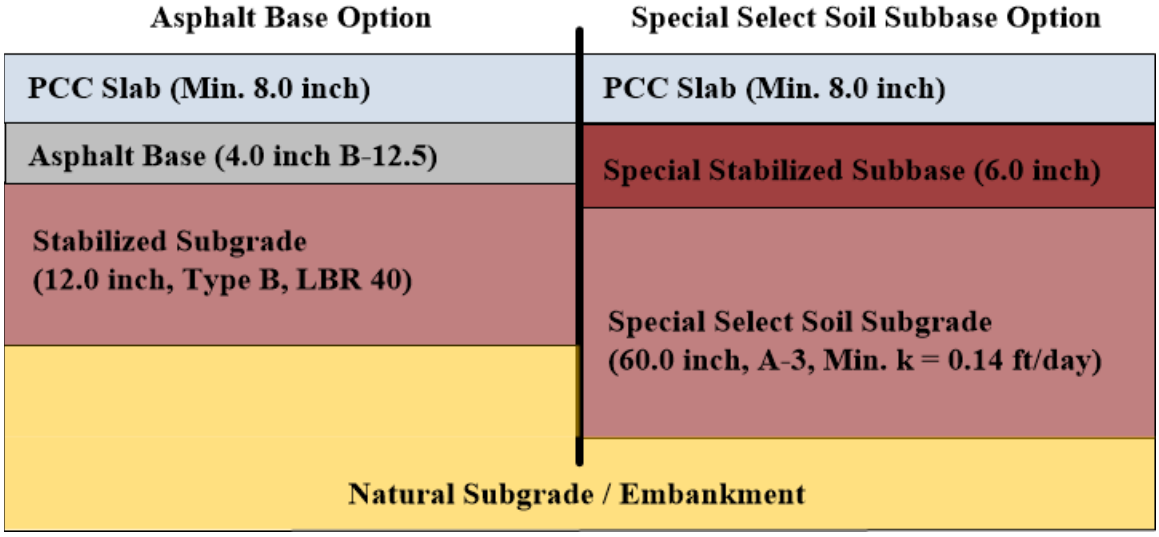

Figure 5. FDOT's rigid pavement design layers.

For each of the design options described above, FDOT's Rigid Pavement Design Manual provides a table of design PCC thicknesses, which was developed using AASHTOWare Pavement ME Design (PMED) software. The design tables allow FDOT's design engineers to determine the required PCC slab thickness quickly based on a few (but important) inputs including traffic (in terms of Equivalent Single Axle Load [ESAL]), climatic region, and design

reliability. In other words, the PCC design thickness can be obtained without running Pavement ME which takes a wide range of inputs pertaining to materials (e.g., PCC modulus, coefficient of thermal expansion, etc.), climate (i.e., historical weather data), traffic (i.e., axle load spectra), and other design features (e.g., dowel bars).

Figure 6 shows different climate regions defined for FDOT's design of rigid pavements. Once the climate region is identified from this figure, the PCC design thickness can be obtained from Table 3 for the asphalt base option and from Table 4 for the special select soil option, respectively.

It should also be noted that although the design tables allow for a quick and efficient means of determining the required PCC thickness, exceptions do exist. For special conditions in which the assumptions behind the design tables are violated (e.g., a reduction in PCC slab width), the design engineers are required to run PMED analysis for determining the required PCC thickness.

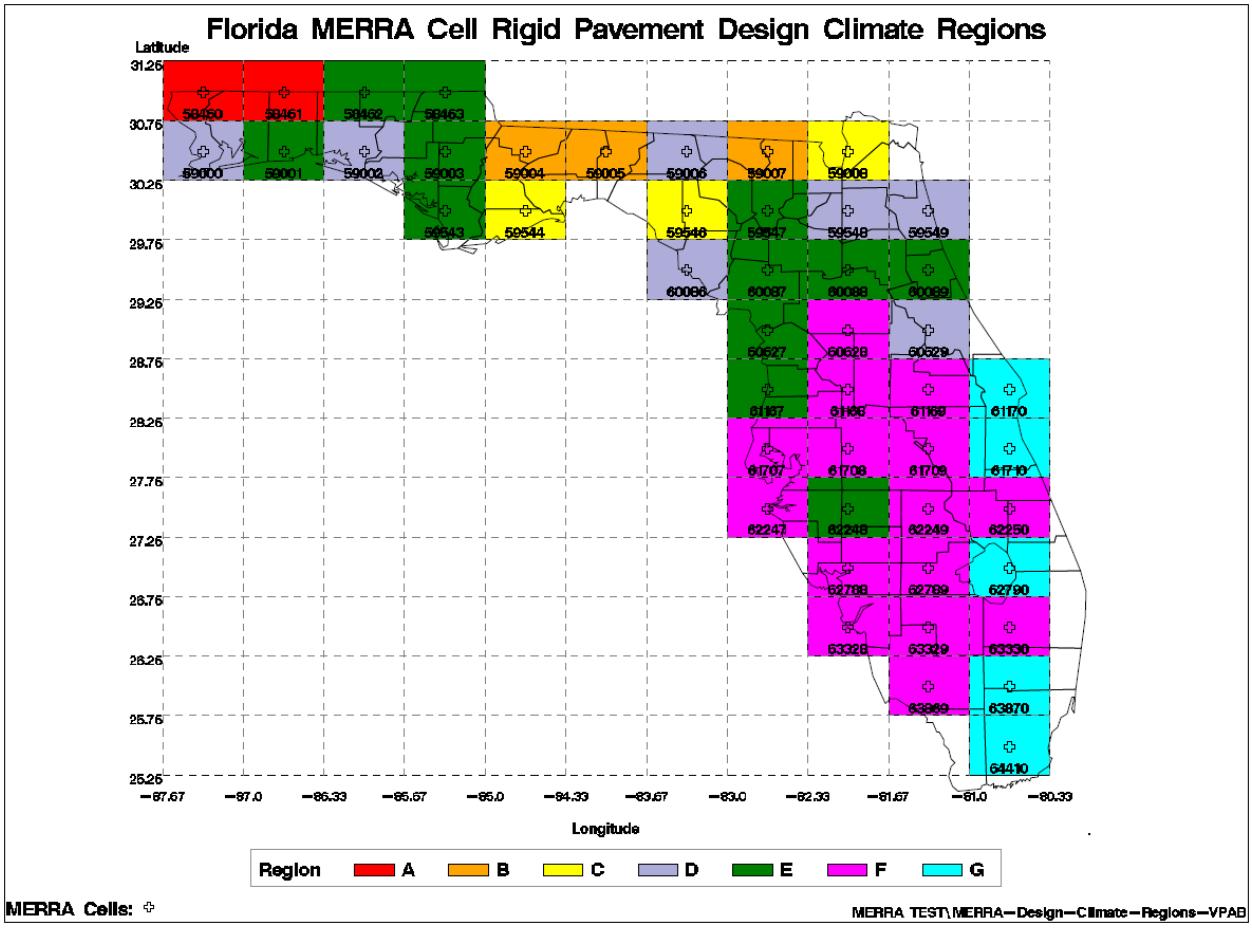

Figure 6. FDOT's climate regions for rigid pavement design (from FDOT, 2021).

Table 3. FDOT's rigid pavement design table for asphalt base option (from FDOT, 2021)

Region		A			B			C			D			E			F			G		
Traffic		Reliability (%)			Reliability (%)			Reliability (%)			Reliability (%)			Reliability (%)			Reliability (%)			Reliability (%)		
ESALs (millions)	AADTT	80	90	95	80	90	95	80	90	95	80	90	95	80	90	95	80	90	95	80	90	95
1	115	8.0	8.5	8.5	8.0	8.0	8.5	8.0	8.0	8.0	8.0	8.0	8.0	8.0	8.0	8.0	8.0	8.0	8.0	8.0	8.0	8.0
2	230	8.5	8.5	8.5	8.0	8.5	8.5	8.5	8.5	8.5	8.0	8.0	8.5	8.0	8.0	8.0	8.0	8.0	8.0	8.0	8.0	8.0
3	345	9.0	9.0	9.0	8.5	9.0	9.0	8.5	8.5	9.0	8.5	8.5	8.5	8.0	8.0	8.5	8.0	8.0	8.0	8.0	8.0	8.0
4	460	9.0	9.0	9.0	9.0	9.0	9.0	9.0	9.0	9.0	8.5	8.5	8.5	8.5	8.5	8.5	8.0	8.0	8.0	8.0	8.0	8.0
5	575	9.0	9.5	9.5	9.0	9.0	9.5	9.0	9.0	9.0	8.5	8.5	9.0	8.5	8.5	8.5	8.0	8.0	8.0	8.0	8.0	8.0
6	690	9.5	9.5	9.5	9.5	9.5	9.5	9.0	9.0	9.5	9.0	9.0	9.0	8.5	8.5	8.5	8.0	8.0	8.5	8.0	8.0	8.0
7	805	9.5	9.5	9.5	9.5	9.5	9.5	9.0	9.5	9.5	9.0	9.0	9.0	8.5	8.5	8.5	8.0	8.5	8.5	8.0	8.0	8.0
8	920	9.5	9.5	10.0	9.5	9.5	9.5	9.5	9.5	9.5	9.0	9.0	9.0	8.5	8.5	9.0	8.5	8.5	8.5	8.0	8.0	8.0
9	1035	9.5	10.0	10.0	9.5	9.5	10.0	9.5	9.5	9.5	9.0	9.0	9.5	8.5	9.0	9.0	8.5	8.5	8.5	8.0	8.0	8.0
10	1150	10.0	10.0	10.5	9.5	10.0	10.0	9.5	9.5	9.5	9.0	9.5	9.5	9.0	9.0	9.0	8.5	8.5	8.5	8.0	8.0	8.5
15	1725	10.5	11.0	11.5	10.5	10.5	11.0	10.0	10.0	10.0	9.5	9.5	9.5	9.0	9.0	9.5	8.5	9.0	9.0	8.5	8.5	8.5
20	2300	11.5	12.0	12.0	11.0	11.5	11.5	10.5	10.5	11.0	9.5	9.5	10.0	9.5	9.5	9.5	9.0	9.0	9.0	8.5	8.5	8.5
25	2875	12.0	12.5	12.5	11.5	12.0	12.0	10.5	11.0	11.5	10.0	10.0	10.0	9.5	9.5	9.5	9.0	9.0	9.0	8.5	9.0	9.0
30	3450	12.5	12.5	12.5	12.0	12.0	12.5	11.0	11.5	11.5	10.0	10.5	10.5	9.5	9.5	9.5	9.0	9.5	9.5	8.5	9.0	9.0
35	4025	12.5	13.0	13.5	12.5	12.5	12.5	11.5	12.0	12.0	10.5	10.5	11.0	9.5	9.5	10.0	9.5	9.5	9.5	9.0	9.0	9.0
40	4600	12.5	13.5	13.5	12.5	12.5	13.0	12.0	12.0	12.5	10.5	11.0	11.5	9.5	10.0	10.0	9.5	9.5	9.5	9.0	9.0	9.0
45	5175	13.0	13.5	14.0	12.5	13.0	13.0	12.0	12.5	12.5	11.0	11.5	11.5	10.0	10.0	10.0	9.5	9.5	10.0	9.0	9.0	9.0
50	5750	13.5	14.0	14.0	13.0	13.0	13.5	12.5	12.5	13.0	11.5	11.5	11.5	10.0	10.0	10.5	9.5	9.5	10.0	9.0	9.0	9.5
60	6900	14.0	14.0	14.5	13.0	13.5	14.0	12.5	13.0	13.0	11.5	12.0	12.5	10.0	10.5	10.5	10.0	10.0	10.5	9.0	9.5	9.5
70	8050	14.0	14.5	15.0	13.5	14.0	14.0	13.0	13.0	13.5	12.0	12.5	12.5	10.5	11.0	11.0	10.5	10.5	10.5	9.5	9.5	9.5
80	9200	14.5	15.0	15.0	14.0	14.0	14.5	13.0	13.5	13.5	12.5	12.5	13.0	11.0	11.0	11.5	10.5	10.5	11.0	9.5	9.5	9.5
90	10350	15.0	15.0	15.5	14.0	14.5	14.5	13.5	13.5	14.0	12.5	13.0	13.0	11.0	11.5	11.5	10.5	11.0	11.5	9.5	9.5	9.5
100	11500	15.0	15.0	15.5	14.5	14.5	15.0	13.5	14.0	14.0	12.5	13.0	13.5	11.5	11.5	12.0	11.0	11.5	11.5	9.5	9.5	9.5

Table 4. FDOT's rigid pavement design table for special select soil option (from FDOT, 2021)

Region		A			B			C			D			E			F			G		
Traffic		Reliability (%)			Reliability (%)			Reliability (%)			Reliability (%)			Reliability (%)			Reliability (%)			Reliability (%)		
ESALs (millions)	AADTT	80	90	95	80	90	95	80	90	95	80	90	95	80	90	95	80	90	95	80	90	95
1	115	9.0	9.0	9.5	9.0	9.0	9.5	9.0	9.0	9.0	8.5	8.5	9.0	8.5	8.5	8.5	8.5	8.5	8.5	8.0	8.0	8.0
2	230	10.0	10.0	10.5	10.0	10.0	10.0	9.5	10.0	10.0	9.5	9.5	9.5	9.0	9.0	9.0	9.0	9.0	9.5	8.5	8.5	8.5
3	345	10.5	10.5	10.5	10.5	10.5	10.5	10.0	10.5	10.5	10.0	10.0	10.0	9.0	9.5	9.5	9.5	9.5	10.0	8.5	8.5	9.0
4	460	11.0	11.0	11.0	10.5	11.0	11.0	10.5	10.5	10.5	10.0	10.0	10.5	9.5	9.5	10.0	10.0	10.0	10.0	9.0	9.0	9.0
5	575	11.0	11.0	11.5	11.0	11.0	11.5	10.5	11.0	11.0	10.5	10.5	10.5	10.0	10.0	10.0	10.0	10.0	10.5	9.0	9.0	9.0
6	690	11.5	11.5	11.5	11.0	11.5	11.5	11.0	11.0	11.5	10.5	10.5	11.0	10.0	10.0	10.5	10.0	10.5	10.5	9.0	9.5	9.5
7	805	11.5	11.5	12.0	11.5	11.5	11.5	11.0	11.5	11.5	10.5	11.0	11.0	10.0	10.5	10.5	10.5	10.5	10.5	9.5	9.5	9.5
8	920	11.5	12.0	12.0	11.5	11.5	12.0	11.5	11.5	11.5	11.0	11.0	11.0	10.5	10.5	10.5	10.5	10.5	11.0	9.5	9.5	10.0
9	1035	12.0	12.0	12.5	11.5	12.0	12.0	11.5	11.5	12.0	11.0	11.0	11.5	10.5	10.5	10.5	10.5	10.5	11.0	9.5	10.0	10.0
10	1150	12.0	12.0	12.5	12.0	12.0	12.0	11.5	11.5	12.0	11.5	11.5	11.5	10.5	10.5	11.0	10.5	11.0	11.0	10.0	10.0	10.0
15	1725	12.5	13.0	13.0	12.5	12.5	12.5	12.0	12.0	12.5	12.0	12.0	12.0	11.0	11.0	11.5	11.0	11.5	11.5	10.0	10.0	10.5
20	2300	13.0	13.5	13.5	12.5	13.0	13.0	12.5	12.0	13.0	12.0	12.0	12.5	11.5	11.5	11.5	11.5	11.5	12.0	10.5	10.5	10.5
25	2875	13.5	13.5	14.0	13.0	13.5	13.5	13.0	13.0	13.0	12.5	12.5	12.5	11.5	12.0	12.0	11.5	12.0	12.0	10.5	11.0	11.0
30	3450	13.5	14.0	14.0	13.5	13.5	13.5	13.0	13.0	13.5	12.5	12.5	13.0	12.0	12.0	12.0	12.0	12.0	12.5	11.0	11.0	11.0
35	4025	14.0	14.0	14.0	13.5	13.5	14.0	13.5	13.5	13.5	13.0	13.0	13.0	12.0	12.0	12.5	12.0	12.5	12.5	11.0	11.0	11.5
40	4600	14.0	14.0	14.5	13.5	14.0	14.0	13.5	13.5	14.0	13.0	13.0	13.5	12.0	12.5	12.5	12.5	12.5	12.5	11.0	11.5	11.5
45	5175	14.0	14.5	14.5	14.0	14.0	14.0	13.5	14.0	14.0	13.5	13.5	13.5	12.5	12.5	12.5	12.5	12.5	12.5	11.5	11.5	11.5
50	5750	14.5	14.5	14.5	14.0	14.0	14.5	13.5	14.0	14.0	13.5	13.5	13.5	12.5	12.5	13.0	12.5	12.5	13.0	11.5	11.5	11.5
60	6900	14.5	15.0	15.0	14.0	14.5	14.5	14.0	14.0	14.5	13.5	13.5	14.0	12.5	13.0	13.0	13.0	13.0	13.0	11.5	12.0	12.0
70	8050	15.0	15.0	15.5	14.5	14.5	15.0	14.0	14.5	14.5	14.0	14.0	14.0	13.0	13.0	13.0	13.0	13.0	13.5	12.0	12.0	12.0
80	9200	15.0	15.5	16.0	14.5	15.0	15.0	14.5	14.5	14.5	14.0	14.0	14.0	13.0	13.0	13.5	13.0	13.5	13.5	12.0	12.0	12.5
90	10350	15.5	15.5	16.0	15.0	15.0	15.5	14.5	14.5	15.0	14.0	14.0	14.5	13.0	13.5	13.5	13.5	13.5	13.5	12.0	12.5	12.5
100	11500	15.5	16.0	16.0	15.0	15.0	15.5	14.5	15.0	15.0	14.5	14.5	14.5	13.5	13.5	13.5	13.5	13.5	13.5	12.0	12.5	12.5

2.5.1. Limitations of FDOT's Rigid Pavement Design Practice

Recently, several studies were conducted to assess the resilience of critical infrastructure failures and to estimate pavement performance before and after flooding in Florida (Bruijn et. al., 2019; Khan et. al., 2017). Results of these studies showed that high resistance to flooding can be achieved through a rigid and strong pavement designed and constructed to a high standard, which may be recommended for areas that are prone to flooding events. Nevertheless, there is still a lack of practical process that can be used by FDOT to assess the functionality of pavement resilience under extreme weather events that can be incorporated into pavement design or evaluation procedures.

Although FDOT's rigid pavement design practice discussed above is working well for Florida's current conditions, it was developed without incorporating the resilience aspect of rigid pavements. In other words, the design practice and the design tables do not consider the effect of short-term severe weather events (e.g., storms) and long-term climate change (e.g., sea level rise). While one may argue that PMED software could provide a means for analyzing the effect of these weather events and climate changes, the software also exhibits limitations which make it unsuitable for this type of analysis. These limitations include the following.

1. While PMED uses the historical climate data for a given location for simulating the performance of a pavement structure, it is not designed to perform a climate analysis over a region. In other words, it does not allow for identifying the locations that are prone to flooding and other weather-related events.

2. PMED is designed to analyze the pavement performance over a long period of time that may span a few decades (i.e., pavement design life). As such, the performance metrics (e.g., damage, cracking, faulting, etc.) are outputted at an interval of a month. In other words, it is not capable of analyzing the short-term flooding effect which may occur within a matter of hours (or days).

3. Similar to the above, the climate module in PMED , namely the Enhanced Integrated Climatic Model (EICM), is implemented to produce the results at every month. Furthermore, while EICM is capable of using a large amount of historical climate data, it is currently not implemented to solve an initial condition problem (e.g., starting from a flooded, fully saturated condition, how much time is required to drain the water out from the pavement system?) nor to predict future climate. Furthermore, infiltration of water from the pavement surface is not simulated in EICM (Brink, 2021).

Due to the above limitations, PMED is considered to be inadequate for analyzing the flood and moisture related resiliency of pavements, especially for the short-term effects, although it may be used for assessing the long-term resiliency of different foundation materials weakened due to the combined effect of temperature and moisture (Brink, 2021).

2.6. RECENT STUDIES ON PAVEMENT RESILIENCY

In light of the above limitations of FDOT's rigid pavement design practice and AASHTOWare PMED, there is a need to develop a Mechanistic-Empirical methodology for assessing the resiliency of Florida's rigid pavements. As such, the relevant literature and available information regarding pavement resiliency tools are reviewed in the following.

2.6.1. Mechanistic and/or Empirical Models for Pavement Resiliency

The literature search did not reveal any studies that have developed mechanistic and/or empirical models/tools for examining the resiliency of inundated rigid pavements. Most of the studies have focused on developing resiliency tools (or methods) for asphalt pavements. These studies are briefly summarized in the following.

- Knott et. al. (2019) developed a hybrid framework for integrating the effect of climate change into asphalt pavement management. The framework uses both bottom-up and top-down approaches; the top-down approach (or scenario-based approach) is used for studying the future pavement life reductions under one or more climate-change scenarios, while the bottom-up approach (or asset-based approach) is used for evaluating the effect of various climate parameters and their combinations on pavement life reduction. In both approaches, the performance of flexible pavements was modeled using MnPAVE which is Minnesota DOT's (MnDOT's) mechanistic-empirical pavement analysis and design software. Similar to the AASHTOWare PMED, MnPAVE uses the layered-elastic theory for simulating the mechanistic response of flexible pavements.

- Mallick et. al. (2014) studied the long-term effect of climate change on pavement performance and maintenance cost using a system dynamics approach. The system dynamics model was developed to provide a link between the long-term pavement performance predicted by PMED and the climate parameters. The results were then used to simulate the effect of climate on multiple pavement factors such as life-cycle cost of flexible pavements including maintenance cost. The framework considers various elements including a change in temperature, precipitation, sea level rise, and number of inundations to estimate the rate of pavement deterioration.

- Elshaer (2017) and Elshaer et. al. (2017) divided the pavement structure (or the unbound layers below the asphalt layer to be more specific) into sublayers of 6 in. thickness for simulating different levels of Ground Water Table (GWT). The GWT was initially located on top of the unbound base layer and sequentially lowered to 112 in. below the top of subgrade at in interval of 6 in. The sublayers below the GWT were assumed to be fully saturated, and the Soil-Water Characteristic Curve was used to estimate the degree of saturation for the layers above GWT. For each case (i.e., for each GWT level), a hydrostatic condition was assumed (i.e., effect of transient flow of water, evaporation, and precipitation events were ignored) and the estimated degree of saturation was used to adjust the resilient modulus of the unbound layers. The pavement structure whose modulus was adjusted for GWT in the above manner was used in a layered elastic

analysis program (KenLayer to be specific) for the analysis of stress, strain, and deflections of the asphalt pavement.

- Asadi (2020) integrated a hydraulic model for simulating the water flow within the pavement foundation layers, with a finite element pavement model for assessing the post-flood impacts on the performance of flexible pavements. The hydraulic analysis was conducted using an open-source finite difference code VS2DI for simulating unsaturated water flow within the pavement layers of a flexible pavement developed by Hsieh et al., (1999). It is a graphical software package for simulating fluid flow and solute or energy transport in variably saturated porous media and is available to download from United States Geological Survey (USGS) website. Pavement responses were calculated using a finite element software known as IntPave developed by Triado et. al. (2007) at the University of Texas, El Paso, which incorporates the moisture-dependent resilient moduli profile. Pavement responses were used to estimate the damage of pavement (i.e., remaining service life of the pavement) due to flood or precipitation through the use of distress models.

- Ghayoomi et. al. (2020) developed a system dynamics model to assess asphalt pavement performance and to identify load restriction decision in Minnesota due to ground water level rise, flood, or precipitation that lead to excessive moisture in pavement foundation layers. The model includes three main elements; hydrological, geotechnical, and pavement response structures (Figure 7). Hydrological structure model inputs include climate information and unsaturated soil hydraulics properties and simulates the moisture movement (i.e., degree of saturation) within the pavement layers. Geotechnical structure model determines the moisture-dependent resilient moduli of unbound layers (base/subbase and subgrade). Lastly, pavement response structure model simulates the stress, strain, and deflection due to traffic loading and the pavement conditions before, during, or after flooding or precipitation, using Boussinesq theory for layered elastic structures.

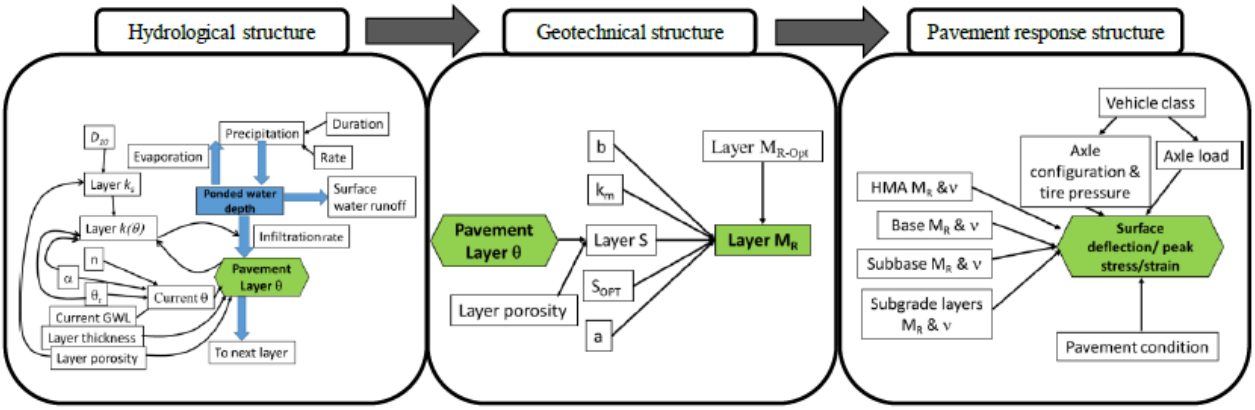

Figure 7. A conceptual framework of system dynamics model along with their variables (Ghayoomi et al., 2020)

In summary, the above studies generally indicate that the structural resiliency assessment of flexible pavement involves 3 general steps: (1) assume or simulate different climate conditions (i.e., temperature, moisture, etc.), (2) adjust the pavement structure (mostly the modulus of affected layers) for the different conditions identified in the previous step, and (3) conduct structural analysis (for stress, strain, or other performance indicators).

2.6.2. Recent Developments on Flood Resiliency of Rigid Pavements

Climate changes have increased the risk of flooding, hurricanes, and precipitation and all States in the U.S have experienced floods or flash floods in the past 5 years (Hemmati et. al., 2020). As such, the impact of flooding (or inundation) on pavements has been widely investigated and several strategies were proposed to mitigate the impact of flooding or hurricane events on pavement systems. Nonetheless, the current state of practice for pavement resiliency is typically limited to general observations and does not adopt any specific strategies (Muench and Van Dam, 2015). The following provides a review of recent studies or developments on rigid pavement resiliency and adaptation options under the climate impact of flooding and inundation.

- Based on the impact of Hurricane Harvey on road networks in Texas and Louisiana, Romanoschi (2019) developed a methodology for examining the performance of pavement sections before and after flooding. Performance modes were used to predict the pavement performance in terms of International Roughness Index (IRI) and Pavement Condition Index (PCI) for flooded and non-flooded conditions. Based on these predictions, the remaining pavement life (i.e., number of years before the next rehabilitation is necessary) for each condition was calculated and compared. These predicted pavement lives were then used to estimate the cost of the rehabilitation incurred by flooding while accounting for several other inputs such as the rehabilitation actions, unit cost trigger value of each action, discount rate, growth rate, and pavements types (e.g., asphalt, concrete, composite).

- Oyediji and Achebe (2019) studied the resilience of Joined Plain Concrete Pavement (JPCP) due to flooding in Canada using AASHTOWare PMED software. The JPCP performance was simulated for scenarios with and without climate changes. For the flooded scenario, the climate was predicted for years 2018 to 2100, corresponding to Representative Concentration Pathway (RCP) of 4.5 W/m^2 precipitation. IRI was used as the main performance parameter for estimating flood damage. The performance difference between no-flood and flood scenarios was calculated as percentage flood damage. It was concluded that the flood damage ranged from 0.31 to 5.99 percent. The researchers also noted that Pavement ME had several limitations for studying the impact of flooding such as the inability to account for degradation of materials.

- Khan et. al. (2017) evaluated the resiliency of different pavement types due to flooding. Roughness and rutting-based Road Deterioration (RD) model was developed to assess pavement performance after a flood. The developed model parameters include the probability (Pr) of flooding, change in roughness (ΔIRI) due to flooding, loss of base/subgrade resilient modulus (MrL), and duration of the flood. Two gradients, ΔIRI/Pr and ΔIRI/MrL using the change in IRI versus the probability of flooding and the loss of

base/subgrade resilient modulus, were calculated to determine the consequence of a flood for pavements and to determine which pavements were flood resilient. Monte Carlo simulation and nonhomogeneous transition probability matrix were used to account for different probability of flooding, gradients, and impact of flooding. It was noted that the model can help agencies to evaluate pavement resilience prior to flooding so that pre-flood maintenance stratagem can be selected in order to reduce the maintenance cost after flooding and to increase the service life of pavements.

- The Missouri River flooding of 1993 significantly damaged pavements, culverts, bridges, building foundations, etc. in Jefferson City, Missouri, resulting in the closure of roadways, delay in traffic, and economic losses to the city. The original pavement design of southbound US-63 at this location near Jefferson City consisted of 9 inches of jointed reinforced concrete pavement (JRCP) with 61-foot joint spacing on 4 inches of dense-graded crushed rock base. Due to the flooding damage, the Missouri DOT conducted a comprehensive study to further enhance the pavement design to resist future damage. The study led to the development of a new standard specification provision of a thick daylighted rock base, which has the capability to drain water from the pavement structure and also improve the load-bearing capacity. The rock base consisted of 1-inch nominal maximum aggregate size crushed limestone (MoDOT 2018). The new design for this section of US-63 consisted of 12 inches of doweled JPCP with 15-foot joint spacing over 24-inch daylighted rock base. This pavement, constructed in 1994, was the first implementation of daylighted rock base in Missouri. After 24 years of relatively heavy traffic, this portion of US-63 is still in excellent structural condition and no repairs have been performed to date. The adaptation option of 24-inch rock fill base was used based on calculations that would be enough for water storage during a storm event. The additional benefit of such adaptation option is the increase in structural capacity.

As mentioned previously, a general tool for structural resilience of rigid pavements was not found in the literature. Instead, the resilience of rigid pavements has generally been assessed using functional performance measures (most frequently the IRI before and after an event or long-term IRI with or without climatic change).

Furthermore, while the Missouri DOT's example of daylighted rock base demonstrates the effectiveness of the most expensive and extreme adaptation option (i.e., both elevating and strengthening the roadway), the effectiveness of other adaptation options (e.g., stabilizing a certain foundation layer or use of ultra-high strength PCC etc. as envisioned in the FMTP) are yet to be assessed.

3. COMPONENTS OF FDOT'S RIGID PAVEMENT RESILIENCY TOOL

As mentioned in the previous chapter, there is a need for a Mechanistic-Empirical methodology for assessing the resiliency of Florida's rigid pavements. Based on the review of available literature, three main components were identified for the mechanistic-empirical flexible pavement resiliency tools developed by previous researchers (Ghayoomi et al., 2020). Similar components were deemed necessary for the "**Rigid Pavement Resilience Tool**" developed as part of this project.

These components are summarized in the following.

1. **Hydrological Model** that can simulate the water flow within the pavement system. The model incorporates precipitation, ground water table, and other environmental inputs to simulate the moisture within any pavement layer over time (before, during, and after flooding).

2. **Geotechnical/Soil Mechanics Model** that can take the moisture content of unbound layers calculated from the hydrological model and adjust their resilient modulus.

3. **Structural Model** that can take the structural inputs (i.e., resilient modulus of unbound layers, PCC modulus, thickness, traffic, etc.) and calculate pavement response, which will ultimately determine the impact and consequence of flood events (e.g., reduction in service life, etc.).

In the following sections, the above components for the proposed rigid pavement resiliency tool are reviewed in detail. In addition, a couple of example problems are provided to demonstrate the capabilities of the above models.

3.1. HYDROLOGICAL MODEL

The purpose of the hydrological model is to simulate the flow of water within the foundation layers of a rigid pavement. A classical equation for the one-dimensional flow of water through unsaturated soils is given by Richards Equation as shown in the following equation (Richards, 1931).

$$\frac{\partial \theta}{\partial t} = \frac{\partial}{\partial z}\left[K(\theta)\left(\frac{\partial h}{\partial z} + 1\right)\right] \tag{1}$$

where θ is the volumetric soil water content, $K(\theta)$ is the moisture dependent hydraulic conductivity of soil, h is the soil pressure head, t is time, and z is elevation. Following Van Genuchten (1980), the hydraulic function of a soil layer can be defined in terms of the relative saturation, Θ, given as the following.

$$\Theta = \frac{\theta - \theta_r}{\theta_s - \theta_r} = \left[\frac{1}{1 + |\alpha h|^n} \right]^m \tag{2}$$

where θs and θr are the saturated and residual soil water contents, α and n are the shape parameters, and $m = 1 - 1/n$ (Van Genuchten, 1980). The hydraulic conductivity of an unsaturated soil is then expressed as the following (Yang et. al., 2009; Ghayoomi et. al. 2020).

$$K(\theta) = K_S \Theta^{0.5} \cdot \left[1 - \left(1 - \Theta^{1/m} \right)^m \right]^2 \tag{3}$$

where Ks is the saturated hydraulic conductivity.

As previously shown in Chapter 2 (i.e., Figure 5 to be more specific), there are five distinct material types used in the foundation layers of FDOT's rigid pavements. These materials are (1) asphalt base, (2) stabilized subgrade, (3) special stabilized subbase, (4) special select soil subgrade, and (5) natural subgrade or embankment. Due to the inherent differences in these materials, it is expected that the drainage characteristics may differ significantly from one material to another. In other words, different models for permeability (or hydraulic conductivity) needed to be implemented into the hydrological model of the resiliency tool. The hydraulic models implemented into the resiliency tool are reviewed in the following.

3.1.1. Hydraulic Conductivity of Asphalt Base

Masad et. al., (2006) developed the following equation for permeability of Asphalt Concrete (AC) materials.

$$K = \frac{C \cdot AV^3}{(1 - AV)^3} \left[D_S \left\{ 1 + \frac{G_{sb}\left[P_b - P_{ba}(1 - P_b) \right]}{G_b (1 - P_b)} \right\}^{1/3} \right]^2 \frac{\gamma}{\mu} \tag{4}$$

where,

K	=	Permeability of asphalt concrete (m/s)
C	=	Empirical calibration coefficient
AV	=	Percent (%) air voids
D_S	=	Average diameter of particles (m)
P_b	=	Percent (%) asphalt content by total weight of mix
P_{ba}	=	Percent (%) of absorbed binder by weight of aggregate
G_b	=	Specific gravity of binder
G_{sb}	=	Bulk specific gravity of aggregate
γ	=	Unit weight of water (9.79 kN/m^3)
μ	=	Viscosity of water (10^{-3} kg/(m·s))

The calibration coefficient, C, in the above equation was determined based on laboratory measurements using FDOT's permeability equipment as well as field measurements using a

device developed by National Center for Asphalt Technology (NCAT) (Cooley et. al., 2002). The *C* values calibrated for different levels of percent air void are summarized in Table 5.

Table 5. Values of calibration coefficient *C* in Equation (4)

Permeability Measurement Device	*C* value for Different Levels of Percent Air Void (*AV*)			
	$AV \leq 5\%$	$5\% < AV \leq 9\%$	$9\% < AV \leq 13\%$	$AV > 13\%$
FDOT Laboratory Device	18.00	78.60	241.00	241.00
NCAT Field Device	50.20	99.10	129.00	129.00

It should be noted that Equation (4) was developed to account for the effect of asphalt content on the permeability of AC mixtures. Consequently, the only parameter that relates to particle size is D_S, which is calculated from the aggregate gradation as the weighted average of the particle diameters retained on different sieves.

In addition to the above, Mohammad et. al. (2003) developed a permeability prediction equation that is more focused on particle distribution. The prediction equation is given as the following.

$$K = 10^{-4}\begin{bmatrix} 76.6AV - 17.2P_{0.075} + 163.4P_{0.3} - 197.5P_{0.6} \\ +33.2P_{2.36} + 4.5P_{12.5} - 1.7H \end{bmatrix} \quad (5)$$

where,

K = Permeability of asphalt concrete (mm/s)
$P_{0.075}$ = Percent passing 0.075 mm sieve
$P_{0.3}$ = Percent passing 0.3 mm sieve
$P_{0.6}$ = Percent passing 0.6 mm sieve
$P_{2.36}$ = Percent passing 2.36 mm sieve
$P_{12.5}$ = Percent passing 12.5 mm sieve
H = Height (or thickness) of specimen (mm)

3.1.2. Hydraulic Conductivity of Coarse-Grained and Fine-Grained Soils

The hydraulic conductivity prediction equation for coarse-grained soils was proposed by Chapuis (2004) and is given as the following.

$$K = 2.4622\left[\frac{d_{10}^2 e^3}{1+e}\right]^{0.7825} \quad (6)$$

where,

K = Permeability (cm/s)
d_{10} = Effective diameter corresponding to 10% passing on the cumulative grain-size distribution curve (mm)
e = Void ratio

The above equation has been implemented into the resiliency tool for special stabilized subbase and subgrade soils comprised of coarse-grained particles (i.e., A-1 through A-3 soils according to AASHTO classification).

For fine-grained soils (i.e., AAASHTO classifications A-4 through A-8), the prediction equation developed by Mbonimpa et al. (2002) was selected as the primary equation for hydraulic conductivity. The reason behind this is that the equation was developed specifically for fine-grained and/or plastic soils (i.e., clayey soils) that are frequently encountered in Florida's roadbed. The equation is given as the following.

$$K_S = C_p \frac{\gamma_w}{\mu_w} \frac{e^{(3+x)}}{(1+e)} \frac{1}{\rho_s^2 w_L^{2x}} \tag{7}$$

where,

K_S = Hydraulic conductivity (cm/s)
C_P = Regression constant (5.6 g^2/m^4)
γ_w = Unit weight of water (kN/m^3)
μ_w = Dynamic viscosity of water (Pa.s)
ρ_s = Density of soil (kg/m^3)
w_L = Liquid limit
x = $7.7\ w_L^{-0.15}-3$

In addition to the above, there are other empirical models exist for *Ks* of soils. For reference purposes (i.e., these equations are not implemented into the Resiliency Tool), Table 6 shows the most widely used empirical equations for determining *Ks*. The most well-known (but simple) equation is given by Hazen (1911).

Table 6. Empirical equations for saturated hydraulic conductivity of soils (White et. al., 2004).

Saturated hydraulic conductivity equation (cm/s)	Parameters	Application	Proposed by
$K_S = cD_{10}^2$	c = Hazen's empirical coefficient, c ≈ 1	Applicable for loose, uniform sands	Hazen (1911)
$K_S = 10.2\eta^{3.287} D_{10}^2$	$\eta = porosity$	Applicable for grain size between 0.01 – 5 mm	Slichter (1898)
$K_S = 1.2C_u^{0.75} D_{10}^{0.89} (\frac{e^3}{1+e})$	e = void ratio of soil	Applicable for medium to fine sands	Shahabi et al. (1984)
$K_S = \frac{D_s^2 \gamma e^3 C}{\mu(1+e)}$	$\eta = porosity$ μ = viscosity of water	Applicable for soils	Taylor (1984)

3.1.3. Implementation of Hydrological Model

Although the Richards Equation (shown in Equation (1)) represents one-dimensional flow of water, it is still a non-linear differential equation which is very difficult to solve (i.e., requires a

sophisticated numerical method such as the Finite Element Method). To overcome this difficulty, Yang et. al. (2009) proposed a spatially-integrated form of Richards Equation by integrating it with respect to *z*, which led to the following expression.

$$\frac{\Delta\overline{\theta_i}}{\Delta t} = \frac{1}{z}\left[K_{i+1}\left(\frac{\Delta h_{i+1,i}}{\Delta z} + 1 \right) - K_i\left(\frac{\Delta h_{i,i-1}}{\Delta z} + 1 \right) \right] \tag{8}$$

where i is the soil layer number, Δt is the discrete time step, $\Delta\overline{\theta_i}$ is the average water content change in soil layer i, Δz is the soil layer thickness, $\Delta h_{i+1,i}$ and $\Delta h_{i,i-1}$ are the differences in soil pressure head between layers $i + 1$ and i, and i and $i - 1$, respectively. (Yang et. al. 2009). Note that Equation (8) allows for a direct, numerical integration over time (t) for calculating the average change in water content within a soil layer of given thickness (Δz).

To demonstrate the use of Equation (8) for simulating the flow of water within a rigid pavement foundation, FDOT's rigid pavement structure with asphalt base option (see left half of Figure 5) was modeled using discrete layers (with each layer having a thickness of 4.0 in.) composed of the following (starting from the bottom): (1) 10 layers of natural subgrade or embankment, (2) 3 layers of stabilized subgrade, and (3) 1 layer of asphalt base.

For the first example, the above pavement structure was subjected to a heavy rainfall similar to that from a severe storm. The simulated rainfall intensity is shown in Figure 8. As shown in the figure, the pavement was subjected to 10 hours of rain event having an intensity of 8 in/hr. The simulation was conducted for a total duration of 30 hours. To simulate a humid environment after the storm, the evaporation rate was set to zero within the 20-hour period after the rainfall.

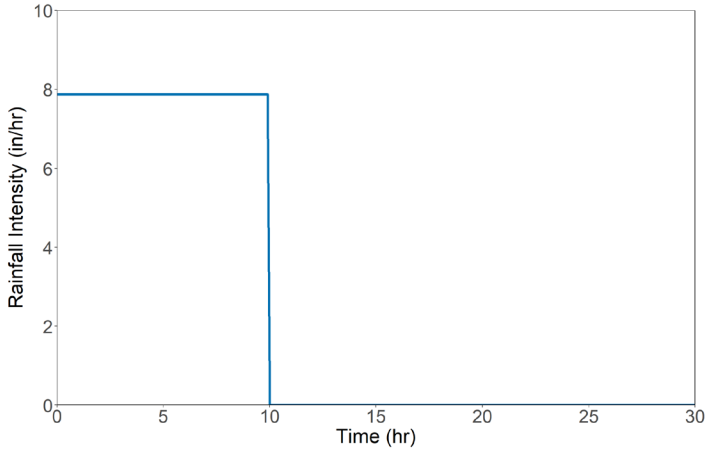

Figure 8. Artificial rainfall intensity of a severe storm.

Figure 9 shows the results of the rainfall simulation. Figure 9(a) shows the initial degree of saturation (i.e., just before the rainfall) using Equation (2), with the GWT located at the bottom of the natural subgrade. The moisture condition during and after the rainfall event is shown in Figure 9(b) through Figure 9(f). The results indicate that at the end of the rainfall, the base, stabilized subgrade, and approximately the top half of the natural subgrade (embankment) layers

were fully saturated (Figure 9(c)). However, the bottom half of the natural subgrade continues to absorb more water after the rainfall due to the flow of water from the upper layers (Figure 9(d)). Figure 9(f) shows the moisture condition at the end of the simulation (i.e., 20 hours after the rain event), which indicates that the stabilized subgrade and the upper half of the natural subgrade layers are still holding some level of water from the storm – i.e., it may take a long period of time to completely drain the water out of these layers.

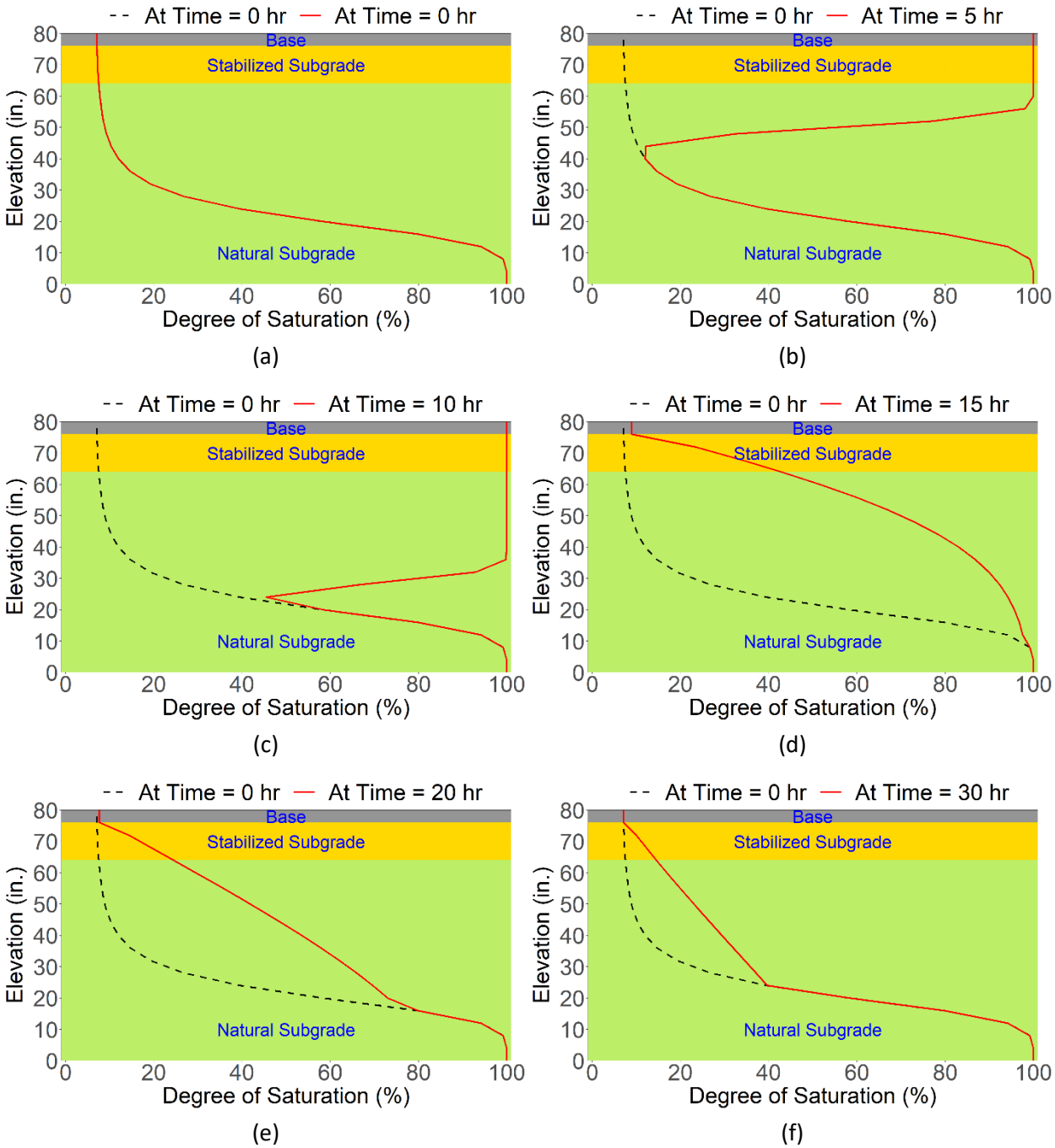

Figure 9. Results from a hydrological simulation of a heavy rainfall at (a) $t = 0$ hr, (b) $t = 5$ hr, (c) $t = 10$ hr, (d) $t = 15$ hr, (e) $t = 20$ hr, and (f) $t = 30$ hr.

For the second example of one-dimensional water flow, the same pavement structure was assumed to be fully saturated at the beginning of the simulation, similar to a severe sea level rise or a pavement that had been submerged under water for an extended period of time. To simulate a relatively dry environment, the pavement was not subjected to a rainfall but subjected to a water evaporation rate of 0.06 in/hr (1.4 in/day).

Figure 10 shows the results of the 30-hour simulation. Figure 10(b) through Figure 10(e) show that the base and stabilized subgrade layers are losing water at a faster rate, due to the evaporation occurring at the pavement surface. Nonetheless, the natural subgrade (especially the bottom half) may need a longer period of time to fully drain the water due to inundation (Figure 10(d) through Figure 10(f)).

As shown in the above examples, the simple one-dimensional simulation of water flow may be used for short-term effect of rainfall and sea level rise on the moisture content within the unbound layers of the rigid pavement structure.

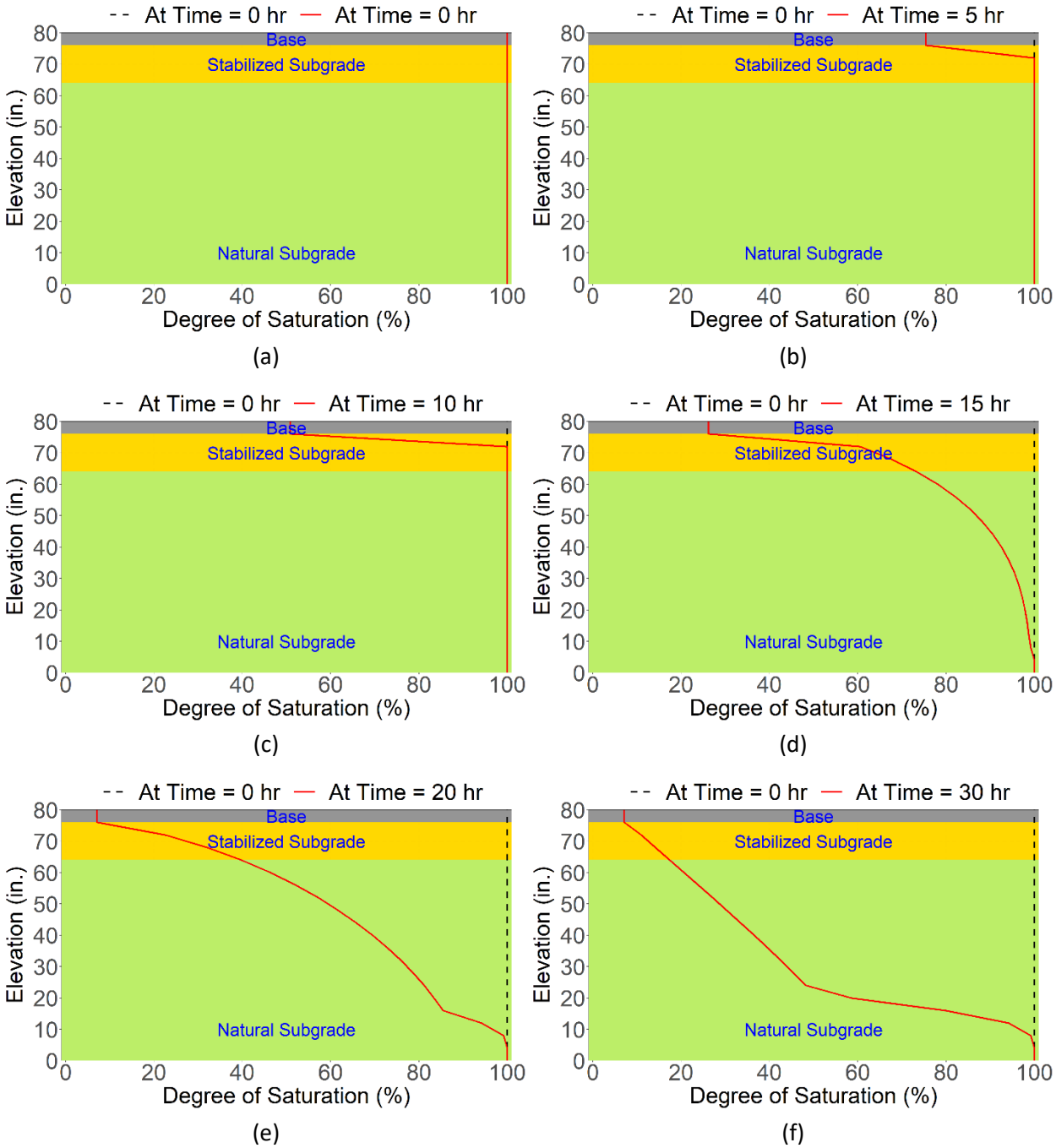

Figure 10. Results from a hydrological simulation of a flooded pavement at (a) $t = 0$ hr, (b) $t = 5$ hr, (c) $t = 10$ hr, (d) $t = 15$ hr, (e) $t = 20$ hr, and (f) $t = 30$ hr.

3.2. GEOTECHNICAL AND SOIL MECHANICS MODEL

The purpose of the soil mechanics model is to estimate the effect of moisture on the resilient modulus of the unbound layer. The most commonly used equation for this purpose is the one developed as part of NCHRP 1-37A project, which is shown below.

$$\log\left(\frac{M_R}{M_{Ropt}}\right) = a + \frac{b-a}{1+\exp\left(\beta + k_m \cdot \left(S - S_{opt}\right)\right)} \tag{9}$$

where M_R is the soil's resilient modulus at a given degree of saturation S, and M_{Ropt} is the resilient modulus corresponding to the degree of saturation at optimum water content S_{opt}, and a, b, β, and k_m are regression parameters whose values are provided in Table 7.

Table 7. Regression parameters for NCHRP 1-37A soil mechanics model (ARA, 2000)

Soil Type	Regression Parameters			
	a	***b***	***β***	***k_m***
Coarse-Grained	-0.3123	0.3	-0.0401	6.8157
Fine-Grained	-0.5934	0.4	-0.3944	6.1324

Note that the advantage of the above equation is that it provides a simple means for estimating the effect of moisture on the resilient modulus of unbound layers. However, a relatively more complicated model was found in literature for Florida's unbound layers. Based on the materials sampled and tested from 25 flexible pavement section in Florida, Oh and Fernando (2011) and Oh et. al. (2012) concluded that the following, stress-dependent resilient modulus model works reasonably well for FDOT's base, subgrade, and embankment materials.

$$M_R = k_1 P_a \left(\frac{\sigma_{bulk} + 3k_4 S\theta}{P_a}\right)^{k2} \left(\frac{\tau_{oct}}{P_a} + 1\right)^{k3} \tag{10}$$

where σ_{bulk} is the bulk stress, τ_{oct} is the octahedral shear stress, S is the soil suction in psi, P_a is the atmospheric pressure (14.5 psi), and k_1 through k_4 are model parameters. The relationship between soil suction (S) and the volumetric water content (θ) is given by the following Soil-Waver Characteristic Curve (SWCC).

$$\theta = C(S)\left[\frac{\theta_{sat}}{\left\{\ln\left(e^1 + \left(S/a_f\right)^{bf}\right)\right\}^{cf}}\right] \tag{11}$$

where

$$C(S)=\left[1-\frac{\ln\left(1+\left(S/h_r\right)\right)}{\ln\left(1+\left(1.45\times10^{5}/h_r\right)\right)}\right] \tag{12}$$

and a_f, b_f, c_f, and h_r are model parameters. Based on their test results, Oh and Fernando (2008) determined that the SWCC (or the model parameters a_f, b_f, c_f, and h_r) for the embankment soil varied substantially depending on the region, and provided the model parameters for each County within the State. However, for the limerock base and stabilized subgrade materials, they observed that the SWCC was relatively more uniform (i.e., regardless of the region) and provided the model parameters shown in Figure 11 (for limerock base) and Figure 12 (for stabilized subgrade).

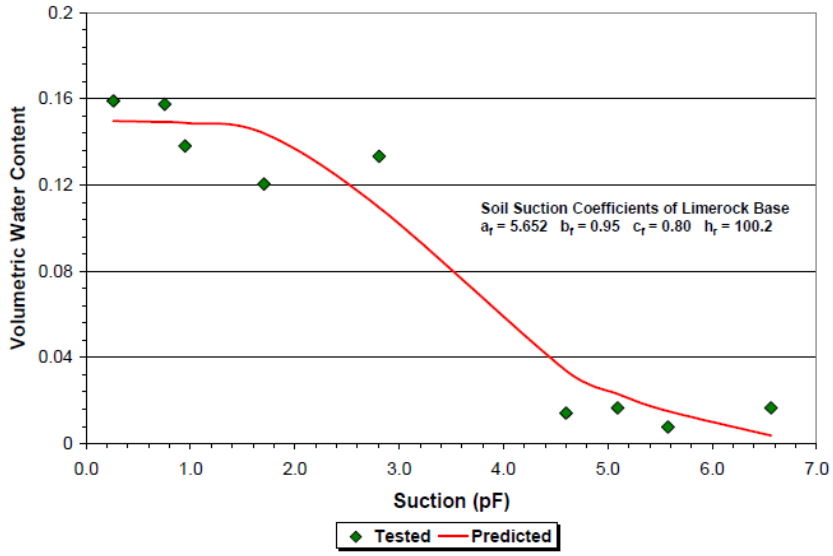

Figure 11. Soil-water characteristic curve for Florida's limerock base material (Oh and Fernando, 2008).

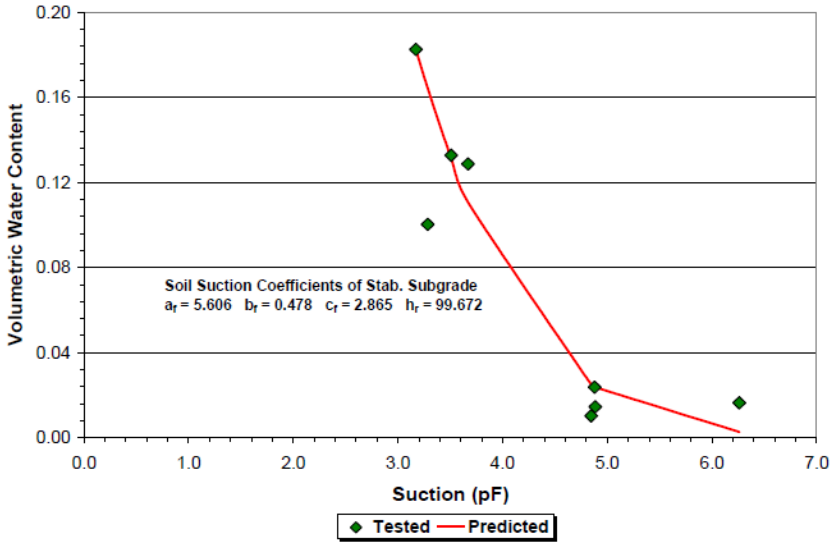

Figure 12. Soil-water characteristic curve for Florida's stabilized subgrade material (Oh and Fernando, 2008).

In addition to the above, several resilient modulus models have been developed that incorporate the effect of moisture content. For references purposes only (i.e., these models are not implemented into the Resiliency Tool), Table 8 summarizes some of the additional resilient modulus models that were identified in the literature.

Table 8. Resilient modulus models for unsaturated soils (ARA 2000).

Resilient modulus	Application	Proposed by
$\frac{M_R}{M_{Ropt}} = 0.98 - 0.28(w - w_{opt}) + 0.029(w - w_{opt})^2$	Applicable for fine-grained soils	Li and Selig (1994)
$M_{R(wet)} = M_{Ropt} + \frac{dM_R}{dS} \cdot \Delta S$ $\frac{dM_R}{dS} = 1,690 - 194 \cdot (CLASS) - 11.2 \cdot [M_{R(out)}]$	Applicable for fine-grained soils	Dumm et al. (1997)
$\log M_R = c_1 + c_2 \cdot \log(\theta) + c_3 \cdot (w\%) + c_4 \cdot (T) + c_5 \cdot (\gamma_d)$	Applicable for coarse-grained soils	Jin et al. (1994)
$\log M_R = c_1 + c_2 \cdot (w\%) + c_3 \cdot (S)$	Applicable for fine-grained soils	Jones and Witczak (1977)
$\log M_R = c_1 + c_2 \cdot (S) + c_3 \cdot PC + c_4 \cdot \log(\theta)$	Applicable for Base/Subbase Materials	Rada and Witczak (1981)
$\log M_R = k_1 \cdot p_a \cdot (\frac{\theta}{p_a})^{k2} \cdot (\frac{\tau_{oct}}{p_a})^{k3}$	Applicable for coarse-grained and fine-grained soils	Santha (1994)

To provide an example of the soils model, Figure 13 shows the degree of saturation as a function of time for the stabilized subgrade at depth 12 in. (or elevation of 68 in. in Figure 9) and the natural subgrade at depth 50 in. (or elevation of 30 in. in Figure 9) that was extracted from the hydrologic simulation of 10-hr rainfall previously presented. Clearly, the figure shows that the stabilized subgrade which is closer to the pavement surface gets saturated faster due to rain but also drains faster after the rainfall. Similarly, Figure 14 shows the degree of saturation for the same layers from the flooding example. It can be seen again that although both layers started at the fully saturated initial condition, the upper stabilized subgrade drains water at a faster rate than the natural subgrade.

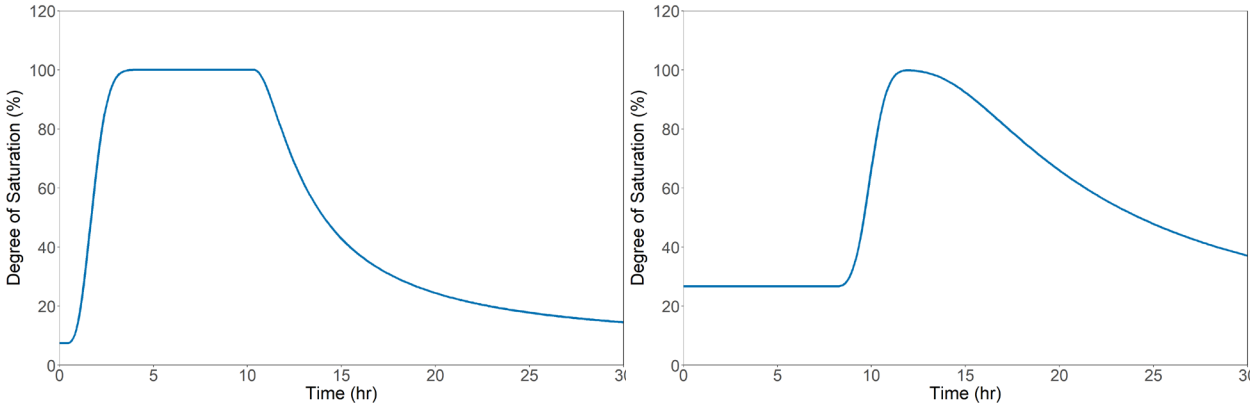

Figure 13. Rainfall example degree of saturation for (a) stabilized subgrade at depth 12 in. and (b) natural subgrade at depth 50 in.

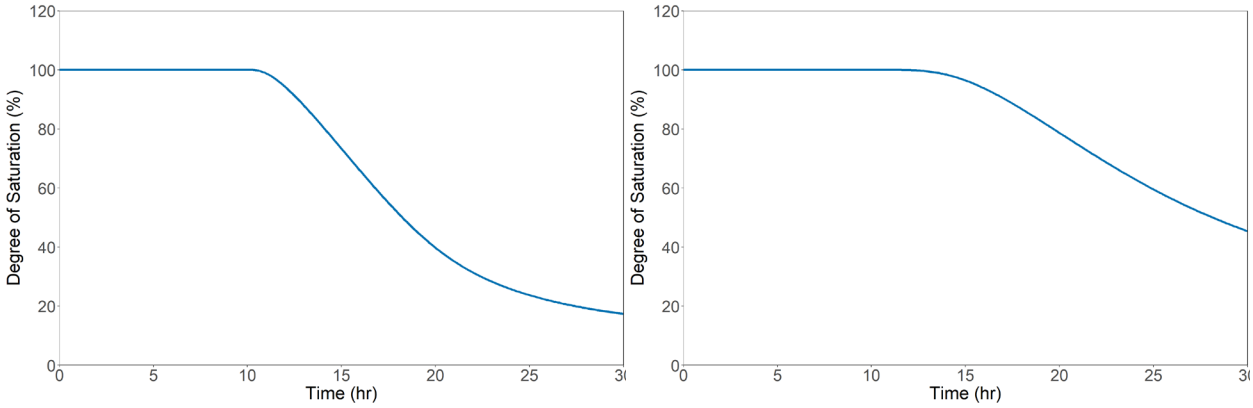

Figure 14. Flooding example degree of saturation for (a) stabilized subgrade at depth 12 in. and (b) natural subgrade at depth 50 in.

Based on the degree of saturation shown in Figure 13 and Figure 14, the resilient moduli of the respective layers were calculated using Equation (9), due to its simple form. The relevant inputs used for this equation is shown in Table 9. To better simulate Florida's conditions, it was assumed that the resilient modulus at optimum moisture content was 16 ksi and 12 ksi for the stabilized subgrade and natural subgrade, respectively. These values correspond to standard values used in FDOT's rigid pavement design (FDOT, 2021).

Table 9. Properties assigned for unbound layers.

Variables	Values
Stabilized subgrade, M_{Ropt}	16,000 psi
Natural subgrade, M_{Ropt}	12,000 psi
Optimum degree of saturation for stabilized subgrade, S_{opt}, (A-1)	11 %
Optimum degree of saturation for natural subgrade, S_{opt}, (A-3)	14 %
Coarse-grained materials regression parameters, a, β, k_m	-0.3123, 0.3, 6.8517
Fine-grained materials regression parameters, a, β, k_m	-0.5934, 0.4, 6.1324

Figure 15 and Figure 16 show the resulting resilient modulus as a function of time for rainfall example and the flooding example, respectively.

For the rainfall example, Figure 15(a) shows that the resilient modulus of the stabilized subgrade undergoes a significant reduction soon after the rainfall. Then, the modulus remains at the saturated level for the duration of rainfall (i.e., 10 hours) but recovers relatively quickly after the rainfall. On the other hand, the natural subgrade (Figure 15(b)) does not show a significant modulus reduction approximately for the first 10 hours (i.e., during rainfall). Nevertheless, due to the rainwater propagating downwards, the natural subgrade shows a significant modulus reduction after the rain event and takes longer to recover.

For the flooding example, Figure 16 shows that both the stabilized subgrade and natural subgrade layers exhibit degraded modulus at the beginning of the simulation (due to flooding which fully saturated the entire pavement). However, as the water starts to recede from the pavement surface due to evaporation, both layers start to recover with the stabilized subgrade recovering at a faster rate than the natural subgrade.

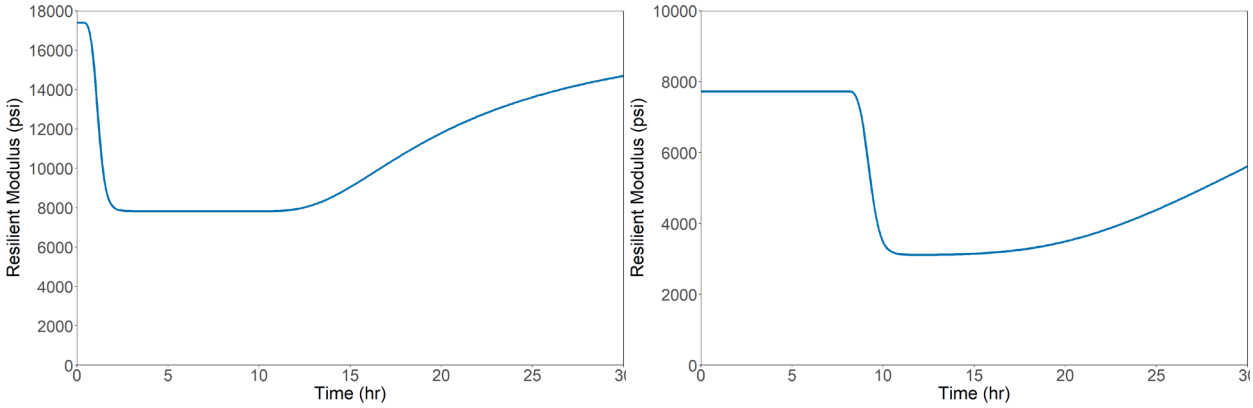

Figure 15. Rainfall example resilient modulus for (a) stabilized subgrade at depth 12 in. and (b) natural subgrade at depth 50 in.

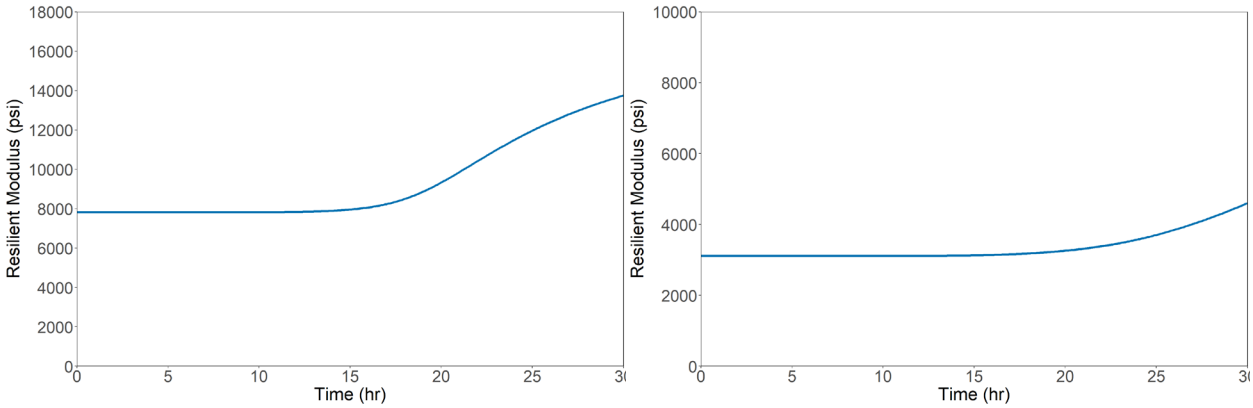

Figure 16. Flooding example resilient modulus for (a) stabilized subgrade at depth 12 in. and (b) natural subgrade at depth 50 in.

3.3. RIGID PAVEMENT STRUCTURAL MODEL

The purpose of the structural model is to estimate the pavement response and the allowable number of load passes that will subsequently be used for performance assessment. The moisture-dependent resilient modulus calculated from the geotechnical and soil mechanics model will be a critical input into the rigid pavement structural model, which is anticipated to have a crucial effect on the allowable number of axle loads. The structural model includes three steps summarized as the following:

- Step 1: Estimate the composite modulus of subgrade reaction (k-value) based on the moisture-dependent resilient modulus of the pavement foundation.
- Step 2: Calculate critical pavement responses.
- Step 3: Estimate the allowable number of loads.

The analytical models frequently used for computing the response of rigid pavement slabs typically utilize the "Winkler spring" foundation model in which all of the foundation layers below the PCC slabs are converted to a set of springs with a constant stiffness known as the composite modulus of subgrade reaction or the k-value (see Figure 17).

It is noted that when the concept of k-value was first introduced by Westergaard (1925), it was assumed that the PCC slabs were placed directly on top of the subgrade (i.e., no base or subbase layers), whose reaction was proportional to the slab deflection only in the vertical direction (hence the name "modulus of subgrade reaction"). Westergaard (1925) also noted that because the PCC slabs are substantially stiffer than any subgrade materials, minor changes in k-value do not result in any appreciable changes in the critical stresses calculated for the PCC slabs, and hence, a reasonable approximation of the k-value is sufficient for obtaining the critical stresses within the PCC slabs.

However, recent rigid pavement designs typically include one or more foundation layers between the PCC slabs and the subgrade (as an example, see Figure 17 for FDOT's rigid pavement design options). In this case, the foundation layers, including the base, subbase, and subgrade, are

combined and then transformed into the Winkler spring foundation (hence called "composite modulus of subgrade reaction"). The use of composite k-value is still considered to be reasonable for the same reason mentioned by Westergaard (i.e., PCC slabs are much stiffer than the foundation layers). In addition, using the k-value also allows for a more efficient computation of the stresses and strains within the PCC slabs (as opposed to time-consuming 3-dimensional Finite Element Method analysis).

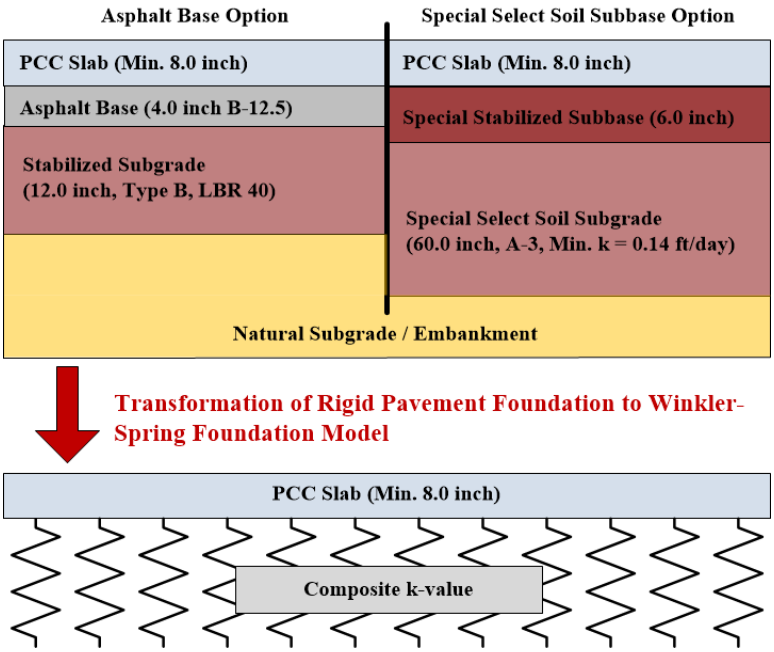

Figure 17. Transformation of rigid pavement foundation layers for structural response computations.

As seen from the above, the first step in rigid pavement response computation involves calculating a composite k-value for all foundation layers below the PCC slabs. The composite k-value impacts the magnitude of stresses and deflection in the PCC slab caused by traffic loads and environmental loads.

Several models have been developed for calculating the k-value from resilient or elastic modulus of the foundation (Darter et al. 1995). The most commonly used composite k-value model for this purpose is the one developed by 1993 AASHTO Design Guide, which is shown below.

$$\ln k = -2.807 + 0.1253\left(\ln H_{SB}\right)^2 + 1.062\left(\ln M_R\right) + 0.1282\left(\ln H_{SB}\right)\left(\ln E_{SB}\right) \\ -0.4114\left(\ln H_{SB}\right) - 0.05851\left(\ln E_{SB}\right) - 0.1317\left(\ln H_{SB}\right)\left(\ln M_R\right) \quad (13)$$

where H_{SB} and E_{SB} are the thickness and modulus of the subbase layer, and M_R is the subgrade modulus (Schwartz and Boudreau, 2006). However, it should be noted that while the above equation only allows for a single subbase layer above the subgrade, FDOT's rigid pavement design includes two distinct layers above the natural subgrade and below PCC (i.e., the Asphalt Base / Stabilized Subgrade or Special Stabilized Subbase / Special Select Soil Subgrade). Furthermore, both these layers need to be subdivided into thinner sublayers for the hydrological

model. As such, it is necessary that a method for combining all of the sublayers (having different modulus depending on moisture content) be used to transform the pavement foundation into a single subbase for Equation 9. The most well-known method for this purpose is Odemark's Equivalent Thickness Method whose equation is shown below and its schematics shown in Figure 18.

$$H_{i,e} = H_i \sqrt[3]{\frac{E_i}{M_R} \times \frac{1-\upsilon_s^2}{1-\upsilon_i^2}} \tag{14}$$

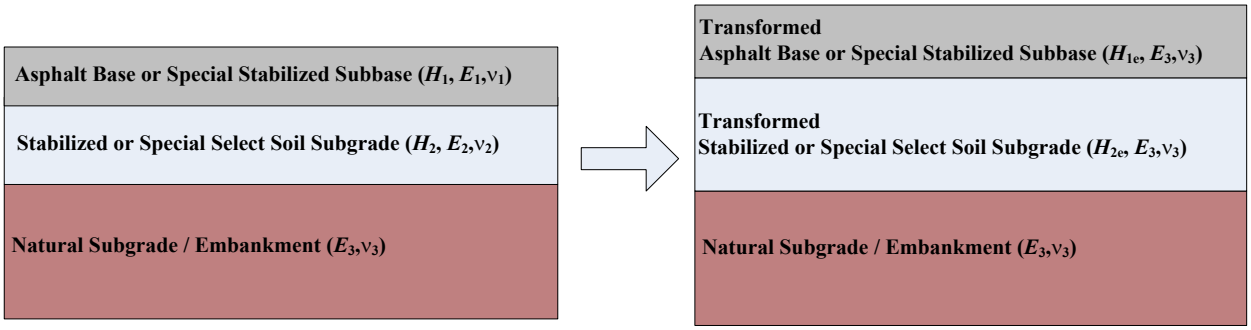

Pavement Foundation **Transformed Pavement Foundation**

Figure 18. Schematics of Odemark's equivalent thickness method

To continue the examples of extreme rainfall and flooding, the asphalt base layers and the 3 sublayers for the stabilized subgrade were transformed using Odemark's method and combined into a single layer. This combined layer was regarded as a subbase and its thickness and modulus were used in Equation (13) for estimating the composite k-value. The composite k-values for the rainfall and the flooding examples are shown in Figure 19(a) and Figure 19(b), respectively.

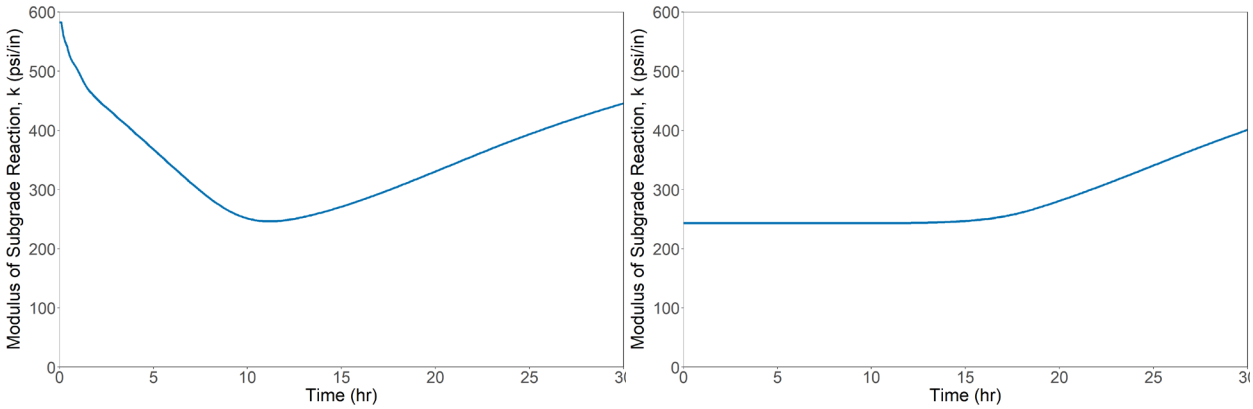

(a) (b)

Figure 19. Composite modulus of subgrade reaction for (a) rainfall example and (b) flooding example.

The second step is to calculate the critical stresses for the rigid pavement with moisture-dependent k-value estimated as above. While a variety of pavement models such as layered-elastic models, finite element models, and Boussinesq equations were used for flexible

pavements, there are two primary models that can be used for this purpose, namely the Westergaard's theory and finite element methods.

3.3.1. Westergaard Theory

Westergaard theory provides simple equations for critical stresses (σ) and deflections (Δ) within the PCC slab for three locations of the load: (1) in the interior of a slab, (2) at the edge of a slab, and (3) at the corner of a slab. These equations are provided in the following.

For interior loading:

$$\sigma = \frac{3(1+\mu)P}{2\pi H^2}\left(\ln\frac{l}{b} + 0.6159\right) \tag{15}$$

$$\Delta = \frac{P}{8kl^2} \tag{16}$$

For edge loading:

$$\sigma = \frac{0.572P}{H^2}\left(\log_{10}\left(H^3\right) - 4\log_{10}\left(\sqrt{1.6a^2 + H^2} - 0.675H\right) - \log_{10} k + 5.767\right) \tag{17}$$

$$\Delta = \frac{1}{\sqrt{6}}(1+0.4\upsilon)\frac{P}{kl^2} \tag{18}$$

and for corner loading:

$$\sigma = \frac{3P}{H^2}\left(1 + \left(\frac{a\sqrt{2}}{l}\right)^{0.6}\right) \tag{19}$$

$$\Delta = \left(1.1 - 0.88\frac{a\sqrt{2}}{l}\right)\frac{P}{kl^2} \tag{20}$$

where H and μ are the thickness and Poisson's ratio of PCC slab, P and a are the magnitude and radius of the load, l is the radius of relative stiffness given as:

$$l = \sqrt[4]{\frac{EH^3}{12\left(1-\mu^2\right)k}} \tag{21}$$

and

$$b = \begin{cases} a & \text{when } a \geq 1.724H \\ \sqrt{1.6a^2 + H^2} - 0.675H & \text{when } a < 1.724H \end{cases} \quad (22)$$

where *E, H, μ, and k* are the modulus of elasticity of PCC slab, thickness and Poisson's ratio of PCC slab, and the modulus of subgrade reaction (i.e., k-value).

3.3.1.1. Limitations of Westergaard Equations

While the closed-form equations developed by Westergaard provides a very simple and efficient means for computing the critical stresses within the PCC layer under wheel load positioned at different locations, these equations also come with several limitations. These limitations are summarized as the following.

- Applicable only to single wheel load with circular contact area.
- Load locations are fixed (i.e., interior, edge, and corner as shown above).
- Applicable only to very large slabs (e.g., it is assumed that the load is at a sufficient distance from any joints or corner for the interior loading)
- Assumes full subgrade support (i.e., while curling of PCC slabs may result in partial loss of foundation support, these are not accounted for in the closed-form solutions).
- No consideration is given to load transfer across joints (e.g., aggregate interlock or dowel/tie bars).

3.3.2. Finite Element Methods (FEM)

As seen from the above, while Westergaard's closed-form solutions offer efficient estimation of the critical stresses and displacements within the PCC slabs, they also have numerous limitations that may not be well-suited for more general analysis conditions (e.g., multiple loads, effect of load transfer, etc.). Furthermore, due to the complexity of rigid pavement structures (with joints, dowels, tie bars, etc.), conventional layered theory (which is frequently used for flexible pavements) has not been used frequently for rigid pavement modeling.

On the other hand, Finite Element Method (FEM) of analysis gained popularity for modeling rigid pavement systems since the 1970's, and a number of FEM solutions tailored for rigid pavements have been developed. While a thorough review of the theory behind FEM and the characteristics of each FEM solution are deemed beyond the scope of this literature review, it is worth noting that the FEM programs developed specifically for rigid pavement systems include JSLAB (Tayabji and Colley, 1986), WESLIQID (Huang and Wang, 1973), ILLISLAB (Tabatabaie, 1978; Tabatabaie and Barenberg, 1978), FEACONS (Tia et. al., 1987), and KENSLABS (Huang, 1974).

Among the above-mentioned FEM solutions, the ARA research team recently implemented ILLISLAB, which utilizes 2-dimensional (2D), medium-thick plate elements for modeling the PCC slabs (Tabatabaie, 1978). The 2D plate element is schematically shown in Figure 20. As shown in the figure, the plate element has 4 nodes (1 at each corner) with each node having 3

degrees of freedom: a vertical deflection (w) along the Z-direction and the rotations about the 2 horizontal axes (θ_X and θ_Y).

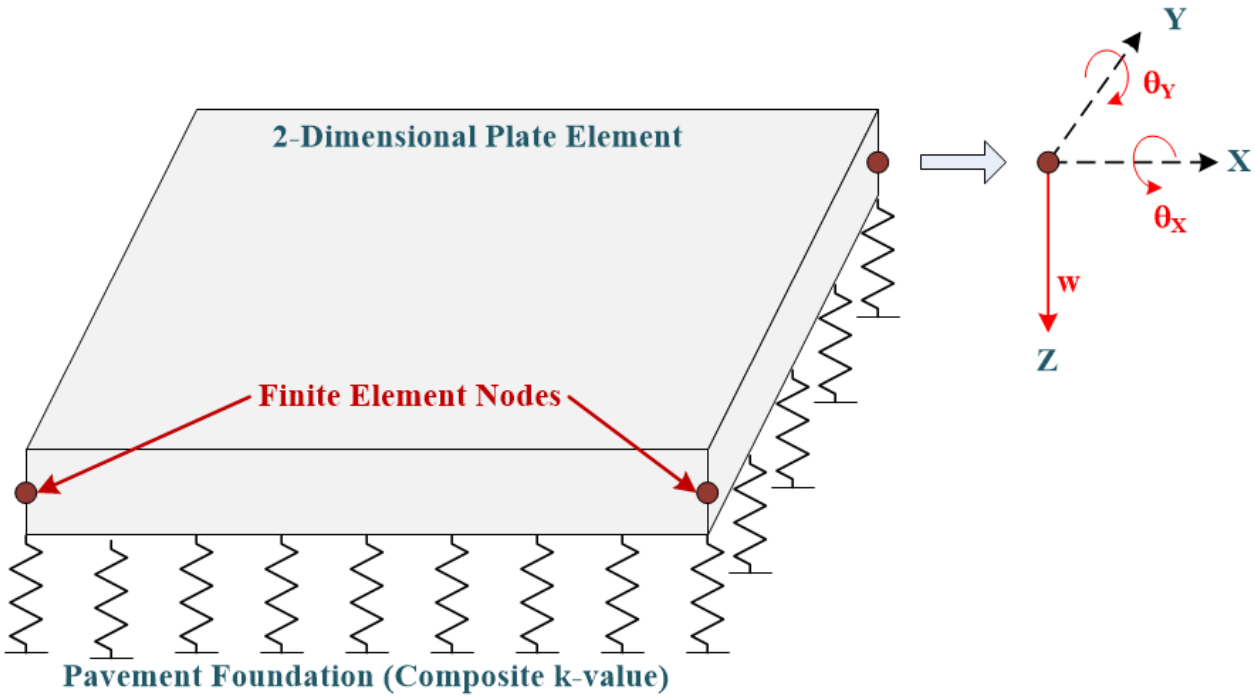

Figure 20. 2D plate element used in ILLISLAB.

In ILLISLAB, each PCC slab is modeled using several of the above plate elements stitched at the nodes (i.e., the 2 adjacent element share the same node along the edge they meet). Joints are modeled by 2 distinct nodes at the same location (e.g., one node for the approach slab and another for the leave slab) that can move independently of each other. Load transfer at the joints can be modeled using the aggregate interlock and/or load transfer mechanisms such as dowels that are modeled using 2D beam elements at the nodes. These elements are supported on by the pavement foundation represented by the composite k-value discussed previously.

The original ILLISLAB developed by Tabatabaie (1978) was limited to simulating the PCC slab response under traffic wheel loads. In a follow up study by Korovesis (1990), the original ILLISLAB was enhanced to simulate the effect of temperature loading or more specifically, curling of PCC slabs due to thermal gradient. Essentially, this was accomplished by iterating the FEM solutions such that the Winkler springs not in contact with the curled shape of the PCC slabs are eliminated from the analysis.

The above features of ILLISLAB, including the capability of analyzing the effect of thermal gradient, has recently been implemented by the Principal Investigator (PI). While the core engine of ILLISLAB algorithm was implemented in open-source language R, the interface was built in MS Excel and Visual Basic for Applications (VBA). For the purpose of illustration, Figure 21 shows a screen capture of the current user interface. In addition, Figure 22 and Figure 23 show the FEM mesh that was generated automatically and an example displacement output from the ILLISLAB core in R.

Although the use of ILLISLAB will overcome some of the limitations of the closed-form solutions, it is also acknowledged that the FEM solution does have limitations as well. The limitations of current ILLISLAB (specifically for the version implemented by the PI) are summarized in the following.

1. It is not capable of modeling any friction between the PCC slabs and the layer beneath them. Therefore, the effect of lateral confinement (if any) provided by the foundation layers are not simulated.
2. Analysis of multiple PCC layers (e.g., Econocrete) with varying quality or modulus has not been implemented. I.e., the PCC slabs must be simulated as a single, uniform layer.
3. The foundation is modeled as a uniform Winkler foundation. In other words, localized variation in foundation or localized loss of foundation support (e.g., due to erosion or pumping) cannot be simulated.

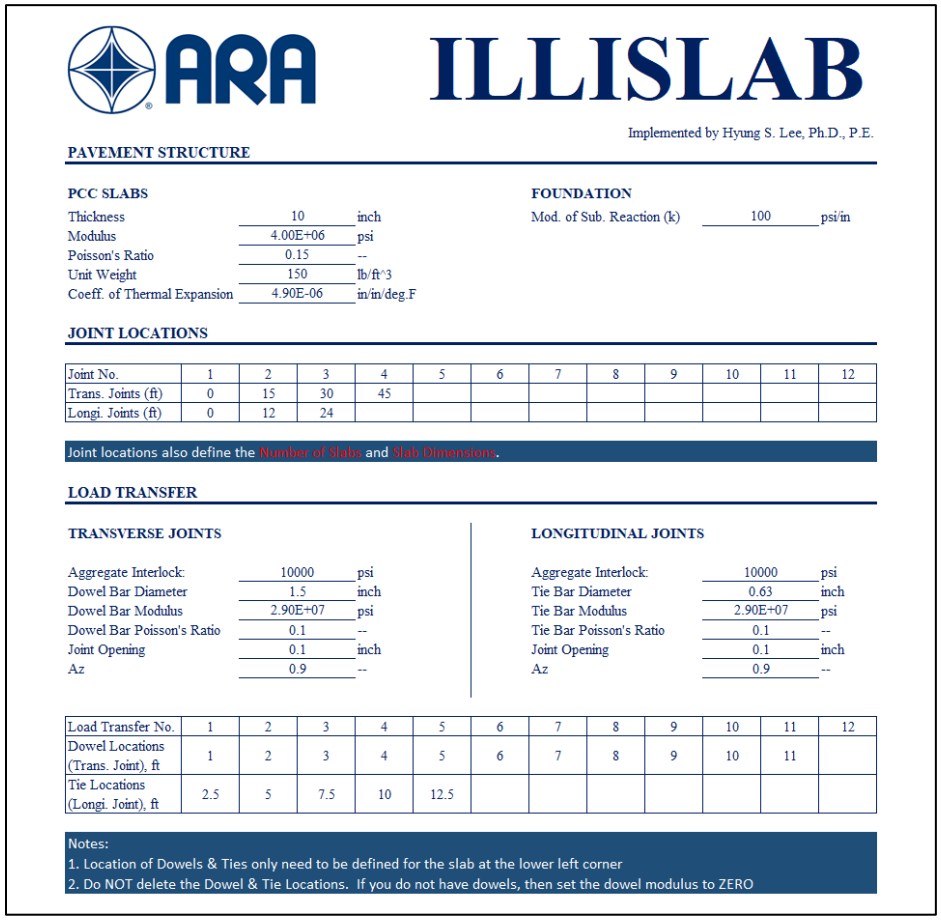

ARA **ILLISLAB**

Implemented by Hyung S. Lee, Ph.D., P.E.

PAVEMENT STRUCTURE

PCC SLABS

Thickness	10	inch
Modulus	4.00E+06	psi
Poisson's Ratio	0.15	--
Unit Weight	150	lb/ft^3
Coeff. of Thermal Expansion	4.90E-06	in/in/deg.F

FOUNDATION

Mod. of Sub. Reaction (k)	100	psi/in

JOINT LOCATIONS

Joint No.	1	2	3	4	5	6	7	8	9	10	11	12
Trans. Joints (ft)	0	15	30	45								
Longi. Joints (ft)	0	12	24									

Joint locations also define the Number of Slabs and Slab Dimensions.

LOAD TRANSFER

TRANSVERSE JOINTS

Aggregate Interlock:	10000	psi
Dowel Bar Diameter	1.5	inch
Dowel Bar Modulus	2.90E+07	psi
Dowel Bar Poisson's Ratio	0.1	--
Joint Opening	0.1	inch
Az	0.9	--

LONGITUDINAL JOINTS

Aggregate Interlock:	10000	psi
Tie Bar Diameter	0.63	inch
Tie Bar Modulus	2.90E+07	psi
Tie Bar Poisson's Ratio	0.1	--
Joint Opening	0.1	inch
Az	0.9	--

Load Transfer No.	1	2	3	4	5	6	7	8	9	10	11	12
Dowel Locations (Trans. Joint), ft	1	2	3	4	5	6	7	8	9	10	11	
Tie Locations (Longi. Joint), ft	2.5	5	7.5	10	12.5							

Notes:
1. Location of Dowels & Ties only need to be defined for the slab at the lower left corner
2. Do NOT delete the Dowel & Tie Locations. If you do not have dowels, then set the dowel modulus to ZERO

Figure 21. Excel-based ILLISLAB interface.

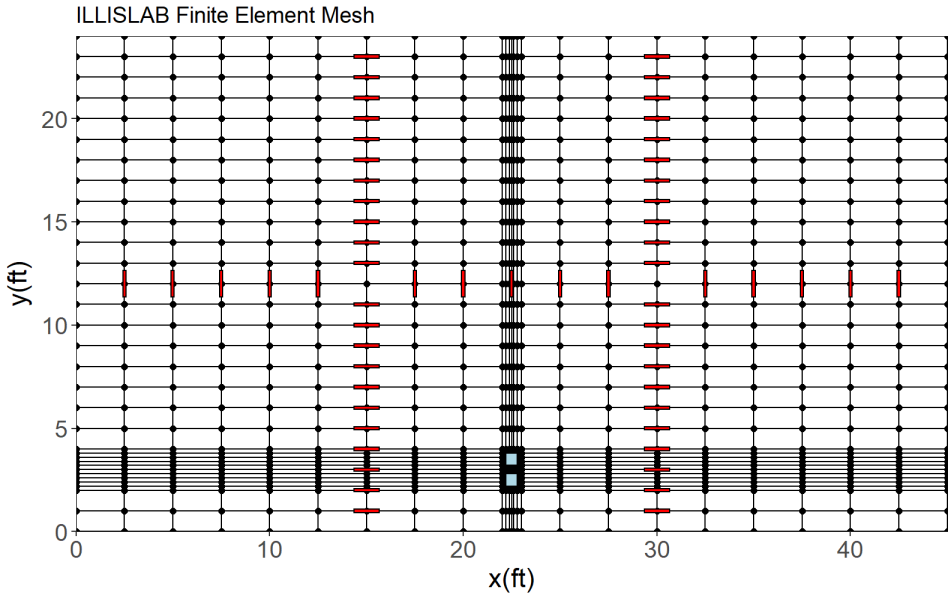

Figure 22. FEM mesh generated using ILLISLAB.

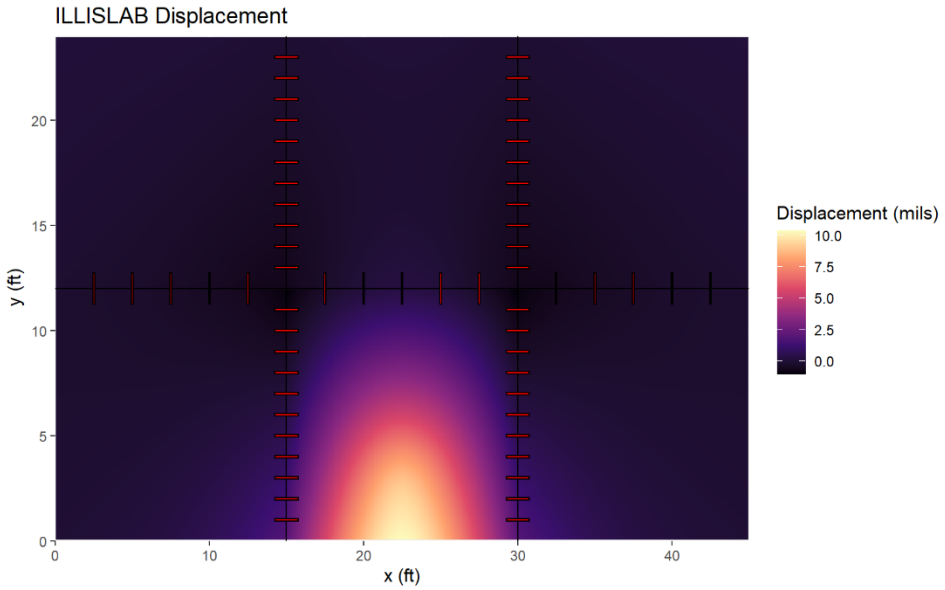

Figure 23. Example contour output from ILLISLAB.

3.3.3. Estimating Damage and Fatigue Life

Using the stress calculated from the above structural models, the allowable number of axle loads can be calculated. According to the Pavement ME model, the allowable number of load applications is the number of load cycles at which fatigue failure is expected (corresponding to 50 percent slab cracking) and is a function of the applied stress and PCC strength (AASHTO, 2015). The equation is given as the following.

$$\log N = C_1 \cdot \left(\frac{M}{\sigma} \right)^{C_2} \tag{23}$$

where N is the allowable number of load application, M is the PCC modulus of rupture, σ is the applied stress, and C_1 and C_2 are calibration coefficients. The damage due to a single load pass, D, is then calculated using Miner's hypothesis as the following.

$$D = \frac{1}{N} \tag{24}$$

To complete the above examples, the allowable number of load repetitions and the corresponding damage were calculated using the moisture-dependent k-value shown in Figure 19 and the additional inputs shown in Table 10. For this simple example, the stress was calculated using Westergaard's equation for slab interior (Equation (15)). In addition, the PCC properties were assumed to remain unchanged (i.e., the only factor affecting stresses and performance was the moisture within the foundation).

Table 10. Pavement properties assumed for structural analysis.

Variables	Value
Elastic modulus of PCC slab	4,000,000 psi
Modulus of PCC rupture	500 psi
Poisson's ratio of PCC	0.15
calibration coefficient C_1, C_2	2.0, 1.22
Wheel load	9 kips

Figure 24(a) and Figure 24(b) show the damage per pass of a 9-kip axle at the slab interior for the rainfall and flooding examples, respectively. Figure 24(a) shows that the damage starts to increase with rainfall and reaches its peak soon after the end of the 10-hour rain event. Then, the damage starts to reduce gradually as the water is drained out of the pavement, but did not fully recover at the end of the simulation. On the other hand, Figure 24(b) shows that the flooded pavement exhibits maximum damage for the first 15 hours after the water started draining from the pavement surface.

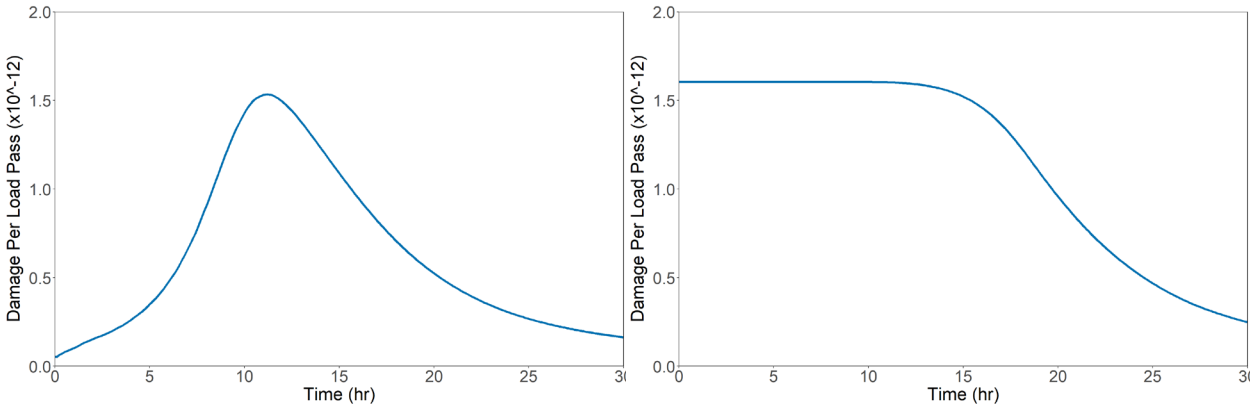

(a) (b)

Figure 24. PCC damage due to a single pass of 9-kip load for (a) rainfall example and (b) flooding example.

4. DEVELOPMENT OF FDOT'S RIGID PAVEMENT RESILIENCY TOOL

4.1. INTRODUCTION

The objectives of this study are (1) to evaluate the impact of inundation (due to flooding, sea level rise, and rainfall) on concrete pavements and (2) to identify cost-effective and implementable solutions to improve resiliency of rigid pavement systems subjected to inundation. To meet the above objectives, a Mechanistic-Empirical (ME) rigid pavement resiliency tool was developed to allow for evaluating not only the impact of inundation on Florida's rigid pavements but also the effectiveness of different strategies for improving the resiliency of rigid pavements.

The rigid pavement resiliency tool (referred to as the "Resiliency Tool" hereafter) is primarily composed of three major components. These components are (1) a hydrological model for simulating the water flow within the pavement foundation, (2) a geotechnical model for estimating the soil strength (or modulus) under different moisture conditions, and (3) a structural model for simulating the response and assessing the performance of inundated rigid pavement systems.

This chapter documents the development of the Resiliency Tool and its features, and provides example scenarios where and how the tool can be used for evaluating the effect of inundation on rigid pavement performance. A user manual for the Resiliency Tool is provided in Appendix A.

4.2. DEVELOPMENT OF THE RIGID PAVEMENT RESILIENCY TOOL

Figure 25 shows the analysis flow of the Resiliency Tool along with some of the necessary inputs for each of the ME components. The user interface of the Resiliency Tool has been developed in the Microsoft (MS) Excel environment with Visual Basic for Application (VBA) codes to allow the users to easily navigate through the inputs and outputs as well as different menu options. Figure 26 shows the top portion of the Excel interface that has been implemented.

In addition to Excel and VBA, the Resiliency Tool is also accompanied by the open source, portable-R programming language. The R language is only used for ILLISLAB, which is a finite element method (FEM) of structural analysis for rigid pavements. All of the necessary R code is stored within the VBA environment and automatically executed using the portable-R that is installed along with the Excel interface. In other words, the end user does not need to have any knowledge about R language or install R separately. However, it is emphasized that although R is generally more efficient than VBA, considering the amount of simulations and calculations needed for the FEM, the Resiliency Tool may still take a significant amount of time when the FEM is selected as the primary structural model for the analysis.

Additional description on the components and the analysis options of the Resiliency Tool are provided in the following sections of this chapter.

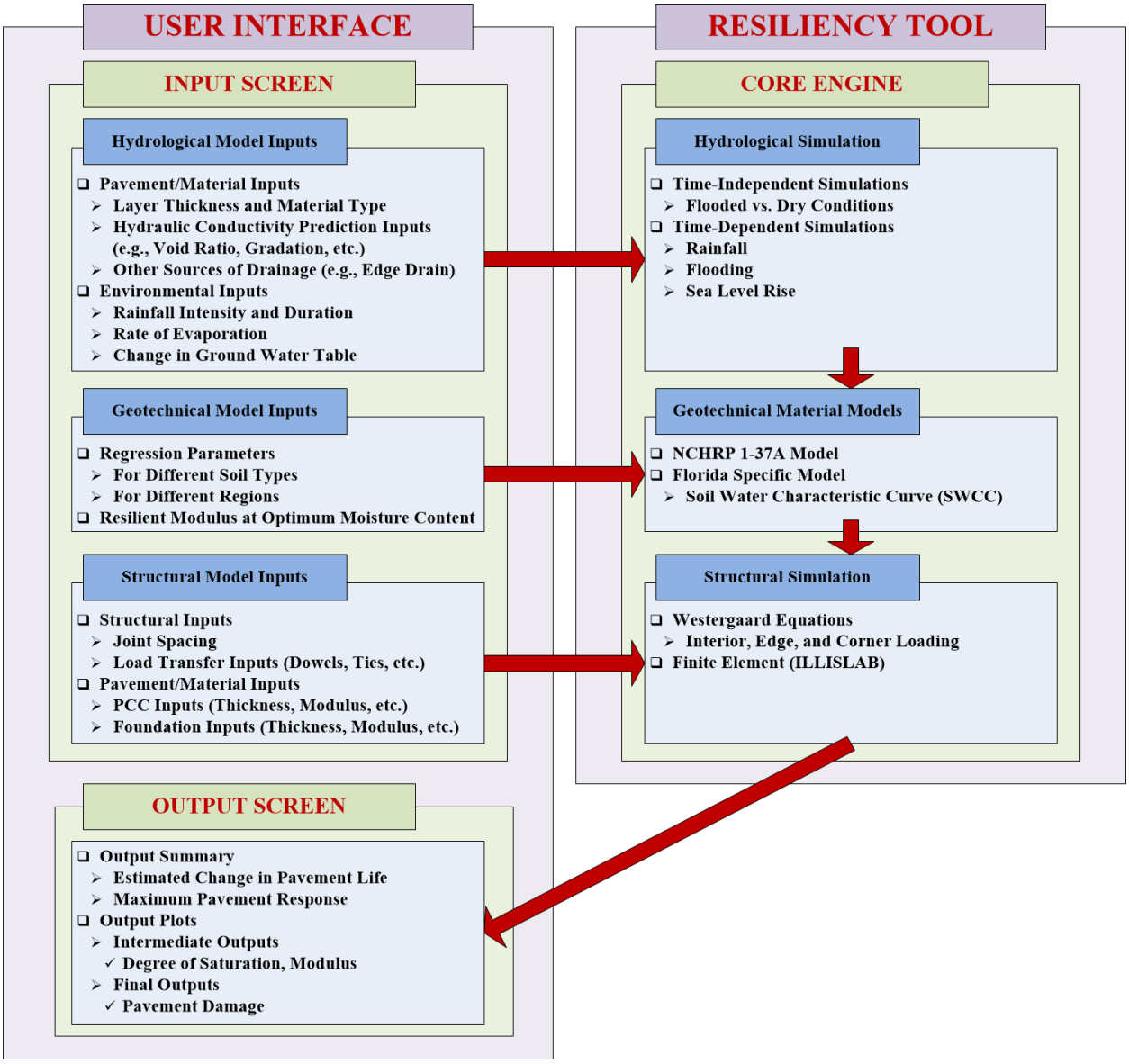

Figure 25. Analysis flow of the rigid pavement resiliency tool.

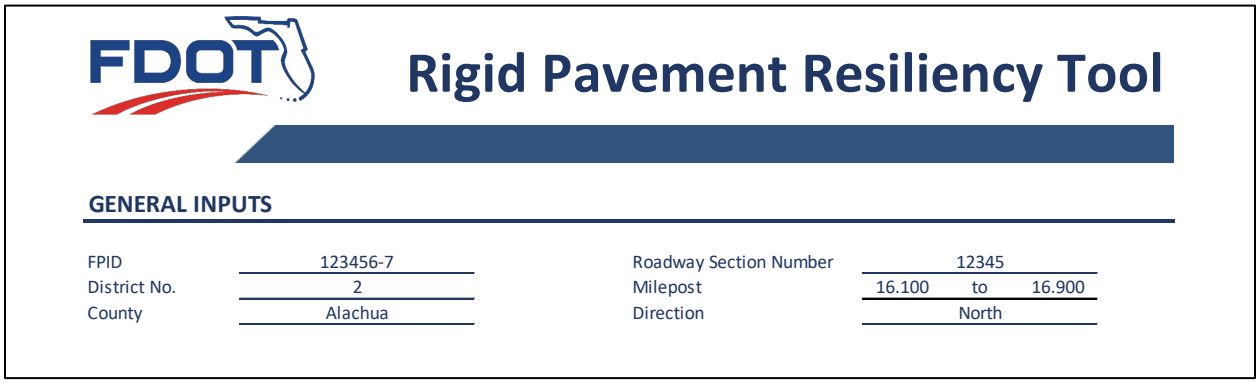

Figure 26. FDOT's rigid pavement resiliency tool interface.

4.3. RIGID PAVEMENT RESILIENCY TOOL INTERFACE AND ITS FEATURES

4.3.1. General Inputs

A screen capture of the tool interface for the general inputs was previously shown in Figure 26. These inputs are the general project-related information that defines the location of the project as well as other information pertaining to the project (i.e., similar project information as included in FDOT's nondestructive testing reports). These inputs include the financial project number (FPN), District, County, roadway section number, direction, and limiting mileposts.

4.3.2. Hydrological Analysis Options

Figure 27 shows the Resiliency Tool interface where the user may select the hydrological analysis options. The two primary analysis options are (1) Long-Term simulation and (2) Short-Term simulation. These options are described subsequently.

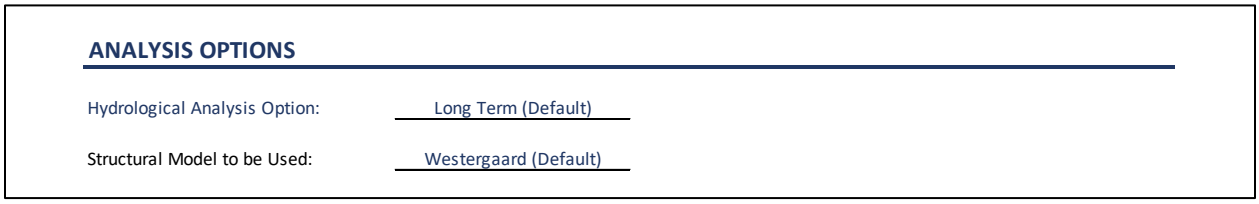

Figure 27. Selection of hydrological analysis options.

4.3.2.1. Long-Term simulation

The purpose of the Long-Term simulation is to allow the user to compare different situations that are considered to be permanent (i.e., those that do not change over a short period of time). Examples of these scenarios are provided in the following.

- Change in pavement performance under different, but permanent levels of sea level rise (e.g., 10 ft. or 5 ft.) versus no change in sea level.
- Change in pavement performance under different levels of Ground Water Table (GWT) versus no change in GWT.
- Difference in pavement life between a flooded versus non-flooded pavement (for the condition that the flooded pavement remains flooded for an extended period of time).

Note that since this type of simulation does not involve any "changes in moisture condition", the use of Richard's Equation for moisture flow within the foundation layers (described in Section 5.1 of the Task 1 report) is not required for this type of analysis. Instead, the hydrological model only involves calculating the residual moisture content for different layers of pavement foundation given the permanent moisture condition (e.g., sea level, GWT, etc.).

Figure 28 shows the additional inputs needed for the Long-Term simulation. As shown in the figure, the user may simulate different depths of Ground Water Table (GWT) with or without flooded condition. Note the following for these additional inputs.

- **Ground Water Table (GWT)**: The GWT should be specified as a depth from the "Pavement Surface" which includes the Portland Cement Concrete (PCC) thickness. The layers below the GWT are assumed to be fully saturated.

- **Flooded Condition**: If this option is selected, it assumes that all foundation layers within the pavement are fully saturated (i.e., degree of saturation is equal to 1.0).

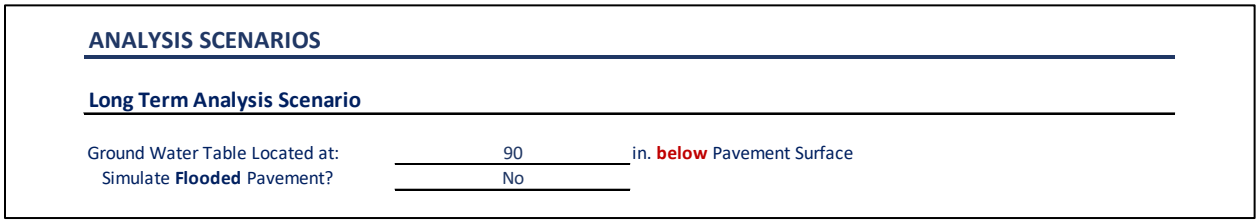

Figure 28. Long-term simulation inputs.

4.3.2.2. Short-Term simulation

The Short-Term simulation is intended for simulating a pavement structure experiencing changes in moisture level within a relatively short period of time (i.e., within a few hours, days, or weeks). Examples of these scenarios are provided as the following.

- Reduction in pavement life due to a severe rainfall combined with traffic loading.
- Recovery of a flooded pavement due to evaporation and other sources of drainage.

The short-term simulation requires the use of Richard's Equation for estimating the vertical flow of water through the pavement foundation layers over time. As such, it also requires the appropriate initial conditions (e.g., rainfall intensity, GWT level at the beginning of simulation, etc,) as shown in Figure 29. Additional information is provided in the following for these inputs.

- **Ground Water Table (GWT)**: The GWT should be specified as a depth from the "Pavement Surface" which includes the PCC thickness. The layers below the GWT are assumed to be fully saturated.

- **Flooded Condition**: If this option is selected, the analysis starts with a flooded pavement draining naturally. To provide any additional drainage at the pavement surface (i.e., evaporation), a drainage rate should be specified in the "Rainfall / Evaporation" table with a negative number.

ANALYSIS OPTIONS

Hydrological Analysis Option: Short Term

Structural Model to be Used: Westergaard (Default)

ANALYSIS SCENARIOS

Short Term Analysis Scenario

Ground Water Table Located at: 90 in. **below** Pavement Surface

Start with **Flooded** Pavement? No

Time Duration for Analysis 30 hr(s)

Time Interval for Analysis, Δt 0.1 hr(s)

Run Short-Term Analysis

Rainfall / Evaporation

Rain Event	Starting Time (hr)	Ending Time (hr)	Rainfall Intensity (in/hr)
Event No. 1	0.0	5.0	5.0
Event No. 2	10.0	15.0	2.0
Event No. 3			
Event No. 4			
Event No. 5			

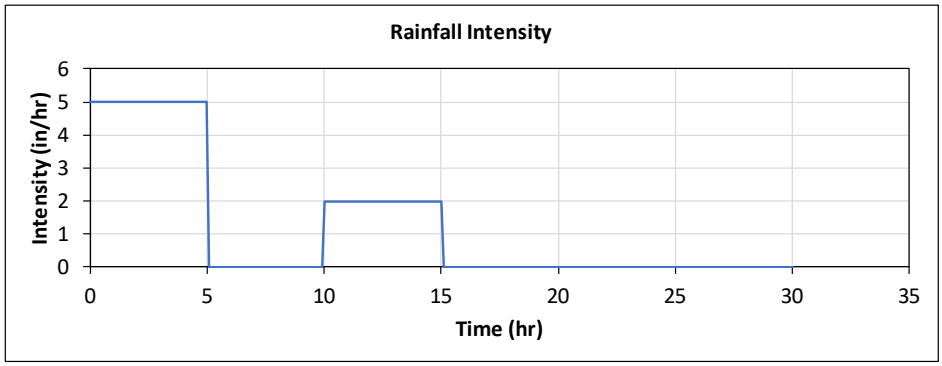

Figure 29. Short-term simulation inputs.

4.3.3. Mechanistic-Empirical Transfer Coefficients

The empirical equation for calculating the allowable number of load passes (N_f) is shown in Figure 30. The default coefficients shown in the figure correspond to those from the AASHTOWare Pavement ME (AASHTO, 2015).

TRANSFER FUNCTION COEFFICIENTS

C_1 = 2 C_2 = 1.22 N_f Equation: $\log N = C_1 \cdot \left(\frac{M}{\sigma}\right)^{C_2}$

Figure 30. Transfer function inputs.

4.3.4. Portland Cement Concrete (PCC) Layer and External Load Input

There are two structural models built into the Resiliency Tool. These models are (1) Westergaard's equations and (2) the ILLISLAB FEM model. The structural model for the analysis can be selected from the "Analysis Options" menu (Figure 27).

The PCC layer inputs as well as the external load inputs for the respective analysis options are described in the following sections.

4.3.4.1. Analysis Using Westergaard Equations

The PCC inputs needed for the Westergaard equations are the **thickness, elastic modulus (i.e., Young's modulus), and Poisson's ratio** (see Figure 31). Note that the **PCC modulus of rupture (*M*)** is not a direct input for the Westergaard equations, but it is needed for calculating the N_f using the transfer function shown in Figure 30.

Since Westergaard equations are applicable for circular loads, it is necessary to input the **load radius and the load magnitude** for the structural analysis.

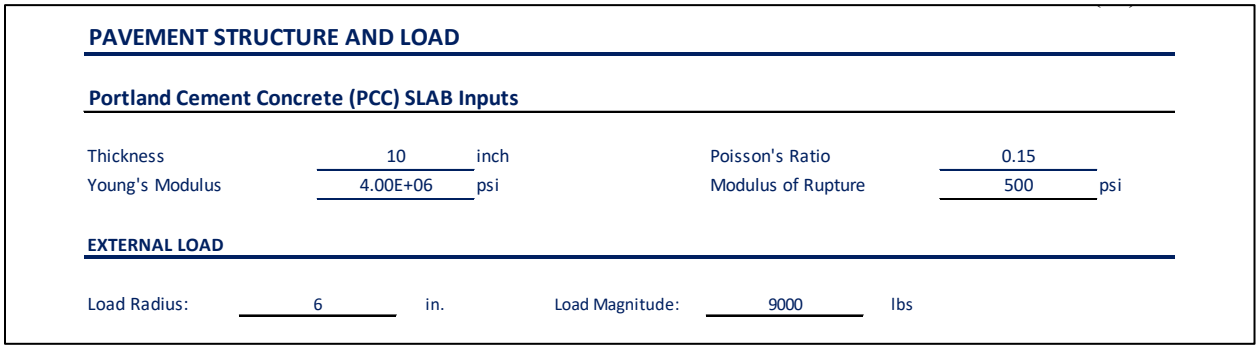

Figure 31. PCC and external load inputs for Westergaard equations.

4.3.4.2. Analysis Using ILLISLAB FEM

Prior to discussing the inputs for ILLISLAB, the readers (and the users) are warned that the FEM code may take a significant amount of time to finish running, especially for the Short-Term analysis, where the structural model needs to be evaluated for each time step.

The PCC and load related inputs are shown in Figure 32, and include most of the basic inputs (e.g., modulus) discussed previously. Additional inputs needed for ILLISLAB analysis are described as the following.

- **Unit weight of PCC** and **coefficient of thermal expansion (α)** of PCC material – these inputs are needed for simulating the PCC slab response under thermal load (i.e., curling).
- **Joint Locations** – the first joint location has to be at 0.0 ft. for both joint types.

- **Transverse joint locations** define the slab dimensions in the direction of travel. The example shown in Figure 32 corresponds to 3 slabs in the travel direction, each having a length of 15 ft.

- **Longitudinal joint locations** define the slab dimensions in the lateral direction (e.g., for different lanes and/or shoulder). The example shown in Figure 32 defines 2 slabs in the lateral direction, each having a width of 12 ft.

PAVEMENT STRUCTURE AND LOAD

Portland Cement Concrete (PCC) SLAB Inputs

Thickness	10	inch	Unit Weight	150	lb/ft^3
Modulus	4.00E+06	psi	Coeff. of Thermal Expansion	4.90E-06	in/in/deg.F
Poisson's Ratio	0.15		Modulus of Rupture	500	psi

Joint Locations

Joint No.	1	2	3	4	5	6	7	8	9	10	11	12
Trans. Joints (ft)	0	15	30	45								
Longi. Joints (ft)	0	12	24									

Joint locations also define the Number of Slabs and Slab Dimensions.

LOAD TRANSFER

TRANSVERSE JOINTS

Aggregate Interlock:	10000	psi
Dowel Bar Diameter	1.5	inch
Dowel Bar Modulus	2.90E+07	psi
Dowel Bar Poisson's Ratio	0.1	--
Joint Opening	0.1	inch
Az	0.9	--

LONGITUDINAL JOINTS

Aggregate Interlock:	10000	psi
Tie Bar Diameter	0.63	inch
Tie Bar Modulus	2.90E+07	psi
Tie Bar Poisson's Ratio	0.1	--
Joint Opening	0.1	inch
Az	0.9	--

Load Transfer No.	1	2	3	4	5	6	7	8	9	10	11	12
Dowel Locations	1	2	3	4	5	6	7	8	9	10	11	
Tie Locations	2.5	5	7.5	10	12.5							

Notes:
1. Location of Dowels & Ties only need to be defined for the slab at the lower left corner
2. Do NOT delete the Dowel & Tie Locations. If you do not have dowels, then set the dowel modulus to ZERO

EXTERNAL & THERMAL LOADS

EXTERNAL LOADS

Load ID	1	2	3	4	5	6	7	8	9	10	11	12
Magnitude (lb)	4500	4500	4500	4500								
X.Coord (ft)	22.5	22.5	22.5	22.5								
X.Length (ft)	0.6	0.6	0.6	0.6								
Y.Coord (ft)	2	3	9	10								
Y.Length (ft)	0.6	0.6	0.6	0.6								

THERMAL LOAD Linear Temperature Gradient (Ttop - Tbottom) 0 deg.F

Figure 32. PCC and external load inputs for ILLISLAB.

- **Load Transfer** – there are two types of load transfer mechanisms modeled in ILLISLAB as discussed below.

- **Dowel bars** (for transverse joints) and **tie bars** (for longitudinal joints) must be specified by the diameter, elastic modulus, and Poisson's ratio of the dowel/tie bar materials (usually steel).

  The dowel and tie bar locations must be specified for the first PCC slab located at the bottom-left corner (see Figure 33), even if there are no dowel and tie bars. This is because these dowel and tie locations are also used to develop the basic FEM mesh for the PCC slabs.

  Note: If there are no dowel bars or tie bars, the modulus of the bar material should be set to zero.

- **Aggregate Interlock** should be specified in the same unit as modulus, i.e., in psi.

- **External Loads** – up to a total of 12 external loads (or tires) can be specified in ILLISLAB, each having a rectangular contact area. As shown in Figure 32, the load magnitude as well as the center coordinates and their length in both the X and Y directions need to be specified for each load.

- **Thermal Load** can be specified using a linear thermal gradient (ΔT) within the PCC layer, which is calculated as the difference in temperature between the top (T_{top}) and the bottom (T_{bottom}) of the PCC (i.e., $\Delta T = T_{top} - T_{bottom}$).

Figure 33 shows an example of the FEM mesh generated based on the sample inputs provided in Figure 32.

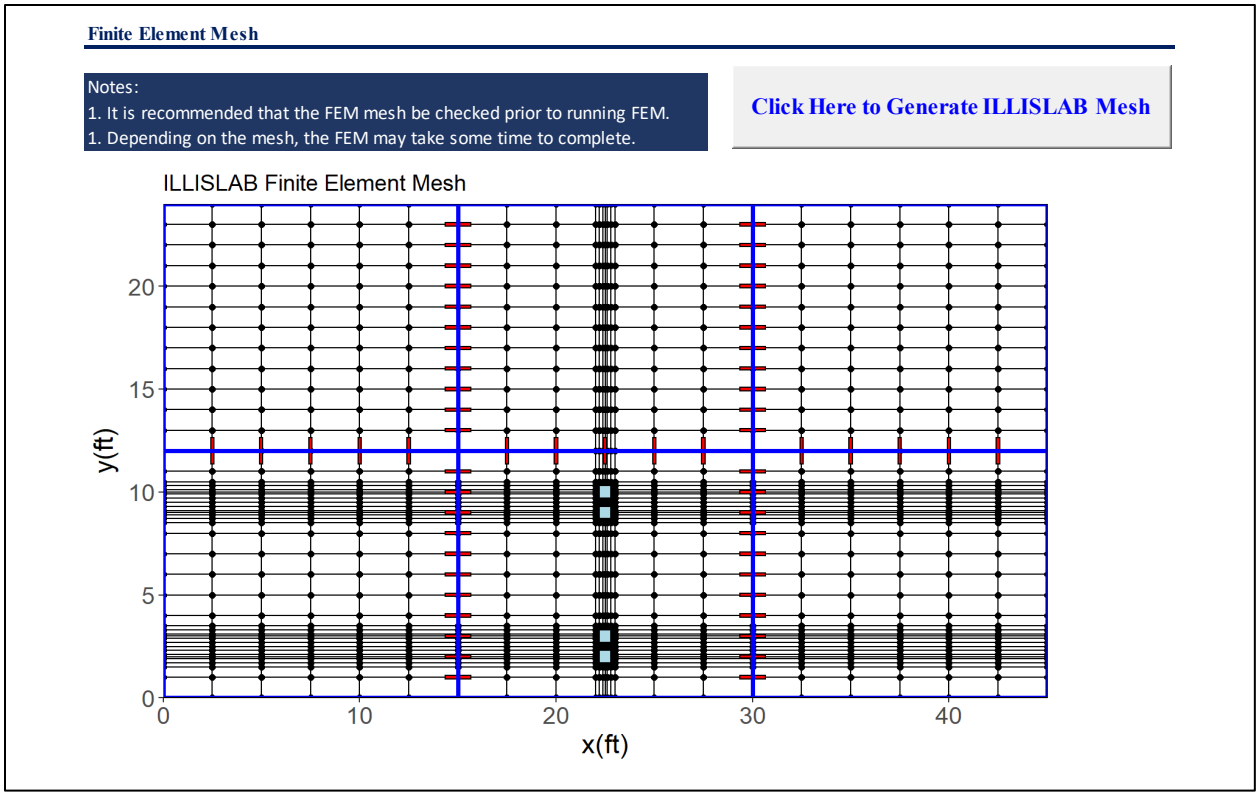

Figure 33. Finite element mesh generated from ILLISLAB.

4.3.5. Foundation Layer Inputs

As discussed in the previous chapter, the foundations under the rigid pavement structure are characterized using the composite modulus of subgrade reaction (i.e., k-value) in both the Westergaard equations and the FEM. As such, the user may choose to use a constant k-value for the analysis, as shown in Figure 34. It should be noted that this option is only available for the Long-Term analysis where the foundation properties do not change within the analysis.

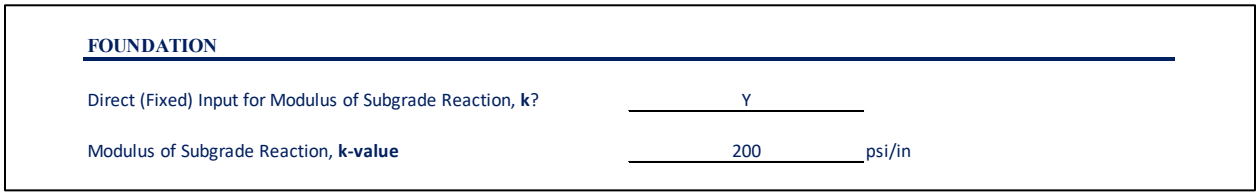

Figure 34. Manual input of the k-value.

In addition to the above, the user may use the k-value that is calculated from other foundation-related input parameters such as the moisture content, modulus, etc. This option is available for both the Short-Term and Long-Term analyses. Figure 35 shows an example including the total thickness and the modulus of the transformed foundation layers (using Odemark's method), as well as the corresponding k-value.

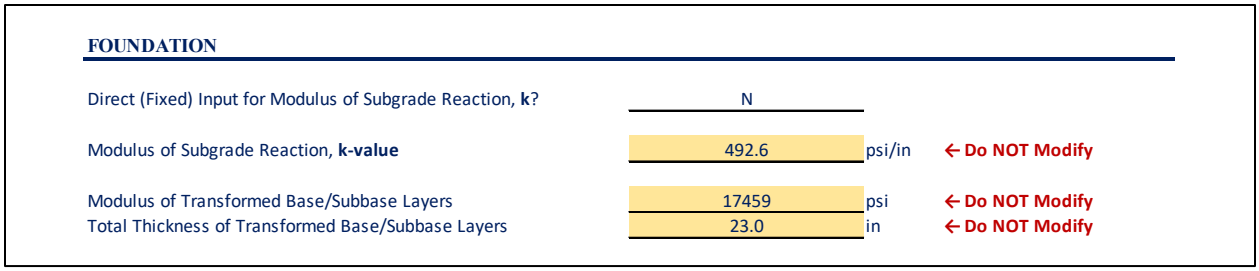

Figure 35. Calculating the k-value from foundation modulus.

4.3.5.1. Available Material Types

For calculating the k-value from the layer modulus that may change with moisture content, the user is provided with several base/subbase types that are frequently used by FDOT. These foundation layers are described in the following.

Asphalt Base

The primary inputs needed for the asphalt base include the layer thickness, resilient modulus, and Poisson's ratio, as shown in Figure 36.

In addition, the user must provide the necessary inputs for the hydraulic analysis which include the **saturated and residual volumetric water contents** (θ_{sat} and θ_R, respectively) as well as the coefficients for the Van Genuchten equation shown in Figure 36.

If known, the user may choose to input a fixed value for the **hydraulic conductivity** of the asphalt material, as shown in Figure 36. It is also possible to estimate the hydraulic conductivity from the gradation and other mixture parameters, as discussed in the following paragraphs.

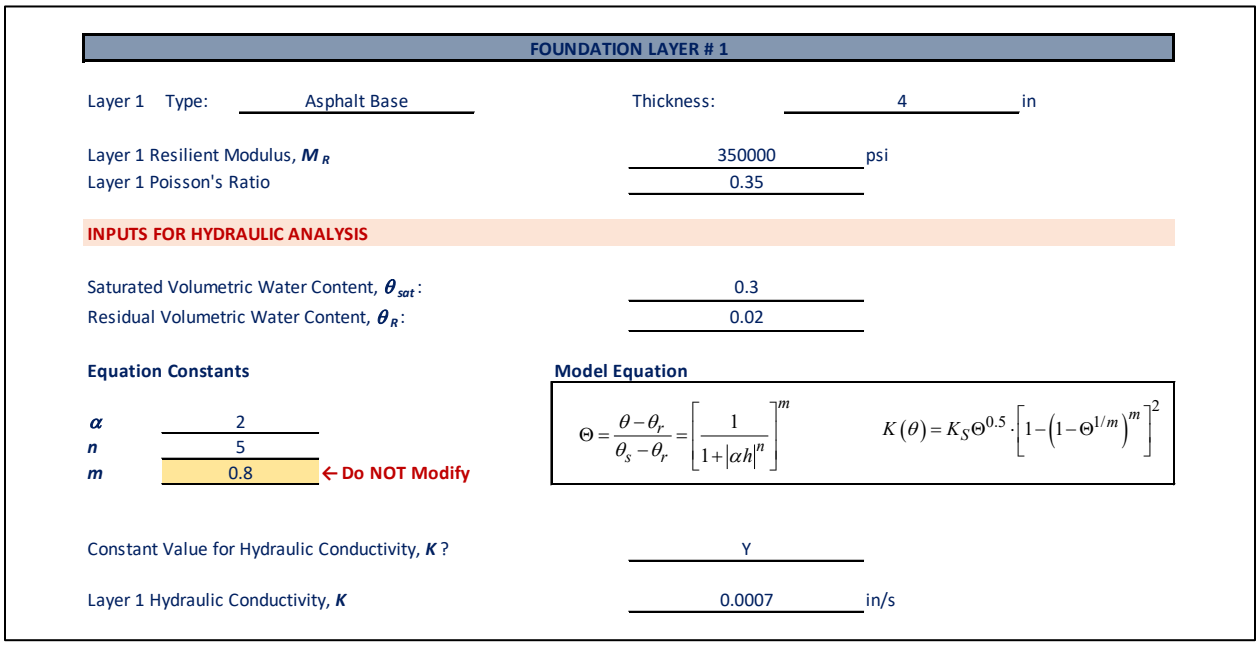

Figure 36. Basic inputs for asphalt base with constant hydraulic conductivity.

There are two different models built into the Resiliency Tool for estimating the hydraulic conductivity of asphalt concrete from mix design inputs. These models are the Masad model (Masad et. al., 2006) and the Mohammad model (Mohammad et. al., 2003) that were previously discussed in Chapter 2.

Figure 37 and Figure 38 show the input screens for the Masad and Mohammad models, respectively. For the gradation input, only the percent passing column needs to be filled in by the user – which can be easily pasted from FDOT's typical mix design spreadsheets. In addition to gradation, the user needs to provide the additional inputs for the respective models that include air voids (which is the only additional input needed for Mohammad model), binder content, specific gravity, etc.

It is also observed that the hydraulic conductivity from the Masad model (Figure 37) is significantly higher than from the Mohammad model (Figure 38) for the same mixture shown in the figures. Although further calibration of these models may reduce the gap between them, such effort is beyond the scope of this study. At the time of this writing, it is recommended that the Mohammad model be used for asphalt permeability (i.e., hydraulic conductivity), since this model provided the results that are in the range reported by FDOT (Lee and Ayyala, 2020).

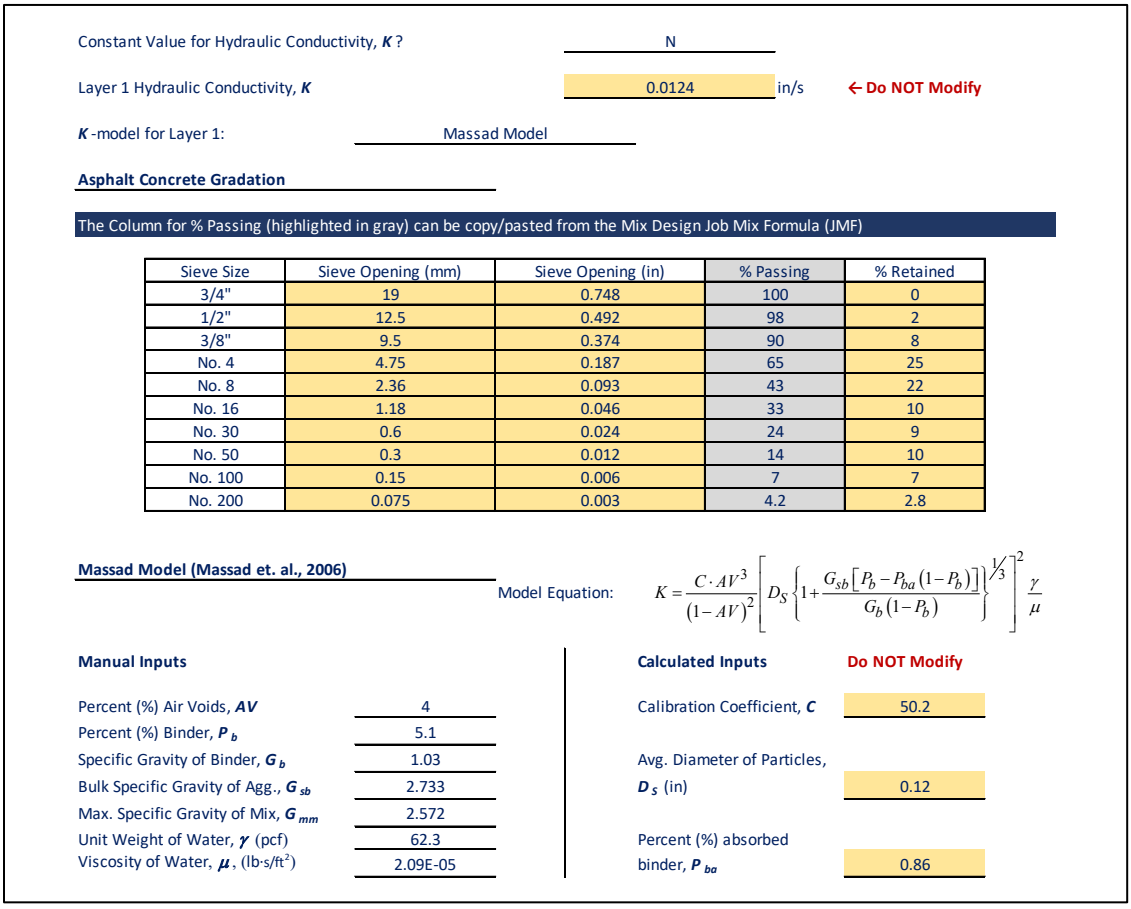

Constant Value for Hydraulic Conductivity, *K*? N

Layer 1 Hydraulic Conductivity, *K* 0.0124 in/s ← Do NOT Modify

K-model for Layer 1: Massad Model

Asphalt Concrete Gradation

The Column for % Passing (highlighted in gray) can be copy/pasted from the Mix Design Job Mix Formula (JMF)

Sieve Size	Sieve Opening (mm)	Sieve Opening (in)	% Passing	% Retained
3/4"	19	0.748	100	0
1/2"	12.5	0.492	98	2
3/8"	9.5	0.374	90	8
No. 4	4.75	0.187	65	25
No. 8	2.36	0.093	43	22
No. 16	1.18	0.046	33	10
No. 30	0.6	0.024	24	9
No. 50	0.3	0.012	14	10
No. 100	0.15	0.006	7	7
No. 200	0.075	0.003	4.2	2.8

Massad Model (Massad et. al., 2006)

Model Equation: $K = \frac{C \cdot AV^3}{(1-AV)^2}\left[D_S\left\{1+\frac{G_{sb}\left[P_b - P_{ba}(1-P_b)\right]}{G_b(1-P_b)}\right\}^{1/3}\right]^2 \frac{\gamma}{\mu}$

Manual Inputs		**Calculated Inputs**	**Do NOT Modify**
Percent (%) Air Voids, *AV*	4	Calibration Coefficient, *C*	50.2
Percent (%) Binder, P_b	5.1		
Specific Gravity of Binder, G_b	1.03	Avg. Diameter of Particles,	
Bulk Specific Gravity of Agg., G_{sb}	2.733	D_S (in)	0.12
Max. Specific Gravity of Mix, G_{mm}	2.572		
Unit Weight of Water, γ (pcf)	62.3	Percent (%) absorbed	
Viscosity of Water, μ, (lb·s/ft^2)	2.09E-05	binder, P_{ba}	0.86

Figure 37. Input screen for calculating asphalt base hydraulic conductivity using Masad Model .

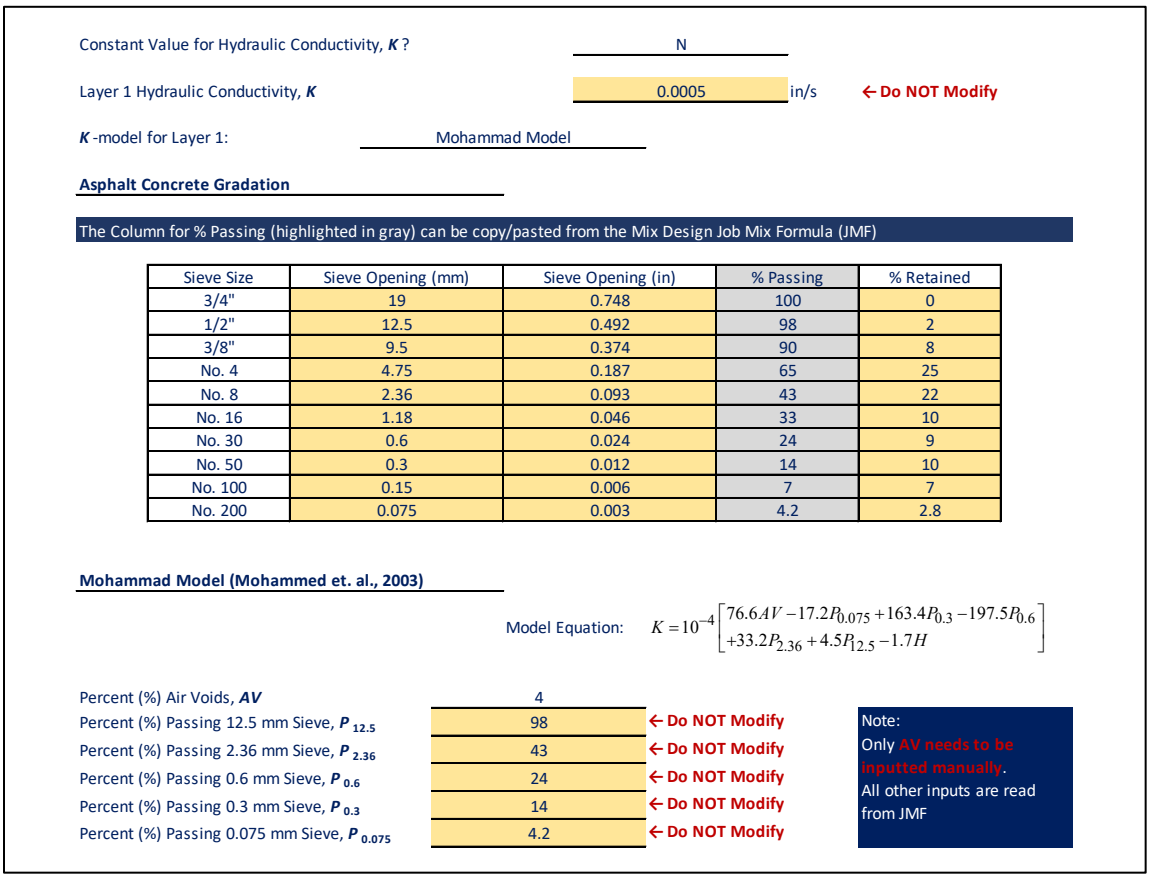

Figure 38. Input screen for calculating asphalt base hydraulic conductivity using Mohammad Model.

Coarse-Grained Soil

For coarse-grained soils, the hydraulic conductivity model developed by Chapuis (2004) has been implemented into the Resiliency Tool. The corresponding input screen is shown in Figure 39. It is recommended that this model be used for FDOT's stabilized subbase and in areas with coarse-grained subgrade materials (i.e., A-1 through A-3 soils according to AASHTO classification).

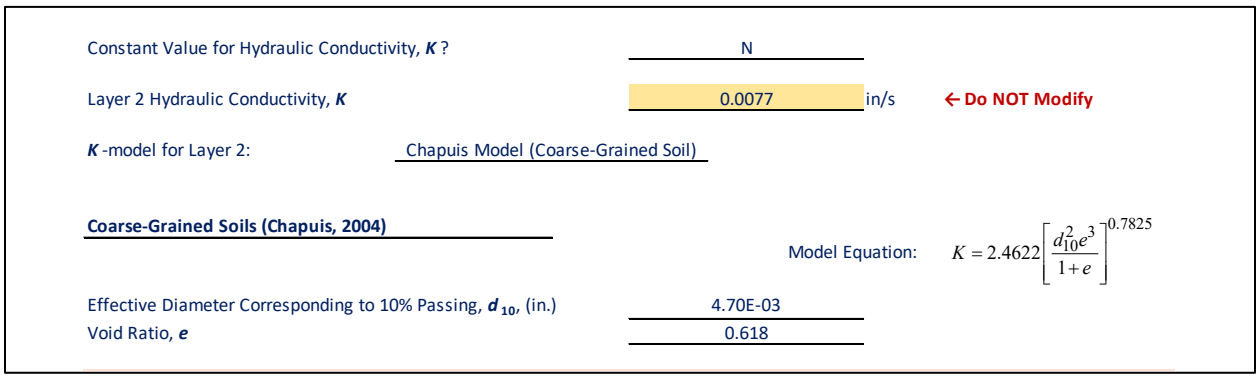

Figure 39. Inputs for hydraulic conductivity of coarse-grained soils.

Fine-Grained Soil

For fine-grained soils (i.e., AAASHTO classifications A-4 through A-8), the Resiliency Tool incorporates the prediction equation developed by Mbonimpa et al. (2002) for hydraulic conductivity. The input screen for this model is shown in Figure 40.

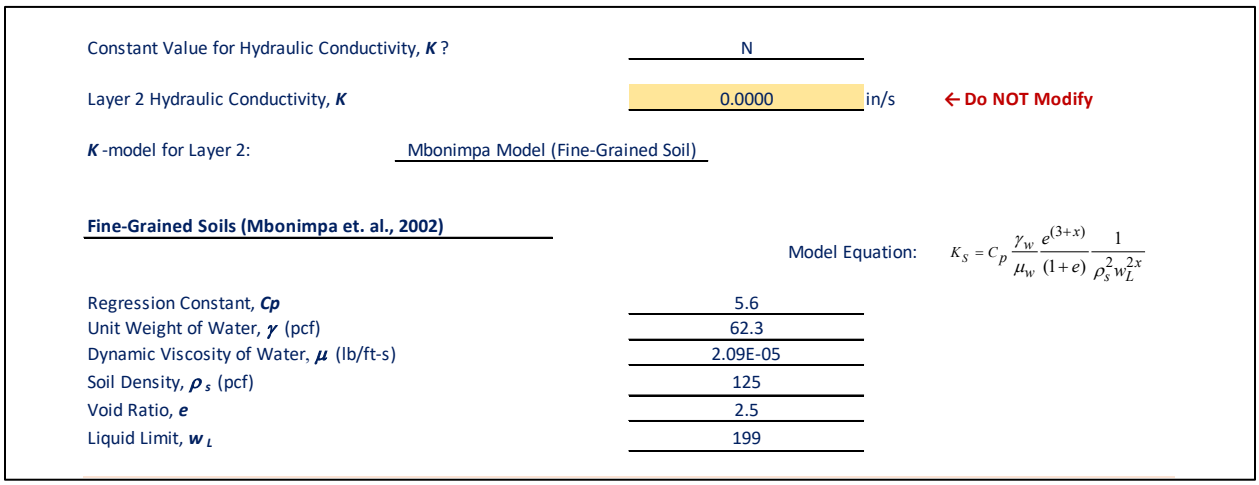

Figure 40. Inputs for hydraulic conductivity of fine-grained soils.

4.3.6. Foundation Layer Modulus

The change in foundation modulus due to change in moisture content (or degree of saturation) can be assessed using one of the two models implemented into the Resiliency Tool. These models are the NCHRP 1-37A model and the Soil-Water Characteristic Curve (SWCC) model.

4.3.6.1. NCHRP 1-37A Model

The NCHRP 1-37A model (ARA, 2000) provides a simple means for estimating the change in soil's resilient modulus as a function of degree of saturation, *S*. The equation as well as the inputs needed for this model are shown in Figure 41.

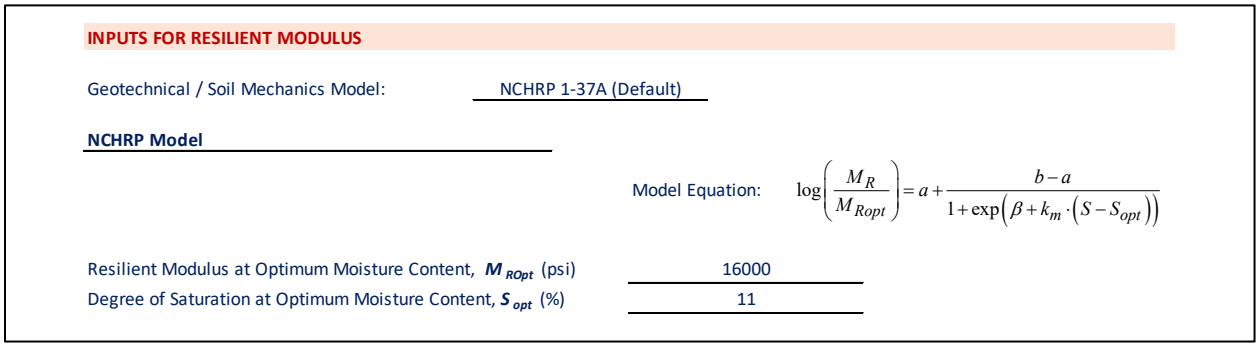

Figure 41. Inputs for NCHRP 1-37A resilient modulus model.

It should be noted that the user only needs to input the **resilient modulus and the degree of saturation at the soil's optimum water content (M_{Ropt} and S_{opt}, respectively)**. The remaining regression coefficients, i.e., a, b, β, and k_m are built into the spreadsheet for the appropriate soil types (coarse vs. fine).

4.3.6.2. Soil-Water Characteristics Curve (SWCC) Model

Figure 42 shows the equations as well as the necessary inputs needed for the SWCC model that was tailored to Florida's soils by Oh and Fernando (2011) and Oh et. al. (2012).

Prior to further discussion on the model inputs, it is emphasized that using the SWCC model requires iteration for finding the soil suction (S_c) for a given volumetric water content (θ) – from the equations shown at the bottom of Figure 42. In other words, the SWCC model is not as efficient as the NCHRP 1-37A model and may require a long time to run the analysis (especially for the Short-Term analysis).

INPUTS FOR RESILIENT MODULUS

Geotechnical / Soil Mechanics Model: SWCC

Florida Soil Water Characteristic Curve (SWCC) Model:

Select a District to Load Defaut Coefficients: D1

Stresses (psi)			MR Model Coefficients				SWCC Coefficients			
Atm	Bulk	Oct. Sh.	k1	k2	k3	k4	af	bf	cf	hr
14.7	6.7	0.9	1352.7	1.0	-0.3	0.8	1.9	0.8	2.8	99.5

MR Model: $$M_R = k_1 P_a \left(\frac{\sigma_{bulk} + 3k_4 S_c \theta}{P_a} \right)^{k_2} \left(\frac{\tau_{oct}}{P_a} + 1 \right)^{k_3}$$

SWCC Model: $$\theta = C(S_c) \left[\frac{\theta_{sat}}{\left\{ \ln\left(e^1 + \left(S_c / a_f \right)^{b_f} \right) \right\}^{c_f}} \right] \quad \text{where} \quad C(S_c) = \left[1 - \frac{\ln\left(1 + (S_c / h_r)\right)}{\ln\left(1 + \left(1.45 \times 10^5 / h_r\right)\right)} \right]$$

Figure 42. Inputs for SWCC resilient modulus model.

According to the previous studies conducted by Oh and Fernando (2011) and Oh et. al. (2012), it was recommended that the **SWCC model coefficients a_f, b_f, c_f, and h_r** shown in Table 11 be used for Florida's limerock base, stabilized subgrade, and embankment materials.

However, the above referenced FDOT research reports did not provide the representative **coefficients for the stress-dependent resilient modulus model (i.e., k_1 through k_4 in the top equation of Figure 42)**. Furthermore, since the previous research was focused on flexible pavements, the representative **bulk (σ_{bulk}) and octahedral shear (τ_{oct}) stresses** were not made available for use with rigid pavements.

To develop the default coefficients for the stress-dependent resilient modulus model, the data made available in Appendix D of the FDOT report by Oh and Fernando (2011) were extracted,

and the coefficients corresponding to the average of the available test data were calculated. This effort was repeated for all material types and FDOT Districts shown in Table 11. As an example, Figure 43 shows the stress-dependent modulus model for the embankment material in District 5. The average coefficients (i.e., the default values for k_1 through k_4) in this manner are shown in Table 12.

Table 11. SWCC Model Parameters for Florida Specific Model (From Oh and Fernando, 2011)

Material	District	SWCC Model Coefficients			
		a_f (psi)	b_f	c_f	h_r (psi)
Limerock Base	All Districts	5.652	0.950	0.800	100.200
Stab. Subgrade	All Districts	5.606	0.478	2.865	99.672
Embankment	1	1.858	0.828	2.804	99.479
	2	3.446	0.884	2.811	100.090
	3	6.585	1.210	3.430	99.952
	4	3.160	0.869	3.430	99.946
	5	3.009	0.640	4.223	100.748
	6	8.111	10.044	1.068	99.728
	7	1.363	0.746	3.343	100.765

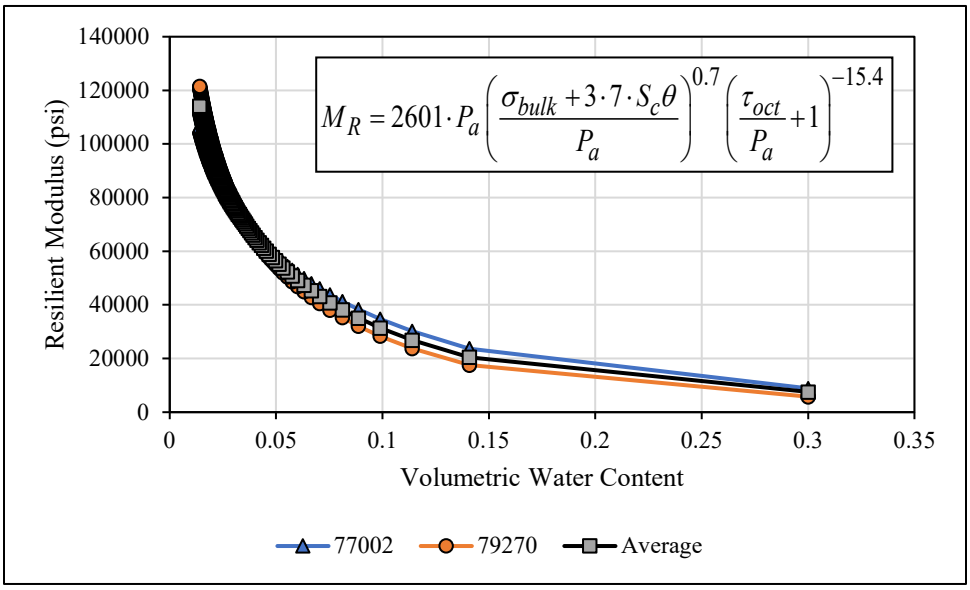

Figure 43. Fitting of stress-dependent resilient modulus model (for embankment material in District 5).

Table 12. Stress-dependent resilient modulus model parameters

Material	District	Model Coefficients			
		k_1	k_2	k_3	k_4
Limerock Base	All Districts	1,047.5	1.0	-0.4	2.4
Stab. Subgrade	All Districts	861.3	0.8	6.6	0.2
Embankment	1	1,352.7	1.0	-0.3	0.8
	2	1,123.8	0.6	-0.2	0.8
	3	543.9	0.9	-0.2	0.1
	4	15,801.6	0.8	-46.3	2.0
	5	2,601.5	0.7	-15.4	7.0
	6	15,801.6	0.8	-46.3	2.0
	7	703.0	1.0	6.1	0.2

The default values for the bulk and octahedral shear stresses were obtained by simulating a typical pavement structure in a Layered Elastic Analysis (LEA) program, known as KenLayer. Table 13 shows the pavement structure simulated in KenLayer. The external load was modeled to be a circular load with a magnitude of 9.0 kips and a radius of 6.0 in.

Table 13. Pavement structure for simulating bulk and octahedral shear stresses

Layer	Elastic Modulus (ksi)	Poisson's Ratio	Thickness (in)	Unit weight (pcf)
PCC	4000	0.15	10.0	145
AC Base	350	0.35	4.0	140
Stabilized Subgrade	16	0.40	12.0	135
Embankment	16	0.45	∞	110

As outlined in Oh and Fernando (2011), the corresponding bulk and octahedral shear stresses were calculated under the combination of the external load mentioned above and the gravimetric load (i.e., overburden). The stresses calculated at the mid-depth of the stabilized subgrade and at 12 in. depth of the embankment are summarized in Table 14.

Table 14. Default values for bulk and octahedral shear stresses

Layer	Bulk Stress, σ_{bulk} (psi)	Shear Stress, τ_{oct} (psi)
Stabilized Subgrade	4.6	0.8
Embankment	6.7	0.9

Note that for the embankment layer (i.e., Foundation Layer No. 7 in the Resiliency Tool), the default values for the SWCC coefficients (Table 11) as well as the resilient modulus model coefficients (Table 12) depend on FDOT's District. These default values can be loaded by selecting the District number (e.g., "D1") in the input screen shown in Figure 42. The default values for stabilized subgrade and special soil (that are independent of FDOT's District) are loaded when the material is first selected.

4.4. ANALYSIS RESULTS

Once the analysis is completed, the user can scroll down within the same worksheet to see the results. The results displayed on the worksheet depend on the analysis options, as discussed in the following sections.

4.4.1. Long-Term Analysis Results

As mentioned previously, the long-term analysis does not involve any changes in the moisture condition of the foundation layers. As such, the results of the long-term analyses are independent of time, and the hydrological model is only used to calculate the moisture condition at the prescribed (i.e., permanent) condition.

4.4.1.1. Hydrologic Equilibrium and Resilient Modulus Results (Long-Term)

Figure 44 shows an example of the hydrologic analysis results provided for the long-term analysis option. As shown in this figure, the results include two plots.

The first plot on the left shows the degree of saturation for the foundation layers at the state of hydrological equilibrium. The second plot on the right shows the resilient modulus of the foundation layers corresponding to the degree of saturation shown on the left. Note that both these plots show the results from the bottom of the PCC layer (i.e., depth of 0.0 in. in the plot) to the top of the GWT.

The user can also access the data used for plotting these results from the worksheet named "Long-Term".

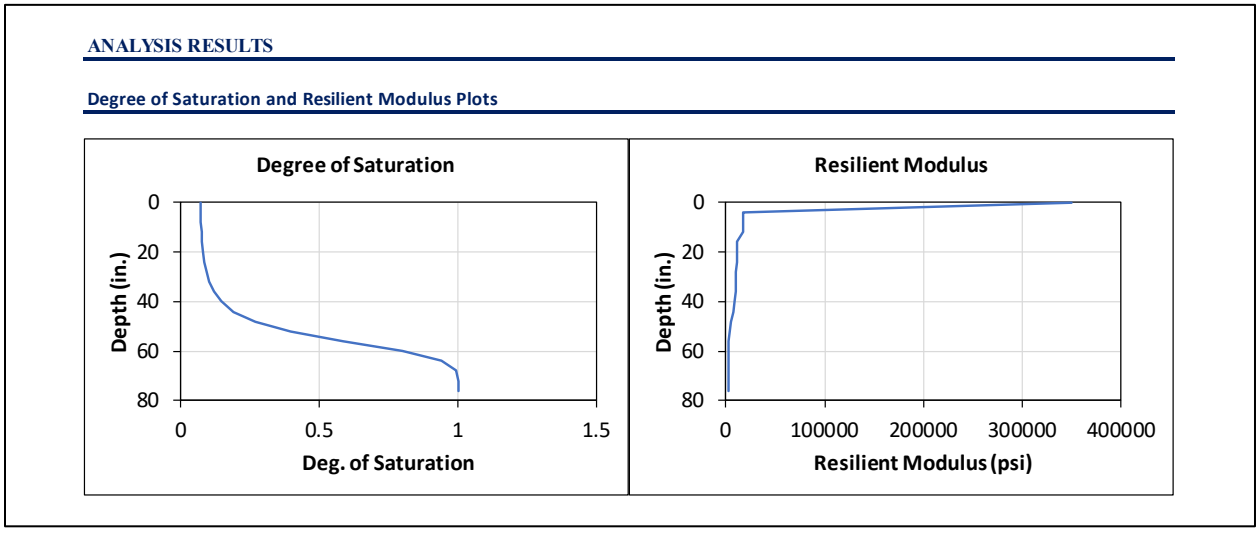

Figure 44. Long-term analysis results using Westergaard equations.

4.4.1.2. Westergaard Results (Long-Term)

When the Westergaard equations are selected for the structural analysis option, the Long-Term analysis results are provided instantaneously (i.e., there are no buttons that need to be clicked to see the results).

The structural analysis results are provided in a table format (see Figure 45) below the hydrologic results. The results include the maximum deflection and tensile stresses obtained from the Westergaard equations, as well as the maximum allowable number of load repetitions (N_f) and the damage corresponding to a single pass of the load ($1/N_f$).

Structural Model Results

Parameters	Interior	Edge	Corner
Deflection (mils)	2.7	9.5	18.5
Stress (psi)	109.7	155.5	399.6
Nf	5.4E+12	2.1E+08	4.3E+02
Damage (1/Nf)	1.9E-13	4.8E-09	2.3E-03

Figure 45. Long-term analysis results using Westergaard equations.

4.4.1.3. ILLISLAB Results (Long-Term)

Figure 46 shows an example of the Long-Term analysis results from ILLISLAB.
Unlike the Westergaard option, the ILLISLAB results are not automatically populated by the tool. To obtain the structural results from ILLISLAB, the user must specify the **locations within the PCC slab (X and Y coordinates as well as the depth)** where the responses are to be extracted from the FEM solution. Then the user needs to click on the "Click Here to Run ILLISLAB" button, which calls the Portable-R and runs the FEM solution.

Once the FEM analysis completes, the ILLISLAB results (i.e., deflections, stresses, and the corresponding N_f and damage values) for the specified locations can be loaded into the spreadsheet by clicking on the "Import ILLISLAB Results" button.

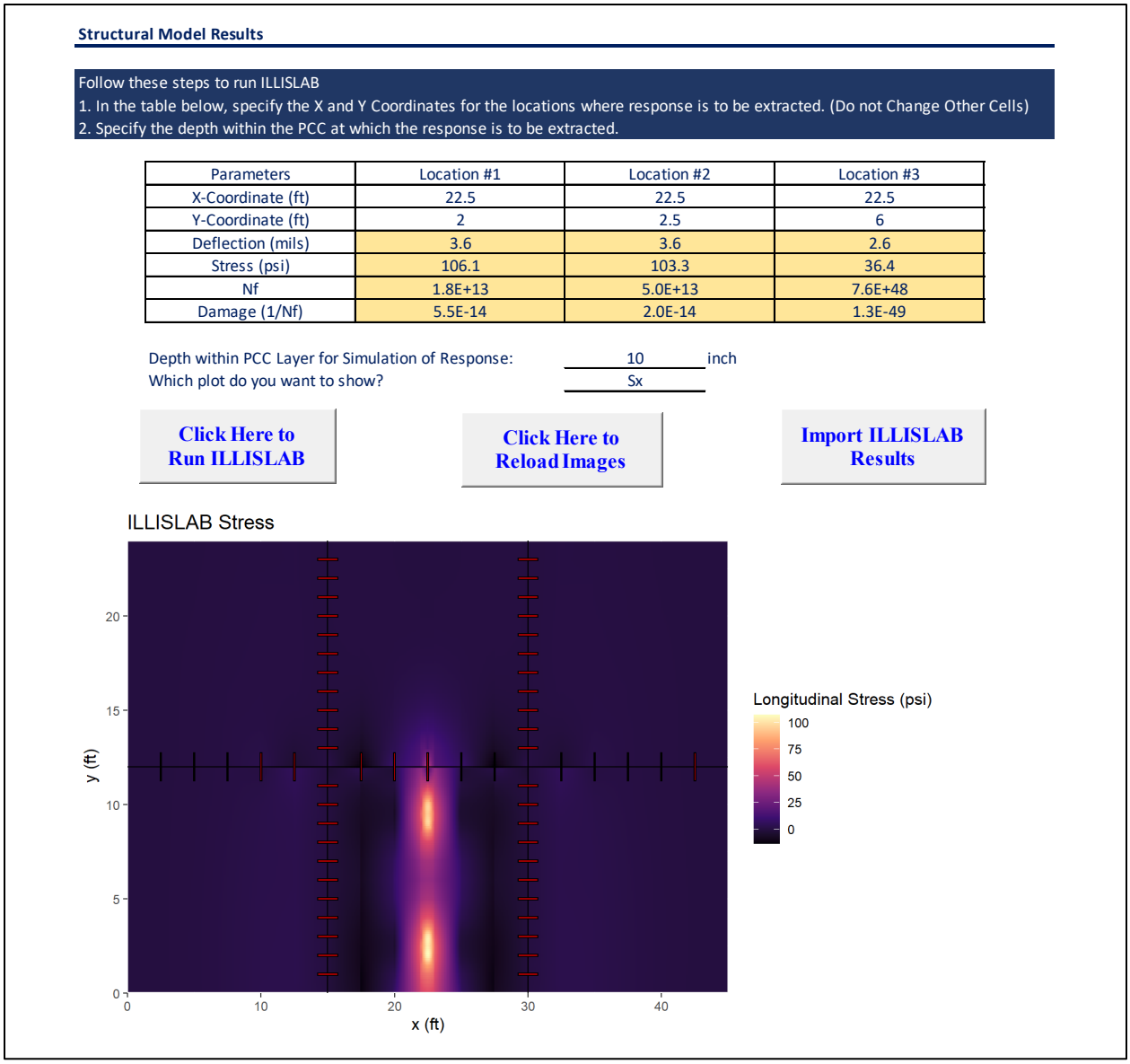

Figure 46. Long-term analysis results rsing ILLISLAB.

4.4.2. Short-Term Analysis Results

The Short-Term analysis involves simulating the moisture flow within the pavement foundation over the prescribed duration, so this option usually requires more time to complete than the Long-Term analysis option.

4.4.2.1. Hydrologic Equilibrium and Resilient Modulus Results (Short-Term)

Figure 47 shows an example of the hydrological analysis results from the Short-Term analysis. The plot on the left shows the degree of saturation over time, at a depth specified by the user. On the other hand, the plot on the right shows the degree of saturation as a function of depth (below the PCC layer) at any time specified by the user.

Similarly, Figure 48 shows the corresponding plots for the resilient modulus. Again, the one on the left is a plot over the analysis duration as a depth specified by the user, while the one on the left is a plot with respect to depth at a given time specified by the user.

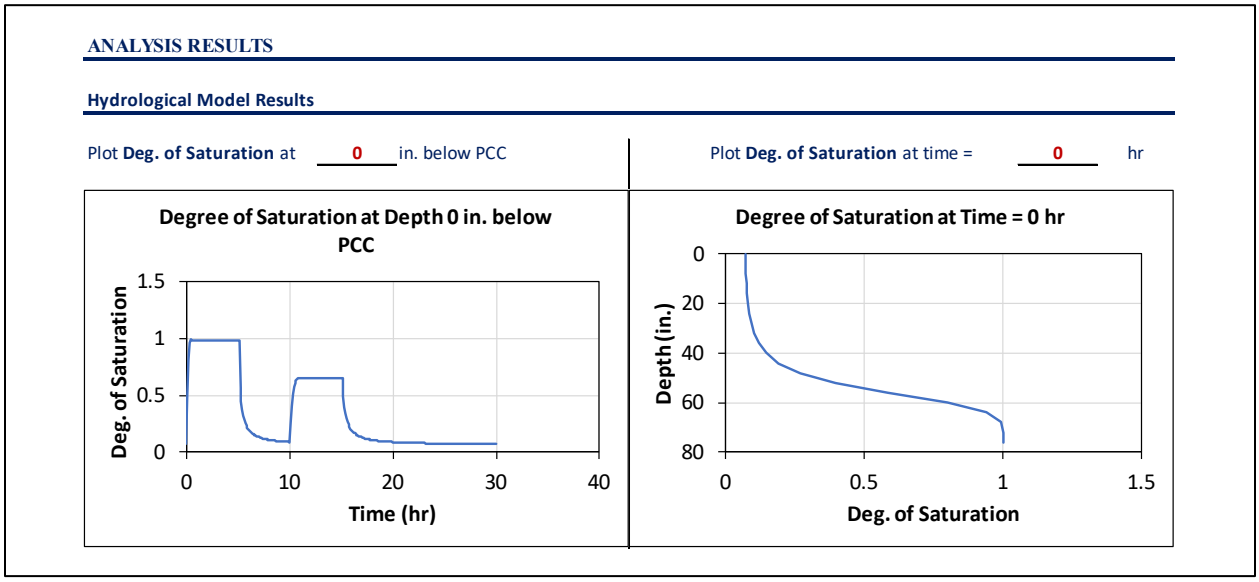

Figure 47. Short-term analysis results – hydrological analysis.

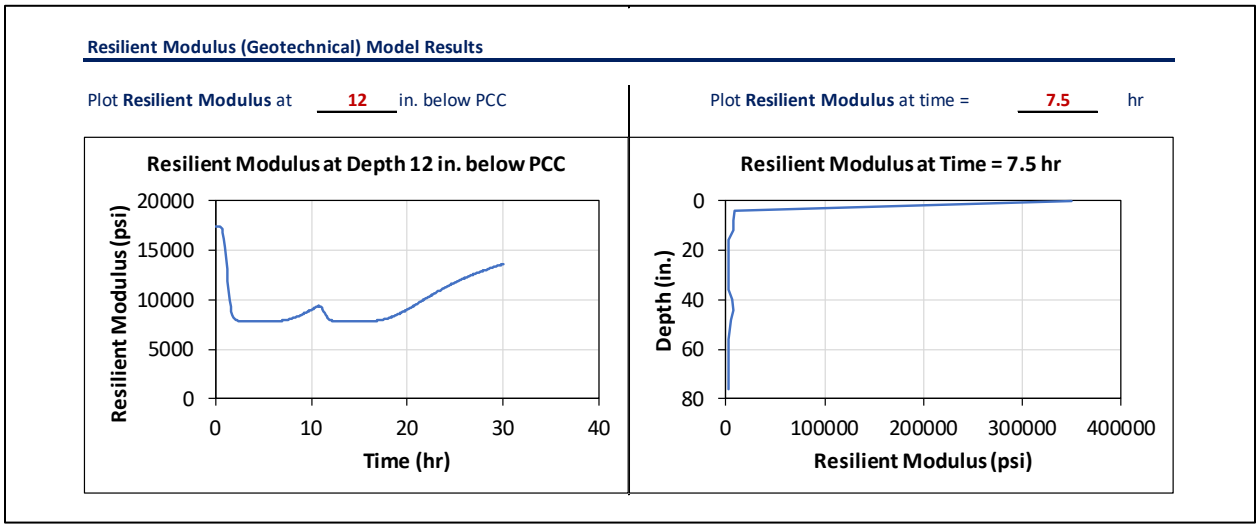

Figure 48. Short-term analysis results – resilient modulus analysis.

4.4.2.2. Westergaard Results (Short-Term)

Figure 49 shows an example of the Westergaard results for the Short-Term analysis. As shown in the figure, there are five plots that include the composite k-value, critical tensile stress, maximum deflection, the allowable number of load passes (N_f), and the damage per pass ($1/N_f$), all of which are plotted as functions of time. The user may choose to plot the corresponding results at different locations made available by Westergaard equations (i.e., slab interior, edge, or corner).

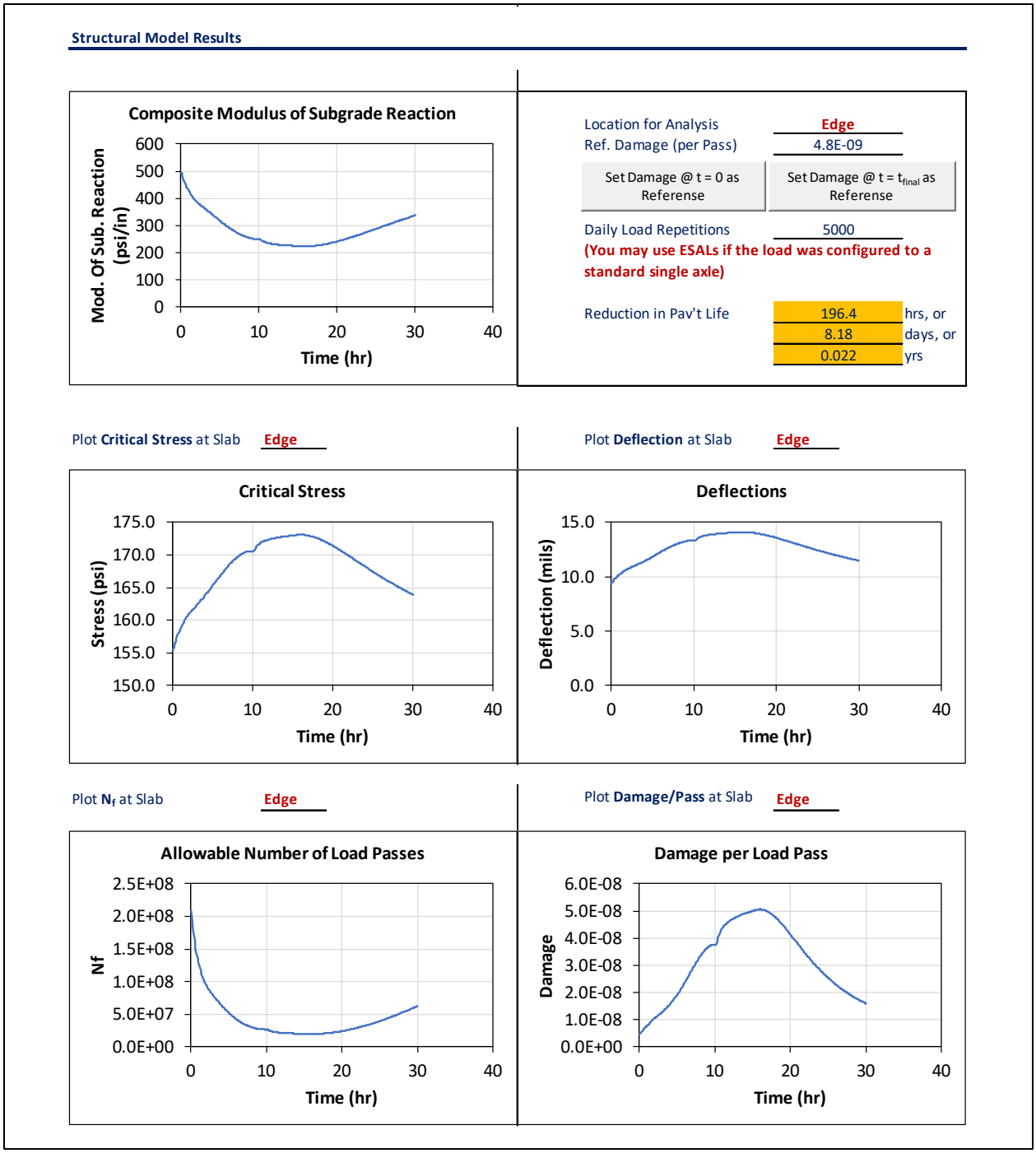

Figure 49. Short-term analysis results – structural analysis using Westergaard equations.

The user is also allowed to carry out the performance analysis based on the structural results (see top-right corner of Figure 49). The procedure for running the performance analysis is described as the following.

1. Select the PCC location for the analysis (i.e., **Interior, Edge, or Corner**). For most cases, it is recommended that the edge location be used for this analysis.

2. Input the **Reference Damage per Pass** for a given load. The reference damage can be obtained in one of the three ways described below.

   a. By clicking on the "**Set Damage @ t = 0 as Reference**" button. As indicated by the name of the button itself, this option allows the user to set the reference damage to that corresponding to the beginning (i.e., time = 0.0 hr) of the simulation.

      This option is feasible and is the recommended method for simulating rainfall events where the condition just before the rainfall is the reference condition.

   b. By clicking on the "**Set Damage @ t = t_{final} as Reference**" button. In contrast to the above, this option sets the reference damage equal to that the end of the simulation.

      This option is to be used when the user simulates a pavement that starts at a flooded condition and goes through the draining process over time. Note that for this method to provide a feasible estimate of the reference damage, the duration of the Short-Term analysis should be long enough to allow for the water to drain and the foundation of the pavement is at the end of simulation is representative of the reference (i.e., before flooding) condition.

   c. From the Long-Term analysis results (e.g., Figure 45) obtained using the hydrological inputs that correspond to the reference condition (e.g., before rainfall).

      This option is made available for special conditions where the two options described above are not deemed feasible.

3. Input the **Daily Load Repetitions** of the corresponding load. This is used to calculate the additional reduction in pavement life caused by the increased pavement damage due to continued traffic loading.

   It is also noted that the additional pavement life reduction is estimated using the well-known Miner's hypothesis. The primary assumption behind this calculation is that the normal pavement life reduction (i.e, without the rain or other adverse event being simulated) is equal to the Short-Term analysis duration. For example, if the pavement was subjected to 30 hours (corresponding to the analysis duration of the example in Figure 49) of normal traffic under the reference condition (i.e., no rainfall), the reduction in pavement life is simply obtained to be 30 hours.

   However, for the adverse condition such as the one shown in Figure 49, the pavement will undergo an increased amount of damage, if it was subjected to the same amount of traffic (as the reference condition). For convenience, the ratio between these two damage values are defined as the Damage Ratio (*DR*) herein.

$$DR = \frac{TD_{Adverse}}{TD_{Normal}} \tag{25}$$

where $TD_{Adverse}$ and TD_{Normal} are the total damage caused during adverse and normal conditions, respectively. Then, the reduction in pavement life due to the adverse event ($\Delta N_{Adverse}$) is obtained as the following.

$$\Delta N_{Adverse} = \Delta N_{Normal} \times DR \tag{26}$$

where ΔN_{Normal} is the life reduction under normal condition, which is set to be equal to the analysis duration.

4.4.2.3. ILLISLAB Results (Short-Term)

It is emphasized again that running the ILLISLAB model for the Short-Term analysis requires a very long time to run and a lot of computer storage area to save all of the results from the ILLISLAB runs. As such, it is recommended that this option be used with caution.
Figure 50 shows the user interface for Short-Term ILLISLAB analysis and results. Similar to the Long-Term analysis, the user must specify the **locations within the PCC slab (X and Y coordinates as well as the depth)** where the responses are to be extracted from the FEM solution, and click on the "Click Here to Run ILLISLAB" button, which calls the Portable-R and runs the FEM solution for each time step within the analysis duration.

Once the FEM analysis completes, the ILLISLAB results (i.e., deflections, stresses, and the corresponding N_f and damage values) for the specified locations can be loaded into the spreadsheet by clicking on the "Import ILLISLAB Results" button. Once the pavement responses are loaded, the user may proceed to the performance analysis as shown in Figure 51. The procedure for running the performance analysis (i.e., calculating the pavement life reduction) was previously described under the Westergaard option, and shall not be repeated here.

Structural Model Results

Follow these steps to run ILLISLAB
1. In the table below, specify the X and Y Coordinates for the locations where response is to be extracted.
2. Specify the depth within the PCC at which the response is to be extracted.
WARNING: ILLISLAB for Short-Term Analysis WILL take a Long Time to Finish

Location Coords.	Location #1	Location #2	Location #3
X-Coordinate (ft)	22.5	22.5	22.5
Y-Coordinate (ft)	2	2.5	6

Depth within PCC Layer for Simulation of Response: 10 inch
Which plot do you want to show? Sx at Time = 0.1 hr

Click Here to Run ILLISLAB | Click Here to Reload Images | Import ILLISLAB Results

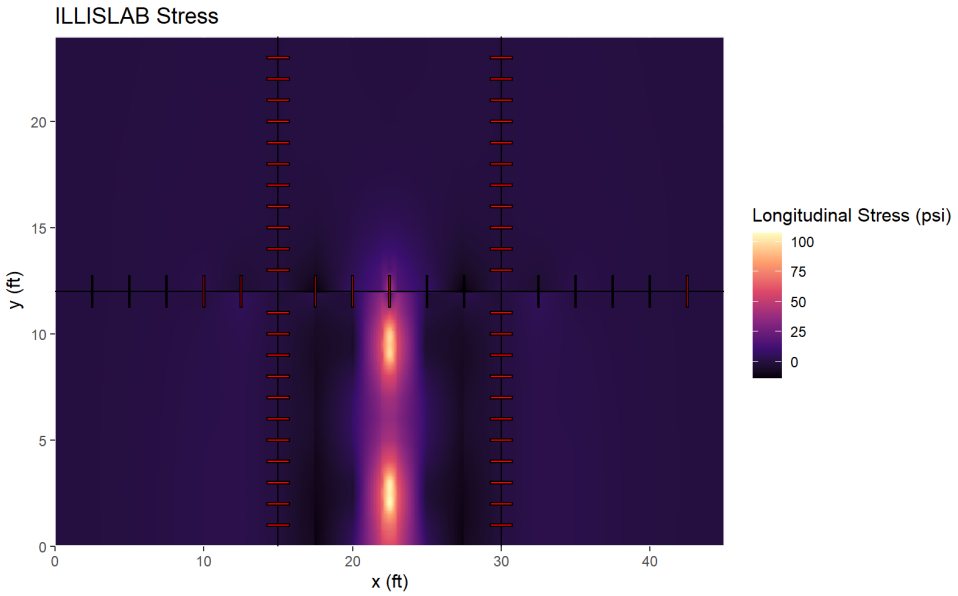

Figure 50. Short-term analysis results – structural analysis using ILLISLAB.

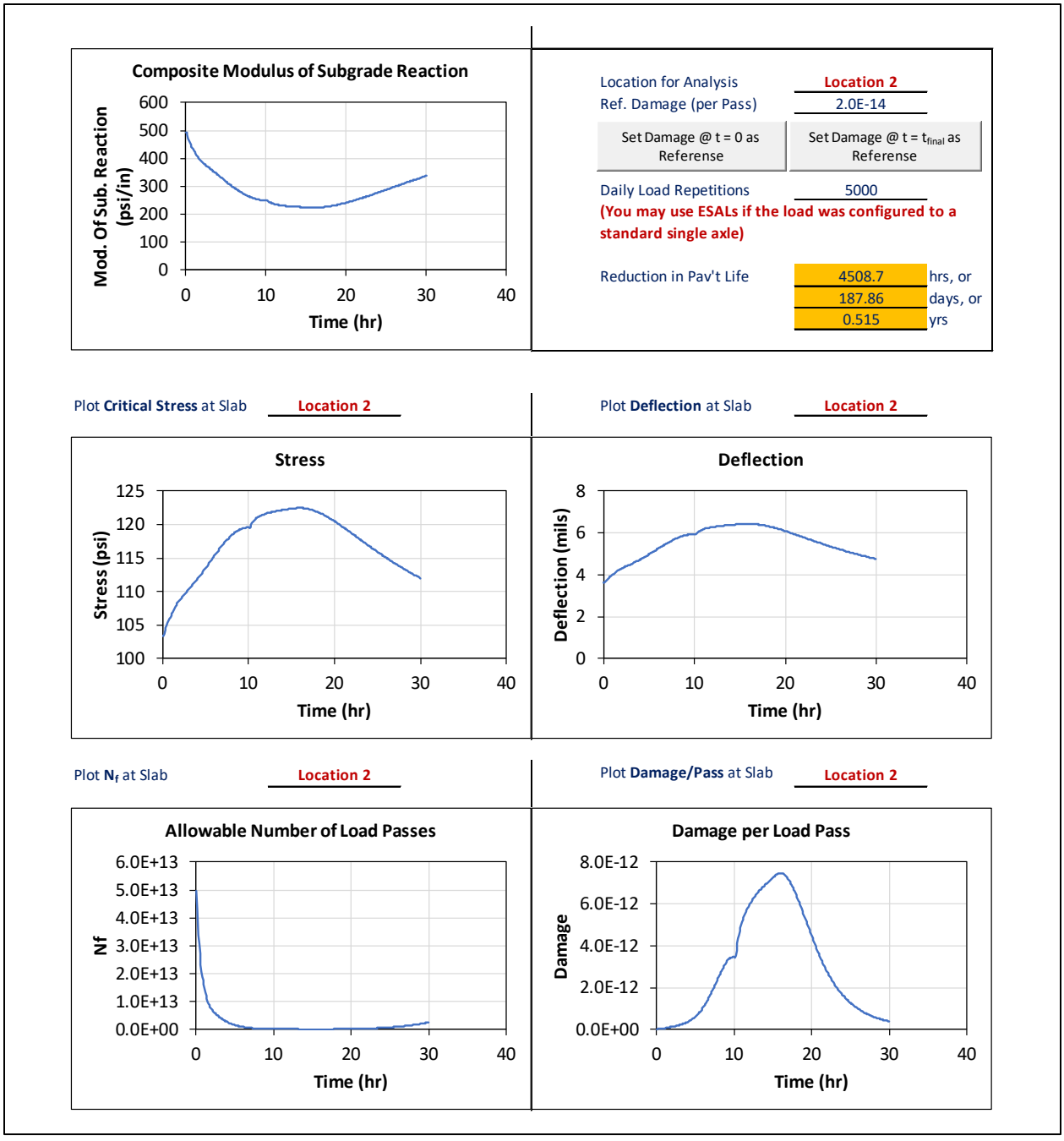

Figure 51. Short-term analysis results – performance analysis using ILLISLAB.

4.5. SAMPLE PROBLEMS

In this section of the report, a few example problems are solved using the Resiliency Tool. The examples are intended to further guide the user to get started with the resiliency tool and its features.

4.5.1. Long-Term Analysis Examples

A couple of example problems that demonstrate the Long-Term analysis option of the Resiliency Tool are provided in the following.

4.5.1.1. Long-Term Analysis Example No. 1: Effect of GWT

Problem Statement: Consider the pavement structure given in Table 15, which is assumed to have a service life of 40 years under a GWT depth of 90 in. below the pavement surface. Using the Westergaard equation for the PCC edge as the structural solution, estimate the effect of GWT rise (at an interval of 5 in.) on pavement service life. Assume that the traffic remains unchanged for all scenarios and use default values for the parameters not shown in Table 15.

Table 15. Pavement layer properties for long-term analysis Example No. 1

Layer	Input Paramter	Value
PCC	Thickness (in.)	10.0
	Young's Modulus (ksi)	4,000
	Modulus of Rupture (psi)	500
	Poisson's Ratio	0.15
Asphalt Base	Thickness (in.)	4.0
	Resilient Modulus (ksi)	350
	Poisson's Ratio	0.35
Stabilized Subgrade	Thickness (in.)	12.0
	Poisson's Ratio	0.4
	Resilient Modulus (ksi)	Calculated Using NCHRP 1-37A Model (M_{ROpt} = 16 ksi, S_{Opt} = 11%)
Embankment	Poisson's Ratio	0.4
	Resilient Modulus	Calculated Using NCHRP 1-37A Model (M_{ROpt} = 10 ksi, S_{Opt} = 11%)

Solution: The pavement life for the respective GWT depth can be estimated by running the long-term analysis option multiple times. More specifically, the GWT depth is changed from 90 in. to 10 in. (corresponding to the bottom of PCC) at an interval of 5 in., and the corresponding pavement damage at the PCC edge is stored at a separate spreadsheet. Table 16 shows these results.

Taking the pavement damage corresponding to GWT depth at 90 in. as the reference damage, $D_{Reference}$, (i.e., damage due to a single load pass under normal condition), the Damage Ratio (DR) is calculated for each GWT depth using the following equation.

$$DR = \frac{D_{GWT}}{D_{Reference}} \tag{27}$$

where D_{GWT} is the damage due to a single load pass for the respective GWT depths. Then, the pavement life for the respective GWT depth (N_{GWT}) is estimated using the following equation.

$$N_{GWT} = \frac{N_{Reference}}{DR} \tag{28}$$

where $N_{Reference}$ is the reference pavement life (= 40 yrs for this example). The calculated results are provided in Table 16 and a plot of the pavement life with respect to the GWT depth is shown in Figure 52.

Table 16. Summary of results for long-term Example No. 1

GWT Depth (in.)	Damage at PCC Edge	Damage Ratio (*DR*)	Estimated Service Life (Yrs)
90	4.81E-09*	1.00	40.0
85	6.08E-09	1.26	31.6
80	7.82E-09	1.63	24.6
75	1.03E-08	2.14	18.7
70	1.38E-08	2.86	14.0
65	1.87E-08	3.89	10.3
60	2.54E-08	5.28	7.6
55	3.33E-08	6.93	5.8
50	4.11E-08	8.55	4.7
45	4.81E-08	10.00	4.0
40	5.27E-08	10.96	3.6
35	5.41E-08	11.25	3.6
30	5.42E-08	11.28	3.5
25	5.42E-08	11.28	3.5
20	5.42E-08	11.28	3.5
15	5.42E-08	11.28	3.5
10	5.42E-08	11.28	3.5

Note*: This value is the reference damage, $D_{Reference}$, (i.e., damage under normal conditions).

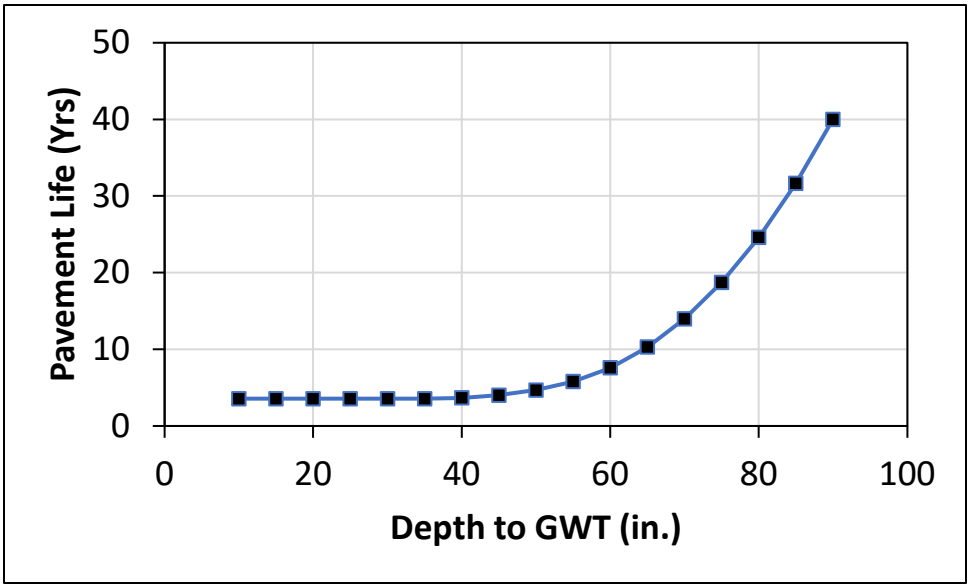

Figure 52. Pavement life vs. GWT depth for long-term Example No. 1

4.5.1.2. Long-Term Analysis Example No. 2: Effect of Resilient Modulus of Stabilized Subgrade

Problem Statement: Consider again the pavement that was analyzed in the previous example. Assume that the same pavement is to be constructed at a different location where the GWT depth is at 80 in. from the surface (rather than 90 in.).

According to Table 16, this pavement will have an estimated service life of 24.6 years under the same amount of traffic. Consider increasing the resilient modulus of the stabilized subgrade to achieve an estimated service life of at least 30 years.

Solution: The Long-Term analysis is repeated for several values of the Resilient Modulus at Optimum Moisture Content, M_{ROpt}, from 16 ksi to 24 ksi at an interval of 2 ksi. Similar to the previous example, the corresponding damage (at PCC edge) from the Westergaard equation is stored for each run. These results are provided in Table 17.

Table 17. Summary of results for long-term Example No. 2

Resilient Modulus (ksi)	Damage at PCC Edge	Damage Ratio (*DR*)	Estimated Service Life (Yrs)
16	7.82E-09	1.63	24.6
18	7.08E-09	1.47	27.2
20	6.47E-09	1.35	29.7
22	5.97E-09	1.24	32.2
24	5.54E-09	1.15	34.7

Note*: This value is the reference damage, $D_{Reference}$, (i.e., damage under normal conditions).

Table 17 also shows the Damage Ratio (*DR*) and the estimated service life using Equations (27) and (28). A plot of the estimated service life is provided in Figure 53. Based on these results, an M_{ROpt} of 22 ksi (approximately) is needed to achieve a service life of 30+ years.

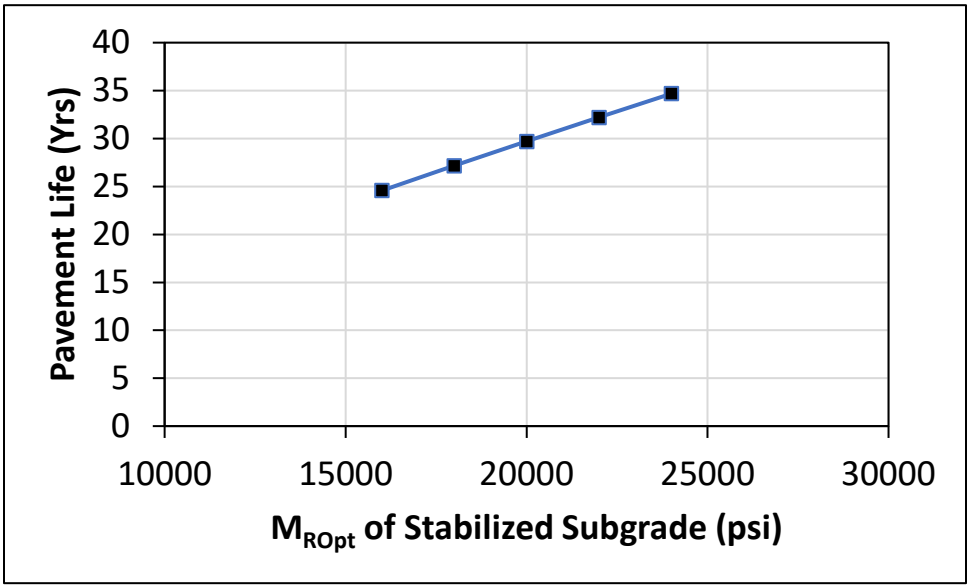

Figure 53. Pavement life vs. M_{Ropt} of stabilized subgrade for long-term Example No. 2

4.5.2. Short-Term Analysis Examples

In the following sections of the report, a couple of Short-Term analysis examples are provided.

4.5.2.1. Short-Term Analysis Example No. 1: Effect of Heavy Rainfall

Problem Statement: Consider again the pavement structure provided in Table 15 with the GWT located at 90 in. below the PCC surface. Assume this pavement is subjected to 5,000 load repetitions per day during normal conditions. It is expected that this pavement will be exposed to the following, severe rainfall events.

1. Five hours of heavy rainfall with an intensity of 5.0 in/hr, starting at time = 0 hr and ending at time = 5 hr.
2. Another five hours of rainfall with an intensity of 2.0 in/hr, starting at time = 10 hr and ending at time = 15 hr.

If the pavement undergoes the above rainfall events, how much time is needed for the pavement foundation to recover 90 and 95 percent of its original strength (in terms of the composite modulus of subgrade reaction, k-value)? In addition, estimate the additional pavement life reduction due to this rainfall event, if the pavement continues to carry the same amount of traffic (i.e., 5,000 load repetitions per day).

Solution: The inputs for the two rainfall events as well as other Short-Term analysis inputs are shown in Figure 54. To ensure that the simulation covers enough time range for the pavement to drain, the analysis duration was set to 100 hrs with an analysis interval of 0.1 hr.

Short Term Analysis Scenario

Ground Water Table Located at:	90	in. **below** Pavement Surface
Start with **Flooded** Pavement?	No	
Time Duration for Analysis	100	hr(s)
Time Interval for Analysis, Δt	0.1	hr(s)

Run Short-Term Analysis

Rainfall / Evaporation

Rain Event	Starting Time (hr)	Ending Time (hr)	Rainfall Intensity (in/hr)
Event No. 1	0.0	5.0	5.0
Event No. 2	10.0	15.0	2.0
Event No. 3			
Event No. 4			
Event No. 5			

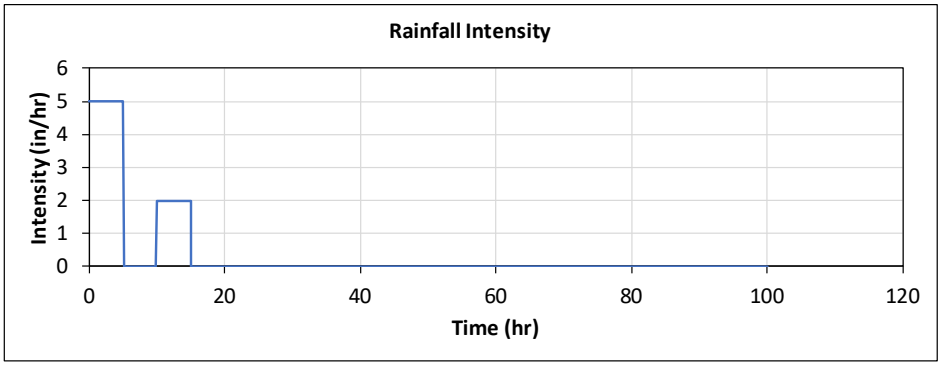

Figure 54. Rainfall inputs for short-term Example No. 1

Figure 55 shows the structural analysis results obtained after clicking the "Run Short-Term Analysis" button in the previous figure. The plot on the top-left corner of this figure shows how the composite modulus of subgrade reaction (k-value) varies over the analysis duration. Clearly, the k-value undergoes a significant reduction during the first 20 hrs of the simulation (due to the rainfall) and starts to recover slowly after the rainfall event.

According to this plot (or based on the data provided separately in the "Short-Term" worksheet, the k-value at the initial condition (or the reference condition just before the rainfall) is equal to 492.6 psi/in. Also based on the results from the plot or the "Short-Term" worksheet, the time needed for the pavement to recover 90 percent (i.e., k-value = 443.3 psi/in) and 95 percent (i.e., k-value = 467.9 psi/in) of the original foundation strength is found to be 48.8 hrs (approximately 2.0 days) and 61.4 hrs (approximately 2.6 days), respectively.

The performance analysis (i.e., calculating the pavement life reduction) can be completed by clicking the "**Set Damage @ t = 0 as Reference**" button (Note again that the reference condition is regarded as the pavement structure just before the rainfall at time = 0.0 hr). The figure shows that the pavement life reduction under the two rainfall events is found to be 292.3 hrs. Since the pavement would have only experienced a reduction of 100 hrs under normal circumstances, it is found that the pavement lost an additional 192.3 hrs (approximately 8.0 days) of service life.

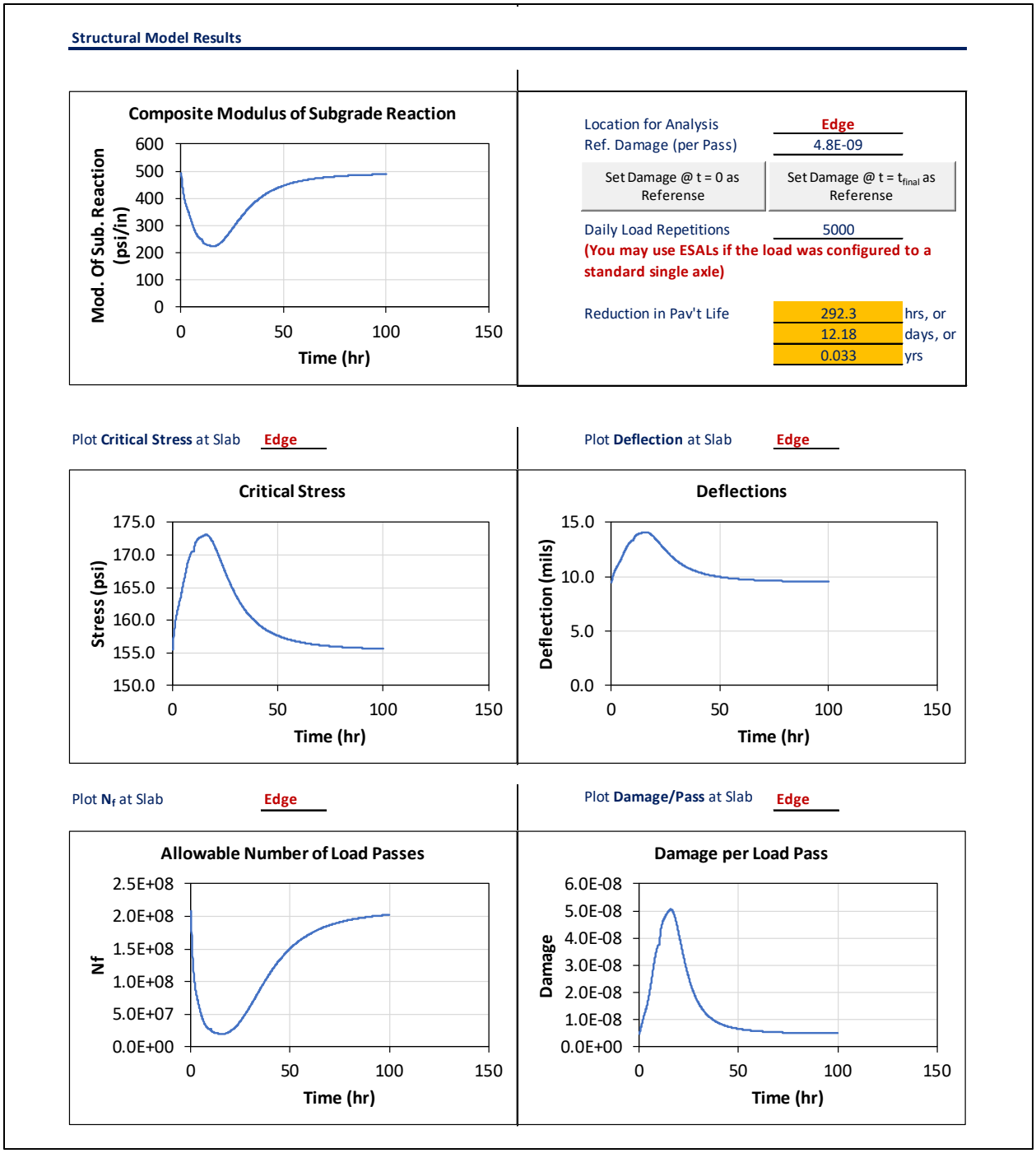

Figure 55. Structural analysis results for short-term Example No. 1

4.5.2.2. Short-Term Analysis Example No. 2: Flooded Pavement

Problem Statement: Consider again the pavement structure provided in Table 15 with the GWT located at 90 in. below the PCC surface. Also assume this pavement is subjected to 5,000 load repetitions per day during normal conditions.

Starting with a flooded condition for this pavement and a moisture evaporation rate of 0.01 in/hr at the pavement surface, estimate the time needed for this pavement foundation to recover 90 and 95 percent of its original strength (which corresponds to k-value = 492.6 psi/in from the previous example). In addition, using an analysis duration of 200 hrs, estimate the additional pavement life reduction for the draining pavement if the pavement continues to carry the same amount of traffic (i.e., 5,000 load repetitions per day).

Solution: The Short-Term analysis inputs for the draining pavement are shown in Figure 56. Note that the evaporation rate is inputted as a negative number (i.e., -0.01 in/hr) to simulate the moisture being removed at the pavement surface. As described in the problem statement, the analysis duration was set to 200 hr. with an analysis interval of 0.1 hr.

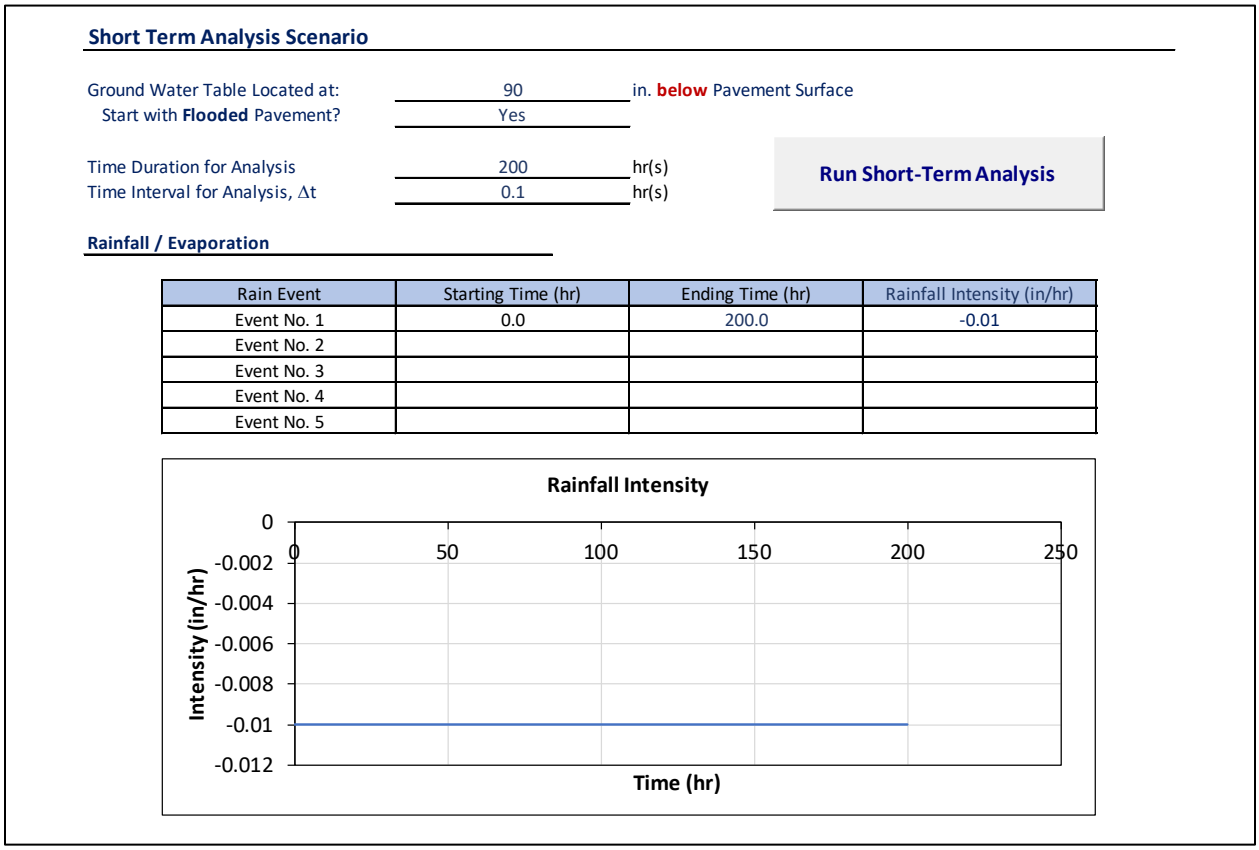

Figure 56. Draining pavement inputs for short-term Example No. 2

Figure 57 shows the structural analysis results obtained for this scenario. As shown in the plot for the composite modulus of subgrade reaction (k-value) on the top-left corner of the figure, the k-value starts at approximately 217.9 psi/in and starts to recover as the moisture is drained within the foundation layers. According to this plot (or based on the data provided separately in the "Short-Term" worksheet, the time needed for the pavement to recover 90 percent (i.e., k-value = 443.3 psi/in) and 95 percent (i.e., k-value = 467.9 psi/in) of the original foundation strength is found to be 33.3 hrs (approximately 1.4 days) and 45.7 hrs (approximately 1.9 days), respectively.

The performance analysis (i.e., calculating the pavement life reduction) can be completed by clicking the "**Set Damage @ t = t_{final} as Reference**" button (Note that the reference condition is reached when the pavement is close to being fully drained at the last time interval). The figure shows that the pavement life reduction under this condition is found to be 315.2 hrs. Since the pavement would have only experienced a reduction of 100 hrs under normal circumstances, it is found that the pavement lost an additional 115.2 hrs (approximately 4.8 days) of service life due to continued traffic loading.

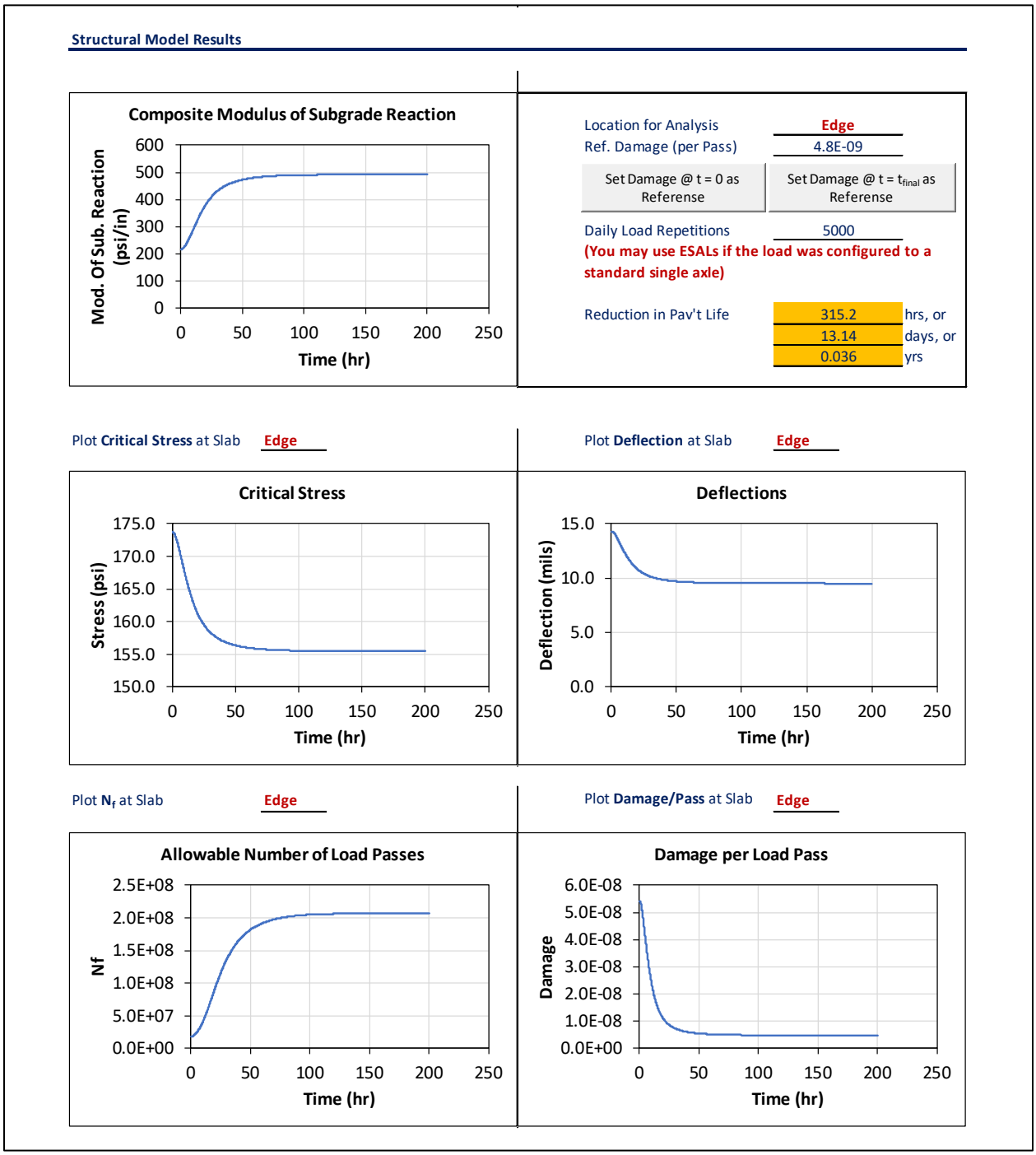

Figure 57. Structural analysis results for short-term Example No. 2

4.6. SUMMARY

FDOT's new Rigid Pavement Resiliency Tool was implemented in a macro-enabled Excel spreadsheet environment. The primary purpose of the Tool is to allow the user analyze the structural response and performance of rigid pavement systems under various moisture-related scenarios. For this purpose, the tool has implemented two analysis options: Long-Term and Short-Term.

The Long-Term analysis option allows the user to compare different situations that are considered to be permanent (i.e., those that do not change over a short period of time). Examples of these scenarios are:

- Change in pavement performance under different, but permanent levels of sea level rise (e.g., 10 ft. or 5 ft.) versus no change in sea level.
- Change in pavement performance under different levels of Ground Water Table (GWT) versus no change in GWT.
- Difference in pavement life between a flooded versus non-flooded pavement (for the condition that the flooded pavement remains flooded for an extended period of time).

The Short-Term analysis option allows the user to simulate a pavement structure experiencing changes in moisture level within a relatively short period of time (i.e., within a few hours, days, or weeks). Examples of these scenarios are:

- Reduction in pavement life due to a severe rainfall combined with traffic loading.
- Recovery of a flooded pavement due to evaporation and other sources of drainage.

The structural analysis can be conducted using the well-known Westergaard equations or the ILLISLAB FEM. Based on the responses obtained from the selected structural analysis option, the tool also calculates some performance measures such as damage and maximum allowable number of load passes using the Transfer function adopted from the AASHTOWare Pavement ME.

As a final note, it is emphasized that the tool was implemented based on various, existing models that were found in literature. These models include those for the moisture flow, hydraulic conductivity, resilient modulus of the soil, structural response, transfer functions, etc. These models were implemented based on the available information documented in literature, without any further calibration or validation. Such effort is beyond the scope of this study, and it is strongly recommended that FDOT examine the results from the Resiliency Tool against any available field data.

5. VULNERABILITY ANALYSIS OF FDOT'S RIGID PAVEMENT SECTIONS

5.1. INTRODUCTION

In the previous chapter, FDOT's new Rigid Pavement Resilience Tool was implemented in the macro-enabled Excel spreadsheet environment. The primary purpose of the tool is to allow the user to analyze the structural response and performance of rigid pavement systems under various moisture-related scenarios.

The purpose of this chapter is to conduct a preliminary vulnerability analysis for FDOT's existing rigid pavement sections under flooding and sea level rise. The secondary objective of this task is to develop a process for assessing the effect of increased layer thickness (especially the base layer) in FDOT's rigid pavement design as a mitigating solution for these moisture-related threats (e.g., SLR).

As discussed previously, sea level rise is one of the major concerns for future inundation of Florida's roadways, especially for those located near the coastline. Similarly, the roadways located close to the inland shorelines (i.e., those of major rivers and lakes) are also of concern, because they may experience higher chances of flooding during a heavy rainfall event.

5.2. MINIMUM DISTANCE TO SHORELINE

As a first step in assessing the vulnerability, the distance between FDOT's rigid pavement sections and the closest shoreline (coastal or inland) was calculated. This effort is briefly described in the following.

First, a list of rigid pavement sections surfaced with Portland cement concrete (PCC) was extracted from FDOT's Pavement Condition Survey (PCS) database. The extracted information included roadway ID (i.e., county section number) and milepost limits for a total of 86 rigid pavement sections managed by FDOT. Since FDOT's PCS database does not include GPS coordinates for the rigid pavement sections, the extracted information was merged with FDOT's roadway GIS data. Figure 58(a) shows a map of the rigid pavement sections identified in this manner while Figure 58(b) shows the midpoint location of the rigid pavement section limits. Then, the GPS coordinates of rigid pavement sections were superimposed on top of the Florida's shoreline GIS dataset that was made available by Florida Fish and Wildlife Conservation (FWC) Commission (FWC, 2023). The FWC data were specifically chosen because they provide information on both the coastal and inland shorelines within the state, as shown by the blue lines in Figure 58(c).

Finally, the data shown in Figure 58(c) were used to calculate the shortest distance to the shoreline for each rigid pavement section. A table of these results, including the latitude, longitude, and the distance to closest shoreline, is provided in Table 18. A quick summary of the results is shown in Figure 59. Essentially, this figure shows that out of 86 rigid pavement sections:

1. Approximately 31 percent (or 27 sections) of rigid pavements are located within 0.5 mile from the shoreline.
2. Another 33 percent (or 28 sections) of rigid pavements are located between 0.5 mile and 2.0 miles from the shoreline.
3. The remaining 36 percent (or 31 sections) of rigid pavements are over 2.0 miles away from the closest shoreline.

Figure 58(b) and Figure 58(c) indicates that many of the rigid pavement sections may be located close to the coastal shoreline, which may be responsible for 31 percent (or 27 sections) within 0.5 mile from the shoreline.

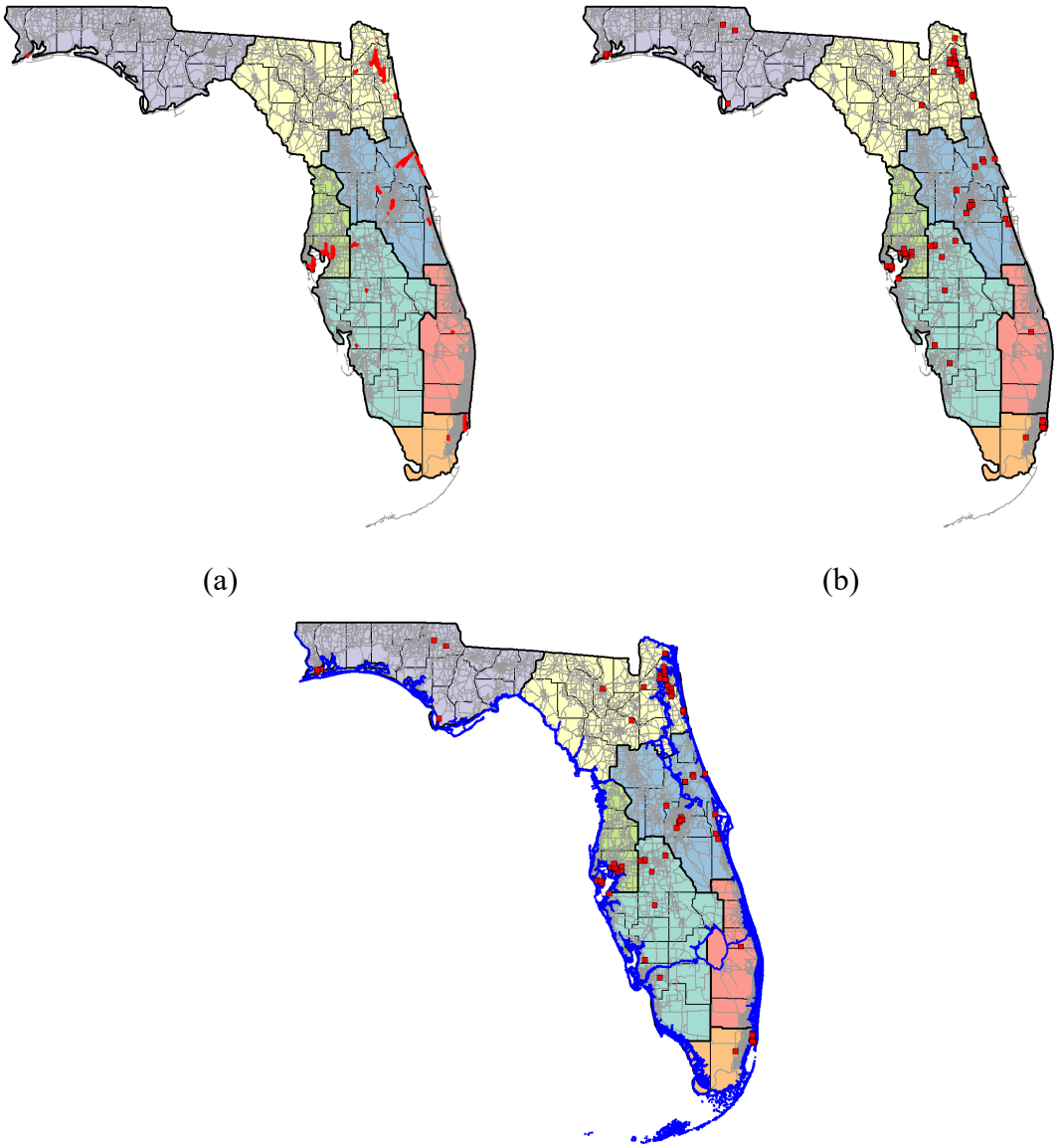

(a) (b)

(c)

Figure 58. Rigid pavement vulnerability (a) FDOT's rigid pavement sections, (b) Midpoint of rigid pavement limits, and (c) FWC shoreline data overlay.

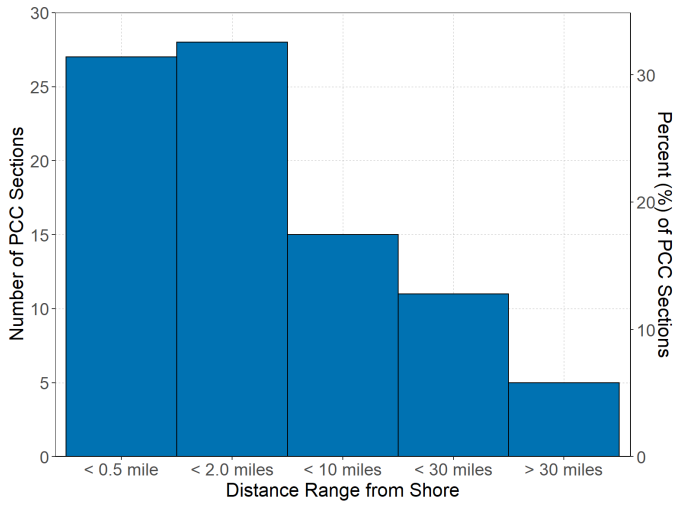

Figure 59. Distance between FDOT's rigid pavements and closest shoreline.

5.3. SEA LEVEL RISE (SLR)

Since the sections near the coastal shorelines are anticipated to be more vulnerable to sea level rise, the rigid pavement locations were superimposed on top of the areas within Florida that are projected to flood at different levels of sea level rise, based on National Oceanic and Atmospheric Administration (NOAA) GIS data (NOAA, 2023). These results are shown in Figure 60. The figure shows that even a 1.0 ft. rise in sea level may cause several rigid pavements near the coast to flood. This may also imply (at least indirectly) that the Ground Water Table (GWT) beneath these coastal roadways is either at a shallow depth from the ground surface already or expected to rise significantly with sea level rise.

To better assess the vulnerability of FDOT's rigid pavement sections, the level of SLR at which the respective rigid pavement sections are projected to be affected by sea level was determined based on NOAA data. For this purpose, the GIS polygons representing the areas affected by 1 ft. to 10 ft. SLR (at an interval of 1 ft.) were extracted from the NOAA data. Then, the rigid pavement sections that are located within the SLR polygons were identified. The corresponding results are shown in Table 18 while a summary is provided in Table 19 which indicates that FDOT's District 2 (Jacksonville area) has the most number of rigid pavement sections that are vulnerable to SLR, followed by District 6 (Miami Area) and District 7 (Tampa area).

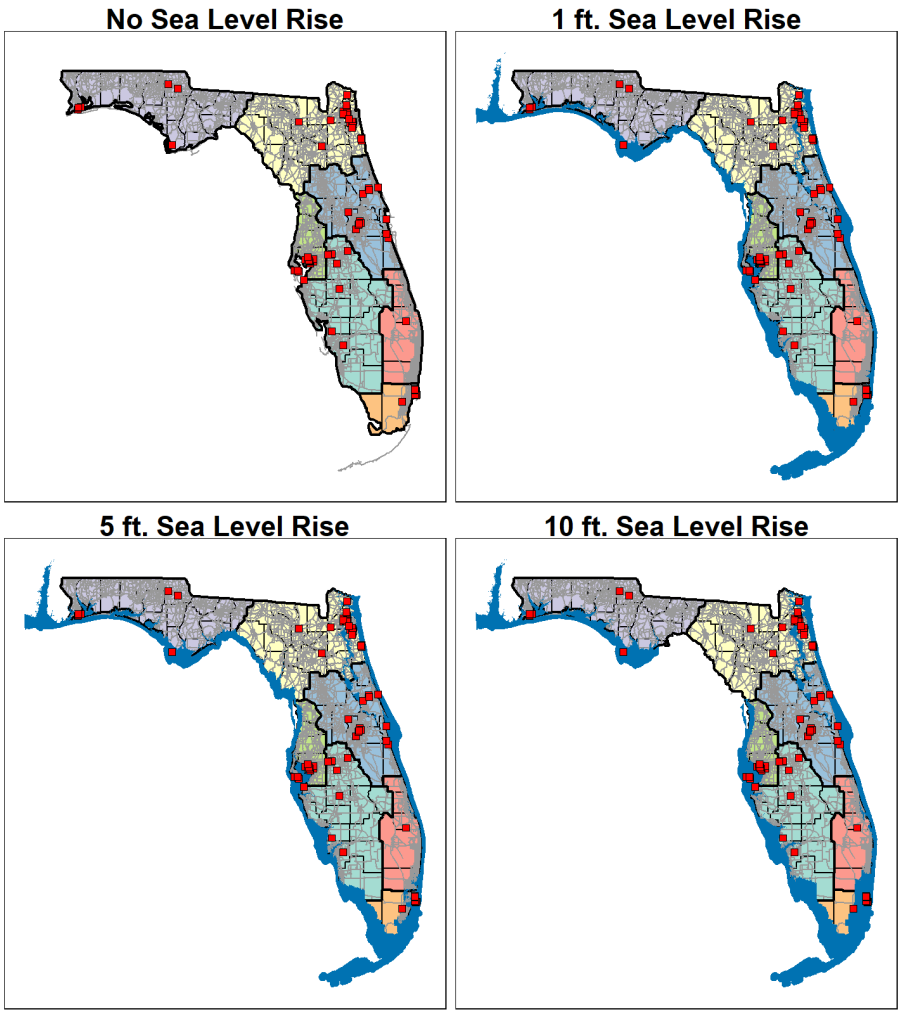

Figure 60. Expected flooding areas due to different sea level rise.

Table 18. Vulnerability of FDOT's rigid pavement sections

District	County	Roadway ID	Latitude	Longitude	Min. Dist. to Shoreline (miles)	Affected by Sea Level Rise?									
						1 ft	2 ft	3 ft	4 ft	5 ft	6 ft	7 ft	8 ft	9 ft	10 ft
1	Charlotte	01010000	26.80964	-81.9566	5.32	Y	Y	Y	Y	Y	Y	Y	Y	Y	Y
	Hardee	06010001	27.49099	-81.7954	33.67										
	Lee	12070000	26.5818	-81.7138	8.79										
	Manatee	13030000	27.63472	-82.539	1.15								Y	Y	Y
	Polk	16003000	28.04292	-81.9606	22.04										
	Polk	16020000	28.10668	-81.6218	42.37										
	Polk	16100000	28.054	-81.9523	22.89										
	Polk	16261000	27.90392	-81.8421	25.61										
	Polk	16320000	28.04387	-82.03	18.74										
2	Alachua	26050065	29.78967	-82.1692	24.53										
	Columbia	29070000	30.1878	-82.6371	45.89										
	Duval	72001000	30.39681	-81.6327	0.10						Y	Y	Y	Y	Y
	Duval	72001200	30.16672	-81.5575	1.59										
	Duval	72001901	30.16725	-81.5664	1.74										
	Duval	72002000	30.1984	-81.5225	4.27										
	Duval	72002027	30.12487	-81.5134	2.16										
	Duval	72020000	30.34792	-81.6617	1.63										
	Duval	72030000	30.30745	-81.711	0.96										
	Duval	72070000	30.31666	-81.6585	0.26							Y	Y	Y	Y
	Duval	72070001	30.3254	-81.6582	0.10				Y	Y	Y	Y	Y	Y	Y
	Duval	72070101	30.31009	-81.6488	0.23							Y	Y	Y	Y
	Duval	72070102	30.31189	-81.6533	0.29						Y	Y	Y	Y	Y
	Duval	72080000	30.35715	-81.7105	1.58										
	Duval	72090000	30.32103	-81.6234	0.21	Y	Y	Y	Y	Y	Y	Y	Y	Y	Y
	Duval	72090200	30.35531	-81.6386	1.06										
	Duval	72090445	30.33235	-81.6366	0.55										

Table 18. Vulnerability of FDOT's rigid pavement sections (Continued)

District	County	Roadway ID	Latitude	Longitude	Min. Dist. to Shoreline (miles)	Affected by Sea Level Rise?									
						1 ft	2 ft	3 ft	4 ft	5 ft	6 ft	7 ft	8 ft	9 ft	10 ft
2	Duval	72090447	30.2996	-81.6135	0.03										
	Duval	72090448	30.30194	-81.6127	0.03									Y	Y
	Duval	72100002	30.3097	-81.6476	0.27										Y
	Duval	72120000	30.20911	-81.9716	11.10										
	Duval	72190100	30.30528	-81.6353	0.38										
	Duval	72270000	30.31914	-81.7159	1.63										
	Duval	72280000	30.23295	-81.589	1.28										
	Duval	72290000	30.45958	-81.6491	1.24										
	Nassau	74040000	30.62588	-81.6264	1.98										
	St Johns	78004000	30.08913	-81.5227	2.63									Y	Y
	St Johns	78010000	29.89472	-81.3226	0.03	Y	Y	Y	Y	Y	Y	Y	Y	Y	Y
	St Johns	78010027	29.89103	-81.3242	0.05			Y	Y	Y	Y	Y	Y	Y	Y
	St Johns	78020000	29.92282	-81.3251	0.21							Y	Y	Y	Y
	St Johns	78060000	29.91567	-81.34	0.55										
3	Escambia	48040000	30.42809	-87.2189	1.41										
	Escambia	48080000	30.39201	-87.2782	0.52										
	Escambia	48080060	30.4081	-87.2691	0.36										
	Escambia	48080062	30.42352	-87.2738	0.90										
	Gulf	51020000	29.81218	-85.3017	0.20								Y	Y	Y
	Jackson	53010000	30.79226	-85.3809	32.34										
	Jackson	53040000	30.72127	-85.1854	33.88										
4	Martin	89020000	26.97307	-80.3966	3.92										
5	Brevard	70030000	28.61953	-80.8133	0.17	Y	Y	Y	Y	Y	Y	Y	Y	Y	Y
	Brevard	70220000	28.31396	-80.7638	3.13										
	Brevard	70225000	28.37924	-80.8073	3.97										
	Orange	75002000	28.45002	-81.4401	20.31										

Table 18. Vulnerability of FDOT's rigid pavement sections (Continued)

District	County	Roadway ID	Latitude	Longitude	Min. Dist. to Shoreline (miles)	Affected by Sea Level Rise?									
						1 ft	2 ft	3 ft	4 ft	5 ft	6 ft	7 ft	8 ft	9 ft	10 ft
5	Orange	75010000	28.52501	-81.397	14.50										
	Orange	75020000	28.73111	-81.6024	16.46										
	Orange	75030000	28.5875	-81.3648	9.77										
	Orange	75060000	28.55325	-81.3452	11.46										
	Orange	75280000	28.5455	-81.3838	12.87										
	Volusia	79010000	29.12578	-80.9783	0.09										
	Volusia	79040000	29.02588	-81.3033	3.13										
	Volusia	79060000	29.11457	-81.1821	8.58										
	Volusia	79070000	29.02808	-81.3014	3.31										
	Volusia	79110000	29.08854	-81.164	7.30										
6	Miami-Dade	87003000	25.81241	-80.2149	1.65										
	Miami-Dade	87004000	25.81219	-80.2039	1.15										
	Miami-Dade	87006000	25.77166	-80.1907	0.09										
	Miami-Dade	87059000	25.78015	-80.1749	0.13	**Y**	**Y**	**Y**	**Y**	**Y**	**Y**	**Y**	**Y**	**Y**	**Y**
	Miami-Dade	87061000	25.77873	-80.1833	0.00		**Y**	**Y**	**Y**	**Y**	**Y**	**Y**	**Y**	**Y**	**Y**
	Miami-Dade	87150000	25.66804	-80.4801	9.44										
	Miami-Dade	87200000	25.78791	-80.2078	0.16								**Y**	**Y**	**Y**
	Miami-Dade	87270000	25.85062	-80.2067	0.25					**Y**	**Y**	**Y**	**Y**	**Y**	**Y**
	Miami-Dade	87270901	25.87882	-80.2085	0.75										**Y**
	Miami-Dade	87270902	25.8654	-80.2082	0.59										**Y**
7	Hillsborough	10002000	27.92783	-82.3331	2.79										
	Hillsborough	10060000	27.90318	-82.4017	0.36					**Y**	**Y**	**Y**	**Y**	**Y**	**Y**
	Hillsborough	10075000	27.96947	-82.3338	1.45										
	Hillsborough	10130000	27.96146	-82.5055	1.59										
	Hillsborough	10150000	27.99607	-82.4527	0.75										
	Hillsborough	10190000	27.95884	-82.4608	0.16										

Table 18. Vulnerability of FDOT's rigid pavement sections (Continued)

District	County	Roadway ID	Latitude	Longitude	Min. Dist. to Shoreline (miles)	Affected by Sea Level Rise?									
						1 ft	2 ft	3 ft	4 ft	5 ft	6 ft	7 ft	8 ft	9 ft	10 ft
7	Hillsborough	10250000	27.92712	-82.4171	0.04	Y	Y	Y	Y	Y	Y	Y	Y	Y	Y
	Hillsborough	10250001	27.94478	-82.4356	0.24					Y	Y	Y	Y	Y	Y
	Hillsborough	10250101	27.95458	-82.4352	0.35							Y	Y	Y	Y
	Hillsborough	10320000	28.00444	-82.454	0.68										
	Pinellas	15002000	27.77704	-82.6523	1.30										
	Pinellas	15003000	27.76588	-82.6443	0.55										
	Pinellas	15010000	27.79304	-82.7303	1.14										
	Pinellas	15190000	27.79274	-82.6651	1.98										

Table 19. Number of FDOT's rigid pavement sections affected by different levels of SLR

District	Number of Sections Affected by SLR									
	1 ft	2 ft	3 ft	4 ft	5 ft	6 ft	7 ft	8 ft	9 ft	10 ft
1	1	1	1	1	1	1	1	2	2	2
2	2	2	3	4	4	6	9	9	11	12
3	0	0	0	0	0	0	0	1	1	1
4	0	0	0	0	0	0	0	0	0	0
5	1	1	1	1	1	1	1	1	1	1
6	1	2	2	2	3	3	3	4	4	6
7	1	1	1	1	3	3	4	4	4	4
Total	**6**	**7**	**8**	**9**	**12**	**14**	**18**	**21**	**23**	**26**
Percent of Total Rigid Sections	**7.0**	**8.1**	**9.3**	**10.5**	**14.0**	**16.3**	**20.9**	**24.4**	**26.7**	**30.2**

5.4. FLOODING HAZARD

In addition to sea level rise, inland flooding due to storm/hurricane events is another major source for inundating Florida's roadways. Therefore, the rigid pavement locations were also superimposed on top of the flood hazard zones made available by Federal Emergency Management Agency, FEMA (FEMA, 2023).

Figure 61 shows a map of Florida's flood hazard zone produced from FEMA data on top of FDOT's roadway network (shown in thin, gray lines) as well as the rigid pavement locations (shown in red squares). The Moderate Flood Hazard Area (MFHA) and Special Flood Hazard Area (SFHA) are defined as those that are prone to 0.2 percent (500-year flood) and 1.0 percent (100-year flood) annual chance of flooding, respectively. As shown in the figure, the hazard zones vary in size and are sporadically spread out within the entire State.

Similar to SLR, the GIS analysis was conducted to determine if any of the rigid pavement sections were located within the SFHA or MFHA polygons. However, none of the 86 rigid pavement sections were found to be within any of these polygons. Nonetheless, as shown in the enlarged map of Hillsborough County (Figure 61), while these rigid pavement sections are not located directly within the hazard zones, they may be located within close proximity of the hazard zones and/or to the shoreline. As such, these rigid pavement sections (especially those near the shoreline, see Table 18) may still experience significant storm surge during an unpredicted natural hazard.

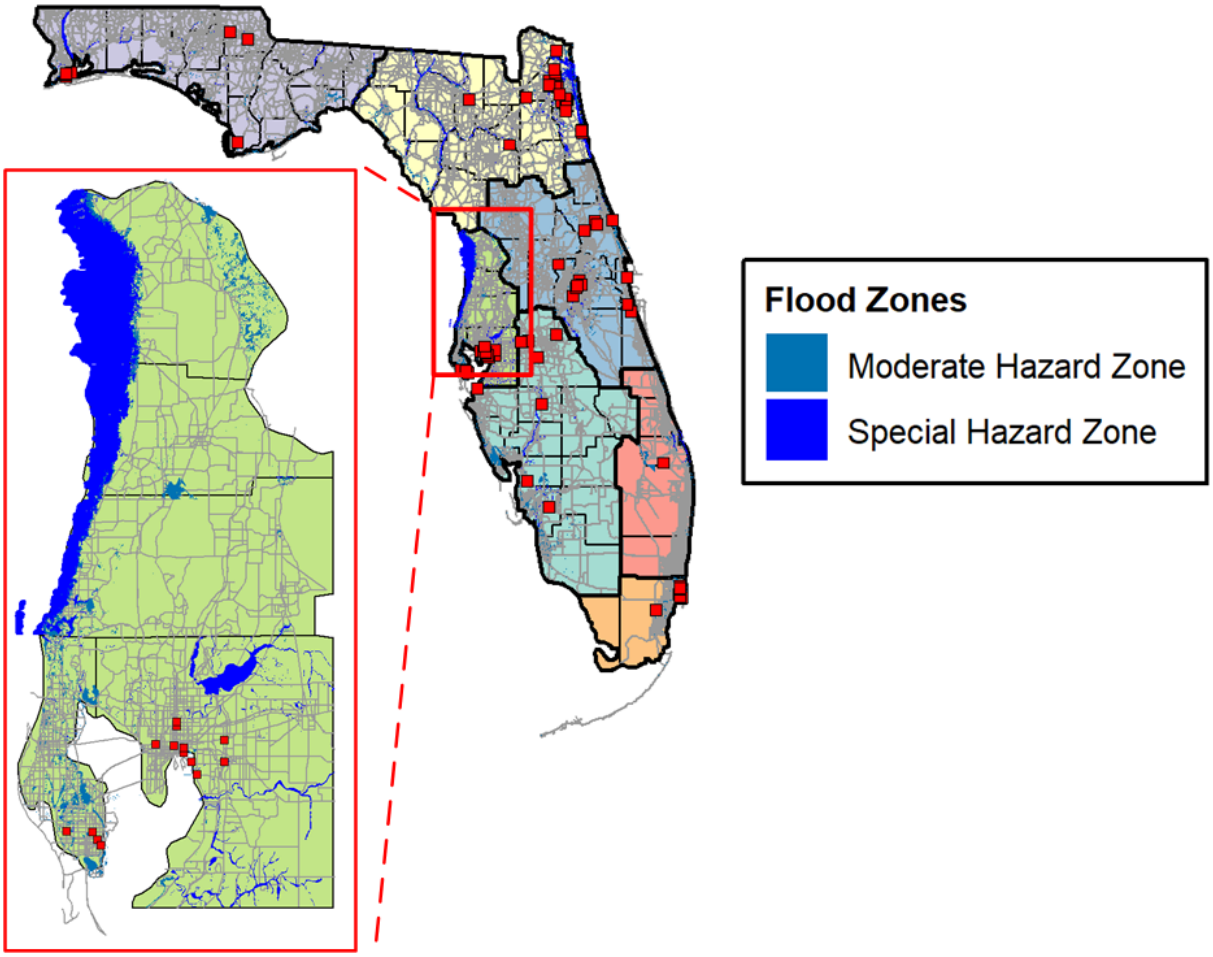

Figure 61. Moderate and special flood hazard zones in Florida.

5.5. SUMMARY OF FDOT'S RIGID PAVEMENT VULNERABILITY

In this section, a preliminary analysis was conducted to assess the vulnerability of FDOT's rigid pavement sections to SLR, GWT rise, and flooding hazard. The analysis showed that out of 86 rigid pavement sections managed by FDOT, 21 sections (i.e., 31 percent) were located within 0.5 mile from the coastal or inland shoreline. Furthermore, 6 sections (i.e., 7 percent) were found to be vulnerable to SLR rise of 1.0 ft.

In a recent study, NOAA updated the near-term SLR projections based on the SLR observations made since 2000 (Sweet et. al., 2022). Using the SLR of 2000 as a baseline, these projections indicated that the SLR around the nation's (including Florida's) shoreline is expected to rise (or has already risen) by 0.36 ft., 0.62 ft., 0.92 ft., and 1.25 ft., by year 2020, 2030, 2040, and 2050, respectively. Said differently, compared to the sea level observed in 2020, the SLR is expected to show an additional increase of 0.26 ft., 0.56 ft., and 0.89 ft. by 2030, 2040, and 2050, respectively.

Although preliminary, the above vulnerability analysis and the SLR projections generally indicate that FDOT's rigid pavements are not free from the threats of SLR rise or other causes of

flooding, and it may be necessary that FDOT start further evaluating the vulnerability of their existing rigid pavement sections and start planning for the projected SLR increase or other events.

It is emphasized again that the vulnerability analysis conducted herein was a preliminary effort. As such, it is recommended that a more detailed vulnerability analysis be conducted in the future to include the following aspects.

1. The preliminary vulnerability analysis was based on the GPS coordinates of the mid-point of the respective rigid pavement sections, regardless of the length of the sections. However, it is possible that the vulnerability (e.g., distance to shoreline) may vary within a project, especially for long sections. For this purpose, it may be useful to conduct the vulnerability analysis based on the GPS coordinates that are available at an interval of 0.001 mile for FDOT's roadways.

2. The preliminary vulnerability analysis discussed above did not take into account the actual elevations of the existing rigid pavement sections nor the elevations of the terrain surrounding the rigid pavements (i.e., the SLR vulnerability was simply based on the GPS coordinates of the respective rigid pavement sections and the areas that may potentially be affected by different levels of SLR, based on NOAA data). If the actual elevations (or the elevations relative to sea level) of the rigid pavement sections are available (especially at short intervals), it is recommended that such information be incorporated into a future SLR vulnerability analysis.

As discussed in Chapter 2, a thorough research documenting all available adaptation options for rigid pavement resiliency was not found. However, based on the limited literature, the following adaptation options are deemed relevant for improving the resiliency of rigid pavements under flooding, SLR, and storm surge (Mack, 2020; Dylla and Hyman, 2018; Pavement Interactive, 2021).

1. Elevating the road above flooding elevation: This is most likely the most expensive option. It is recommended that the actual elevations of the rigid pavements be evaluated as a pre-flood measure and be compared to the expected (or projected) level of flooding due to SLR and GWT rise.

2. Hardening of the pavement system: Although the use of stiffer and/or better-quality materials (especially for the foundation layers) may improve the resiliency of rigid pavements, it is not guaranteed that the "better-quality" materials are available locally. Furthermore, the effect of a stiffer rigid pavement foundation on resiliency is not easily quantified. Additional research (e.g., calibration of the Rigid Pavement Resilience Tool developed in this study and/or verification and validation of rigid pavement performance under various moisture conditions) is recommended before this option is implemented into practice.

3. Stabilized base and subbase layers: It is noted that FDOT is already using stabilized base and subbase materials in rigid pavement foundations. However, it may be beneficial to increase the thickness of these layers in areas where the ground water table may rise or

higher precipitation is expected. However, similar to the use of stiffer materials, the effect of increased foundation thickness on the overall resiliency is difficult to quantify. As such, additional research is recommended for verifying and validating the performance of rigid pavements for different foundation design strategies (e.g., increasing thickness of the stabilized base).

6. PROPOSED PROCEDURE FOR DEVELOPING RIGID PAVEMENT DESIGN STRATEGIES

6.1. INTRODUCTION

To overcome the limitations of FDOT's design practice discussed Chapter 2, a couple of examples are provided in this chapter for developing the preliminary design strategies using FDOT's Rigid Pavement Resiliency Tool.

It is strongly emphasized again that none of the models incorporated into the Resiliency Tool was verified or validated. As such, the relevant efforts documented in this section of the report should only be used as a general guide on how the tool may be used in the future with additional research to support the validity of the Resiliency Tool.

As mentioned in the previous chapter, increasing the stiffness and/or the thickness of the foundation layers may be a reasonable option for improving the resiliency of rigid pavements. However, since the benefit of such improvement cannot be quantified using the available pavement design methodologies, the goal of the examples provided herein is to outline the procedures that FDOT may take in the future for quantifying the benefit of the adaptation options that involve any changes to FDOT's current rigid pavement design practice. The examples are provided in terms of the thickness of the PCC layer as well as the stabilized base layer.

6.2. FLORIDA'S DEPTH TO WATER TABLE

In order to provide recommendations for considering the effect of GWT in FDOT's rigid pavement design, it was deemed necessary that the typical range of GWT be assessed. Figure 62 shows a map of the "minimum" GWT depth that was produced based on the United States Department of Agriculture (USDA) data (Zhou and Geza, 2016). This figure clearly shows that the GWT in Florida is relatively close to the ground surface, with its minimum depth ranging from 0 in. to 80 in. (0 cm to 203 cm).

However, as noted by Zhou and Geza (2016), the depth to GWT is highly variable and depends on the time of measurement, sampling locations, as well as the individual performing the measurements. In addition, the GWT shown in Figure 62 represents the "minimum" depth to GWT that was observed at any time during a year. In other words, it was not possible to derive a "typical" depth to GWT based on the research team's review of available literature and data. As such, a GWT depth of 55 in. was selected as the reference GWT depth for the procedure outlined in this chapter.

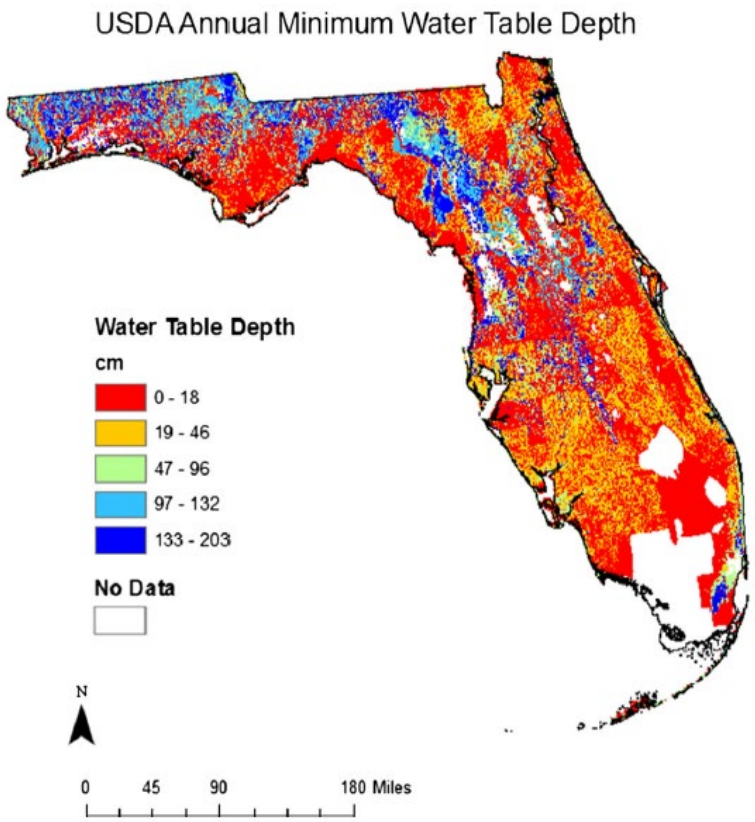

Figure 62. GIS mapping of minimum GWT depth in Florida (from Zhou and Geza, 2016)

6.3. PCC THICKNESS

To demonstrate the development of the design strategies for PCC thickness, a sensitivity analysis was conducted using the new Resiliency Tool developed in this study. For this analysis, the default inputs were used for all material properties. The sensitivity parameters are summarized as the following.

1. The PCC thickness was varied from 8 in. to 14 in. at an interval of 1 in.
2. The depth to GWT was varied from 55 in. to 0 in. at an interval of 5 in.

In addition to the above, modulus of the embankment layer was obtained from the Soil-Water Characteristic Curve (SWCC), since this allows for modeling different soils within FDOT's Districts (see Table 11 and Table 12).

Using the damage obtained at the edge of the PCC slabs, the sensitivity analysis results were used to develop a set of Damage Ratios (DR) for different scenarios. Similar to the examples shown in the previous chapter, the DR is defined herein as the following.

$$DR = \frac{TD_{Adverse}}{TD_{Normal}} \tag{29}$$

where $TD_{Adverse}$ and TD_{Normal} are the total damage caused during adverse and normal conditions, respectively.

For each PCC thickness considered, the normal condition was assumed to have a GWT depth equal to the reference depth of 55 in. within each District. The adverse condition corresponds to any GWT depth that is shallower than the reference. Figure 63 shows the resulting DR values obtained for the asphalt base option, while Figure 64 shows those for the special select soil option. It should be noted that these figures only show the GWT depth from 35 in. to 55 in., as the damage ratio for GWT less than 35 in. only showed negligible changes (i.e., the DR corresponding to 35 in. should be used for any GWT depth shallower than 35 in.).
An example problem is provided in the following to demonstrate how these DR values could be used in design.

Problem Statement: Consider a PCC pavement that is to be designed for 9 million ESALs in District 2 (Jacksonville area). Using a reliability of 90 percent, determine the normal PCC design thickness (without considering GWT).

In addition, determine the PCC design thickness if this pavement expected to experience a GWT rise from 55 in. to 45 in.

Solution: From Figure 6, it is seen that this area is in climate region "D". So, the design PCC thickness for this climate region, along with 90 percent reliability and 9 million ESALs, is found to be 9.0 in from Table 3. This is the design thickness without considering the GWT.

From Figure 63, it is found that the DR corresponding to 9.0 in. PCC with GWT at 45 in. depth in District 2, is equal to 1.25. This indicates that the rise in GWT depth from 55 in. to 45 in. may produce an equivalent damage under 1.25 × 9 million = 11.3 million ESALs of traffic loading. As such, the design thickness for this traffic level is found to be 9.5 in. (from Table 3).

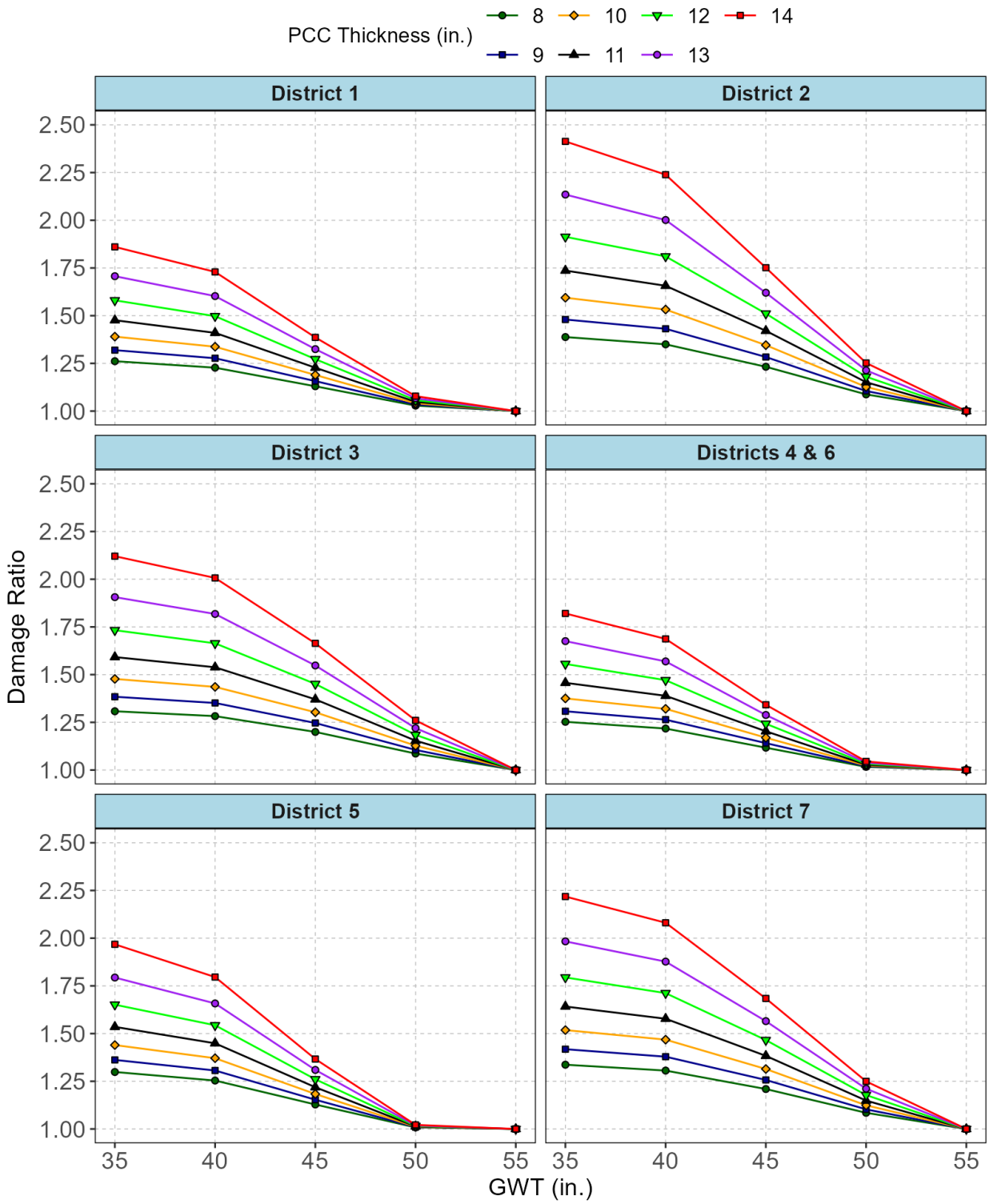

Figure 63. PCC damage ratios for PCC thickness (asphalt base option)

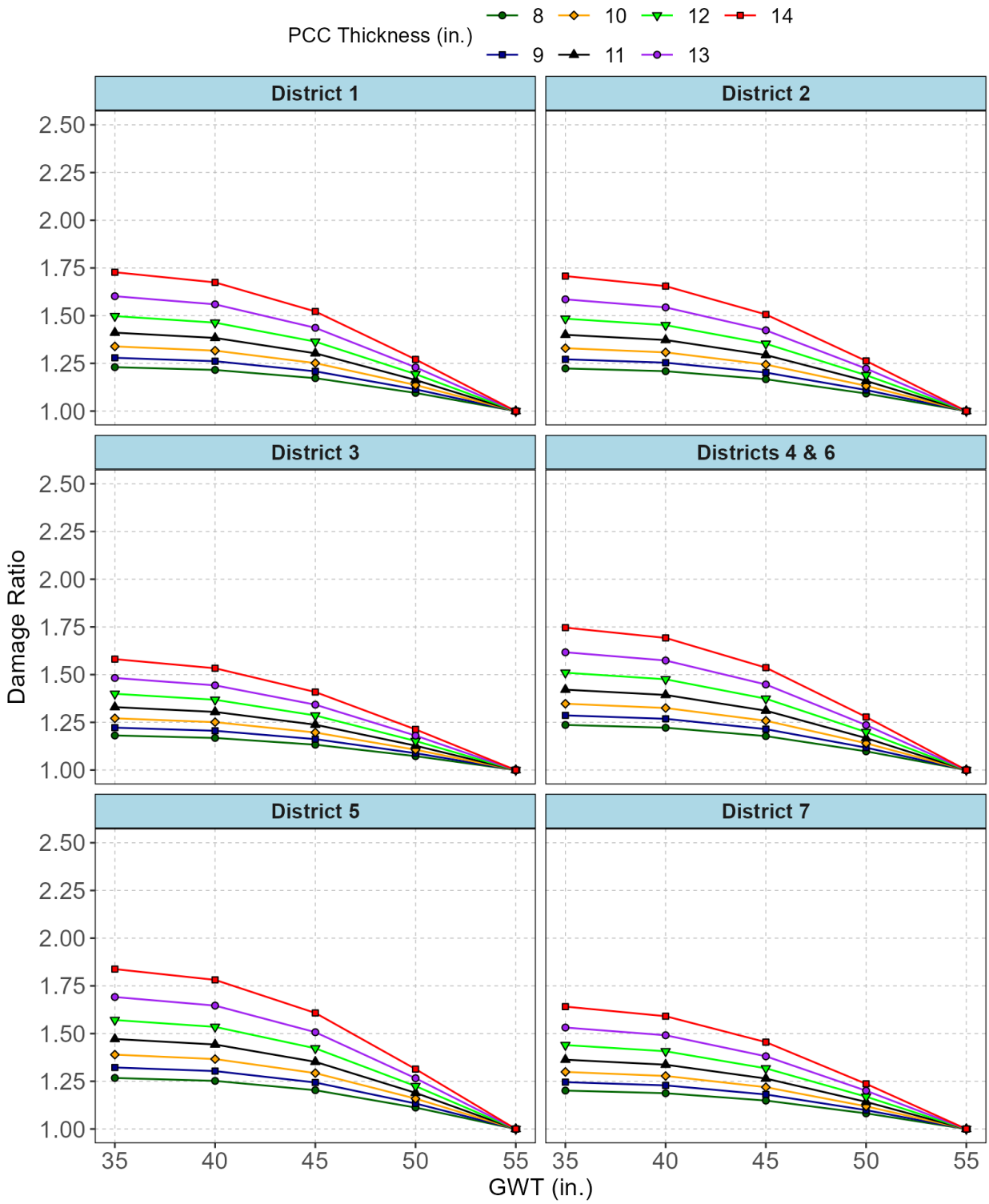

Figure 64. PCC damage ratios for PCC thickness (special select soil option)

6.4. BASE THICKNESS

Although increasing the PCC design thickness may be a viable strategy for improving the resiliency of rigid pavements, it may also be the most expensive strategy. Depending on the situation, it may be feasible to increase the AC base thickness (for the asphalt base option) or the stabilized subbase thickness (for the special select soil option), rather than the PCC thickness. As such, additional sensitivity analyses have been conducted using the Resiliency Tool for both design options. Similar to the previous analysis, the SWCC model was used for the modulus of embankment layer within the respective FDOT Districts (see Table 11 and Table 12).

6.4.1. Asphalt Base Option

The parameters included in the sensitivity analysis of the asphalt base option are described as the following.

1. The PCC thickness was varied from 8 in. to 14 in. at an interval of 1 in.
2. The AC thickness was varied from 4 in. to 8 in. at an interval of 1 in.
3. The depth to GWT was varied from 55 in. to 0 in. at an interval of 5 in.

Again, the sensitivity analysis results (using the damage obtained at PCC edge) were used to develop a set of DR (Equation (29)) for different scenarios.

For each PCC thickness, the normal condition was assumed to have an AC base thickness of 4.0 in. (which is the standard in FDOT's current rigid pavement design) and the GWT located at the reference depth of 55 in. below the pavement surface. The adverse condition corresponds to any changes in the GWT depth and/or the AC base thickness.

Figure 65 through Figure 70 show the DR values obtained from the sensitivity analysis. It is noted again that these figures only show the GWT depth from 35 in. to 55 in., as the damage ratio below 35 in. only showed negligible changes (i.e., the DR corresponding to 35 in. should be used for any GWT depth shallower than 35 in.).

An example problem is provided in the following to demonstrate how these DR values could be used in design.

Problem Statement: Consider the same PCC pavement in the previous example (9.0 in. PCC to carry 9 million ESALs in District 2, Jacksonville area). Determine the necessary AC base thickness to carry the same amount of traffic (without increasing the PCC thickness) if this pavement expected to experience a GWT rise from 55 in. to 45 in.

Solution: From Figure 66 (for District 2), it is found that for a 9.0 in. PCC, an AC base thickness of 7.0 in. is needed to keep the damage ratio below 1.0 (damage ratio = 0.96). Therefore, a minimum of 3.0 in. increase in the AC base thickness is needed to account for the GWT rise from 55 in. to 45 in.

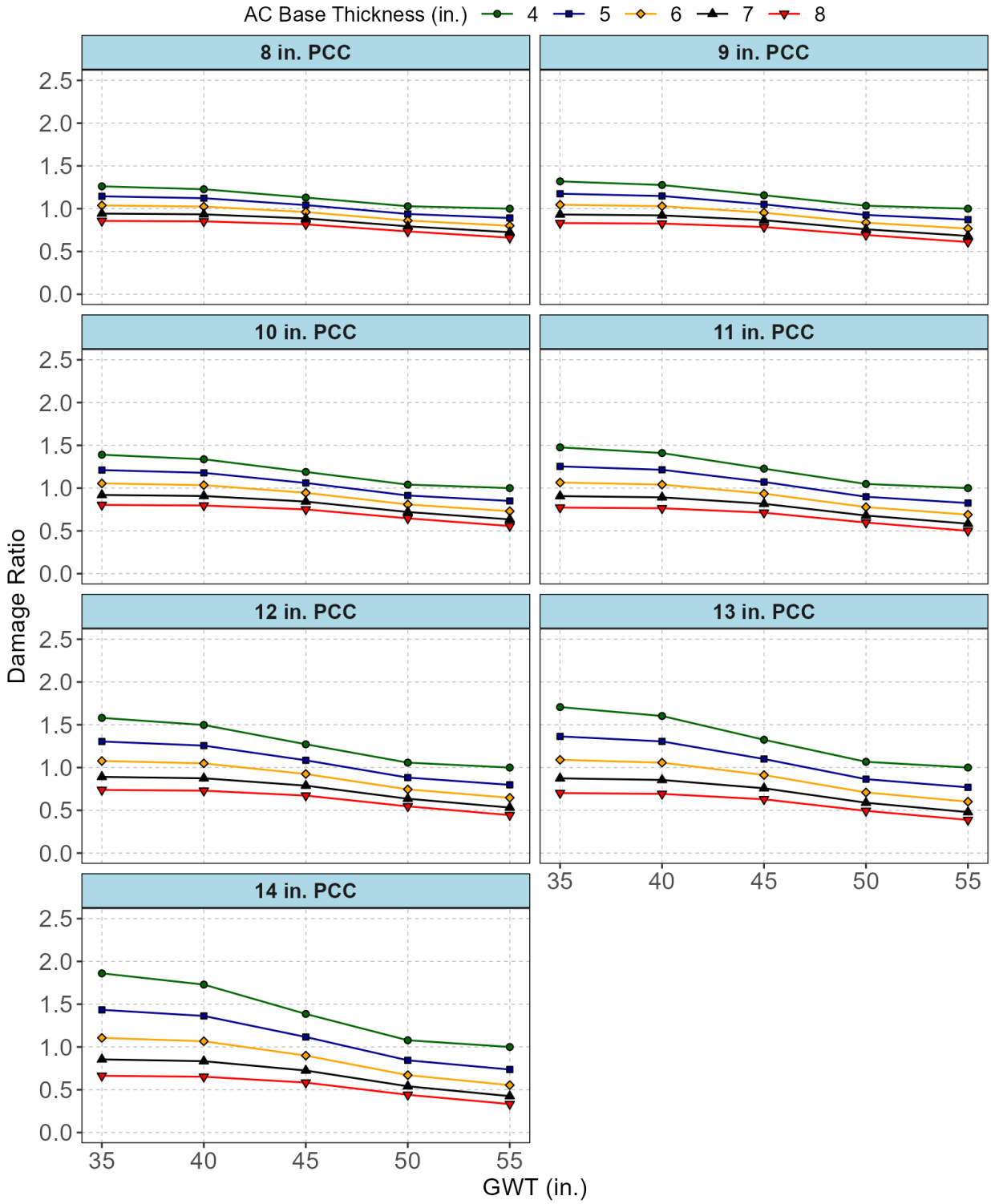

Figure 65. PCC damage ratios for AC thickness (asphalt base option, District 1)

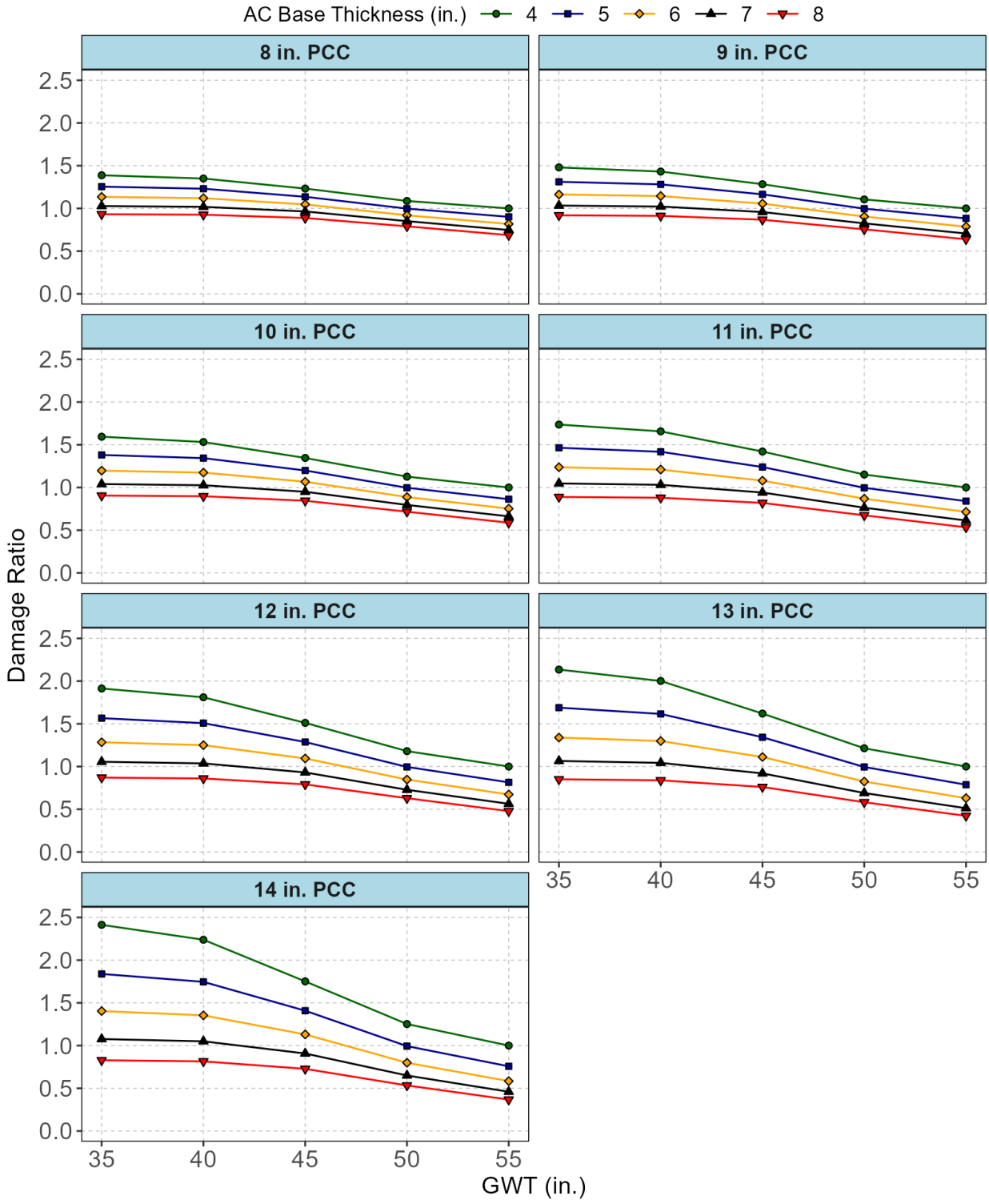

Figure 66. PCC damage ratios for AC thickness (asphalt base option, District 2)

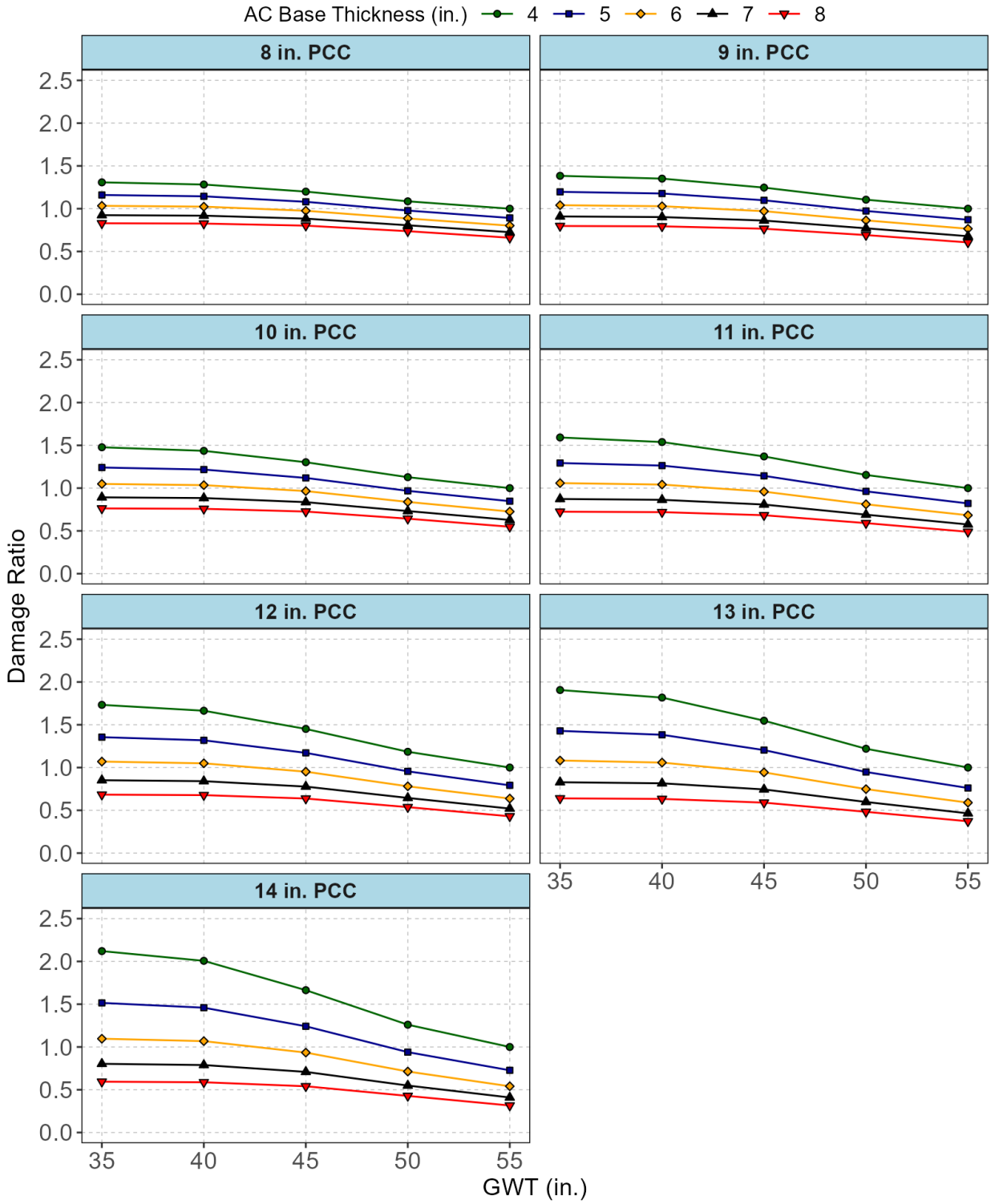

Figure 67. PCC damage ratios for AC thickness (asphalt base option, District 3)

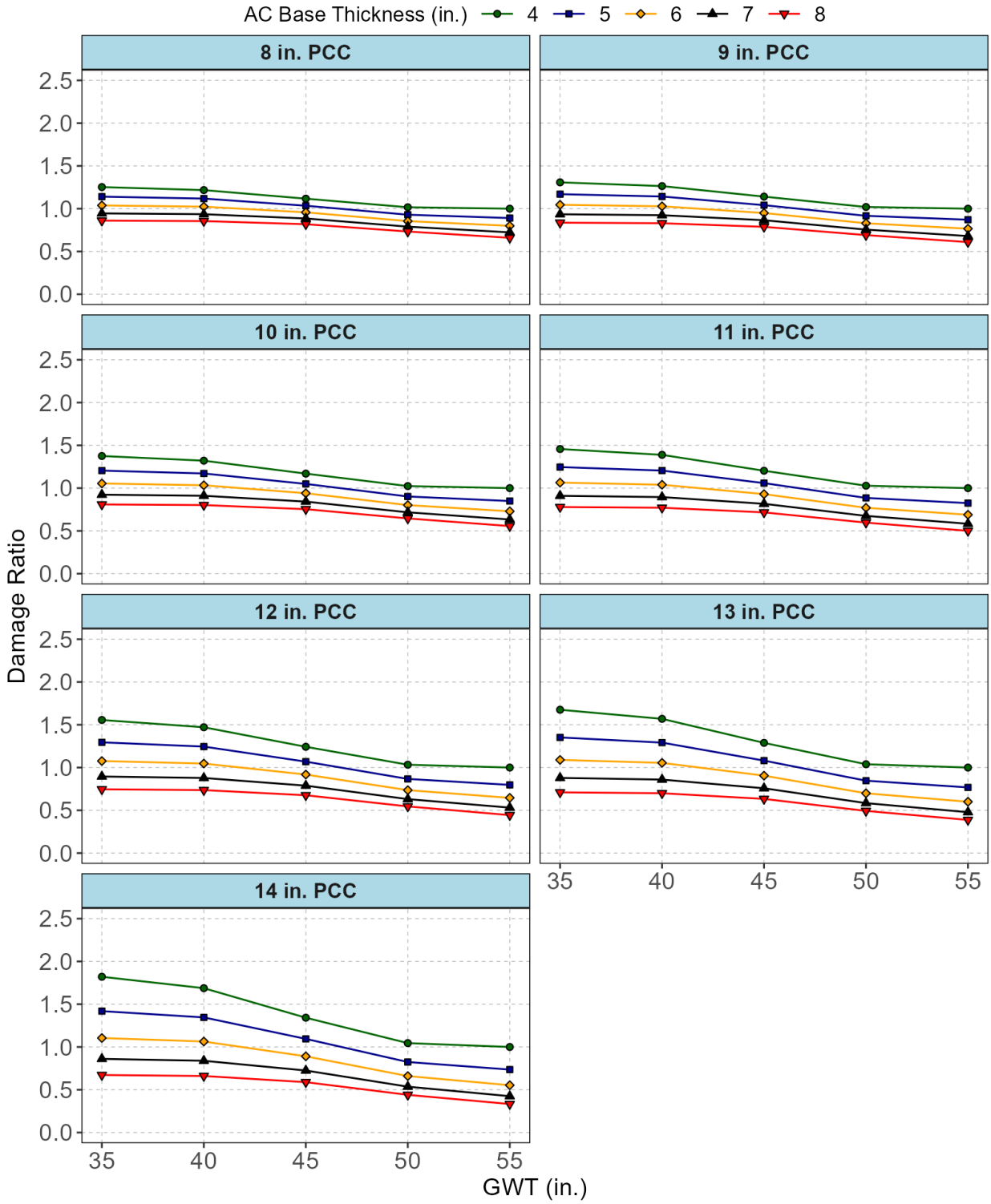

Figure 68. PCC damage ratios for AC thickness (asphalt base option, Districts 4 & 6)

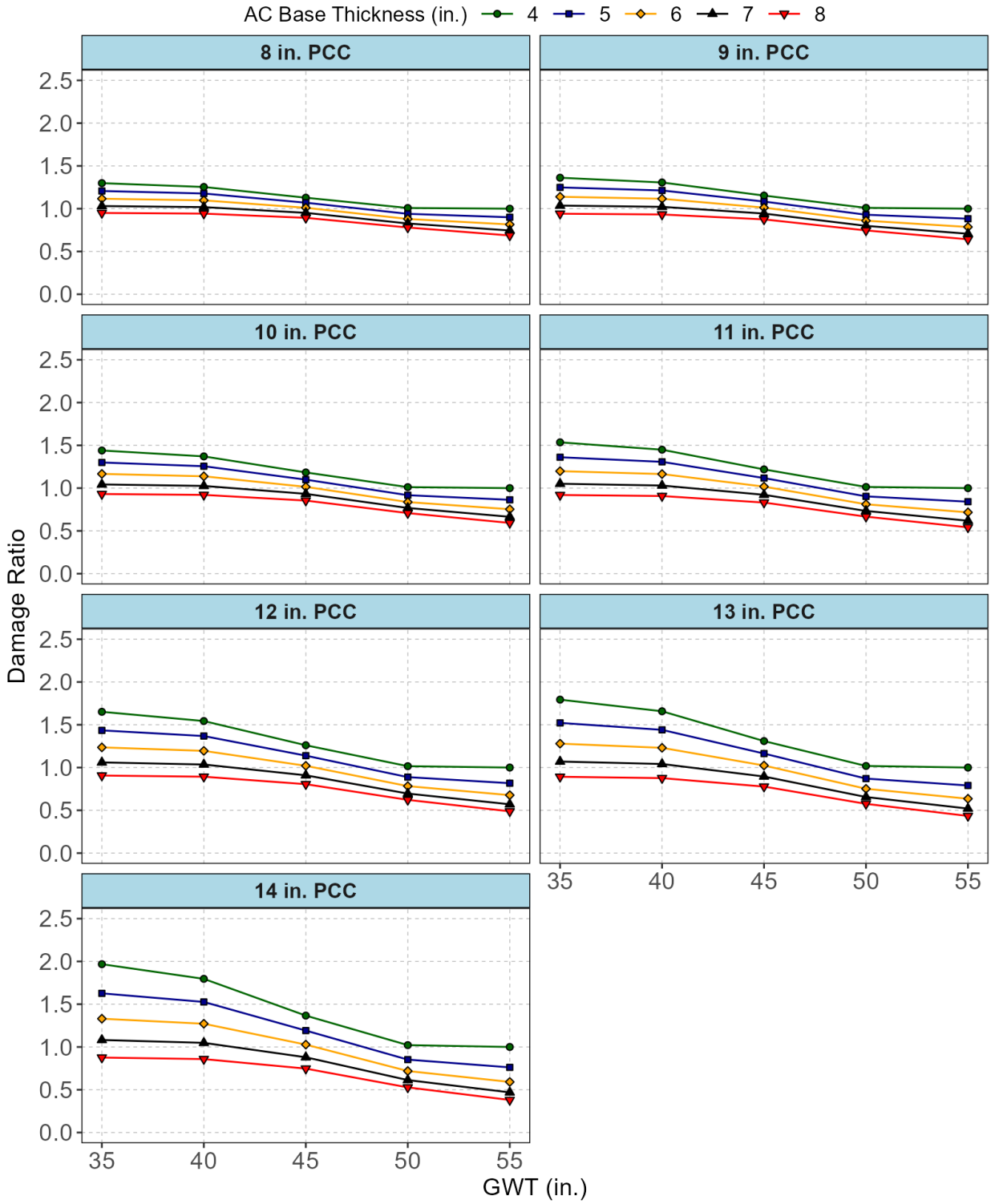

Figure 69. PCC damage ratios for AC thickness (asphalt base option, District 5)

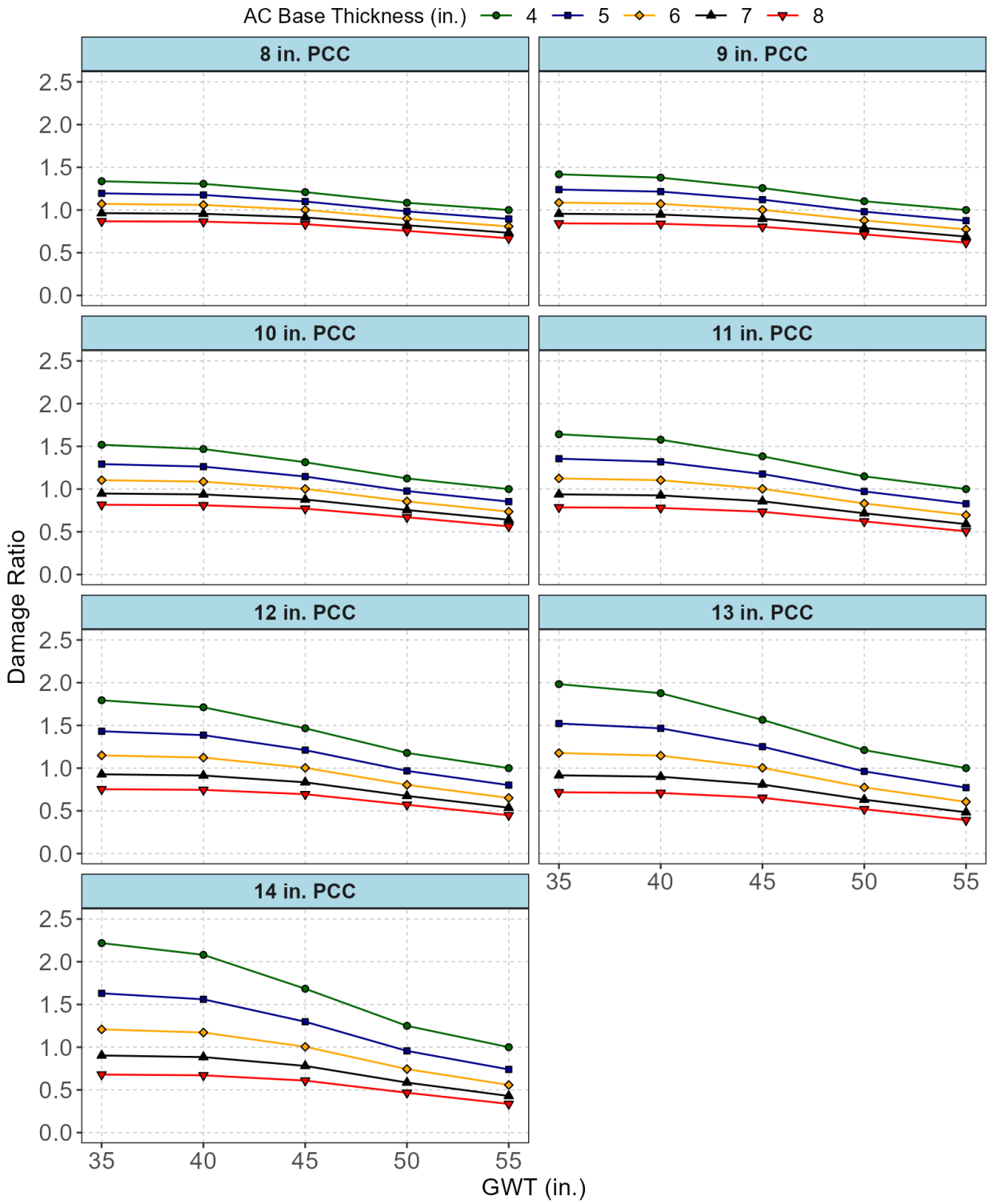

Figure 70. PCC damage ratios for AC thickness (asphalt base option, District 7)

6.4.2. Special Select Soil Option

The parameters included in the sensitivity analysis of the asphalt base option are described as the following.

1. The PCC thickness was varied from 8 in. to 14 in. at an interval of 1 in.
2. The Special Stabilized (SS) subbase thickness was varied from 6 in. to 10 in. at an interval of 1 in.
3. The depth to GWT was varied from 55 in. to 0 in. at an interval of 5 in.

Again, the sensitivity analysis results (using the damage obtained at PCC edge) were used to develop a set of DR (Equation (29)) for different scenarios.

For each PCC thickness, the normal condition was assumed to have a SS subbase thickness of 6.0 in. (which is the standard in FDOT's current rigid pavement design) and the GWT located at the reference depth of 55 in. below the pavement surface. The adverse condition corresponds to any changes in the GWT depth and/or the SS subbase thickness.

Figure 71 through Figure 76 show the DR values obtained from the sensitivity analysis. It is noted again that these figures only show the GWT depth from 35 in. to 55 in., as the damage ratio below 35 in. only showed negligible changes (i.e., the DR corresponding to 35 in. should be used for any GWT depth shallower than 35 in.).

However, all these figures generally indicate that most of the DR values derived for SS subbase thickness of 6 in. to 10 in. were above 1.0. In other words, increasing the SS subbase thickness of up to 4.0 in. from the standard thickness of 6.0 in. was not sufficient to reduce the damage caused by rise in GWT. This also means that the thickness of SS subbase may need to be increased substantially (to the point where it is no longer practical) in order for this design option to be considered a viable option for improving resiliency.

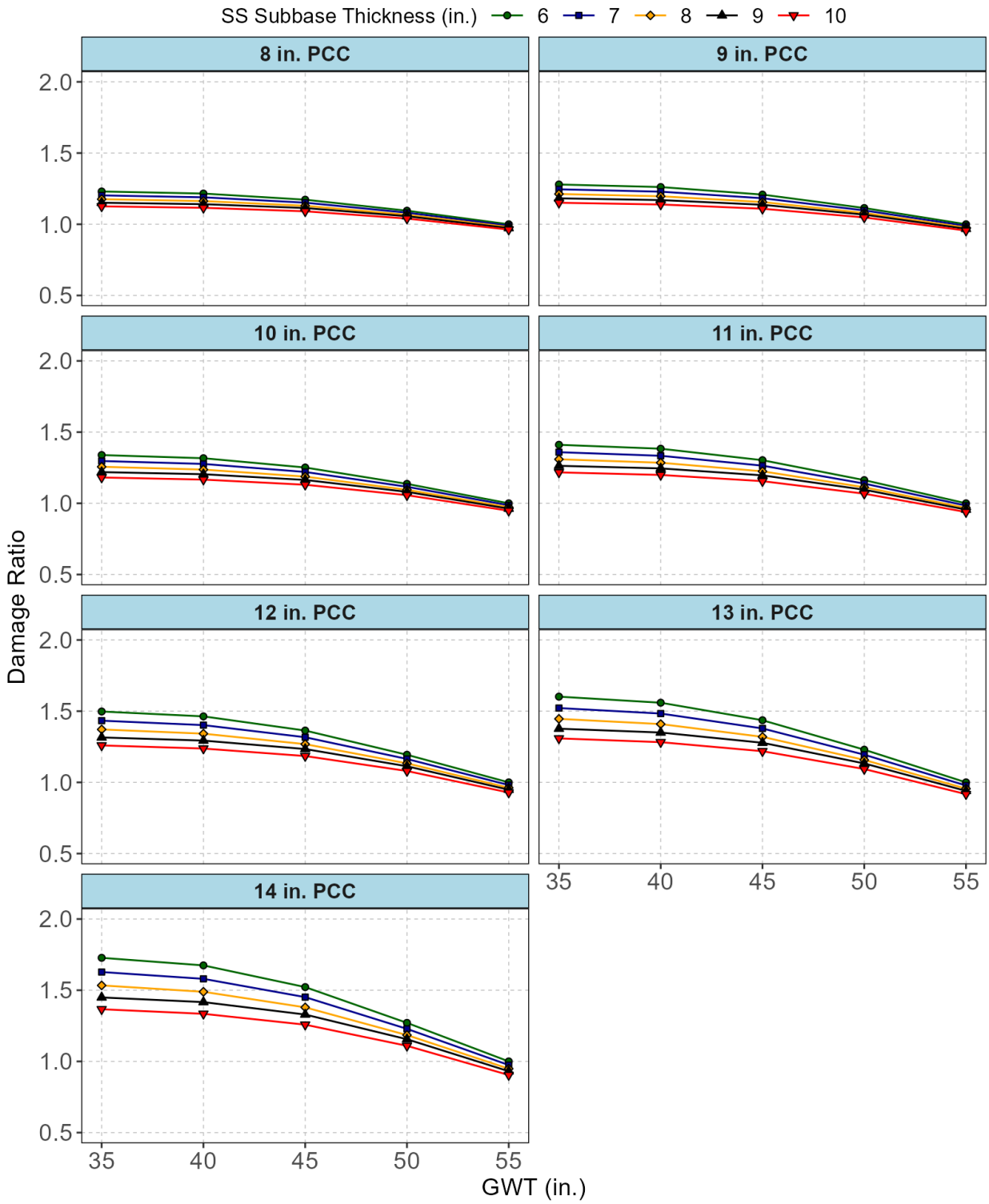

Figure 71. PCC damage ratios for stabilized subbase thickness (special select soil option, District 1)

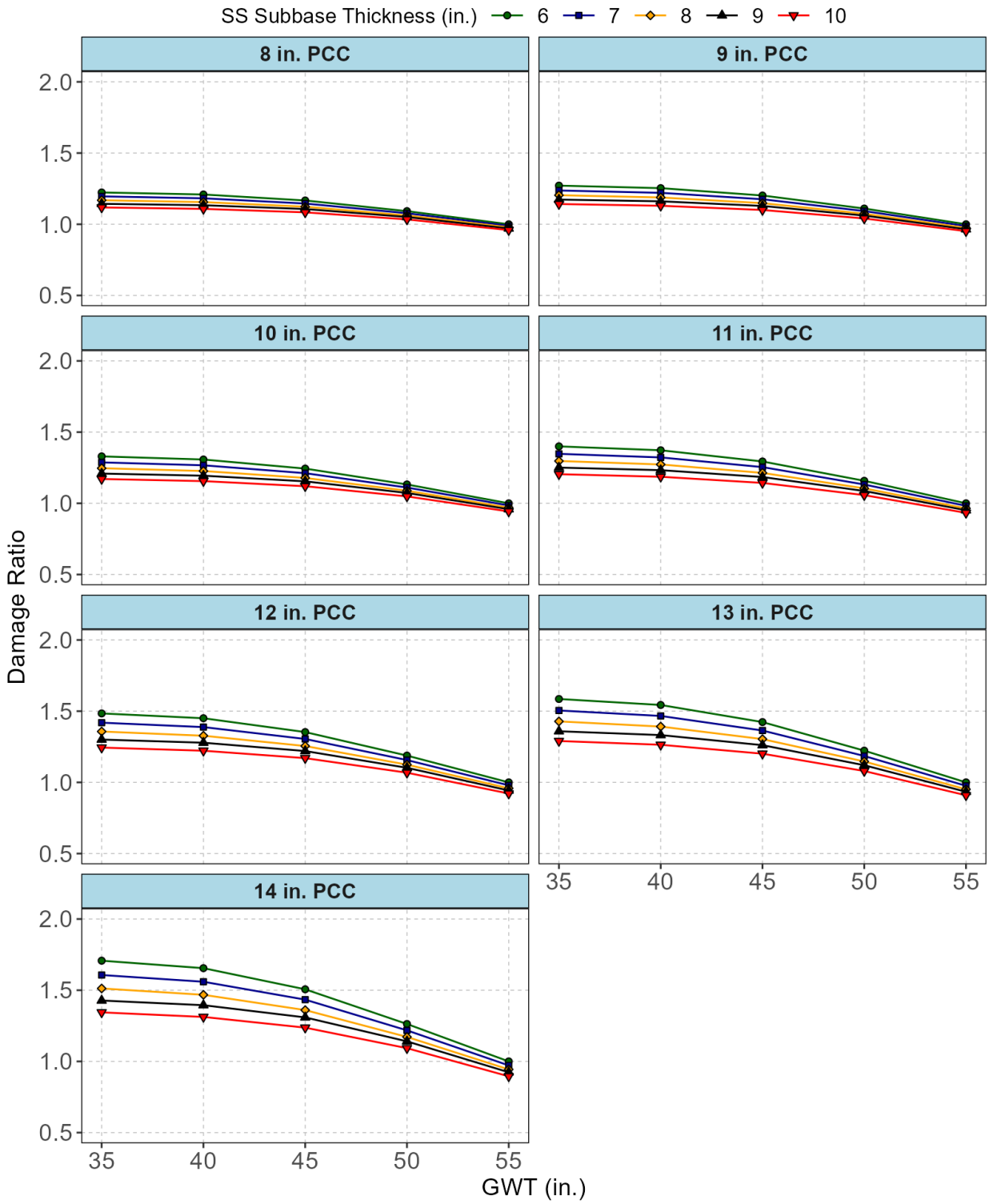

Figure 72. PCC damage ratios for stabilized subbase thickness (special select soil option, District 2)

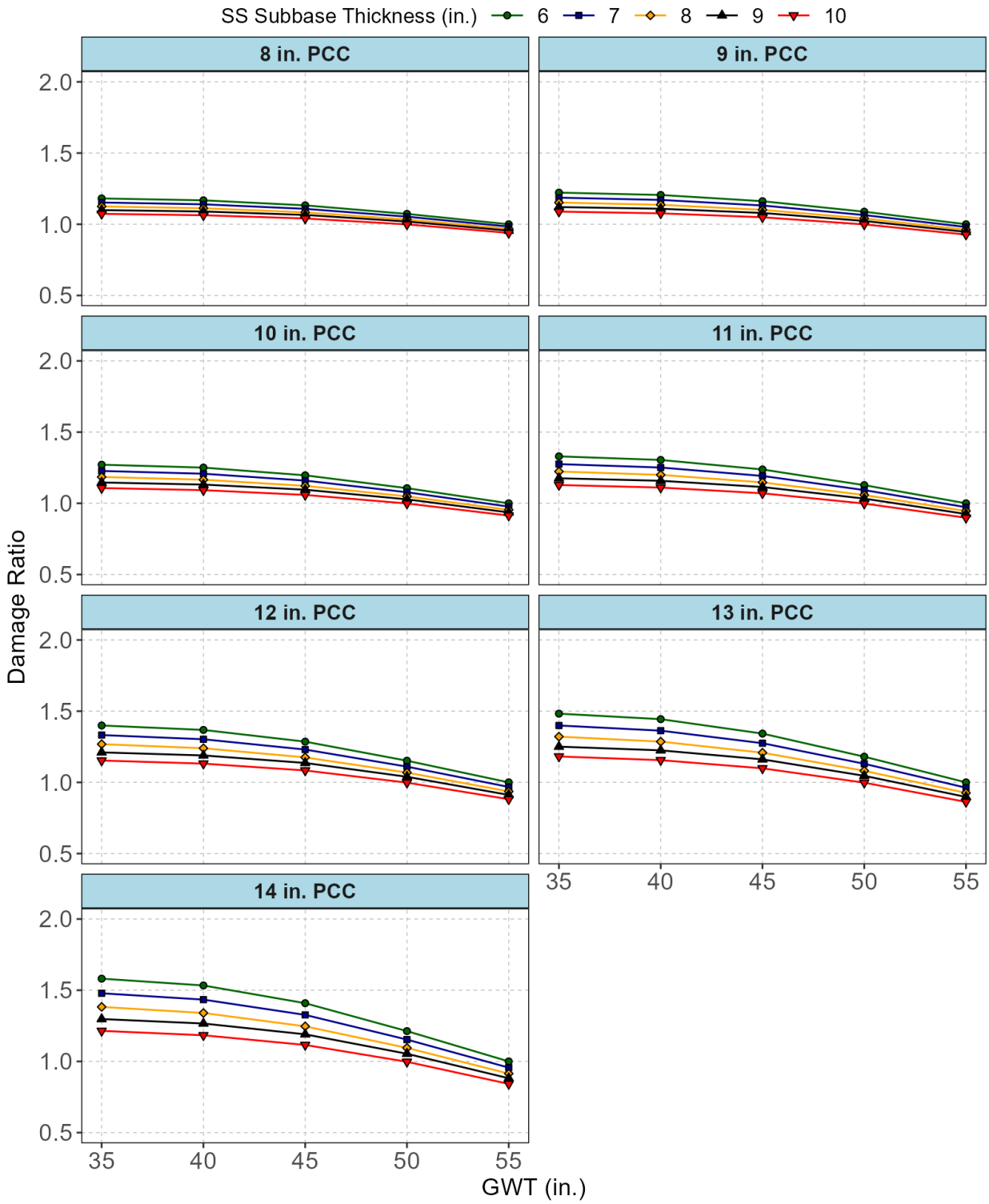

Figure 73. PCC damage ratios for stabilized subbase thickness (special select soil option, District 3)

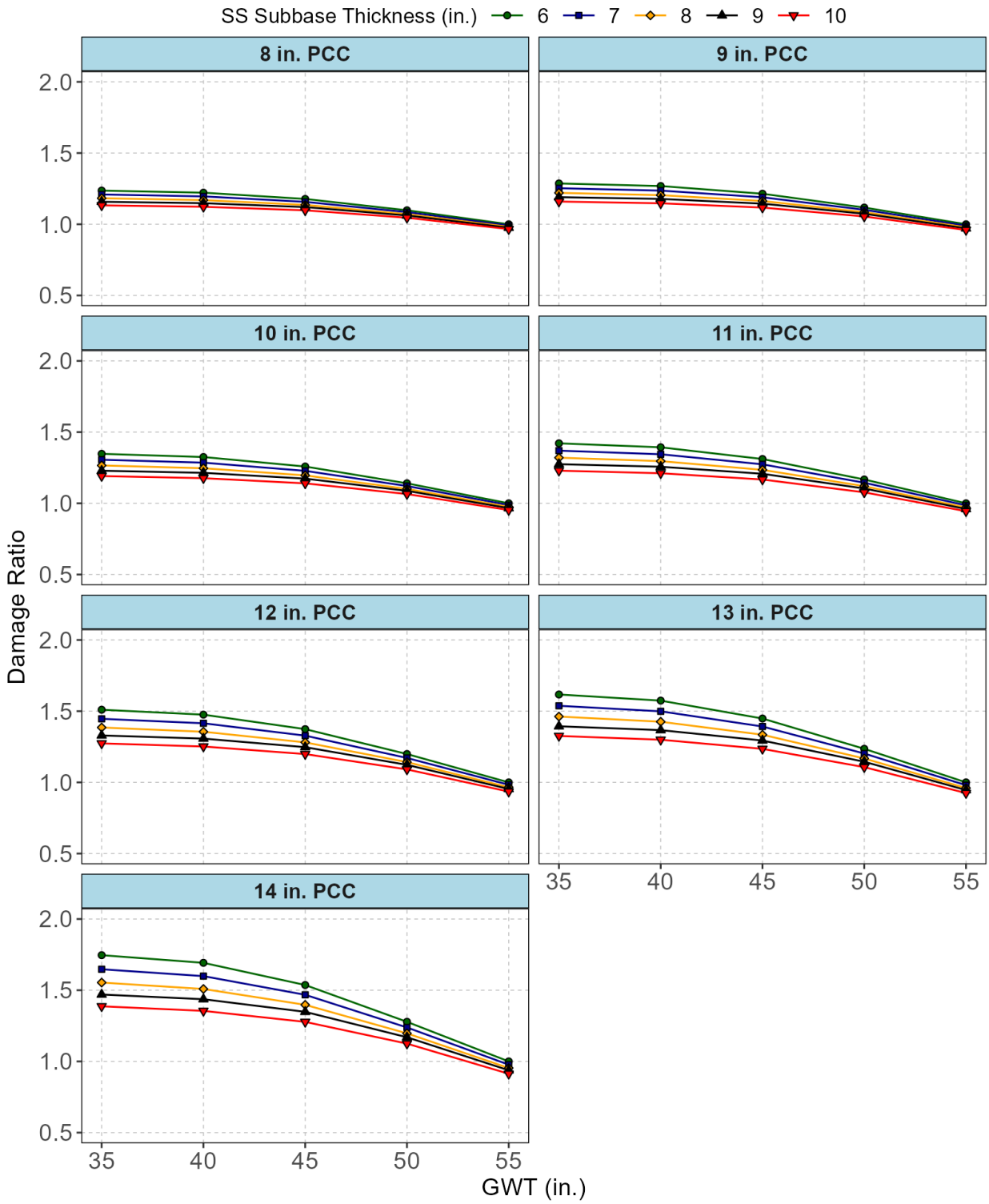

Figure 74. PCC damage ratios for stabilized subbase thickness (special select soil option, Districts 4 & 6)

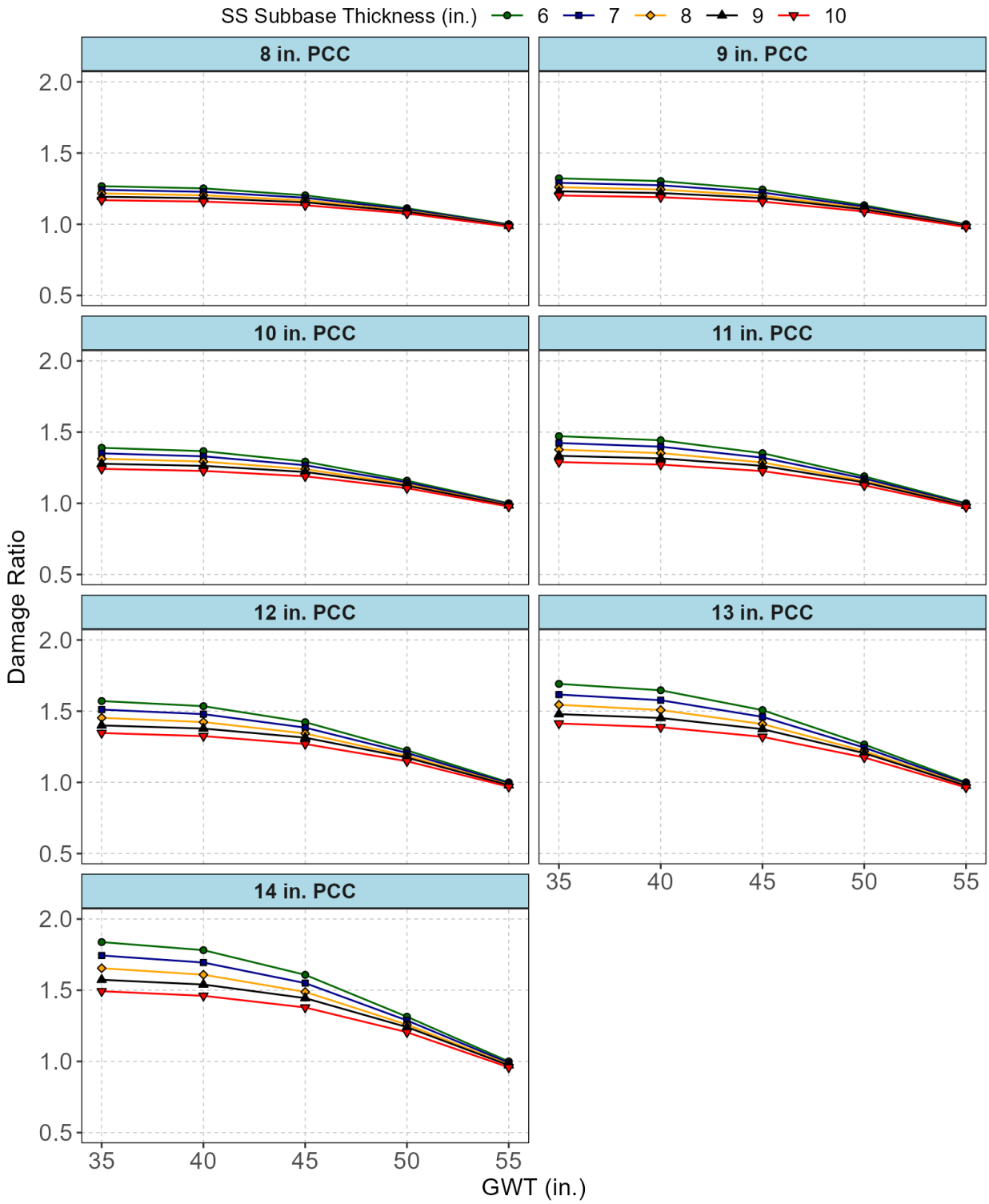

Figure 75. PCC damage ratios for stabilized subbase thickness (special select soil option, District 5)

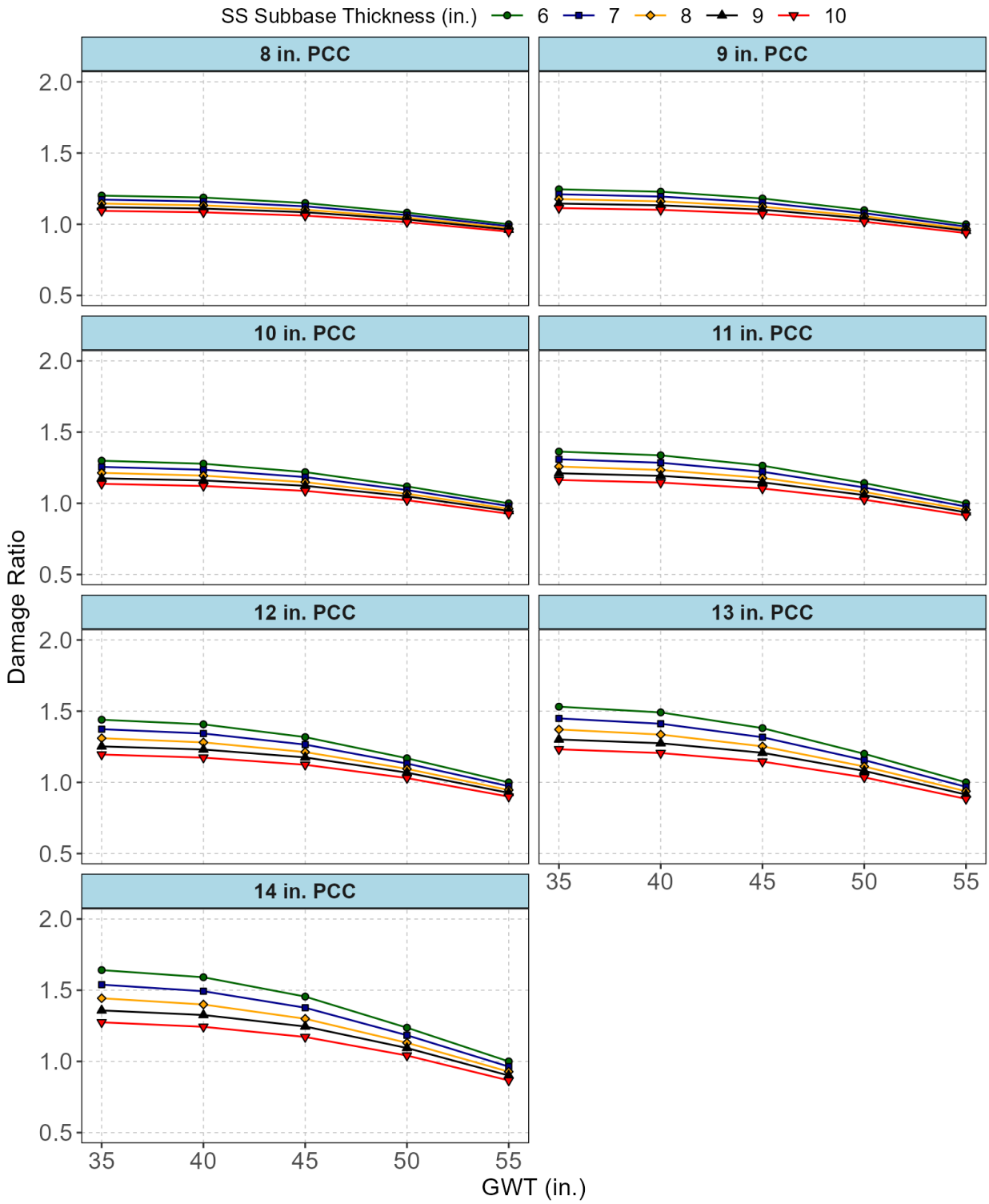

Figure 76. PCC damage ratios for stabilized subbase thickness (special select soil option, District 7)

6.5. SUMMARY

The primary purpose of this chapter was to assess the vulnerability of FDOT's existing rigid pavement sections under flooding and sea level rise. Based on the research team's preliminary analysis, it was found that FDOT's existing rigid pavements may be vulnerable to flooding and SLR. More specifically, out of the 86 rigid pavement sections managed by FDOT, approximately 31 percent (or 27 sections) of rigid pavements are located within 0.5 mile from the shoreline while another 33 percent (or 28 sections) of rigid pavements are located between 0.5 mile and 2.0 miles from the shoreline.

In addition, analysis of the NOAA data for SLR indicated that approximately 7 percent of FDOT's rigid pavement sections may be affected by a SLR of 1.0 ft. It was also found that the most of FDOT's rigid pavements vulnerable to SLR were located in District 2 (Jacksonville area) followed by District 6 (Miami Area) and District 7 (Tampa area).

Another objective of this task was to outline a procedure to assess the effect of increased layer thickness (especially the PCC and the base layer) in FDOT's rigid pavement design as a mitigating solution for these moisture related threats (e.g., SLR). Since FDOT's rigid pavement design tables were not developed to incorporate the effect of SLR, a series of sensitivity analyses were conducted to develop preliminary design strategies using FDOT's Rigid Pavement Resiliency Tool. The results from the sensitivity analyses were used to develop preliminary damage ratios that can be used to adjust the PCC or the base thickness for different levels of ground water table depth. A couple of example problems were provided in which a rigid pavement design could be modified based on the damage ratios provided in this report.

It is strongly emphasized again that none of the models incorporated into the Resiliency Tool was verified or validated. As such, the examples on the damage ratios developed herein should only be used as a general guide on how the tool may be used in the future with additional research to support the validity of the Resiliency Tool.

7. SUMMARY AND RECOMMENDATIONS

Moisture within the foundation of Florida's pavements may lead to detrimental impacts. The consequence may range from total washout of the pavement (under very severe storms and hurricanes) to short-term and long-term inundation that may lead to serviceability loss of the pavement structure. The short-term effect may result from opening the roadway to traffic as soon as the flooded water is receded from the pavement surface while the long-term effect may be caused by excessive moisture within the base, subbase, subgrade, and embankment that requires a long period of time to drain out.

The primary objective of this study was to evaluate the impact that inundation may have on concrete pavements and to identify cost-effective and implementable solutions to improve the resilience of new and existing rigid pavement systems subjected to the combined effects of flooding and sea level rise. To meet these objectives, a Mechanistic-Empirical methodology for assessing the resiliency of Florida's rigid pavements was developed. Based on the thorough review of available literature, three main components were identified and implemented into the mechanistic-empirical "Rigid Pavement Resilience Tool" developed as part of this project. These components are summarized in the following.

1. A Hydrological Model that simulates the water flow within the pavement system. The model incorporates precipitation, ground water table depth, and surface evaporation to simulate the moisture within any pavement layer over time (before, during, and after flooding).

2. A Geotechnical/Soil Mechanics Model that takes the moisture content of unbound layers calculated from the hydrological model and adjust their resilient modulus accordingly.

3. A Structural Model that takes the structural inputs (i.e., resilient modulus of unbound layers, PCC modulus, thickness, traffic, etc.) and calculates pavement response and predicts performance.

FDOT's new Rigid Pavement Resiliency Tool was implemented in a macro-enabled Excel spreadsheet environment. The primary purpose of the Tool is to allow the user analyze the structural response and performance of rigid pavement systems under various moisture-related scenarios. For this purpose, the tool has implemented two analysis options: Long-Term and Short-Term. The Long-Term analysis option allows the user to compare different situations that are considered to be permanent (i.e., those that do not change over a short period of time), while the Short-Term analysis option allows the user to simulate a pavement structure experiencing changes in moisture level within a relatively short period of time (i.e., within a few hours, days, or weeks).

The structural analysis within the tool can be conducted using the well-known Westergaard equations or the ILLISLAB FEM. Based on the responses obtained from the selected structural analysis option, the tool also calculates some performance measures such as damage and maximum allowable number of load passes using the Transfer function adopted from the AASHTOWare Pavement ME.

In addition to the resiliency tool development, a preliminary effort was carried out to assess the vulnerability of FDOT's existing rigid pavement sections under flooding and sea level rise. Based on the results of the preliminary analysis, it was found that FDOT's existing rigid pavements may be vulnerable to flooding and SLR. More specifically, out of the 86 rigid pavement sections managed by FDOT, approximately 31 percent (or 27 sections) of rigid pavements are located within 0.5 mile from the shoreline while another 33 percent (or 28 sections) of rigid pavements are located between 0.5 mile and 2.0 miles from the shoreline.

In addition, analysis of the NOAA data for SLR indicated that approximately 7 percent of FDOT's rigid pavement sections may be affected by a SLR of 1.0 ft. It was also found that the most of FDOT's rigid pavements vulnerable to SLR were located in District 2 (Jacksonville area) followed by District 6 (Miami Area) and District 7 (Tampa area).

Several examples have been provided in the report to demonstrate the use of the newly developed resiliency tool. Since FDOT's rigid pavement design tables were not developed to incorporate the effect of SLR, a series of sensitivity analyses were conducted to develop preliminary design strategies using FDOT's Rigid Pavement Resiliency Tool. The results from the sensitivity analyses were used to develop preliminary damage ratios that can be used to adjust the PCC or the base thickness for different levels of ground water table depth. A couple of example problems were provided in which a rigid pavement design could be modified based on the damage ratios provided in this report.

However, it is emphasized that the tool was implemented based on numerous, existing models that were found in literature. These models include those for the moisture flow, hydraulic conductivity, resilient modulus of the soil, structural response, transfer functions, etc. These models were implemented based on the available information documented in literature, without any further calibration or validation. As such, it is emphasized that the examples on the damage ratios developed herein should only be used as a general guide on how the tool may be used in the future with additional research to support the validity of the Resiliency Tool. Furthermore, it is strongly recommended that FDOT examine the results from the Resiliency Tool against any available field data.

REFERENCES

AASHTO. Mechanistic-Empirical Pavement Design Guide, Interim Edition: A Manual of Practice. Washington, D.C., 2015.

Applied Research Associates (ARA). Guide for Mechanistic-Empirical Design of New and Rehabilitated Pavement Structures. Appendix DD-1: Resilient Modulus as Function of Soil Moisture – Summary of Predictive Models. NCHRP 1-37(A). June, 2000.

Asadi, M. Assessment of Hydraulic and Structural Behavior of Inundated Pavements. Ph.D. Dissertation, University of Texas at El Paso, 2020.

Barami, B. Infrastructure Resilience: A Risk-Based Framework. Summary prepared for Beyond Bouncing Back: A Roundtable on Critical Transportation Infrastructure Resilience. John A. Volpe National Transportation Systems Center, USDOT, 2013.

Berry, L., Arockiasamy, Bloetscher, M., Kaisar, F., Rodriguez-Seda, E., Scarlatos, J., Teegavarapu, P., Hammer, R. N.M. Development of a Methodology for the Assessment of Sea Level Rise Impacts on Florida's Transportation Modes and Infrastructure; Florida Department of Transportation: Tallahassee, FL, USA, 2012.

Bloetscher, F., Berry, L., Rodriguez-Seda, J., Hammer, N.H., Romah, T., Jolovic, D., Heimlich, B. and Cahill, M.A. Identifying FDOT's physical transportation infrastructure vulnerable to sea level rise. Journal of Infrastructure Systems, 20(2), p.04013015, 2014.

Bloetscher, F., Hoermann, S. and Berry, L. Adaptation of Florida's Urban Infrastructure to Climate Change. Florida's Climate: Changes, Variations, and Impacts, 2017.

Bowers, B.F., and Gu, F. Asphalt Pavement: A Critically Important Aspect of Infrastructure Resiliency. Report No. 21-02. National Center for Asphalt Technology, Auburn, AL. July, 2021.
Briaud, J.L. and Maddah, L. Minimizing Roadway Embankment Damage from Flooding. Project No. 20-05, 2016.

Brink, W. Applying Resiliency Concepts for PCC Pavements Using AASHTOWare Pavement ME Design. Presentation at 100th Annual Meeting of Transportation Research Board. Session 1194. Jan. 2021.

Bruijn, K.M., Maran, C., Zygnerski, M., Jurado, J., Burzel, A., Jeuken, C. and Obeysekera, J Flood resilience of critical infrastructure: Approach and method applied to Fort Lauderdale, Florida. *Water*, *11*(3), p.517, 2019.

Carver, J. and Spirio, C. Strategies to Increase Resilience of Florida DOT's Facilities. In Transportation Resilience 2019: 2nd International Conference on Resilience to Natural Hazards and Extreme Events. Transportation Research Circular E-C265. Transportation Research Board, Washington, D.C., 2019.

Cary, C.E. and Zapata, C.E. Resilient Modulus for Unsaturated Unbound Materials. Road Materials and Pavement Design, 12 (3), 615–638, 2011.

Ceylan, H., Gopalakrishnan, K., Kim, S. and Steffes, R.F. Evaluating Roadway Subsurface Drainage Practices. IHRB Project TR-643, 2013.

Chapuis, R.P. Predicting the Saturated Hydraulic Conductivity of Sand and Gravel Using Effective Diameter and Void Ratio. Canadian Geotechnical Journal. Vol. 41. Pp. 787-795. 2004.

Cleary, J., Gurley, K., Marshall, J., Pinelli, J. et al. StEER: Structural Extreme Event Reconnaissance network: Field Assessment Team 1 (FAT-1), Early Access Reconnaissance Report (EARR). Project No. PR-J-2111, 2018.

Cooley, A. L., Prowell, B., and Brown, E.R. Issues Pertaining to the Permeability Characteristics of Coarse-Graded Superpave Mixes. NCAT Report No. 02-06. National Center for Asphalt Technology, Auburn, AL. 2002.

Darter, M.I., Hall, K.T. and Kuo, C.M. Support under Portland Cement Concrete Pavements. National Cooperative Highway Research Program, NCHRP Project 1-30, 1995.

Dean G. Improving a Pavement's Resiliency Part II Concrete Pavement Solutions. VA Concrete Conference, February, 2020.

Dylla, H., and Hyman, R. Boosting Pavement Resilience. FHWA-HRT-19-001. Public Roads, Federal Highway Administration, Washington, D.C., 2018.

Elshaer, M. Assessing the Mechanical Response of Pavements During and After Flooding. Doctoral dissertation. University of New Hampshire.2017.

Elshaer, M. Ghayoomi, M., and Daniel, J.S. Impact of Subsurface Water on Structural Performance of Inundated Flexible Pavements. International Journal of Pavement Engineering, DOI: https://doi.org/10.1080/10298436.2017.1366767. 2017.

FDOT. Florida Department of Transportation Hurricane Response Evaluation and Recommendation. Technical Memorandum. Traffic Engineering and Operations Office Intelligent Transportation Systems (ITS) Section, Tallahassee, Florida, 2005.

FDOT. Risk Assessment on SIS Facilities. http://www.floridatransportationplan.com/pdf/FDOT-SIS_ResiliencePhaseI-TechMemo_wApp_8-22-18.pdf. Tallahassee, FL. 2018.

FDOT. Resiliency of State Transportation Infrastructure. FDOT Policy No. 000-525-053. Tallahassee, FL. April 2020a.

FDOT. Florida Transportation Plan. http://floridatransportationplan.com/index.htm. Tallahassee, FL. 2020b.

FDOT. Freight Mobility and Trade Plan. https://www.fdot.gov/fmtp. Tallahassee, FL. 2020c.
FDOT. Rigid Pavement Design Manual. Florida Department of Transportation. Tallahassee, FL. Jan. 2021.

Federal Emergency Management Agency (FEMA). https://www.fema.gov/flood-maps/national-flood-hazard-layer. Accessed 2023.
Florida Fish and Wildlife Conservation Commission (FWC). https://geodata.myfwc.com/datasets/myfwc::florida-shoreline-1-to-40000-scale/about. Accessed. 2023.

FHWA. Transportation System Preparedness and Resilience to Climate Change and Extreme Weather Events. U.S. Department of Transportation, 2014.

FHWA. Climate Change Adaptation Tools. https://www.fhwa.dot.gov/environment/sustainability/resilience/tools/. April, 2021.

Flannery, A. Pena, M.A., Manns, J. Resilience in Transportation Planning, Engineering, Management, Policy, and Administration. NCHRP Synthesis 527. National Academy of Sciences. Washington D.C., 2018.

Gaspard, K., Martinez, M., Zhang, Z. and Wu, Z. Impact of Hurricane Katrina on Roadways in the New Orleans Area: Technical Assistance. Report No. 07-2TA. Louisiana Transportation Research Center, 2007.

Ghayoomi, M., dave, E.V., and Mousavi, S.M. Mehcanistic Load Restriction Decision Platform for Pavement Systems Prone to Moisture Variations: System Dynamics Framework Development. National Road Research Alliance, Contract 1034192. 2020.

Hazen A. Discussion: Dams on Sand Foundations. Transactions, American Society of Civil Engineers. Vol. 73, pp.199–203. 1911.

Hsieh, P. A., Wingle, W. L., and Healy, R. W. VS2DI-A Graphical Software Package for Simulating Fluid Flow and Solute or Energy Transport in Variably Saturated Porous Media. U.S. Geological Survey Water-Resources Invest. Rep. 99-4130, 1999.

Hemmati, M., Ellingwood, B.R. and Mahmoud, H.N. The Role of Urban Growth in Resilience of Communities under Flood Risk. Earth's Future, 8(3), p.e2019EF001382, 2020.

Huang, Y.H., and Want, S.T. Finite Element Analysis of Concrete Slabs and its Implications for Rigid Pavement Design. Highway Research Record No. 466, Highway Research Board, Washington, D.C. pp. 55-69. 1973.

Huang, Y.H. Finite Element Analysis of Slabs on Elastic Solids. Transportation Engineering Journal, ASCE, Vol. 100. Pp. 403-416. 1974.

Khan, M.U., Mesbah, M., Ferreira, L. and Williams, D.J. Estimating Pavement's Flood Resilience. Journal of Transportation Engineering, Part B: Pavements, 143(3), p.04017009, 2017.

Knott, J.F., Elshaer, M., Daniel, J.S., Jacobs, J.M. and Kirshen, P. Assessing the Effects of Rising Groundwater from Sea Level Rise on the Service Life of Pavements in Coastal Road Infrastructure. Transportation Research Record, 2639(1), pp.1-10, 2017.

Knott, J.F., Jacobs, J.M., Sias, J.E., Kirshen, P. and Dave, E.V., 2019. A Framework for Introducing Climate-Change Adaptation in Pavement Management. Sustainability, 11(16), p.4382, 2019.

Kopp, R.E., Horton, R.M., Little, C.M., Mitrovica, J.X., Oppenheimer, M., Rasmussen, D.J., Strauss, B.H. and Tebaldi, C. Probabilistic 21st and 22nd century sea-level projections at a global network of tide-gauge sites. *Earth's future*, *2*(8), pp.383-406, 2014.

Korovesis, G.T. Analysis of Slab-on-Grade Pavement Systems Subjected to Wheel and Temperature Loadings. Ph.D. Dissertation. University of Illinois. 1990.

Leadon, M.E., Nguyen, N.T., Clark, R. R. Hurricane Opal: Beach and Dune Erosion and Structural Damage along the Panhandle Coast of Florida. Report of the Bureau of Beaches and Coastal systems. 1998.

Lee, H.S. and Ayyala, D. Enhanced Hydroplaning Prediction Tool. Final Report, FDOT Contract No. BE570. Champaign, IL. April, 2020.

Lounis, Z. and McAllister, T.P. Risk-Based Decision Making for Sustainable and Resilient Infrastructure Systems. Journal of Structural Engineering, 142(9), p.F4016005, 2016.

Mack, J. Improving Pavement Resilienty & Disaster Recovery; Flooding Impacts. Presentation. Feb. 2020. https://www.penndot.gov/ProjectAndPrograms/Construction/QAW/2020_QAW_Presentations/Concrete_Session/6-PCC_benefits_for_Flooded_Pavements.pdf

Mallick, R.B., Radzicki, M.J., Daniel, J.S. and Jacobs, J.M. Use of System Dynamics To Understand Long-Term Impact Of Climate Change On Pavement Performance And Maintenance Cost. Transportation Research Record, 2455(1), pp.1-9, 2014.

Masad, E., Al-Omari, A., and Lytton, R. Simple Method for Predicting Laboratory and Field Permeability of Hot-Mix Asphalt. Transportation Research Record: Journal of the Transportation Research Board, No. 1970, Transportation Research Board of the National Academies, Washington, D.C., 2006, pp. 55–63.

Mbonimpa M., Aubertin M., Chapuis R.P., and Bussière B. Practical Pedotransfer Functions for Estimating the Saturated Hydraulic Conductivity. Geotech. Geol. Eng. Vol. 20, No. 3, pp. 235–259., 2002.

Missouri Department of Transportation (MoDOT). Missouri Standard Specification for Highway Construction, Section 303, Rock Base, Base and Aggregate Surface, Jefferson City, MO., 2018.
Muench, S. and Van Dam, T. Climate Change Adaptation for Pavements. Report No. FHWA-HIF-15-015, 2015.

Mohammad, L.N., Herath, A., and Huang, B. Evaluation of Permeability of Superpave Asphalt Mixtures. Transportation Research Record: Journal of the Transportation Research Board, No. 1832, Transportation Research Board of the National Academies, Washington, D.C., 2003, pp. 50–58.

NOAA. Hurricane Costs. National Ocean and Atmospheric Administration. 2020a. https://coast.noaa.gov/states/fast-facts/hurricane-costs.html

NOAA. Flooding in Florida. National Ocean and Atmospheric Administration. 2020b. https://www.weather.gov/safety/flood-states-fl

National Oceanic and Atmospheric Administration (NOAA). https://coast.noaa.gov/slrdata/. Accessed 2023.

Oh, J.H., and Fernando, E.G. MEPDG Program Implementation in Florida. Final Report No. BDH10. Florida Department of Transportation. Tallahassee, FL. 2008.

Oh, J.H., and Fernando, E.G. Comparison of Resilient Modulus Values Used in Pavement Design. Final Report No. BDL76. Florida Department of Transportation. Tallahassee, FL. 2011.

Oh, J.H., Fernando, E.G., Holzschuher, C., and Horhota, D. Comparison of Resilient Modulus Values for Florida Flexible Mechanistic-Empricial Pavement Design. International Journal of Pavement Engineering, Vol. 13, No. 5, pp. 472-484. 2012.

Oyediji, O. and Achebe, J. Towards a Flood Resilient Pavement System in Canada-A Rigid Pavement Design Approach. In Transportation Association of Canada and ITS Canada Joint Conference and Exhibition, 2019.

Pavement Interactive. https://pavementinteractive.org/climate-change-impacts-on-pavements-and-resilience/. Accessed July 2021.

Rada, G. and Witczak, M.W. Comprehensive Evaluation of Laboratory Resilient Moduli Results for Granular Material. In: Transportation Research Record 810, Layered Pavement Systems. Washington, DC: Transportation Research Board, National Research Council, National Academy of Sciences, 1981.

Richards, L.A. Capillary conduction of liquids through porous mediums. Physics, Vol. 1, No. 5, pp. 318–333., 1931.

Romah, T. Advanced Methods in Sea Level Rise Vulnerability Assessment. Florida Atlantic University, Boca Raton, FL, 2012.

Romanoschi, S. The Impact of Hurricane Harvey on Pavement Structures in the South East Texas and South West Louisiana. Project No. 18PUTA02, Transportation Consortium of South-Central States (Tran-SET), Louisiana State University, Baton Rouge, LA, 2019.

Schwartz, C. and Boudreau, R. Geotechnical Aspects of Pavements. FHWA NHI-05-037. Federal Highway Administration, Washington, D.C., 2006.

Smith, A., Lott, N., Houston, T., Shein, K., Crouch, J., Enioe, J. U.S. Billion-Dollar Weather and Climate Disasters 1980-2020. National Centers for Environmental Information. 2020. https://www.ncdc.noaa.gov/billions/events.pdf

Sweet, W.V., B.D. Hamlington, R.E. Kopp, C.P. Weaver, P.L. Barnard, D. Bekaert, W. Brooks, M. Craghan, G. Dusek, T. Frederikse, G. Garner, A.S. Genz, J.P. Krasting, E. Larour, D. Marcy, J.J. Marra, J. Obeysekera, M. Osler, M. Pendleton, D. Roman, L. Schmied, W. Veatch, K.D. White, and C. Zuzak, 2022: Global and Regional Sea Level Rise Scenarios for the United States: Updated Mean Projections and Extreme Water Level Probabilities Along U.S. Coastlines. NOAA Technical Report NOS 01. National Oceanic and Atmospheric Administration, National Ocean Service, Silver Spring, MD. https://oceanservice.noaa.gov/hazards/sealevelrise/noaa-nos-techrpt01-global-regional-SLR-scenarios-US.pdf. 2022.

Tabatabaie, A.M. Structural Analysis of Concrete Pavement Joints. Ph.D. Dissertation. University of Illinois. 1978.

Tabatabaie, A.M., and Barenberg, E.J. Finite-Element Analysis of Jointed or Cracked Concrete Pavements. Transportation Research Record No. 671, Transportation Research Board, Washington, D.C., pp. 11-17. 1978.

Tamvakis, P. and Xenidis, Y. Comparative Evaluation of Resilience Quantification Methods for Infrastructure Systems. Social and Behavioral Sciences. Vol. 74, pp. 339-348. 2013.

Tayabji, S.D., and Colley, B.E. Analysis of Jointed Concrete Pavements. Report No. DOT/FHWA/RD-86/041. Federal Highway Administration, Washington, D.C., 1986.

Tia, M., Armaghani, J.M., Wu, C.L., Lei, S., and Toye, K.L. FEACONS III Computer Program for an Analysis of Jointed Concrete Pavements. Transportation Research Record No. 1136, Transportation Research Board, Washington, D.C., pp. 12-22. 1987.

Tirado, C., Carrasco, C., Nazarian, S. and Osegueda, R. Updates to Software for Estimating Damage Due to Superheavy Loads. Report FHWA/TX-05/9-1502-01-7, El Paso, TX, 2007.
United Nations (UN). 2016. *Report of the Open-Ended Intergovernmental Expert Working Group on Indicators and Terminology Relating to Disaster Risk Reduction*. United Nations Office for Disaster Risk Reduction, United Nations General Assembly, New York, NY. https://www.preventionweb.net/files/50683_oiewgreportenglish.pdf

Van Genuchten, M.T. A Closed-Form Equation for Predicting the Hydraulic Conductivity of Unsaturated Soils. Soil Science Society of America Journal, Vol. 44, pp. 892–898., 1980.
Vennapusa, P., White, D.J. and Miller, D.K. Western Iowa Missouri River Flooding--Geo-Infrastructure Damage Assessment, Repair and Mitigation Strategies. IHRB Project TR-638, 2013.

Vennapusa, P.K., Zhang, Y. and White, D.J. Comparison of Pavement Slab Stabilization Using Cementitious Grout and Injected Polyurethane Foam. Journal of Performance of Constructed Facilities, 30(6), p.04016056, 2016.

Westergaard, H.M. Computation of Stresses in Concrete Roads. Proceedings of Highway Research Board, Vol. 5, Part 1. Pp. 90-112, 1925.

White, D.J., Vennapusa, P. and Jahren, C.T. Determination of the Optimum Base Characteristics for Pavements. Center for Transportation Research and Education, Iowa DOT Project TR-482, 2004.

Yang, D., Zhang, T., Zhang, K., Greenwood, D.J., Hammond, J.P., and White, P.J. An Easily Implemented Agro-Hydrological Procedure with Dynamic Root Simulation for Water Transfer in the Crop-Soil System: Validation and Application. Journal of Hydrology. Vol. 370. pp. 177-190., 2009.

Zhou, W. and Geza, M. GIS-Based Nitrogen Removal Model for Assessing Florida's Surficial Aquifer Vulnerability. Environmental Earth Sciences. DOI: 10.1007/s12665-015-5213-x. March, 2016.

.

APPENDIX A: FDOT RIGID PAVEMENT RESILIENCY TOOL USER GUIDE

Installing the Resiliency Tool and Portable-R

The FDOT Rigid Pavement Resiliency Tool (henceforth the "Resiliency Tool" or simply the "Tool") is essentially a macro-enabled MS Excel workbook. As such, it is possible to manually install the Tool along with Portable-R for ILLISLAB simulations.

However, it is strongly recommended that the installation be carried out executing "FDOT_Rigid_Resiliency_Tool_V1.1.msi" to install both the Excel workbook and Portable-R. Once the installer is called, the user can follow the on-screen instructions as shown in Figure A-1.

🕮 The advantage of using the above msi file is that it installs Portable-R and the necessary packages into the designated path. Therefore, it is strongly recommended that you use the msi file for installing the Resiliency Tool.

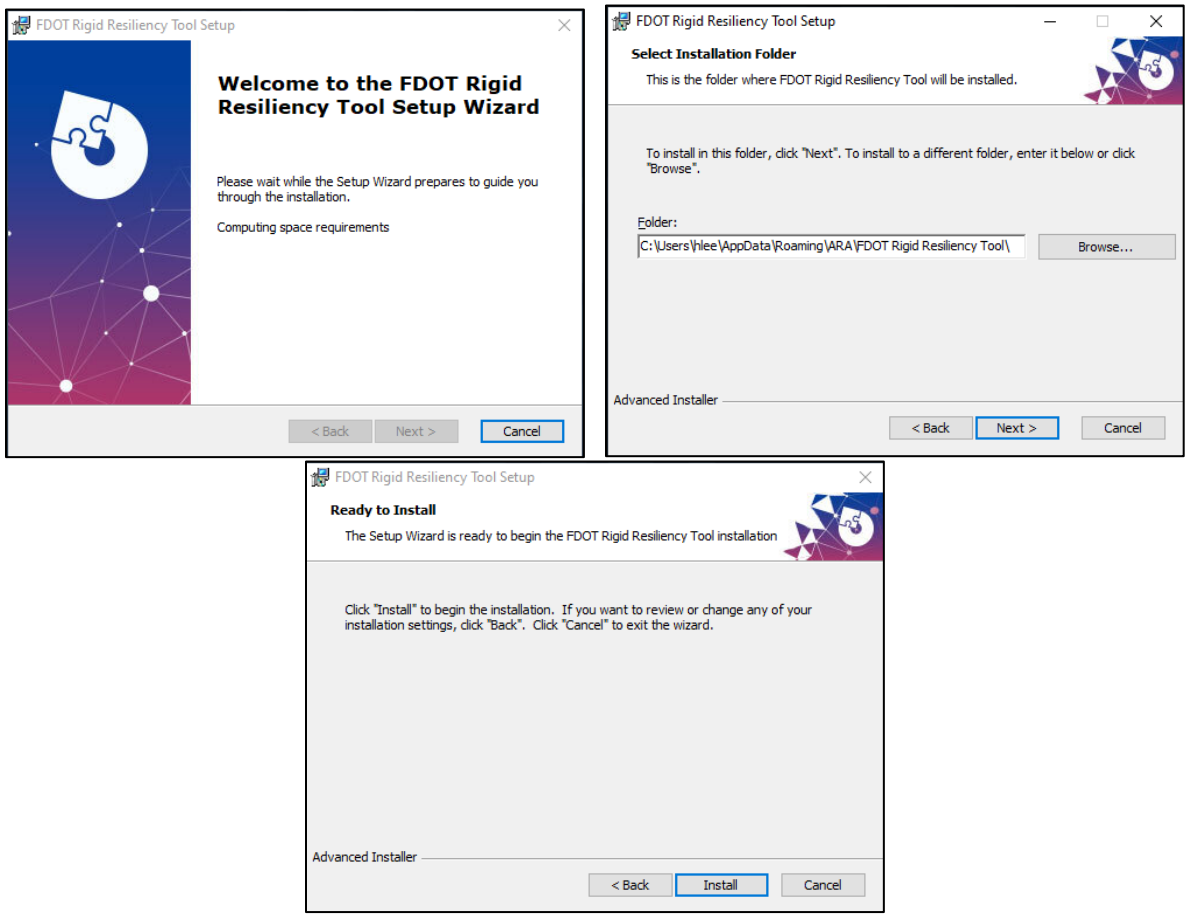

Figure A-1. Installing the Resiliency Tool

To install Portable-R manually, the user needs to download it from SourceForge (https://sourceforge.net/projects/rportable/) and extracting the files to the following path.

- C:\"Username"\AppData\Local\ILLISLAB_R\R-Portable\App\R-Portable

Manual installation of Porttable-R also means that the necessary R packages need to be installed manually. To do so, start R console by double clicking the "R.exe" file located in the following directory, depending on the version of MS Excel being used.

- C:\"Username"\AppData\Local\ILLISLAB_R\R-Portable \bin\R.exe (If you are using **32-bit** version of Excel)
- C:\"Username"\AppData\Local\ILLISLAB_R\R-Portable \bin\i386\R.exe (If you are using **64-bit** version of Excel)

Once the R terminal pops up on the screen, type in the following command to install the necessary packages (Figure 23).

```
install.packages(c('data.table', 'ggplot2', 'plyr', 'dplyr', 'stringr', 'RColorBrewer', 'matlib'))
```

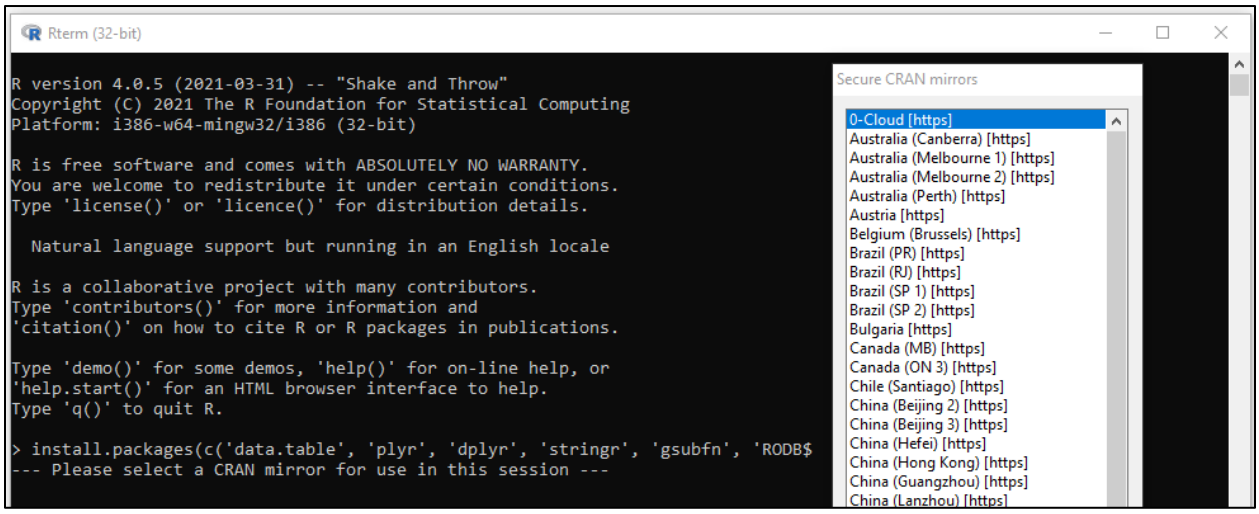

Figure A-2. Manually Installing Packages to Portable R

🕮 If you do not wish to install Portable-R, you will have to run the R-script generated by the Tool in Standard R (with or without RStudio), outside the Resiliency Tool environment. This option is not recommended unless you have sufficient knowledge in R language and the VBA code behind the Tool.

Before Getting Started

Because the Resiliency Tool is implemented in a macro-enabled MS Excel spreadsheet environment, it is important that the macros or code written in Visual Basic for Application (VBA) language be enabled for the interface to function properly.

Figure A-3 shows the Excel window in which a security warning is displayed due to the embedded macros. If you see such a message, simply click the "Enable Content" button to enable the macros within the Tool.

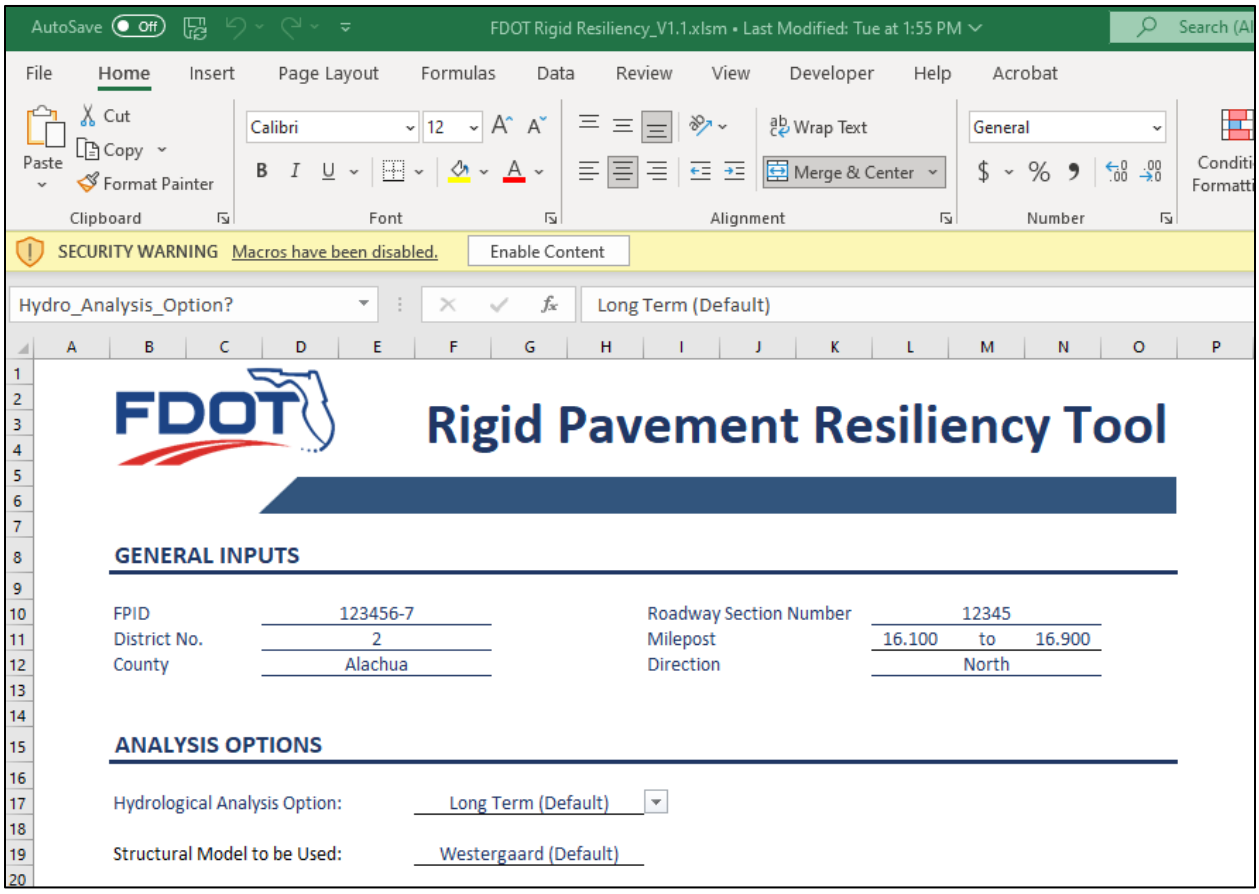

Figure A-3. Security Warning Message in Excel

Furthermore, it is recommended that the user enables all macros within the Excel environment. To do so, follow the steps outlined below.

- Click on the "Developer" tab of the Excel Ribbon
  - If the "Developer" tab is not visible, go to File → Options → Customize Ribbon, and select the check box next to "Developer".
- Select "Macro Security" in the "Developer" tab
- In the new pop-up window, select "Enable All Macros" option and then click "OK" (Figure A-4).

With the above settings in Excel, you are ready to run the Resiliency Tool! The remainder of this manual describes how to use Tool.

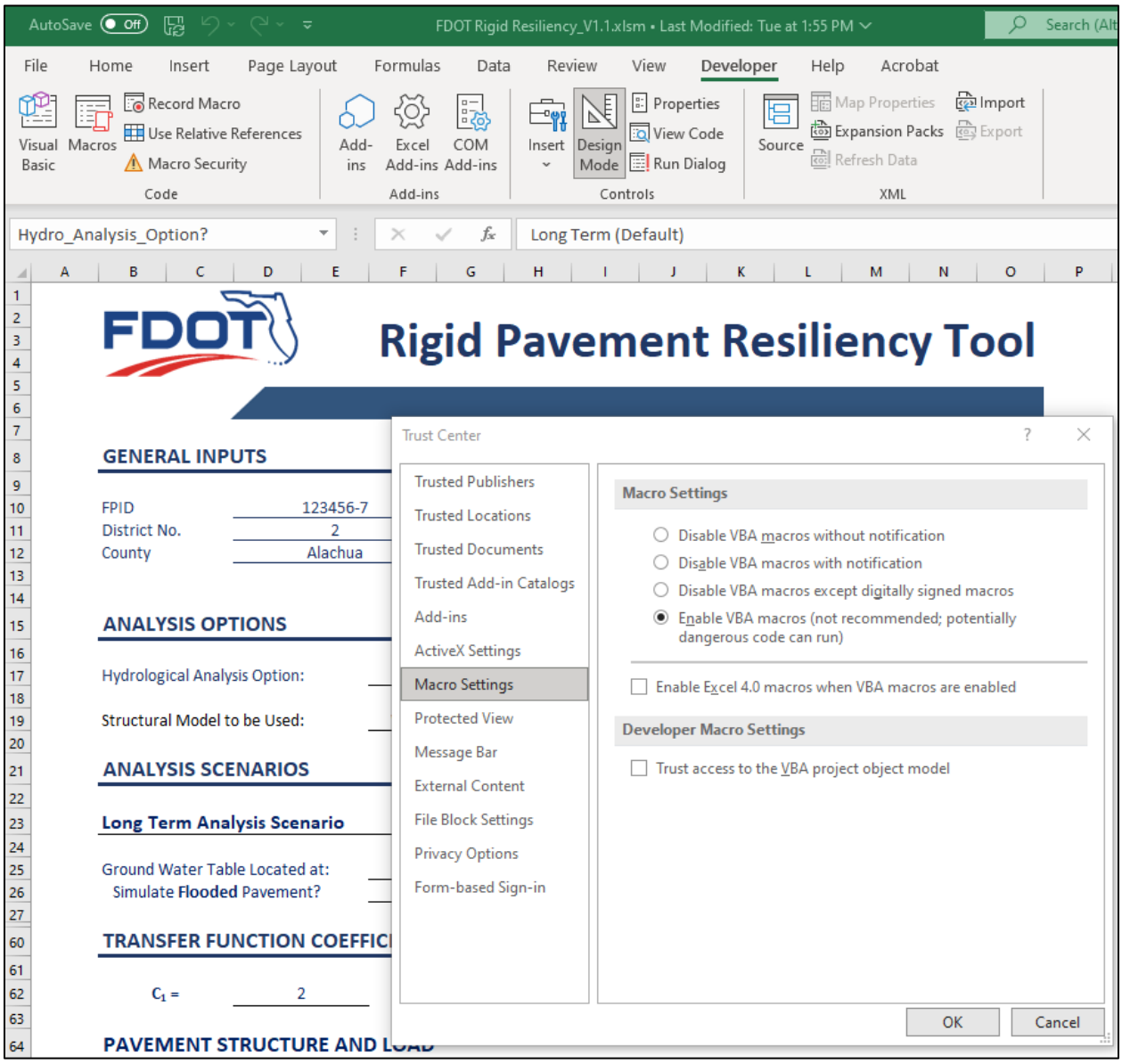

Figure A-4. Enabling all macros in Excel

Getting Started

Once Resiliency Tool is installed, you should see a shortcut created on your Windows Desktop. Double-click on the shortcut to open the Tool interface built in the Microsoft Excel environment.

🕮 The desktop shortcut opens the Resiliency Tool interface which is a "**Read-Only**" file. Please save the template with a different file name if you do not want to lose your changes.

The Resiliency Tool interface has the following 4 tabs:

- **Rigid** – Tab for all inputs and analysis results. This is the only tab that you will interact with.
- **Long-Term** – Tab for storing the results from the Long-Term analysis.
- **Short-Term** – Tab for storing the results from the Short-Term analysis.
- **SWCC_Coeff** – This worksheet stores the default values for the SWCC coefficients. This is also the spreadsheet where the iteration occurs for the SWCC analysis.

Rigid Pavement Resiliency Tool
The Resiliency Tool interface is mainly divided into five sections. These sections are:

1. General Inputs
2. Hydrological Analysis Options
3. Mechanistic-Empirical Transfer Coefficients
4. Portland Cement Concrete (PCC) Layer and External Load Input
5. Foundation Layer Inputs
6. Analysis Results

Detailed description on the above sections are provided subsequently.

General Inputs

Figure A-5 shows the screen capture of the General Inputs section of the Tool. These inputs are the general project-related information that defines the location of the project as well as other information pertaining to the project (i.e., similar project information as included in FDOT's nondestructive testing reports). These inputs include the financial project number (FPN), District, County, roadway section number, direction, and limiting mileposts.

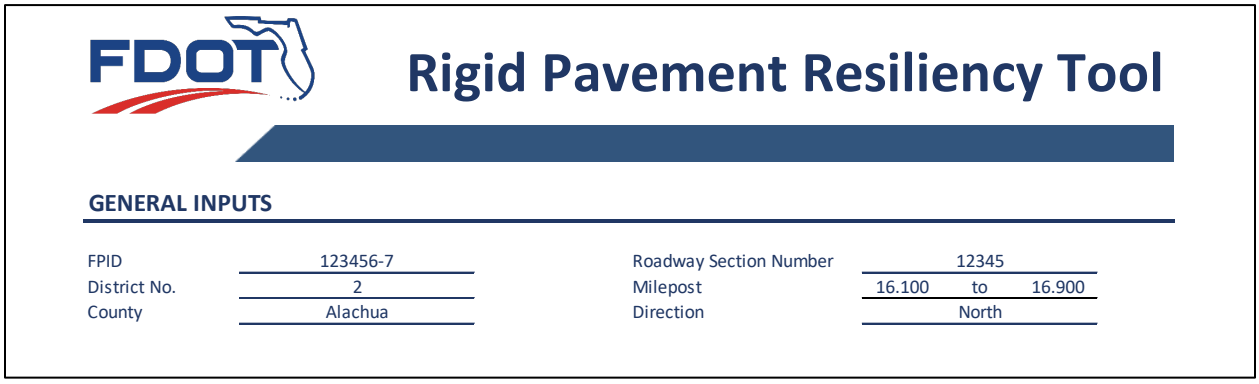

Figure A-5. FDOT's Rigid Pavement Resiliency Tool Interface.

Hydrological Analysis Options

Figure A-6 shows the Resiliency Tool interface where the user may select the hydrological analysis options. The user may select one of the two primary analysis options from the drop-

down menu. These analysis options are (1) Long-Term simulation and (2) Short-Term simulation. These options are described subsequently.

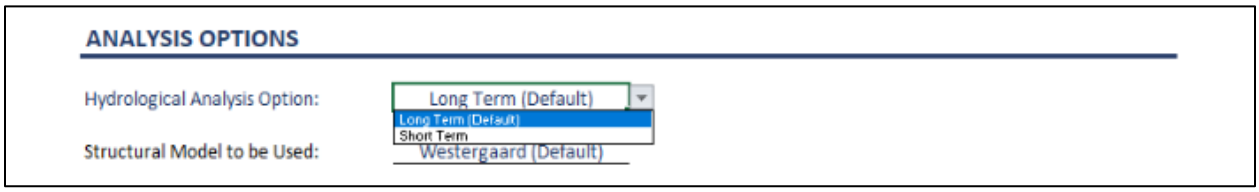

Figure A-6. Resiliency Tool Analysis Options.

Long-term simulation

The purpose of the long-term simulation is to allow the user to compare different situations that are considered to be permanent (i.e., those that do not change over a short period of time). Examples of these scenarios are provided in the following.

- Change in pavement performance under different, but permanent levels of sea level rise (e.g., 10 ft. or 5 ft.) versus no change in sea level.
- Change in pavement performance under different levels of Ground Water Table (GWT) versus no change in GWT.
- Difference in pavement life between a flooded versus non-flooded pavement (for the condition that the flooded pavement remains flooded for an extended period of time).

🕮 The **Long-Term** simulation does **NOT involve any changes in moisture condition**. Thus, the Long-Term simulation should be used for simulating **a permanent moisture condition** (e.g., sea level, Ground Water Table (GWT), etc.).

Figure A-7 shows the additional inputs needed for the long-term simulation. The user may simulate different depths of Ground Water Table (GWT) with or without flooded condition (using the drop-down menu for "Simulate Flooded Pavement?").

Ground Water Table (GWT): The GWT should be specified as a depth from the "Pavement Surface" which includes the Portland Cement Concrete (PCC) thickness. The layers below the GWT are assumed to be fully saturated.

Flooded Condition: If this option is selected, it assumes that all foundation layers within the pavement are fully saturated (i.e., degree of saturation is equal to 1.0).

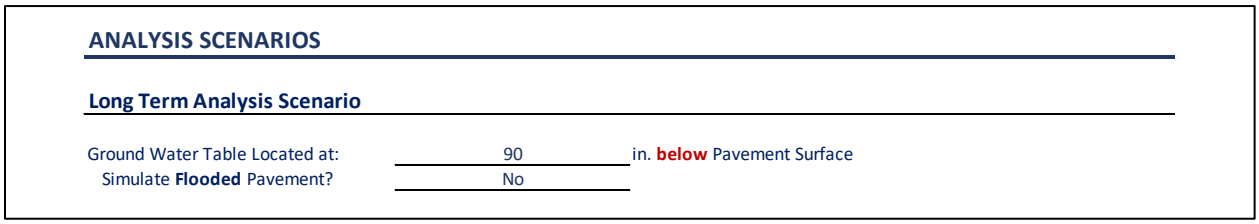

Figure A-7. Long-Term Simulation Inputs.

Short-term simulation

The short-term simulation is intended for simulating a pavement structure experiencing changes in moisture level within a relatively short period of time (i.e., within a few hours, days, or weeks). Examples of these scenarios are provided as the following.

- Reduction in pavement life due to a severe rainfall combined with traffic loading.
- Recovery of a flooded pavement due to evaporation and other sources of drainage.

🕮 The **Short-Term** option allows you to simulate the **(1-Dimensional) vertical flow of water** through the pavement foundation layers over time.

The Short-Term simulation requires appropriate initial conditions (e.g., rainfall intensity, surface evaporation rate, GWT level at the beginning of simulation, etc,) as shown in Figure A-8. Additional information is provided in the following for these inputs.

Ground Water Table (GWT): The GWT should be specified as a depth from the "Pavement Surface" which includes the PCC thickness. The layers below the GWT are assumed to be fully saturated.

Flooded Condition: If this option is selected, the analysis starts with a flooded pavement draining naturally. To provide any additional drainage at the pavement surface (i.e., evaporation), an evaporation rate should be specified in the "Rainfall / Evaporation" table with a negative number.

Mechanistic-Empirical Transfer Coefficients

The empirical equation for calculating the allowable number of load passes (N_f) is shown in Figure A-9. This equation as well as the default coefficients are adopted from the AASHTOWare Pavement ME (AASHTO, 2015).

It is recommended that the transfer function coefficients remain unchanged, unless a local calibration of this function has been conducted.

ANALYSIS OPTIONS

Hydrological Analysis Option: Short Term

Structural Model to be Used: Westergaard (Default)

ANALYSIS SCENARIOS

Short Term Analysis Scenario

Ground Water Table Located at: 90 in. **below** Pavement Surface

Start with **Flooded** Pavement? No

Time Duration for Analysis 30 hr(s)

Time Interval for Analysis, Δt 0.1 hr(s)

Run Short-Term Analysis

Rainfall / Evaporation

Rain Event	Starting Time (hr)	Ending Time (hr)	Rainfall Intensity (in/hr)
Event No. 1	0.0	5.0	5.0
Event No. 2	10.0	15.0	2.0
Event No. 3			
Event No. 4			
Event No. 5			

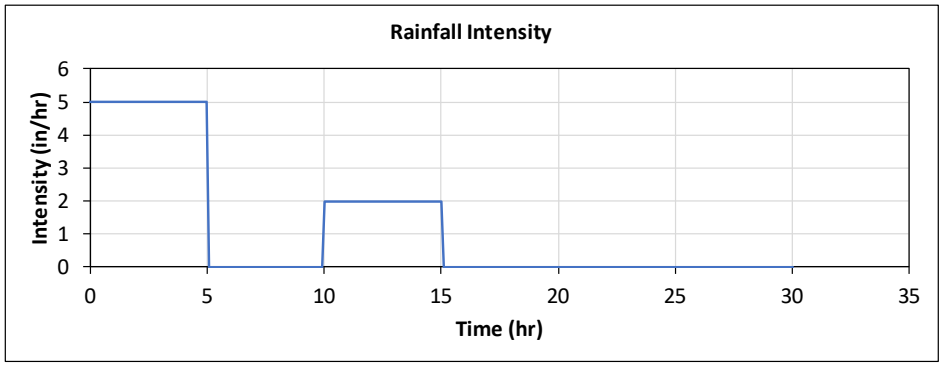

Figure A-8. Short-Term Simulation Inputs.

TRANSFER FUNCTION COEFFICIENTS

C_1 = 2 C_2 = 1.22 N_f Equation: $\log N = C_1 \cdot \left(\frac{M}{\sigma}\right)^{C_2}$

Figure A-9. Transfer Function Inputs.

Portland Cement Concrete (PCC) Layer and External Load Input

There are two structural models built into the Resiliency Tool. These models are (1) Westergaard's equations and (2) the ILLISLAB FEM model. The structural model for the analysis can be selected from the drop-down box in the "Analysis Options" menu, as shown in Figure A-10.

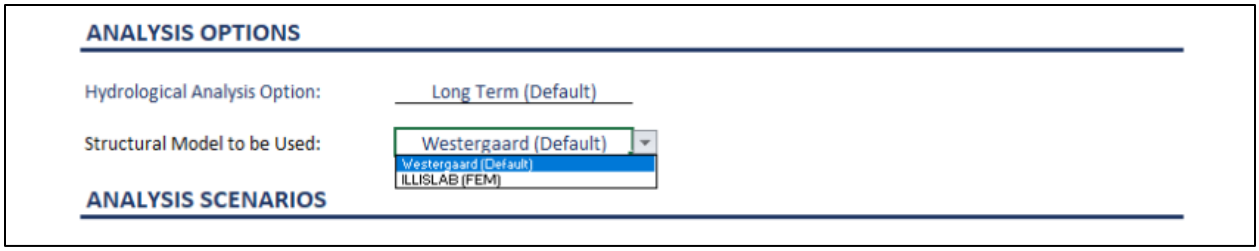

Figure A-10. Resiliency Tool Structural Model Options.

Analysis Using Westergaard Equations

The Portland Cement Concrete (PCC) layer inputs and the load related inputs needed for the Westergaard analysis option are shown in Figure A-11. These inputs are:

- **Thickness** of the PCC layer in inches
- **Elastic modulus** (i.e., Young's modulus) of the PCC layer in psi
- **Poisson's ratio**
- **PCC modulus of rupture (*M*)** which is not used within the Westergaard equations, but needed for calculating the N_f using the transfer function
- **Load radius** in inches.
- **Load magnitude** in lbs.

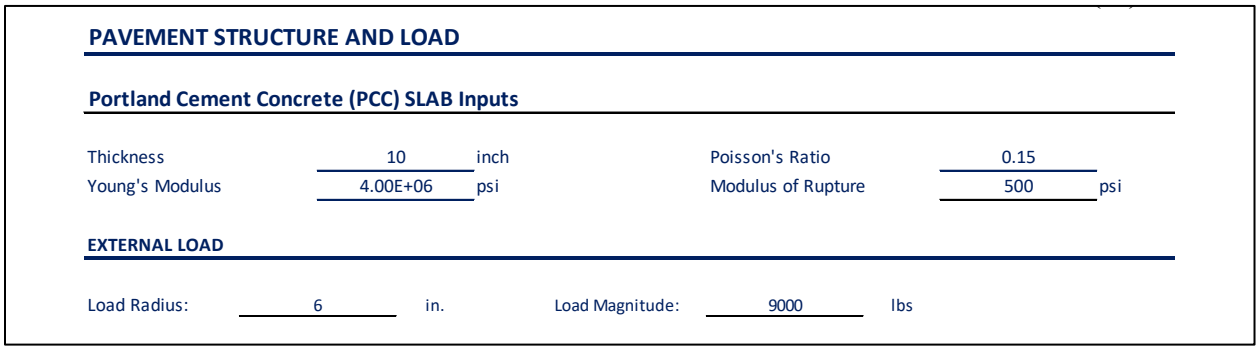

Figure A-11. PCC and External Load Inputs for Westergaard Equations.

Analysis Using ILLISLAB Finite Element Method (FEM)

🕮 The users are warned that the **FEM analysis option may take a significant amount of time to finish** running, especially for the Short-Term analysis, where the structural model needs to be evaluated for each time step.

The PCC and load related inputs for the ILLISLAB FEM are shown in Figure A-12. The inputs include most of the basic inputs (e.g., modulus) discussed above under the Westergaard option. Additional inputs needed for ILLISLAB analysis are described as the following.

- **Unit weight of PCC** and **coefficient of thermal expansion (α)** of PCC material: these inputs are needed for simulating the PCC slab response under thermal load (i.e., curling).

- **Joint Locations:** the first joint location has to be at 0.0 ft. for both joint types.
  - **Transverse joint locations** define the slab dimensions in the direction of travel.

    The example shown in Figure A-12 corresponds to 3 slabs in the travel direction, each having a length of 15 ft.

  - **Longitudinal joint locations** define the slab dimensions in the lateral direction (e.g., for different lanes and/or shoulder).

    The example shown in Figure A-12 defines 2 slabs in the lateral direction, each having a width of 12 ft.

- **Load Transfer:** there are two types of load transfer mechanisms modeled in ILLISLAB as discussed below.

  - **Dowel bars** (for transverse joints) and **tie bars** (for longitudinal joints) must be specified by the following inputs.
    - **Diameter** in inches
    - **Elastic modulus** in psi
    - **Poisson's ratio**
    - **Joint opening** in inches
    - **Az parameter** (non-dimensional) which specifies the effective area of the dowel/tie bars under shear. Use 0.9 for circular cross-section.

  - The dowel and tie bar locations must be specified for the first PCC slab located at the bottom-left corner (see Figure A-12), even if there are no dowel and tie bars. This is because these dowel and tie locations are also used to develop the basic FEM mesh for the PCC slabs.

🕮 The dowel and tie locations must be specified even if there are no dowel/tie bars, because these locations are used to develop the FEM mesh. If there are no dowel bars or tie bars, the modulus of the bar material should be set to zero.

  - **Aggregate Interlock** should be specified in the same unit as modulus, i.e., in psi.

- **External Loads:** up to a total of 12 external loads (or tires) can be specified in ILLISLAB, each having a rectangular contact area. As shown in Figure A-12, the following must be specified for each external load.

  - **Load magnitude** in lbs
  - **Center coordinates** in feet for X and Y directions
  - **Length of the contact area** in both the X and Y directions in feet.

- **Thermal Load** can be specified using a linear thermal gradient (ΔT) within the PCC layer, which is calculated as the difference in temperature between the top (T_{top}) and the bottom (T_{bottom}) of the PCC (i.e., $\Delta T = T_{top} - T_{bottom}$).

Figure A-13 shows an example of the FEM mesh generated based on the sample inputs provided in Figure A-12.

PAVEMENT STRUCTURE AND LOAD

Portland Cement Concrete (PCC) SLAB Inputs

Thickness	10	inch	Unit Weight	150	lb/ft^3
Modulus	4.00E+06	psi	Coeff. of Thermal Expansion	4.90E-06	in/in/deg.F
Poisson's Ratio	0.15		Modulus of Rupture	500	psi

Joint Locations

Joint No.	1	2	3	4	5	6	7	8	9	10	11	12
Trans. Joints (ft)	0	15	30	45								
Longi. Joints (ft)	0	12	24									

Joint locations also define the Number of Slabs and Slab Dimensions.

LOAD TRANSFER

TRANSVERSE JOINTS

Aggregate Interlock:	10000	psi
Dowel Bar Diameter	1.5	inch
Dowel Bar Modulus	2.90E+07	psi
Dowel Bar Poisson's Ratio	0.1	--
Joint Opening	0.1	inch
Az	0.9	--

LONGITUDINAL JOINTS

Aggregate Interlock:	10000	psi
Tie Bar Diameter	0.63	inch
Tie Bar Modulus	2.90E+07	psi
Tie Bar Poisson's Ratio	0.1	--
Joint Opening	0.1	inch
Az	0.9	--

Load Transfer No.	1	2	3	4	5	6	7	8	9	10	11	12
Dowel Locations	1	2	3	4	5	6	7	8	9	10	11	
Tie Locations	2.5	5	7.5	10	12.5							

Notes:
1. Location of Dowels & Ties only need to be defined for the slab at the lower left corner
2. Do NOT delete the Dowel & Tie Locations. If you do not have dowels, then set the dowel modulus to ZERO

EXTERNAL & THERMAL LOADS

EXTERNAL LOADS

Load ID	1	2	3	4	5	6	7	8	9	10	11	12
Magnitude (lb)	4500	4500	4500	4500								
X.Coord (ft)	22.5	22.5	22.5	22.5								
X.Length (ft)	0.6	0.6	0.6	0.6								
Y.Coord (ft)	2	3	9	10								
Y.Length (ft)	0.6	0.6	0.6	0.6								

THERMAL LOAD Linear Temperature Gradient (Ttop - Tbottom) 0 deg.F

Figure A-12. PCC and External Load Inputs for ILLISLAB.

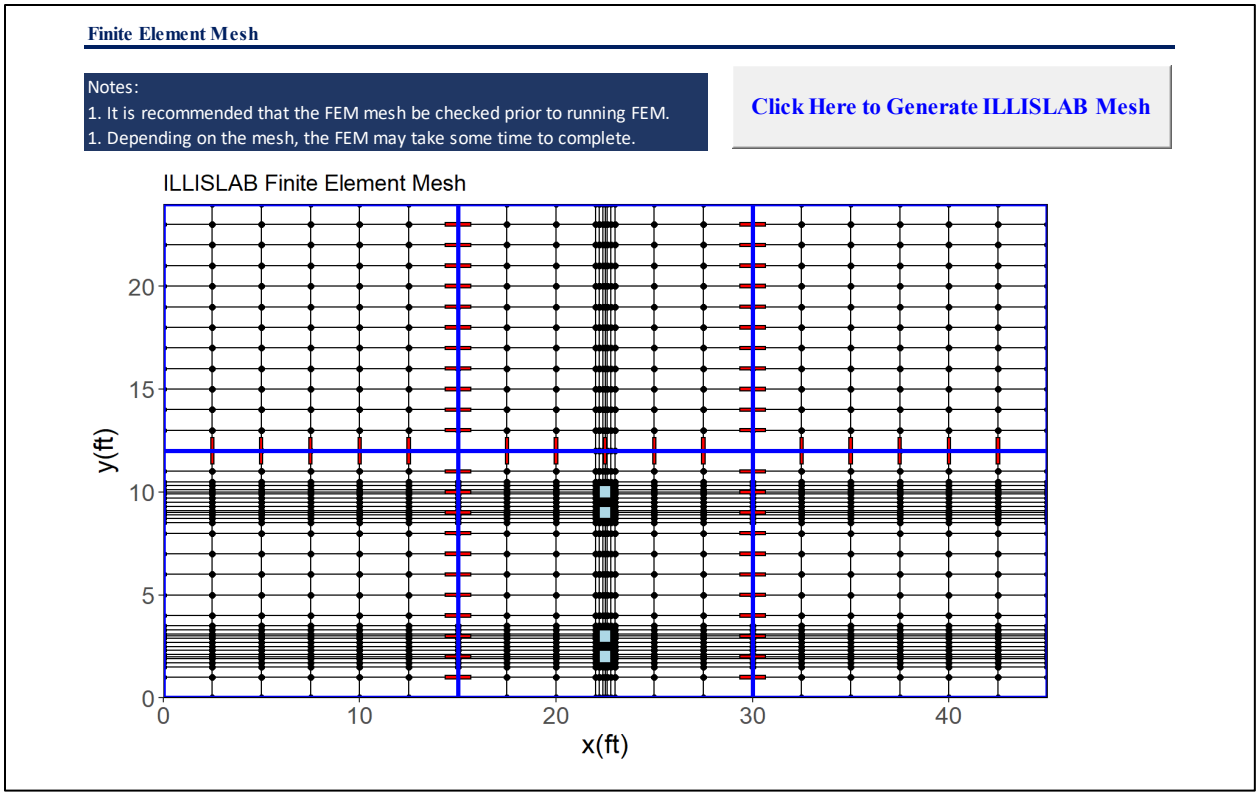

Figure A-13. Finite Element Mesh Generated from ILLISLAB.

Foundation Layer Inputs

Specifying a Fixed k-value for the Foundation

The rigid pavement foundation needs to be characterized in terms of the composite modulus of subgrade reaction (i.e., k-value) for both the Westergaard equations and the FEM. As such, the user may choose to use a constant k-value for the analysis and manually input the k-value for the analysis, as shown in Figure A-14.

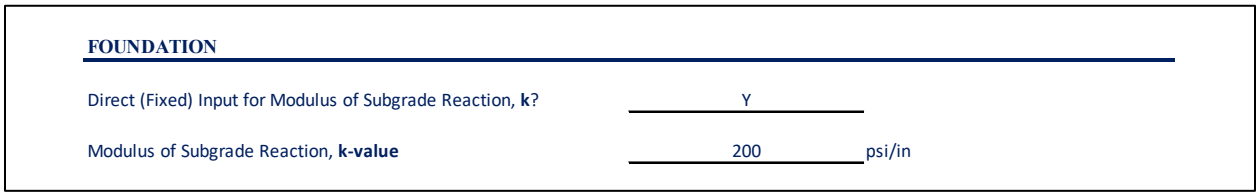

Figure A-14. Manual Input of the k-value.

🕮 This option is **only available for the Long-Term analysis** where the foundation properties do not change within the analysis.

Calculating the k-value for the Foundation

The user may also choose to calculate the k-value from other foundation-related input parameters such as the moisture content, modulus, etc. This option is available for both the Short-Term and Long-Term analyses. Figure A-15 shows an example including the total thickness and the modulus of the transformed foundation layers (using Odemark's method), as well as the corresponding k-value.

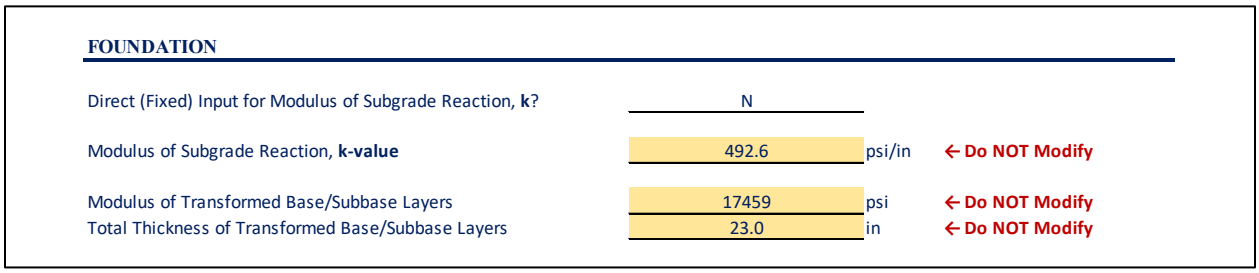

Figure A-15. Calculating the k-value from Foundation Modulus.

For calculating the k-value from the layer modulus that may change with moisture content, the user is provided with several base/subbase types that are frequently used by FDOT. These foundation layers are described in the following.

Asphalt Base

The inputs needed for the asphalt base are shown in Figure A-16. These inputs include:

- **Layer thickness** in inches
- **Resilient modulus** in psi
- **Poisson's ratio**
- **Saturated and Residual volumetric water contents** (θ_{sat} and θ_R, respectively)
- Coefficients for the Van Genuchten equation (Default values are $\alpha = 2$ and $n = 5$)
- **Hydraulic conductivity** of the asphalt material which may be inputted as a fixed value or calculated from other mixture parameters.

There are two different models built into the Resiliency Tool for estimating the hydraulic conductivity of asphalt concrete from mix design inputs. These models are the Masad model (Figure A-17) and the Mohammad model (Figure A-18).

Both models require the gradation input. However, the user only needs to fill in the percent passing column (highlighted in gray) – which can be easily pasted from FDOT's typical mix design spreadsheets. In addition to gradation, the user needs to provide the additional inputs for the respective models that include the following.

- **Air voids** in percent
- **Binder content** in percent
- **Specific gravities of binder, aggregate (bulk), and mixture**
- **Unit weight** and **viscosity** of water (User default values).

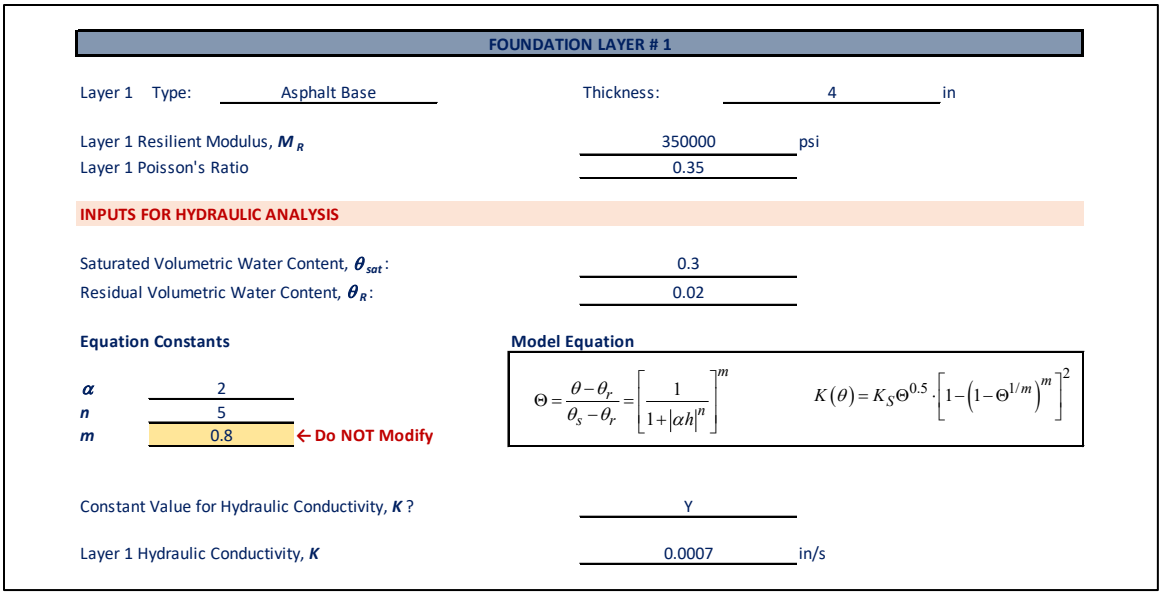

FOUNDATION LAYER # 1

Layer 1 Type: Asphalt Base — Thickness: 4 in

Layer 1 Resilient Modulus, M_R: 350000 psi

Layer 1 Poisson's Ratio: 0.35

INPUTS FOR HYDRAULIC ANALYSIS

Saturated Volumetric Water Content, θ_{sat}: 0.3

Residual Volumetric Water Content, θ_R: 0.02

Equation Constants

α	2
n	5
m	0.8 ← Do NOT Modify

Model Equation

$$\Theta = \frac{\theta - \theta_r}{\theta_s - \theta_r} = \left[\frac{1}{1+|\alpha h|^n}\right]^m \qquad K(\theta) = K_S \Theta^{0.5} \cdot \left[1-\left(1-\Theta^{1/m}\right)^m\right]^2$$

Constant Value for Hydraulic Conductivity, K ? Y

Layer 1 Hydraulic Conductivity, K: 0.0007 in/s

Figure A-16. Basic Inputs for Asphalt Base with Constant Hydraulic Conductivity.

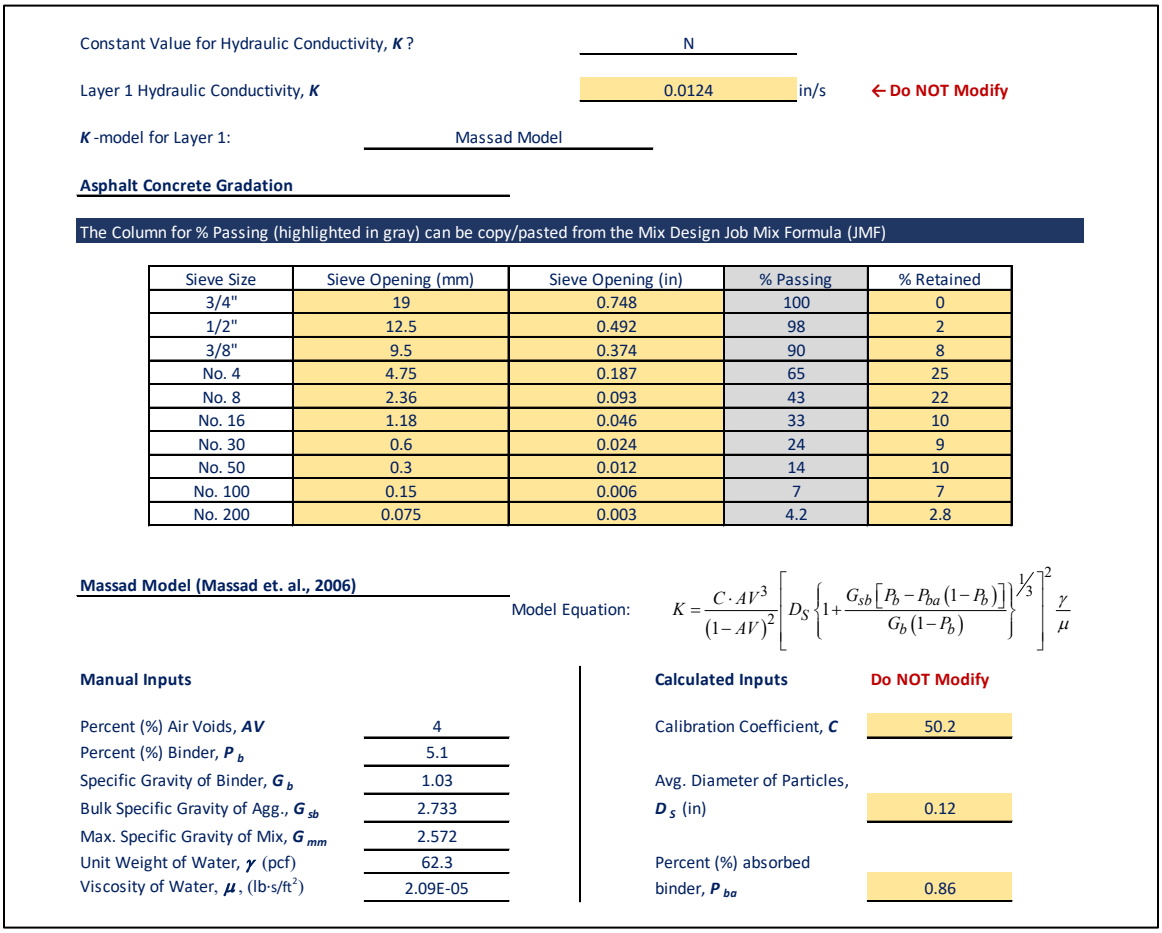

Constant Value for Hydraulic Conductivity, K ? N

Layer 1 Hydraulic Conductivity, K: 0.0124 in/s ← Do NOT Modify

K-model for Layer 1: Massad Model

Asphalt Concrete Gradation

The Column for % Passing (highlighted in gray) can be copy/pasted from the Mix Design Job Mix Formula (JMF)

Sieve Size	Sieve Opening (mm)	Sieve Opening (in)	% Passing	% Retained
3/4"	19	0.748	100	0
1/2"	12.5	0.492	98	2
3/8"	9.5	0.374	90	8
No. 4	4.75	0.187	65	25
No. 8	2.36	0.093	43	22
No. 16	1.18	0.046	33	10
No. 30	0.6	0.024	24	9
No. 50	0.3	0.012	14	10
No. 100	0.15	0.006	7	7
No. 200	0.075	0.003	4.2	2.8

Massad Model (Massad et. al., 2006)

Model Equation:

$$K = \frac{C \cdot AV^3}{(1-AV)^2}\left[D_S\left\{1+\frac{G_{sb}\left[P_b - P_{ba}(1-P_b)\right]}{G_b(1-P_b)}\right\}^{1/3}\right]^2 \frac{\gamma}{\mu}$$

Manual Inputs		Calculated Inputs	Do NOT Modify
Percent (%) Air Voids, AV	4	Calibration Coefficient, C	50.2
Percent (%) Binder, P_b	5.1		
Specific Gravity of Binder, G_b	1.03	Avg. Diameter of Particles, D_S (in)	0.12
Bulk Specific Gravity of Agg., G_{sb}	2.733		
Max. Specific Gravity of Mix, G_{mm}	2.572		
Unit Weight of Water, γ (pcf)	62.3	Percent (%) absorbed binder, P_{ba}	0.86
Viscosity of Water, μ, (lb·s/ft^2)	2.09E-05		

Figure A-17. Input Screen for Calculating Asphalt Base Hydraulic Conductivity Using Masad Model .

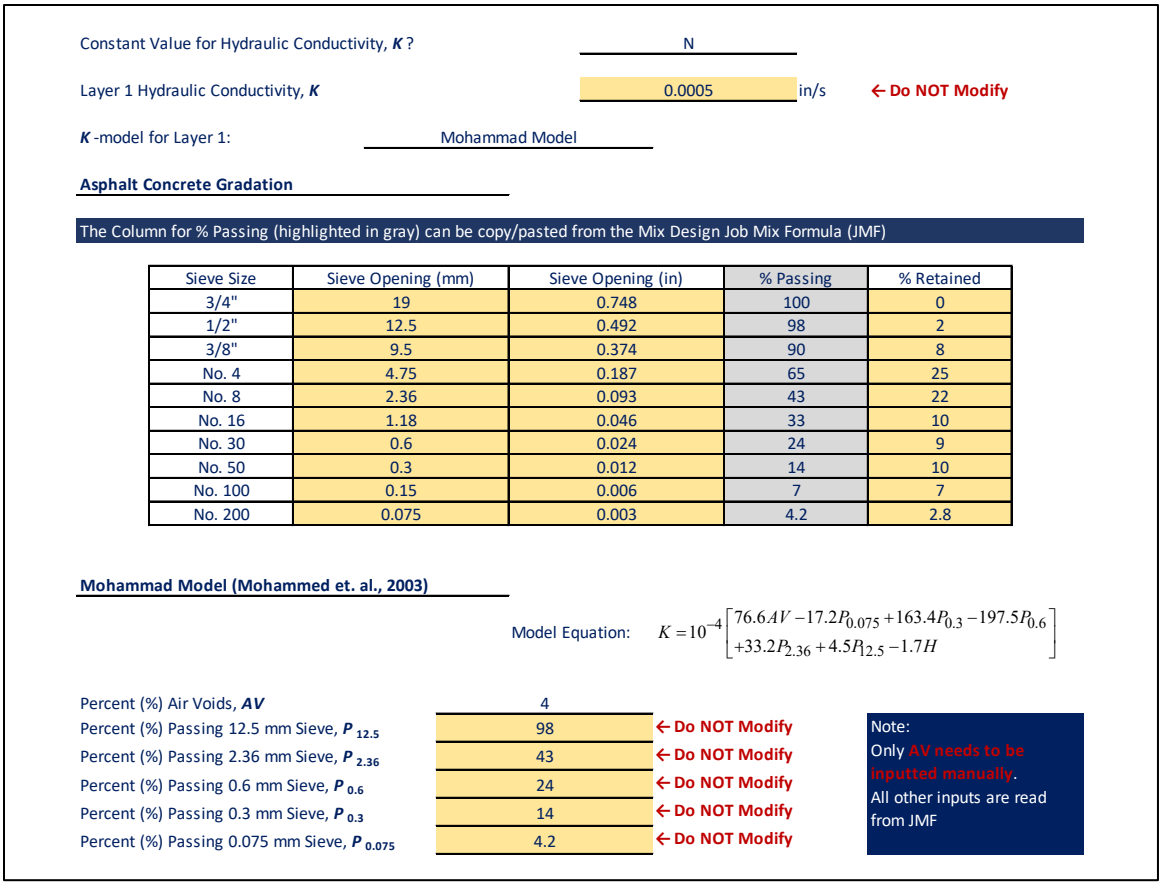

Figure A-18. Input Screen for Calculating Asphalt Base Hydraulic Conductivity Using Mohammad Model.

Coarse-Grained Soil

For coarse-grained soils, the hydraulic conductivity of the coarse-grained soils can either be specified by the user (by selecting "Y" for "Constant Value for Hydraulic Conductivity, K?" in Figure A-19), or calculated using the model developed by Chapuis (2004). The corresponding input screen is shown in Figure A-19. The inputs needed for the Chapuis model are:

- **Effective diameter for 10 percent passing** in inches (default = 0.0047 in.)
- **Void ratio of the soil** (default = 0.618)

It is recommended that this model be used for FDOT's stabilized subbase and in areas with coarse-grained subgrade materials (i.e., A-1 through A-3 soils according to AASHTO classification).

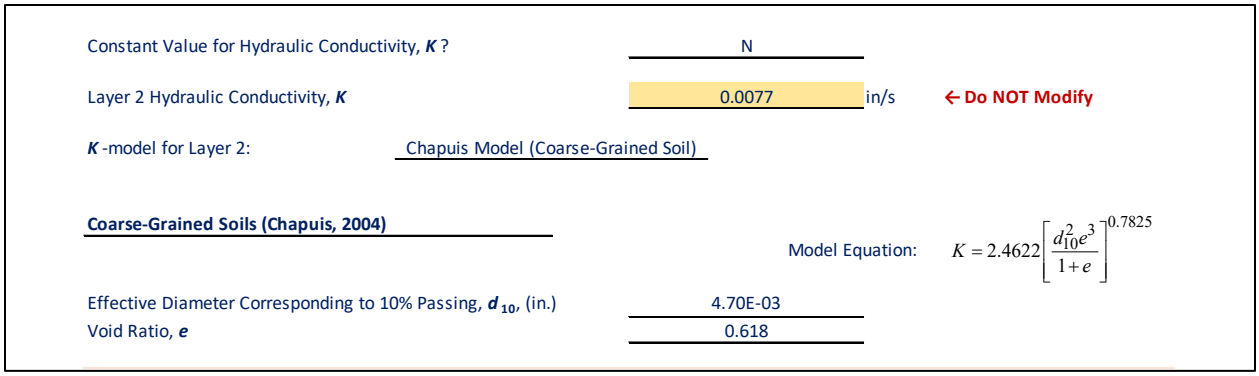

Figure A-19. Inputs for Hydraulic Conductivity of Coarse-Grained Soils.

Fine-Grained Soil

Similar to the coarse-grained soils, the hydraulic conductivity of the fine-grained soils (i.e., AAASHTO classifications A-4 through A-8) can either be specified by the user (by selecting "Y" for "Constant Value for Hydraulic Conductivity, K?" in Figure A-20), or use the model equation Mbonimpa et al. (2002). The inputs needed for the Chapuis model are:

- **Regression Constant** (5.6)
- **Soil Density** in pcf
- **Void ratio of the soil** (default = 2.5)
- **Liquid limit**

The unit weight and the dynamic viscosity of water may also be changed depending on temperature (if desired). However, for most cases, the default values shown in Figure A-20 should be sufficient for the purpose of the Resiliency Tool.

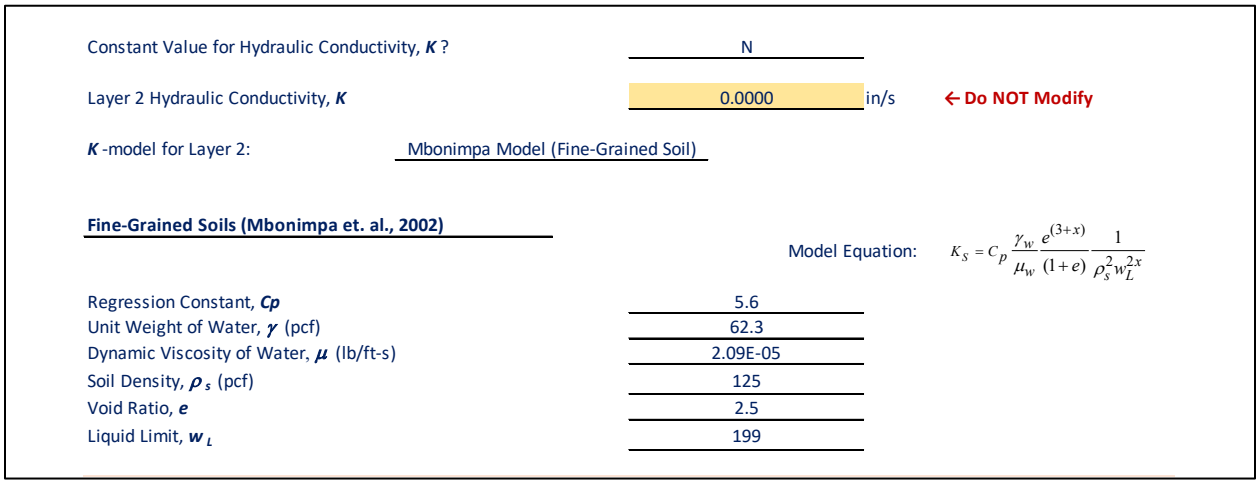

Figure A-20. Inputs for Hydraulic Conductivity of Fine-Grained Soils.

Foundation Layer Modulus

The change in foundation modulus due to change in moisture content (or degree of saturation) can be assessed using one of the two models implemented into the Resiliency Tool. These models are the NCHRP 1-37A model and the Soil-Water Characteristic Curve (SWCC) model.

NCHRP 1-37A Model

The equation as well as the inputs needed for this NCHRP 1-37A model (ARA, 2000) are shown in Figure A-21. These inputs are:

- Resilient modulus at optimum moisture content (M_{ROpt}): Default values are 16,000 psi for stabilized subgrade and the special select soil subgrade, and 10,000 psi for embankment.
- Degree of saturation at optimum moisture content (S_{Opt}): Default value is 11 percent for all soil types.

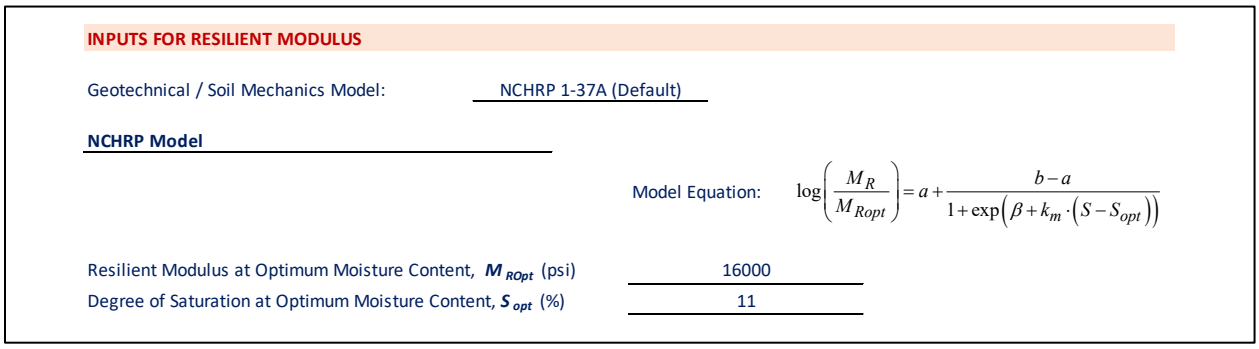

Figure A-21. Inputs for NCHRP 1-37A Resilient Modulus Model.

🕮 The user only needs to input the M_{Ropt} **and** S_{opt}**.** The remaining regression coefficients, i.e., a, b, β, and k_m are built into the spreadsheet for the appropriate soil types (coarse vs. fine).

Soil-Water Characteristics Curve (SWCC) Model

Figure A-22 shows the equations as well as the necessary inputs needed for the SWCC model that was tailored to Florida's soils by Oh and Fernando (2011) and Oh et. al. (2012). The default inputs needed for the SWCC model are stored in the worksheet named "SWCC_Coeff".

🕮 The SWCC model requires iteration for finding the soil suction (S_c) for a given volumetric water content (θ). In other words, the **SWCC model is not as efficient as the NCHRP 1-37A model and may require a long time to run** the analysis (especially for the Short-Term analysis).

Note that for the embankment layer (i.e., Foundation Layer No. 7 in the Resiliency Tool), the default values for the SWCC coefficients (Table 1) as well as the resilient modulus model coefficients (Table 2) depend on FDOT's District. These default values can be loaded by selecting the District number (e.g., "D1") in the input screen shown in Figure A-22. The default

values for stabilized subgrade and special soil (that are independent of FDOT's District) are loaded when the material is first selected.

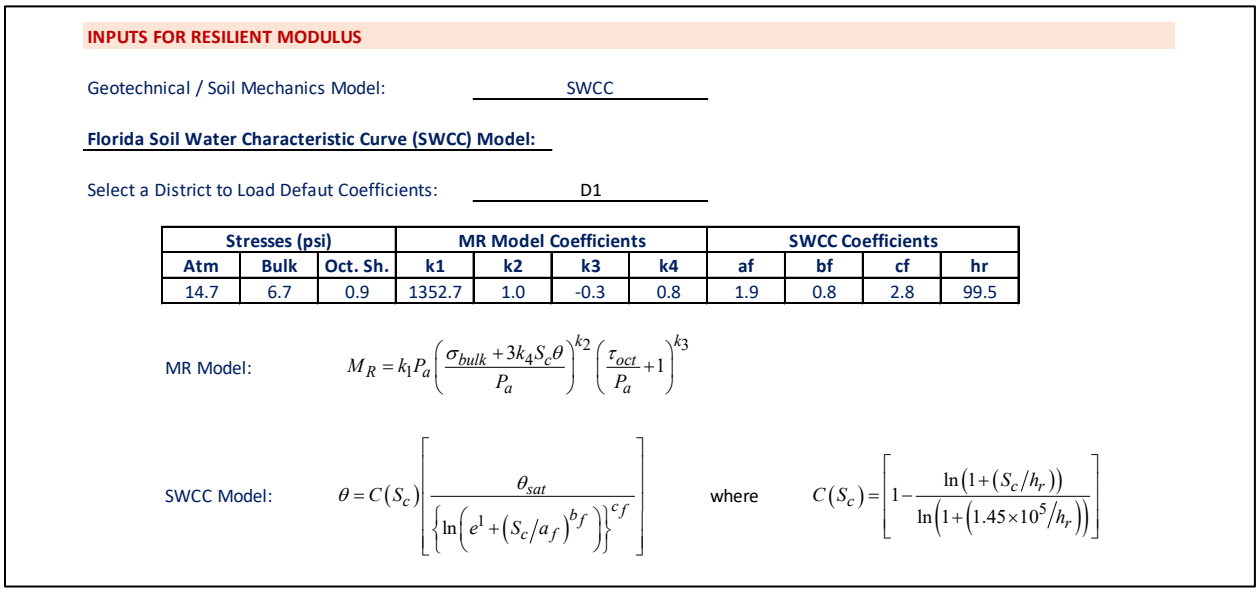

Figure A-22. Inputs for SWCC Resilient Modulus Model.

Analysis Results

Once the analysis is completed, the user can scroll down within the same worksheet to see the results. The results displayed on the worksheet depend on the analysis options, as discussed in the following.

Long-Term Analysis Results

As mentioned previously, the Long-Term analysis does not involve any changes in the moisture condition of the foundation layers. As such, the results of the Long-Term analyses are independent of time, and the hydrological model is only used to calculate the moisture condition at the prescribed (i.e., permanent) condition.

Hydrologic Equilibrium and Resilient Modulus Results (Long-Term)

Figure A-23 shows an example of the hydrologic analysis results provided for the Long-Term analysis option. As shown in this figure, the results include two plots.

- The plot on the left shows the **degree of saturation** for the foundation layers (as a function of depth) at the state of hydrological equilibrium.
- The plot on the right shows the **resilient modulus** of the foundation layers corresponding to the degree of saturation shown on the left.

🕮 Note that both these plots show the results from the **bottom of the PCC layer (i.e., depth of 0.0 in. in the plot) to the top of the GWT**. The user can also **access the data used for plotting these results from the worksheet named "Long-Term"**.

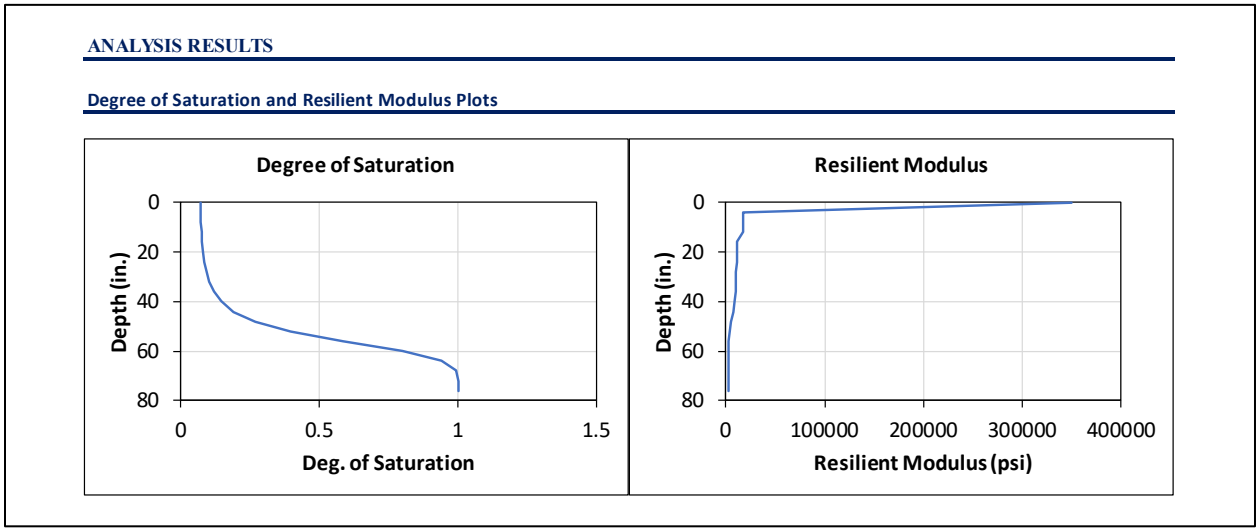

Figure A-23. Long-Term Analysis Results Using Westergaard Equations.

Westergaard Results (Long-Term)

When the Westergaard equations are selected for the structural analysis option, the Long-Term analysis results are provided instantaneously (i.e., there are no buttons that need to be clicked to see the results).

The structural analysis results are provided in a table format (see Figure A-24) below the hydrologic results. The results include the following.

- **Maximum deflection** in mils
- **Critical tensile stresses** in psi for the respective locations (interior, edge, and corner)
- **Maximum allowable number of load repetitions** (N_f)
- **Damage due to a single pass** of the load (1/ N_f).

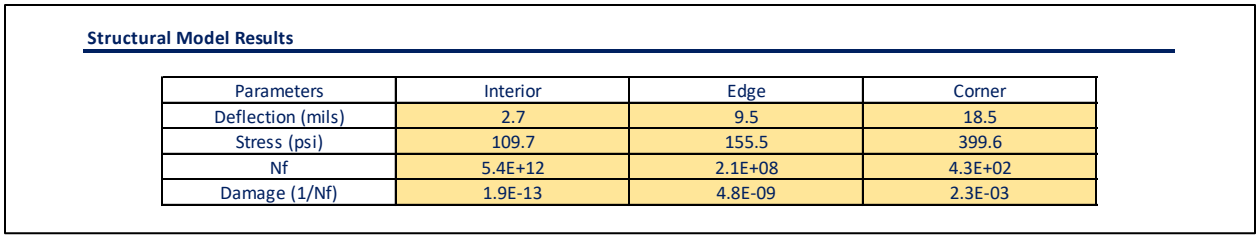

Parameters	Interior	Edge	Corner
Deflection (mils)	2.7	9.5	18.5
Stress (psi)	109.7	155.5	399.6
Nf	5.4E+12	2.1E+08	4.3E+02
Damage (1/Nf)	1.9E-13	4.8E-09	2.3E-03

Figure A-24. Long-Term Analysis Results Using Westergaard Equations.

ILLISLAB Results (Long-Term)

Figure A-25 shows an example of the Long-Term analysis results from ILLISLAB.

🕮 Unlike the Westergaard option, the **ILLISLAB results are not automatically populated** by the Tool.

To obtain the structural results from ILLISLAB, the user must specify the **locations within the PCC slab (X and Y coordinates as well as the depth)** where the responses are to be extracted from the FEM solution. Then the user needs to click on the "Click Here to Run ILLISLAB" button, which calls the Portable-R and runs the FEM solution.

Once the FEM analysis completes, the ILLISLAB results (i.e., deflections, stresses, and the corresponding N_f and damage values) for the specified locations can be loaded into the spreadsheet by clicking on the "Import ILLISLAB Results" button.

The results obtained for each specified location include the following.

- **Maximum deflection** in mils
- **Critical tensile stresses** in psi for the respective locations (interior, edge, and corner)
- **Maximum allowable number of load repetitions** (N_f)
- **Damage due to a single pass** of the load (1/ N_f).

The user may also decide to load a different contour plot from ILLISLAB. This can be done by selecting one of the following options for "Which plot do you want to show?" and clicking on the "Click Here to Reload Images".

- The FEM Mesh
- Vertical displacement (or deflection)
- Longitudinal and transverse Stresses (Sx and Sy) in psi unit
- Longitudinal and transverse Strains (Ex and Ey) in microstrain unit

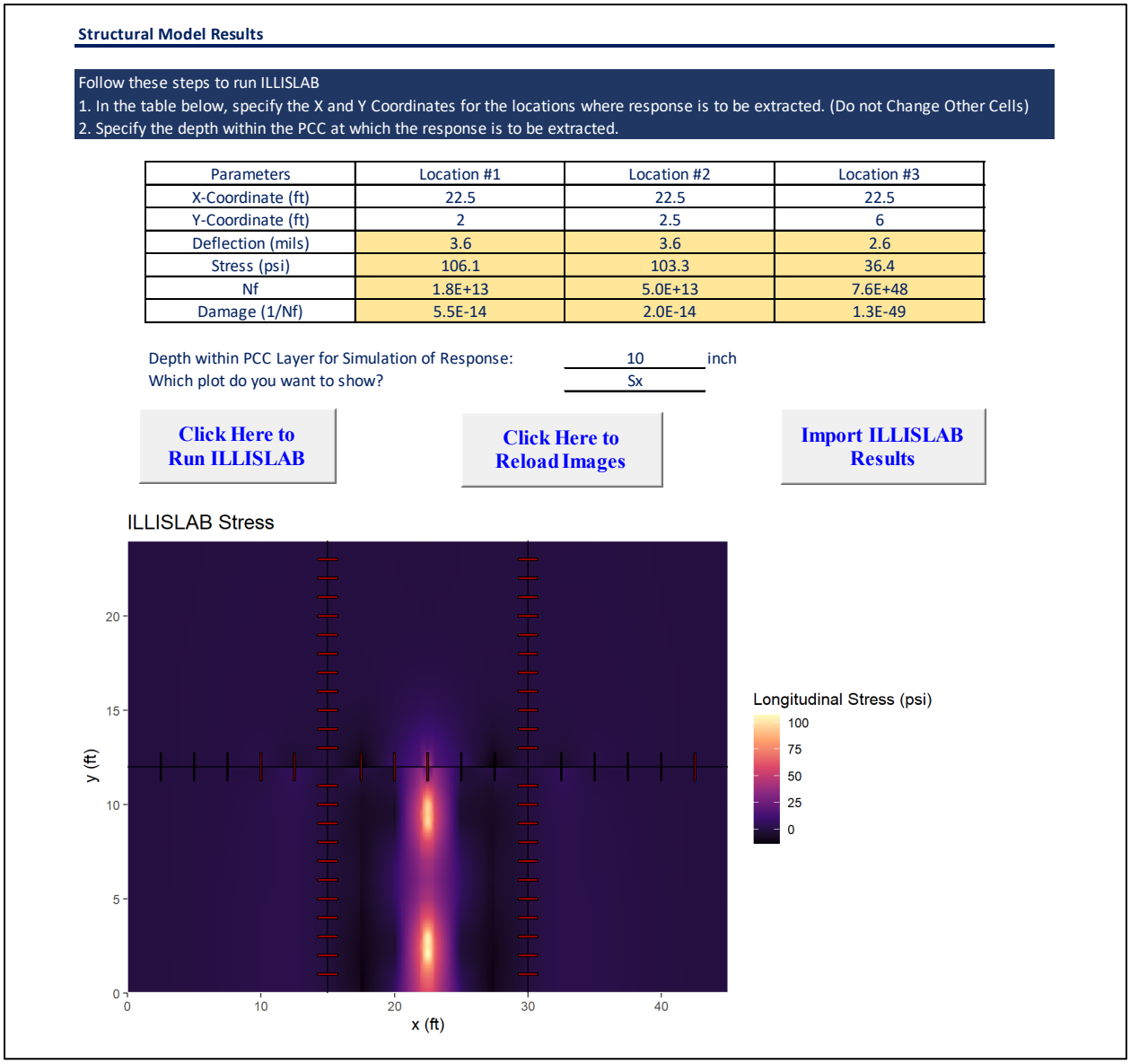

Figure A-25. Long-Term Analysis Results Using ILLISLAB.

Short-Term Analysis Results

The Short-Term analysis involves simulating the moisture flow within the pavement foundation over the prescribed duration, so this option usually requires more time to complete than the Long-Term analysis option.

Hydrologic Equilibrium and Resilient Modulus Results (Short-Term)

Figure A-26 shows an example of the hydrological analysis results from the Short-Term analysis. The plot on the left shows the degree of saturation over time, at a depth specified by the user. On the other hand, the plot on the right shows the degree of saturation as a function of depth (below the PCC layer) at any time specified by the user.

Similarly, Figure A-27 shows the corresponding plots for the resilient modulus. Again the one on the left is a plot over the analysis duration as a depth specified by the user, while the one on the left is a plot with respect to depth at a given time specified by the user.

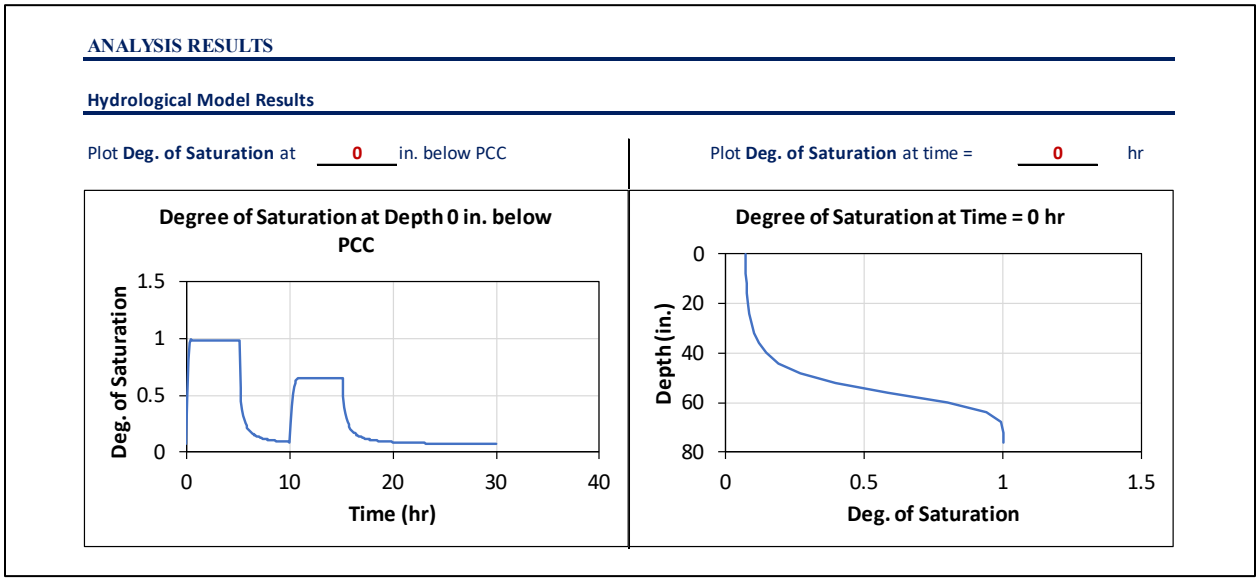

Figure A-26. Short-Term Analysis Results – Hydrological Analysis.

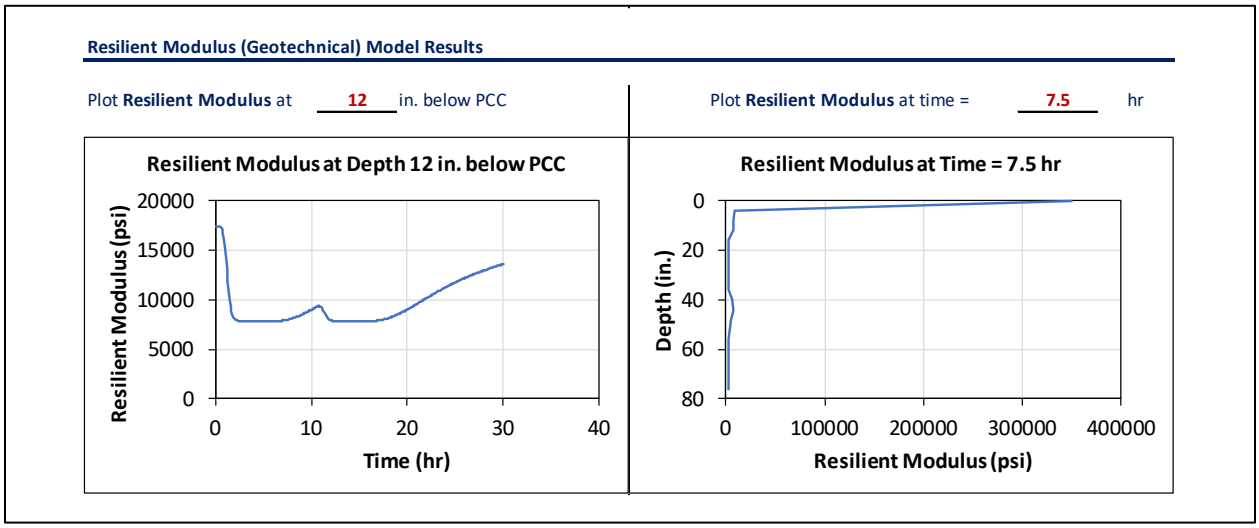

Figure A-27. Short-Term Analysis Results – Resilient Modulus Analysis.

🕮 Changing the Depth or Time for the plots in Figures A-26 and A-27 is easy. Simply select the depth or time using the drop-down menu.

Westergaard Results (Short-Term)

Figure A-28 shows an example of the Westergaard results for the Short-Term analysis. As shown in the figure, there are five plots that include the following:

- Composite k-value
- Critical tensile stress,
- Maximum deflection
- Maximum allowable number of load passes (N_f)
- Damage per pass (1/ N_f),

All of the above plots are shown as functions of time. The user may choose to plot the corresponding results at different locations made available by Westergaard equations (i.e., slab interior, edge, or corner).

The user is also allowed to carry out the performance analysis based on the structural results (see top-right corner of Figure A-28). The procedure for running the performance analysis is described as the following.

- Select the PCC location for the analysis (i.e., **Interior, Edge, or Corner**). For most cases, it is recommended that the edge location be used for this analysis.

- Input the **Reference Damage per Pass** for a given load. The reference damage can be obtained in one of the three ways described below.

    - By clicking on the "**Set Damage @ t = 0 as Reference**" button. As indicated by the name of the button itself, this option allows the user to set the reference damage to that corresponding to the beginning (i.e., time = 0.0 hr) of the simulation.

🕮 This option is feasible and is the recommended method for simulating **rainfall events** where the condition just before the rainfall is the reference condition.

    - By clicking on the "**Set Damage @ t = t_{final} as Reference**" button. In contrast to the above, this option sets the reference damage equal to that the end of the simulation.

🕮 This option is to be used when the user **simulates a pavement that starts at a flooded condition and goes through the draining process over time**.
Note that for this method to provide a feasible estimate of the reference damage, **the duration of the Short-Term analysis should be long enough to allow for the water to drain** and the foundation of the pavement is at the end of simulation is representative of the reference (i.e., before flooding) condition.

- Input the **Daily Load Repetitions** of the corresponding load. This is used to calculate the additional reduction in pavement life caused by the increased pavement damage due to continued traffic loading.

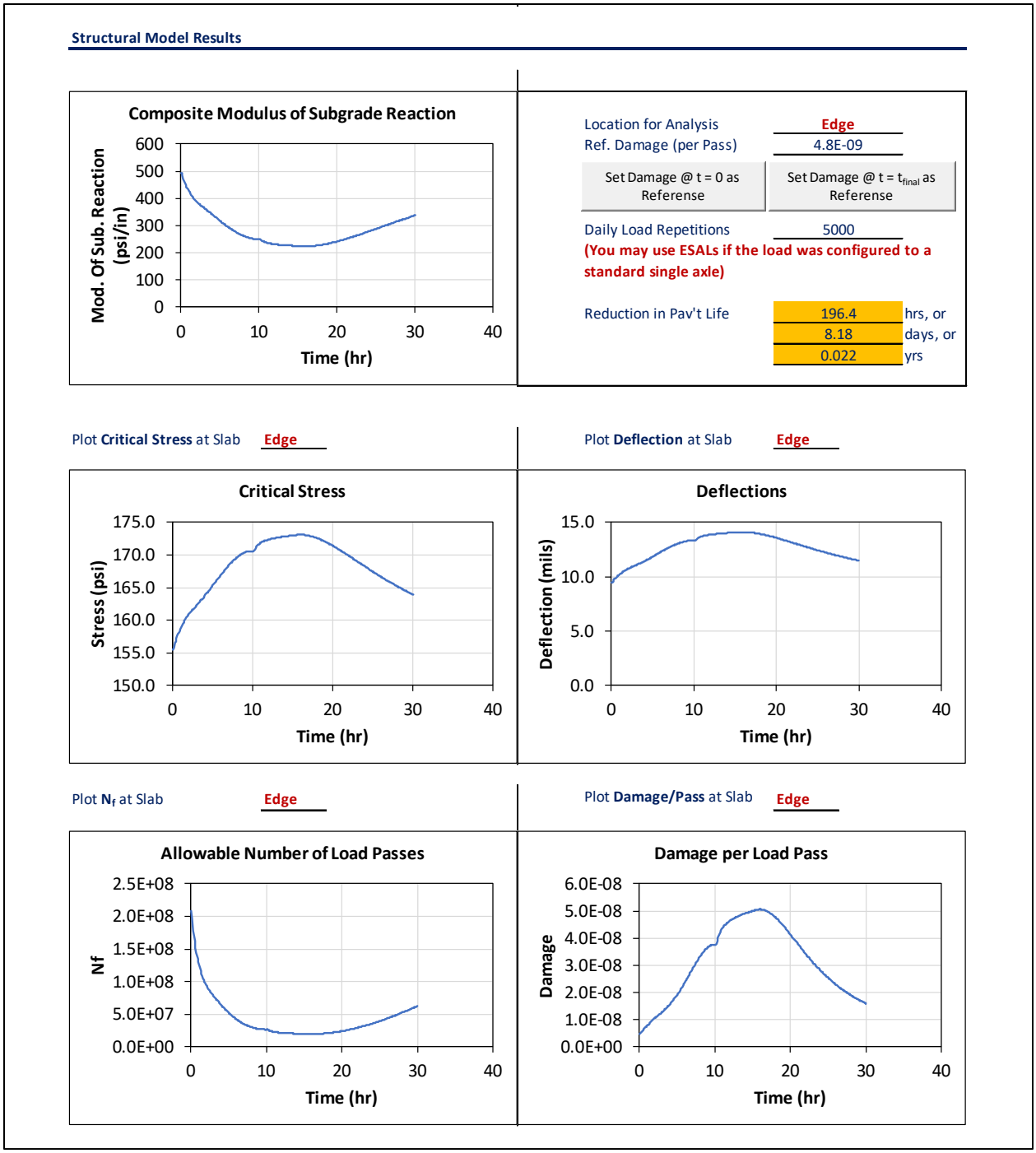

Figure A-28. Short-Term Analysis Results – Structural Analysis Using Westergaard Equations.

ILLISLAB Results (Short-Term)

🕮 It is emphasized again that **running the ILLISLAB model for the Short-Term analysis requires a very long time to run and a lot of computer storage area to save all of the results** from the ILLISLAB runs.

As such, it is recommended that this option be used with caution.

Figure A-29 shows the user interface for Short-Term ILLISLAB analysis and results. Similar to the Long-Term analysis, the user must specify the **locations within the PCC slab (X and Y coordinates as well as the depth)** where the responses are to be extracted from the FEM solution, and click on the "**Click Here to Run ILLISLAB**" button, which calls the Portable-R and runs the FEM solution for each time step within the analysis duration.

Once the FEM analysis completes, the ILLISLAB results (i.e., **deflections, stresses, and the corresponding N_f and damage values**) for the specified locations can be loaded into the spreadsheet by clicking on the "**Import ILLISLAB Results**" button.

Once the pavement responses are loaded, the user may proceed to the performance analysis as shown in Figure A-30. The procedure for running the performance analysis (i.e., calculating the pavement life reduction) was previously described under the Westergaard option, and shall not be repeated here.

Structural Model Results

Follow these steps to run ILLISLAB
1. In the table below, specify the X and Y Coordinates for the locations where response is to be extracted.
2. Specify the depth within the PCC at which the response is to be extracted.
WARNING: ILLISLAB for Short-Term Analysis WILL take a Long Time to Finish

Location Coords.	Location #1	Location #2	Location #3
X-Coordinate (ft)	22.5	22.5	22.5
Y-Coordinate (ft)	2	2.5	6

Depth within PCC Layer for Simulation of Response: 10 inch
Which plot do you want to show? Sx at Time = 0.1 hr

Click Here to Run ILLISLAB | Click Here to Reload Images | Import ILLISLAB Results

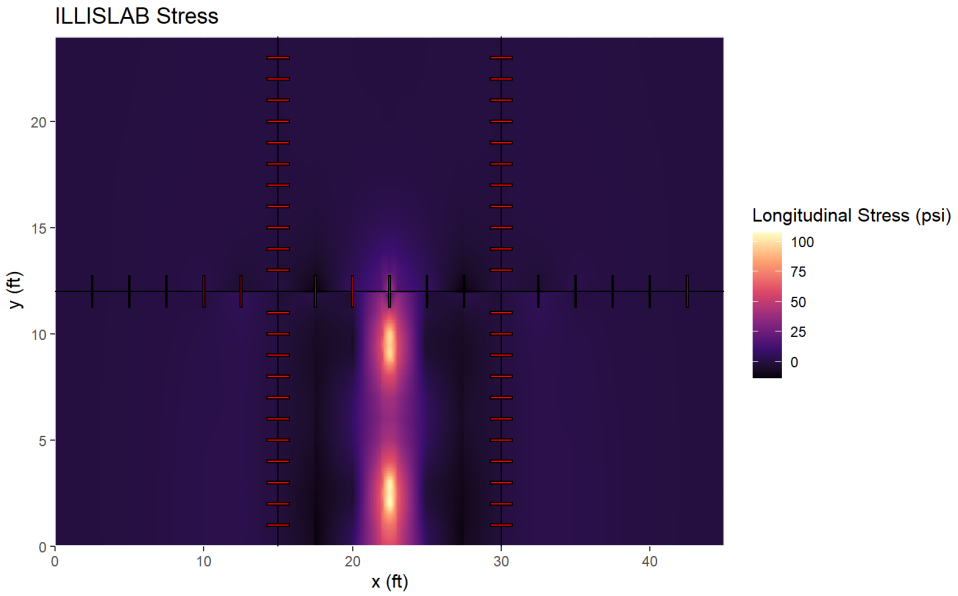

Figure A-29. Short-Term Analysis Results – Structural Analysis Using ILLISLAB.

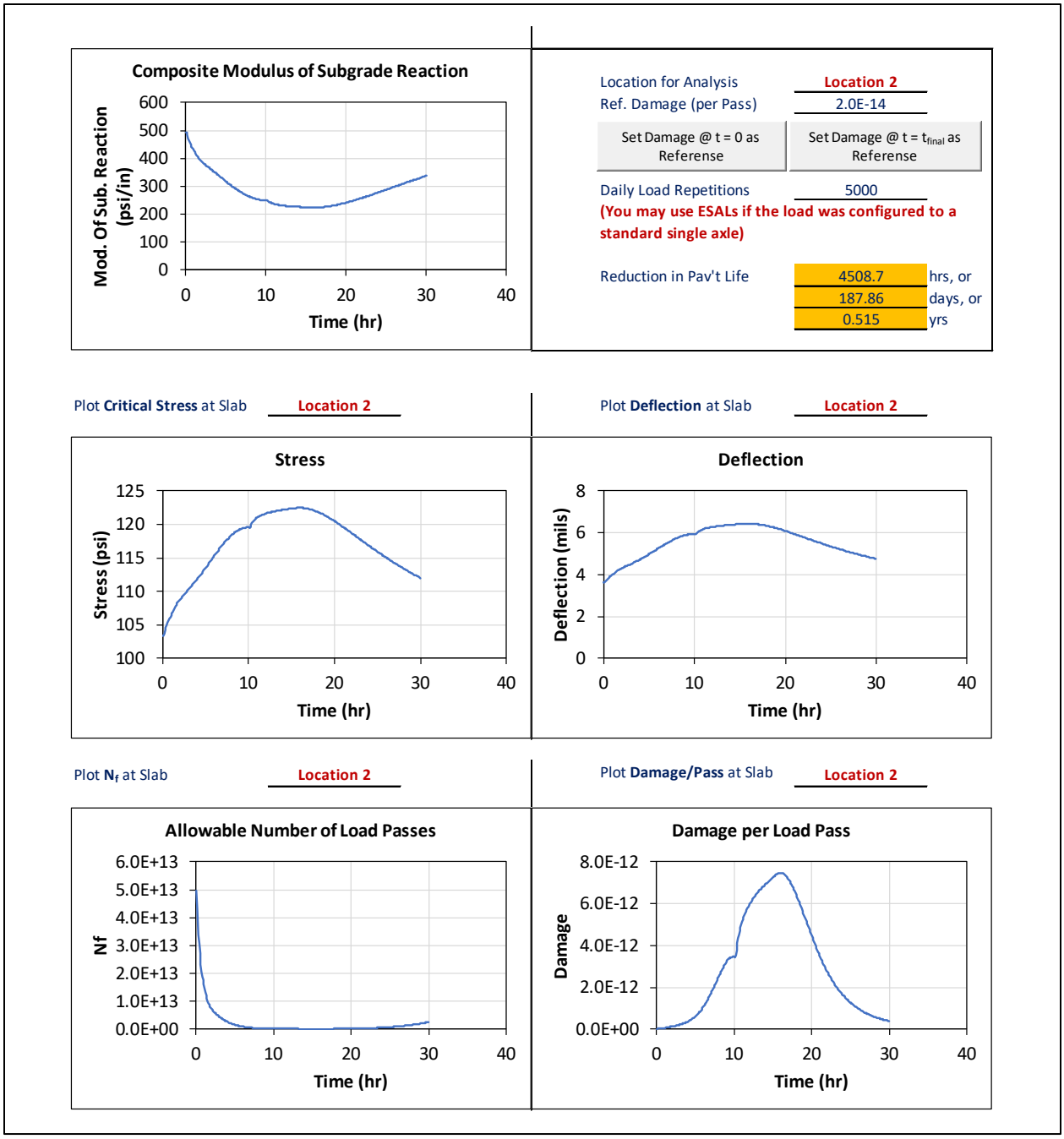

Figure A-30. Short-Term Analysis Results – Performance Analysis Using ILLISLAB.